Developing Tools for Late-Stage Regimen Development for Tuberculosis

by
Vincent Chang

DISSERTATION
Submitted in partial satisfaction of the requirements for degree of
DOCTOR OF PHILOSOPHY

in

Pharmaceutical Sciences and Pharmacogenomics

in the

GRADUATE DIVISION
of the
UNIVERSITY OF CALIFORNIA, SAN FRANCISCO

Approved:

DocuSigned by:
Patrick Phillips
F39BACE611F44E6...

Patrick Phillips
Chair

DocuSigned by:
Radojka Savic
DocuSigned by:

Radojka Savic

DocuSigned by:
Payam Nahid
D5DBF2347A6A427...

Payam Nahid

Committee Members

Acknowledgements

Just as it takes a village to raise a child, it takes a lab community to raise a graduate student.

First, thank you to all the study participants and volunteers, the staff at clinical sites, and all investigators for each of the clinical trials that are the foundation of this dissertation. This work would not be possible without your contributions.

My sincerest gratitude to my mentor and advisor, Dr. Rada Savic, for fostering a nurturing environment for myself and other academic trainees. She has designed a setting that simultaneously has space for people to learn and grow while answering important global health research questions with sweeping ramifications to change the world. I feel so fortunate to be part of this lab and so honored to be trusted with such impactful research. She has protected my time and encouraged me when I felt stressed and challenged me when there was room to improve. My experience here has taught me not only about pharmacometrics research, but also about myself as a person.

I would like to express my deepest appreciation for my dissertation committee members, Dr. Payam Nahid and Dr. Patrick Phillips. They have been a valuable resource and have acted as a second set of mentors and advisors for my research. Patrick and I worked closely together for the adaptive trial design manuscript presented in chapter 5 of this dissertation. He was consistently available and offered insightful troubleshooting sessions, constructive comments, and continuous support at all stages of my research. Payam has brought valuable clinical and programmatic perspectives to my work, shaping the main messages to have larger global health and drug development impacts.

I would also like to thank the members of my qualifying exam committee, Drs. Kathy Giacomini, Patrick Phillips, and Payam Nahid for your expertise and support. Along with the PSPG Graduate Program Directors, Drs. Deanna Kroetz, Nadav Ahituv, and Rada Savic, thank you for shaping and providing a path for me to develop as a research scientist.

I have had the honor of working with data from the first successful phase III clinical trial in drug-susceptible tuberculosis in approximately 50 years. I am incredibly thankful for the opportunity to work with our numerous collaborators who have spent much of their career working towards implementing and conducting Tuberculosis Trials Consortium Study 31/AIDS Clinical Trial Group A5349. William Whitworth and Kia Bryant tirelessly fulfilled and managed our data requests. Ekaterina Kurbatova, Susan Dorman, Kelly Dooley, Andrew Vernon, Susan Swindells, Patrick Phillips, Payam Nahid, Rada Savic, and Gustavo Velásquez edited and reviewed this work. The following is not an exhaustive list of those who contributed to TBTC Study 31/ACTG A5349: Susan E. Dorman, M.D., Payam Nahid, M.D., M.P.H., Ekaterina V. Kurbatova, M.D., Ph.D., M.P.H., Patrick P.J. Phillips, Ph.D., Kia Bryant, M.P.H., Kelly E. Dooley, M.D., Ph.D., Melissa Engle, C.R.T., C.C.R.C., Stefan V. Goldberg, M.D., Ha T.T. Phan, Dr.P.H., M.D., James Hakim, M.D., John L. Johnson, M.D., Madeleine Lourens, M.B., Ch.B., Ph.D., Neil A. Martinson, M.B., B.Ch., M.P.H., Grace Muzanyi, M.B., Ch.B., Kim Narunsky, M.B., Ch.B., Sandy Nerette, M.D., Nhung V. Nguyen, M.D., Ph.D., Thuong H. Pham, M.D., M.P.H., Samuel Pierre, M.D., Anne E. Purfield, Ph.D., Wadzanai Samaneka, M.B., Ch.B., Radojka M. Savic, Ph.D., Ian Sanne, M.B., B.Ch., D.T.M.H., Nigel A. Scott, M.S., Justin Shenje, M.B., Ch.B., Erin Sizemore, M.P.H., Andrew Vernon, M.D., M.H.S., Ziyaad Waja, M.B., B.Ch., M.P.H., Marc Weiner, M.D., Susan Swindells, M.B., B.S., and Richard E. Chaisson, M.D.

To my mentors in the Savic lab, Marjorie Imperial and Nan Zhang, your guidance was instrumental in the research presented here. Nan taught me population pharmacokinetic modeling and together with others in the lab, we completed pharmacokinetic analysis of the six drugs administered in Study 31/A5349. Marjorie has worked closely together with me from beginning to the end of my time here, and she has always been an inspiration and role model. Much of my research is built on top of the TB-ReFLECT analysis and models that Marjorie had completed during her own PhD. She mentored me through many of my projects and advised me on time to event analysis, clinical trial simulations, general model building principles, linear and logistic regressions, toxicity and safety analyses, pharmacokinetic-pharmacodynamic analyses, etc. I am sad that the pandemic led to us working together remotely, but you always made yourself available and I appreciate your guidance and friendship immensely.

To my fellow PSPG graduate students, Janice Goh, Jackie Ernest, Emma Hughes, Kendra Radtke, and Marjorie Imperial, thank you for charting a path for me to follow. Your trail blazing has made the time of each successive graduate student simpler and more straightforward. I have enjoyed our friendships and I value this time together immensely. Emma and Kendra, I especially appreciate the Savic lab infrastructure that you two tirelessly provided.

To all others in the Savic lab, María García-Cremades, Natasha Strydom, Priya Jayachandran, Belén Pérez Solans, Leah Gonzalez Jarlsberg, Erika Wallender, Huy Ngo, Hwi-yeol Yun, Isaac Cohen, Agathe Béranger, Ségolène Siméon, Mikhail Zastrozhin, Pieter Van Brantegem, Rob Christiaan van Wijk, Ryo Miyakawa, Jordan Brooks, Yamine White, Silver Alkhafaji, Anu Patel, Hoang-Anh Vu, Ava Xu, Erwin Dressen, Lorezno Flori, and Anna Fochesato, thank you for the time we have spent together. I have learned from you and with you, and through mentoring some of you I have gained a deeper understanding of the work we do here. Thank you for all the time we have spent together, the coffee times, board games, potlucks, lab retreats, nailed it ceremonies, happy hours, etc. Your friendship, company, and good nature defined Savic lab culture and I'm so happy to be one of us.

I would like to thank my remaining PSPG classmates for the camaraderie, memories, and support over the last five years. Thank you to the cohorts above, especially Bianca Vora, Marcus Chin, and Dina Buitrago Silva for being so welcoming and warm in the early years. A special thank you to my own cohort, Emily Connelly, Jackie Ernest, Colin Germer, Janice Goh, Nilsa La Cunza, Michelle Wang, Will Connell, Xujia Zhou, and Kendra Radtke. We did it!

To my LYF camp family, you may not think you have had much impact on my PhD path, but LYF has shaped me and made me who I am. You have taught me how to love myself, how to be true to myself, how to community build, and how to inspire others. Even as I moved on from attending LYF camp each year, these lessons remain at the core of my identity, and I have continued to grow into a more authentic self with each passing year. Thank you for being my home and thank you for your love and care.

To my parents, Jody 吳麗雪 and Tom Chang 張鴻德, thank you for your support over my entire life. You have prepared me so well and offered me resources and opportunities that most people never receive. The pride the two of you have for me for pursuing a PhD at UC San Francisco is so tangible and palpable, and I feel so loved and supported. I always left home going back to San Francisco with arms full of homecooked meals and groceries. Words cannot express the deep gratitude, appreciation, and love I feel for you.

To my brother, Johnny Chang, you are the best brother anyone can ask for. You have loved me for who I am and provided a safe space for me, from when I was small and throwing tantrums at you until this day as adults. Your patience, acceptance, and intentionality are seen, valued, and appreciated.

This dissertation is dedicated to my mentors, colleagues, friends, and family.

Contributions

Several chapters in this dissertation contain material that has been published previously or is currently under consideration/review. They do not necessarily represent the final published form and in all cases have been edited slightly.

Chapter 2 is modified from a manuscript in preparation, “Rifapentine Population Pharmacokinetics and Dosing Recommendations for the Novel WHO-recommended 4-Month Rifapentine-Moxifloxacin Regimen for Drug-Susceptible Tuberculosis”, by Chang V, Imperial MZ, Zhang N, and Savic RM. Rada Savic contributed to the study design. Marjorie Imperial and Nan Zhang reviewed and edited the manuscript. Execution, analysis, and manuscript preparation were carried out by Vincent Chang.

Chapter 3 is modified from a manuscript in preparation, “Moxifloxacin Population Pharmacokinetics for the Novel WHO-recommended 4-Month High-Dose Rifapentine-Moxifloxacin Regimen for Drug Susceptible Tuberculosis”, by Chang V, Imperial MZ, Zhang N, and Savic RM. Rada Savic contributed to the study design. Marjorie Imperial and Nan Zhang reviewed and edited the manuscript. Execution, analysis, and manuscript preparation were carried out by Vincent Chang.

Chapter 4 is modified from a manuscript in preparation, “Risk Stratified Treatment for Drug-Susceptible Tuberculosis”, by Chang V, Imperial MZ, Phillips PPJ, Velásquez GE, Vernon A, Kurbatova E, Swindells S, Chaisson R, Dorman S, Johnson J, Weiner M, Sizemore E, Whitworth W, Carr W, Bryant K, Burton D, Dooley K, Engle M, Nsubuga P, Diacon A, Nhung NV, Dawson R, and Savic RM for the AIDS Clinical Trials Group and the Tuberculosis Trials Consortium. All authors contributed to the study design, conducted the study, and edited the manuscript. Vincent Chang and Marjorie Imperial carried out the analysis and prepared the manuscript.

Chapter 5 is modified from an accepted manuscript, “A Comparison of Clinical Development Pathways to Advance Tuberculosis Regimen Development”, by Chang V, Phillips PPJ, Imperial MZ, Nahid PN, and Savic RM. VC co-built the clinical trial simulation tool, performed the simulations, interpreted the

simulation data, designed the figures, and wrote the manuscript. PJPP conceived and designed the study, interpreted the simulation data, and was a major contributor in writing the manuscript. MZI co-built the simulation tool and made significant revisions to figures and writing. PN conceived and designed the study and edited the manuscript. RMS conceived and designed the study, interpreted the simulation data, and made significant revisions to figures and writing. All authors read and approved the final manuscript.

Developing Tools for Late-Stage Regimen Development for Tuberculosis

Vincent K. Chang

Abstract

Tuberculosis was the leading infectious disease killer, prior to the COVID-19 pandemic, and infected approximately 10 million people each year and kills approximately 1.5 million. Currently. drug-susceptible TB is treated with rifampin, isoniazid, pyrazinamide, and ethambutol for a minimum of six months, however even with full adherence to this long treatment, relapse and treatment failure each occur in approximately 5-10% of cases. Crucially, these treatments for drug-susceptible TB have not appreciably changed in over 50 years and current drug discovery and clinical development pipelines are in dire need of rapid innovation.

In 2020, a landmark phase III trial successfully demonstrated noninferiority of a novel 4-month regimen compared to the current 6-month standard of care. TBTC Study 31/A5349 was a multicenter randomized controlled phase III non-inferiority trial that compared two four-month regimens (both replace rifampin with rifapentine, and one tests the additional substitution of ethambutol replaced by moxifloxacin) with the standard six-month regimen for treating drug-susceptible pulmonary tuberculosis. The regimen containing high dose rifapentine, moxifloxacin, isoniazid, and pyrazinamide successfully demonstrated noninferiority. Remarkably, Study 31/A5349 collected study wide pharmacokinetic samples of all six drugs offering us the first opportunity in the history of TB-research to link drug exposures to long term clinical outcomes.

Each of the six drugs were analyzed by non-linear mixed effects modeling and the typical population pharmacokinetic behavior, between subject variability of F, CL, and V_c, and their relationships with clinical characteristics and demographic covariates were thoroughly characterized. Model derived maximal plasma concentration and area under the curve (exposure) were then used in pharmacodynamic efficacy and toxicity analyses to determine optimal dosing. We conducted an integrated analysis of

demographic, clinical, microbiologic, radiographic, and pharmacokinetic data from 2343 participants with drug-susceptible tuberculosis from Study 31/A5349. We compared two 4-month rifapentine-based regimens with and without moxifloxacin to a 6-month control regimen. We demonstrated the importance of achieving a high exposure to rifapentine in the 4-month rifapentine-moxifloxacin regimen to reduce the risk of TB-related unfavorable outcomes. We identified a low-risk subgroup where further treatment shortening, and simplification is likely possible and a high-risk subgroup where longer treatment may be needed.

The integrated models built from this work were used in a variety of simulation work, (1) optimal dosing of the rifapentine-moxifloxacin regimen (Chapters 2 and 3), (2) design of a novel risk-stratification duration-randomization phase II trial (not described in this thesis), (3) development of a clinical trial simulation tool to calculate statistical power and determine sample size (Chapter 5), and (4) optimization of adaptive trial designs for phase II and III anti-tuberculosis agent (Chapter 5).

Collectively, the dissertation research described here contributes to the optimal use of the first 4-month regimen for drug-susceptible tuberculosis and develops simulation tools for future development of novel therapeutics and interventions for the treatment and prevention of tuberculosis.

Table of Contents

List of Figures

List of Supplemental Figures

List of Tables

List of Supplemental Tables

List of Abbreviations

TB – Tuberculosis

US – United States

FDA – Federal Drug Administration

HRZE – Isoniazid, Rifampicin, Pyrazinamide, Ethambutol regimen

HPZE – Isoniazid, Rifapentine, Pyrazinamide, Ethambutol regimen

HPZM – Isoniazid, Rifapentine, Pyrazinamide, Moxifloxacin regimen

S31 – Study 31/A5349

TB-ReFLECT – Patient database of ReMOX, RIFAQUIN, and OFLOTUB

BPaL – Bedaquiline, Pretomanid, Linezolid regimen

MAMS – Multi-Arm Multi-Stage

BAR – Bayesian response Adaptive Randomization

PaMZ – Pretomanid, Moxifloxacin, Pyrazinamide regimen

TCC – Time to Culture Conversion

TTR – Time To Relapse

%CV – percent coefficient of variation

HR – hazard ratio

TS-X – treatment success at week X

MIC – Minimum inhibitory concentration

VPC – Visual Predictive Check

Chapter 1 - Introduction

TB remains a major global health issue: In 2022, there were an estimated 10 million new cases of TB, and 1.5 million TB deaths, including 251,000 HIV-positive people[1]. Prior to the COVID-19 pandemic, TB was the leading cause of death from a single infectious agent. Currently. drug-susceptible TB is treated with rifampin, isoniazid, pyrazinamide, and ethambutol for a minimum of six months, however even with full adherence to this long treatment, relapse and treatment failure each occur in approximately 5-10% of cases[2,3]. Crucially, these treatments for drug-susceptible TB have not appreciably changed in over 50 years and current drug discovery and clinical development pipelines are in dire need of rapid innovation[4,5].

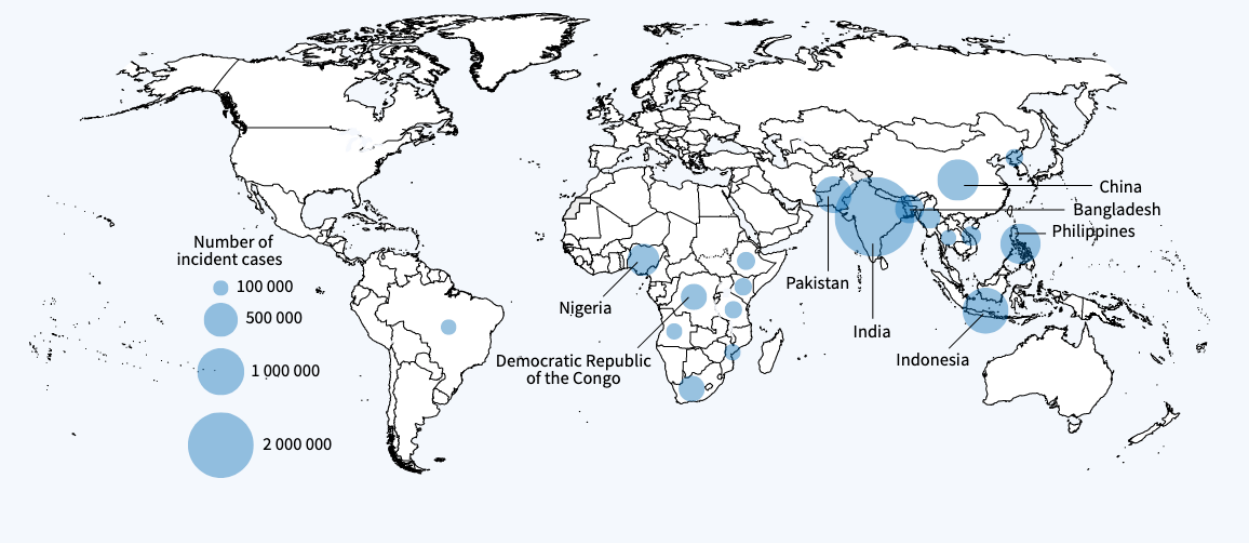

Figure 1-1 Estimated global TB incidence adapted from 2022 WHO Global TB Report

Tuberculosis is one of humanity's oldest and most resilient infectious diseases. Every country is affected by TB, but the vast majority of cases occur in the developing world. Combined, Sub-Saharan Africa, South Asia, and Southeast Asia accounts for greater than 87% of the incidence of TB worldwide. This disproportionate economic and geographic spread of TB has led to the perception in wealthy nations that TB has been eradicated, even as the number of new TB cases continue to rise every year (TB incidence rate is falling, but number of new cases still continue to rise due to population growth)[6]. This

also leads to little incentive for pharmaceutical companies (which largely reside in wealthy nations) to invest into improving the current standard of care, which has proven inadequate to manage the TB epidemic. Additionally, novel therapies and technologies that are primarily developed in wealthy nations are expensive and slow to reach these TB endemic regions. The work described here aims to push forward two main TB treatment goals: (1) establish patient centric treatment protocols which minimize treatment duration and maximize treatment success in low and high resource settings, and (2) develop new treatment shortening regimens which will enable treating more patients with the same resources.

In 2020, a landmark phase III trial successfully demonstrated noninferiority of a novel 4-month regimen compared to the current 6-month standard of care. TBTC Study 31/A5349[7] was a multicenter randomized controlled phase III non-inferiority trial that compared two four-month regimens (both replace rifampin with rifapentine, and one tests the additional substitution of ethambutol replaced by moxifloxacin) with the standard six-month regimen for treating drug-susceptible pulmonary tuberculosis (Figure 1-2). The regimen containing high dose rifapentine, moxifloxacin, isoniazid, and pyrazinamide successfully demonstrated noninferiority (Regimen 3: 2PHZM/2PHM). Although the regimen demonstrated noninferiority on the trial level, this registration-quality trial provides host, bacterial, pharmacokinetic, and clinical data across all patients enrolled, offering an unprecedented opportunity to investigate subpopulations to determine for whom this novel regimen worked for and for whom it did not, develop PKPD models, and provide stratified treatment algorithms. We envision a stratified medicine approach that will take full advantage of the clinical characteristics and biomarkers available to a healthcare clinic to stratify patients into subpopulations of minimal, moderate, and severe disease risk. We will utilize the various models built from S31/A5349 which span the spectrum of precision and simplicity built from different sets of clinical characteristics and biomarkers. The simplest model utilizes standard and cost effective clinical and disease markers, resulting in the greatest benefit at a low cost. The most precise model will require time to culture conversion, MICs, and other resource intensive measures. We hope that this approach will equip clinicians all around the world with new tools to combat over and under treatment of TB and help manage the TB epidemic.

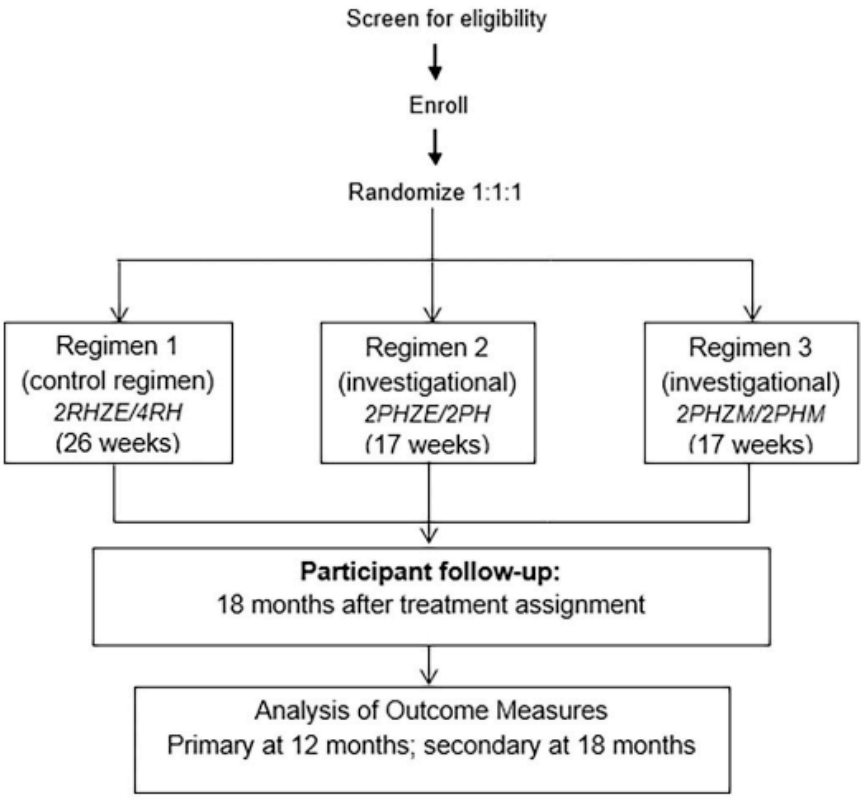

Figure 1-2 Study schematic for Study 31/A5349.

R = rifampin, H = isoniazid, Z = pyrazinamide, E = ethambutol, P = rifapentine, M = moxifloxacin
Adapted from "High-dose rifapentine with or without moxifloxacin for shortening treatment of pulmonary tuberculosis: Study protocol for TBTC study 31/ACTG A5349 phase III clinical trial" Dorman SE et al., Contemporary Clinical Trials 2020

The S31/A5349 database also lends a wealth of simulation opportunities to explore novel approaches for stratified treatment and late-stage drug development. Standard clinical development strategies for TB regimens are slow (Phases II and III take >8.5 years) and have not yet taken advantage of newly profiled patient risk phenotypes and new adaptive clinical trial designs, both advancements well recognized in oncology. Stratified treatments and adaptive designs can make clinical trials more flexible by utilizing results accumulating in the trial to modify treatment and/or the trial's course according to pre-specified rules[5]. These strategies permit shorter trials, seamless transitions between phases, and more efficient regimen selection from a larger pool of candidates. The primary goal of our simulations will be to optimize new tools, such as patient stratification algorithms and adaptive trial designs for TB regimen

development and provide recommendations on when, where, and how these tools may be applied to greatest impact.

Thesis Aims

This thesis aims to address important and policy-driven questions around dose and treatment optimization for anti-TB drugs. This work is focused on the optimization and utilization of the first 4-month regimen to demonstrate noninferiority compared to the 50-year-old 6-month standard of care regimen. As such, the findings will have important implications on treatment guidelines and TB programs all around the world.

Chapters 2 and 3 are focused on evaluating the population pharmacokinetics of rifapentine and moxifloxacin, the two primary drugs of interest in the novel 4-month regimen. Chapter 2 focuses on characterizing the variability in rifapentine pharmacokinetics, determining its role in driving treatment response, and recommending optimal dosing guidelines. Chapter 3 focuses on characterizing the variability in moxifloxacin pharmacokinetics, determining its contribution to the novel rifapentine-based regimen, and exploring optimal dosing.

Chapter 4 addresses an important knowledge gap in TB treatment. The role of pharmacokinetics has been evaluated with many different surrogate endpoints, ie. early bactericidal activity, time to positivity, and time to culture conversion, but it has never been linked to long term clinical outcomes. The research determines the primary pharmacokinetic drivers of treatment response and identifies demographic and baseline clinical risk factors for treatment failure and relapse. These findings are used to develop a risk stratification algorithm where patients can be stratified by baseline disease burden into a low-risk subgroup in which further treatment shortening and simplification are likely to be possible and a high-risk subgroup in which longer treatment may be needed.

Chapter 5 aims to demonstrate the feasibility of adaptive trial designs in TB regimen development. Advances in the field of oncology have demonstrated that biomarker stratified trials and adaptive trial designs can rapidly bring treatment innovation from bench to clinic, and the work here utilizes individual

patient data, integrated models predicting treatment outcomes, and clinical trial simulation tools to demonstrate the suitability of adaptive trial designs in TB regiment development.

References

1. World Health Organization. *Global tuberculosis report 2022*. (World Health Organization, 2022).
2. Nahid, P. *et al.* Official American Thoracic Society/Centers for Disease Control and Prevention/Infectious Diseases Society of America Clinical Practice Guidelines: Treatment of Drug-Susceptible Tuberculosis. *Clin. Infect. Dis.* **63**, e147–e195 (2016).
3. World Health Organization. *Guidelines for treatment of drug-susceptible tuberculosis and patient care: 2017 update.* (2017).
4. Davies, G., Boeree, M., Hermann, D. & Hoelscher, M. Accelerating the transition of new tuberculosis drug combinations from Phase II to Phase III trials: New technologies and innovative designs. *PLOS Med.* **16**, e1002851 (2019).
5. Phillips, P. P. J. *et al.* Innovative Trial Designs Are Practical Solutions for Improving the Treatment of Tuberculosis. *J. Infect. Dis.* **205**, S250–S257 (2012).
6. WORLD HEALTH ORGANIZATION. *GLOBAL TUBERCULOSIS REPORT 2019.* (WORLD HEALTH ORGANIZATION, 2019).
7. Dorman, S. E. *et al.* High-dose rifapentine with or without moxifloxacin for shortening treatment of pulmonary tuberculosis: Study protocol for TBTC study 31/ACTG A5349 phase 3 clinical trial. *Contemp. Clin. Trials* **90**, 105938 (2020).

Chapter 2 - Optimal Rifapentine Dosing in the Novel 4-Month Rifapentine-Moxifloxacin Regimen for Drug-Susceptible Tuberculosis

Introduction

Since their first use in clinical trials in the 1970s, rifamycins have remained a cornerstone in treatments for drug-susceptible tuberculosis[1]. Rifapentine is a cyclopentyl derivative of rifampicin, the rifamycin in the current 6-month standard of care regimen, and was approved by the U.S. FDA in 1998 for the treatment of TB using intermittent dosing[2]. As focus has shifted from intermittent dosing to shortening the duration of treatment, rifapentine's higher potency and longer half-life makes the drug an attractive option for replacing rifampicin in short course treatments. Subsequent animal studies demonstrated that daily rifapentine in a combination regimen had potent antimycobacterial activity able to achieve cure without relapse after three months of treatment in the relapsing mouse model.[3] Phase 1 and 2 clinical trials confirmed safety and tolerability of rifapentine at daily doses up to 20 mg/kg (up to 1500 mg) and demonstrated a strong exposure-response relationship with time to stable culture conversion, the primary on-treatment surrogate biomarker.[4,5]

In the phase 2b dose ranging study Study 29/29x[4,6], Savic et.al. previously described rifapentine population pharmacokinetics with a first order absorption, one compartment model with metabolite clearance.[5] Male sex, HIV seropositivity, older age, absence of food, and dose limiting bioavailability were all found to be covariates on either bioavailability or clearance decreasing rifapentine exposure. Higher rifapentine steady state individual participant area under the concentration-time curve from 0-24 hours ($AUC_{0\text{-}24h}$) was found to improve time to stable liquid culture conversion with maximum achievable effect observed at an exposure of 350 μg·h/mL. Additionally, 73% of phase 2b participants achieved this target by taking a 1200 mg dose while consuming food. Therefore, S31/A5349 selected to administer a flat 1200 mg dose with food. Rifamycins are well known to have highly variable pharmacokinetics[7–9]. The Savic model found high between subject variability in clearance, metabolite clearance, and bioavailability

resulting in up to 5-fold $AUC_{0\text{-}24h}$ range with the same dose and meal underscoring the need to accurately characterize rifapentine pharmacokinetics in a larger population.

As a follow up to S29/29x, the Tuberculosis Trials Consortium recently completed Study 31/ACTG A5349 (S31/A5349), an international, multicenter, randomized, open-label, phase III, noninferiority trial, successfully demonstrated noninferiority of a short course 4-month regimen of once-daily rifapentine, isoniazid, pyrazinamide, and moxifloxacin (rifapentine-moxifloxacin regimen) when compared to the 6-month standard of care regimen of once-daily rifampicin, isoniazid, pyrazinamide, and ethambutol (control regimen).[10,11] S31/A5349 also tested 4-month rifapentine, isoniazid, pyrazinamide, and ethambutol (rifapentine regimen), but this regimen failed to demonstrate noninferiority. Notably, S31/A5349 is the first phase III anti-tuberculosis agent trial that had near study-wide pharmacokinetic sampling for all drugs. It offers the first opportunity to build robust population pharmacokinetic models and link exposure to long-term clinical outcomes. In chapter 4, we report in a pharmacokinetic-pharmacodynamic analysis of S31/A5349 that low rifapentine exposure is a risk factor for TB-related unfavorable outcomes (Figure 2-1). From this analysis we determined the target exposure of rifapentine to be 570 μg·h/mL which corresponds to 5% TB-related unfavorable outcomes in participants receiving the rifapentine-moxifloxacin regimen.

In this work, using the largest PK dataset from S31/A5349, a Phase III clinical trial, we characterized rifapentine pharmacokinetics using a nonlinear mixed effects population approach to (1) quantify the patient characteristics and clinical factors that underpin variability in rifapentine exposure, (2) identify subpopulations at risk for low drug exposure, (3) characterize PK-safety relationships, and (4) perform simulations to determine optimal dosing strategies across subpopulations.

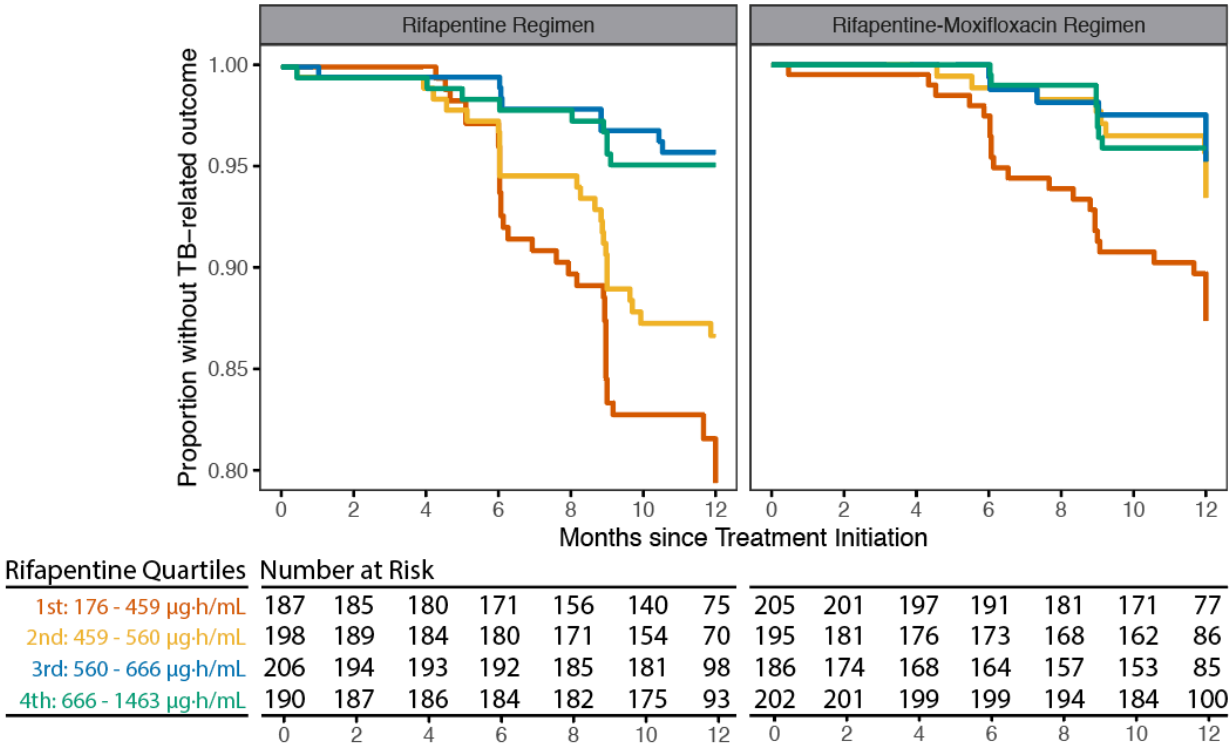

Figure 2-1 Kaplan Meier estimates of TB-related Unfavorable Outcomes Stratified by Rifapentine Exposure Quartiles Shows Participants with Low Rifapentine Exposure are at Higher Risk of TB-related Unfavorable Outcomes

Participants in the microbiologically eligible population were stratified by regimen and quartiles of rifapentine exposure. A clear exposure response relationship can be seen in both rifapentine and rifapentine-moxifloxacin regimens.

Methods

Study Design

Study 31/A5349 was a phase III randomized controlled trial conducted in 13 countries at 34 clinical sites by the CDC funded Tuberculosis Trials Consortium and the National Institutes of Health funded AIDS Clinical Trials Group (ACTG). The participants were ≥12 years of age and had newly diagnosed pulmonary tuberculosis that was confirmed on culture to be susceptible to isoniazid, rifampicin, and fluoroquinolones. All participants provided written informed consent. The participants were randomly assigned in a 1:1:1 ratio to one of three previously described regimens. Isoniazid was administered at 300 mg once daily, rifampin at 600 mg once daily, rifapentine 1200 mg once daily, and moxifloxacin at 400 mg once daily. Pyrazinamide and ethambutol were administered according to weight bands: 1000 mg and

800 mg for < 55 kg, respectively; 1500 and 1200 mg for ≥ 55-75 kg, respectively; and 2000 mg and 1600 mg for > 75 kg, respectively. The 4-month rifapentine and rifapentine-moxifloxacin regimens were administered within 1 hour after ingesting food and the 6-month control regimen was administered on an empty stomach Additional details on the study design are available in the original study protocol publication.

Sample Collection and Assays

Patients were dosed with 1200 mg rifapentine flat dose daily; samples were taken in between the 2 week and 8 week visit windows, after enzyme induction reached steady state. Intensive sampling was performed on a small number of participants (targeting 53 participants for 85% power to detect up to an 8% difference in apparent clearance assuming 20% variance between individuals), half from 2HPZE/2HP and half from 2HPZM/2HPM regimens, samples were taken at 0.5, 3, 5, 9, 12, and 24 hours in 2-3 separate occasions. The remaining participants were sampled sparsely with time points at 0.5, 5, and 24 hours in 1-2 occasions. Plasma concentrations of rifapentine and its main metabolite, 25-desacetyl-rifapentine, were determined using validated high-performance liquid chromatography assays.

Modeling Software and Methods

Pharmacokinetic data were randomly split into an analysis cohort for model development and validation cohort for model validation, where one-third of the data was conserved for the validation cohort and covariates (clinical site and HIV) were balanced between cohorts. Rifapentine and its metabolite 25-desacetyl-rifapentine plasma concentrations were analyzed using nonlinear mixed-effects modeling with NONMEM version 7.41 (ICON Development Solutions). Population pharmacokinetic model building followed standard procedures by first characterizing the base structural model and estimating typical pharmacokinetic parameters using a first-order conditional estimation method with interaction (FOCE INTER).[12] Interindividual variability, which describes the observed population variability in pharmacokinetic parameters, are assumed to follow a log normal distribution and the variance of this distribution is estimated.

One- and two-compartment distribution models with first-order elimination were tested. First-order models or a sequence of zero- and first-order models that incorporate lag times or transit compartments were evaluated to describe rifapentine absorption.

Age, sex, African/non-African site, race (Black, Asian, White, and Mixed), weight, BMI, study arm, cavity existence, cavity size classification, extent of disease classification, smear grade, HIV status, diabetes history and karnofsky score, were evaluated for potential inclusion as covariates on the PK parameters: bioavailability (F1), apparent clearance (CL/F) and apparent volume of the central compartment (V/F). Covariate effects were selected through a stepwise procedure with forward selection (P<0.05) and backward elimination (P<0.01). Final inclusion of covariates was based on statistical significance, scientific plausibility, and clinical relevance.[13]

Model development was guided by assessment of goodness of fit plots, condition number, and the likelihood ratio test. Simulation based diagnostics (e.g., visual predictive checks [VPCs] and bootstraps) were used for model development and validation.

R software (version 3.5.2; R Foundation for Statistical Computing) was used for all data management, analyses, and graphical visualization. The Xpose (version 0.4.4) and vpc (version 1.0.1) packages were used for visual diagnostics. Nonparametric bootstrap and covariate modeling were performed with Perl-speaks-NONMEM (version 4.7.0).

Safety Outcomes and Analysis

The primary safety outcome in the trial was any grade 3 or higher adverse events during the on-treatment period (the time during which the participants were receiving the trial medications and up to 14 days after the last dose)[10,11]. Additional analyses were performed for: (i) treatment related grade 3 or higher adverse events, (ii) serious adverse events, (iii) tolerability, and (iv) death. Tolerability was defined as discontinuation of the assigned treatment for any reason other than microbiological ineligibility. 3x and 5x upper limit of normal ALT and AST levels and grade 3 or above neutropenia were investigated further for

a pharmacokinetic-toxicity relationship, as these adverse events are well documented in rifapentine literature[14,15]. See Table 2-1 for counts of each of the safety outcomes. Rifapentine $AUC_{0\text{-}24h}$ and maximal plasma concentration (C_{max}) were analyzed with independent logistic regressions with each of the safety outcomes described above.

Dosing Simulations

Dosing simulations were performed with the final model to (1) assess the impact of clinically relevant patient factors (e.g. HIV and sex) on rifapentine exposure, and (2) propose pragmatic dosing strategies for rifapentine that maximizes achieving target exposure (570 μg·h/mL) and minimizes safety concerns. Since bioavailability of rifapentine is dose dependent, simulations were performed using the following equation [EQ1] from Hibma and Radtke et. al to calculate bioavailability relative to the 1200 mg dose used in S31/A5349.[16]

[EQ1] F = (1-0.0167*DOSE/100)/(1-0.0167*1200/100)

Results

Study Design and Dataset

The S31/A5349 rifapentine pharmacokinetic data were received from the US Centers for Disease Control on July 20, 2020, and consisted of 1523 participants, an additional cohort of data with 65 participants were received on June 30, 2021. 27 participants were intensively sampled, and 759 participants were sparsely sampled from the 2HPZE/2HP regimen, and 26 participants were intensively sampled and 768 were sparsely sampled from the 2HPZM/2HPM regimen. In total, 472 intensive samples and 4556 sparse samples were collected and measured for both parent drug rifapentine and metabolite 25-desacetyl-rifapentine concentrations (see raw data in Figure 2-2). Patient demographics, clinical factors, and demographics were similar across the two investigational arms and across the model development and validation datasets (Table 2-1 and Supplemental Table 2-1). Twenty-four samples were reported as below the limit of quantification (lower limit of quantification=0.25 μg/mL) and were fixed to half the LLOQ concentration, 0.125 μg/mL.

Table 2-1 Summary of Pharmacokinetic, Demographic, Clinical, and Safety data
(*) rifapentine and 25-desacetyl rifapentine were measured in each sample. N (%) given for categorical variables and median (95th percentiles) given for continuous variables. (▼) 12 participants were missing aggregate cavity size and disease extent, 3 participants were missing baseline smear grade.

	Arm 2 2HPZE/2HP	Arm 3 2HPZM/2HPM	Total
PHARMACOKINETIC SAMPLING *			
Total Participants	N=786	N=794	N=1580
Intensive Sampling Participants	N=27 (486 samples)	N=26 (458 samples)	N=53 (944 samples)
Sparse Sampling Participants	N=759 (4528 samples)	N=768 (4584 samples)	N=1527 (9112 samples)
Below Limit of Quantification	10 samples	14 samples	24 samples
DEMOGRAPHIC FACTORS			
Age [years]	31 (18 – 59)	31 (17 – 60)	31 (17-60)
Male Sex	558 (71.0)	567 (71.4)	1125 (71)
Height [cm]	167 (151 – 182)	167 (151 – 183)	167 (151 – 182)
Weight [kg]	53 (41 – 75)	53 (41 – 77)	53 (41 -76)
BMI [kg/m2]	19.00 (14.87 – 27.61)	18.99 (15.21 – 28.83)	19.00 (15.05 – 28.02)
Race			
Black	564 (72)	558 (70)	1122 (71)
Mixed/Multi-racial	126 (16)	134 (17)	260 (16)
Asian	88 (11)	90 (11)	178 (11)
White	8 (1)	12 (2)	20 (1)
CLINICAL FACTORS			
African Clinical Site	585 (74)	584 (74)	1169 (74)
Baseline Chest X-Ray Cavity	571 (73)	574 (72)	1145 (73)
Baseline Aggregate Cavity Size ▼			
No cavities	209 (27)	212 (27)	421 (27)
Cavities < 4cm	246 (31)	274 (35)	520 (33)
Cavities ≥ 4cm	326 (42)	301 (38)	627 (40)
Baseline Chest X-Ray Disease Extent ▼			
Lesions < 1/4 thoracic area	138 (18)	150 (19)	288 (18)
Lesions 1/4 to < 1/2 thoracic area	339 (43)	368 (47)	707 (45)
Lesions ≥ 1/2 thoracic area	304 (39)	269 (34)	573 (37)
Baseline Smear Grade ▼			
Negative	39 (5)	24 (3)	63 (4)
Scanty	131 (17)	154 (19)	285 (18)
Grade 1	177 (23)	170 (21)	347 (22)
Grade 2	219 (28)	224 (29)	443 (28)
Grade 3	211 (27)	215 (27)	426 (27)
Positive WHO scale not used	8 (1)	6 (1)	14 (1)
Karnofsky Score	90 (70 – 100)	90 (70 – 100)	90 (70 – 100)
HIV	67 (8)	66 (8)	133 (8)
Diabetes	13 (2)	30 (4)	43 (3)
SAFETY OUTCOMES			
Number of Patients (Safety Population)	835	846	1681
Grade 3 or higher adverse event	119 (14.3)	159 (18.8)	278 (16.5)
Treatment-related grade 3 or higher adverse event	64 (7.7)	109 (12.9)	173 (10.3)
Any serious adverse event	39 (4.7)	37 (4.4)	76 (4.5)
Death	4 (0.5)	3 (0.4)	7 (0.4)
Any adverse event resulting in discontinuation of assigned treatment	11 (1.3)	16 (1.9)	27 (1.6)
Any grade 3 or higher adverse event within 28 weeks after randomization	138 (16.5)	194 (22.9)	332 (19.8)
ALT or AST level ≥5×ULN	13 (1.6)	16 (1.9)	29 (1.7)
ALT or AST level ≥10×ULN	5 (0.6)	4 (0.5)	9 (0.5)
Serum total bilirubin level ≥3×ULN	20 (2.4)	28 (3.3)	48 (2.9)
Hy's law criteria of ALT or AST level ≥3×ULN plus serum total bilirubin level ≥2×ULN	8 (1.0)	10 (1.2)	18 (1.1)
Premature discontinuation of assigned regimen for any reason in the microbiologically eligible population	37/784 (4.7)	55/791 (7.0)	92/1575 (5.8)
Neutropenia	42 (5.0)	77 (9.1)	119 (7.1)

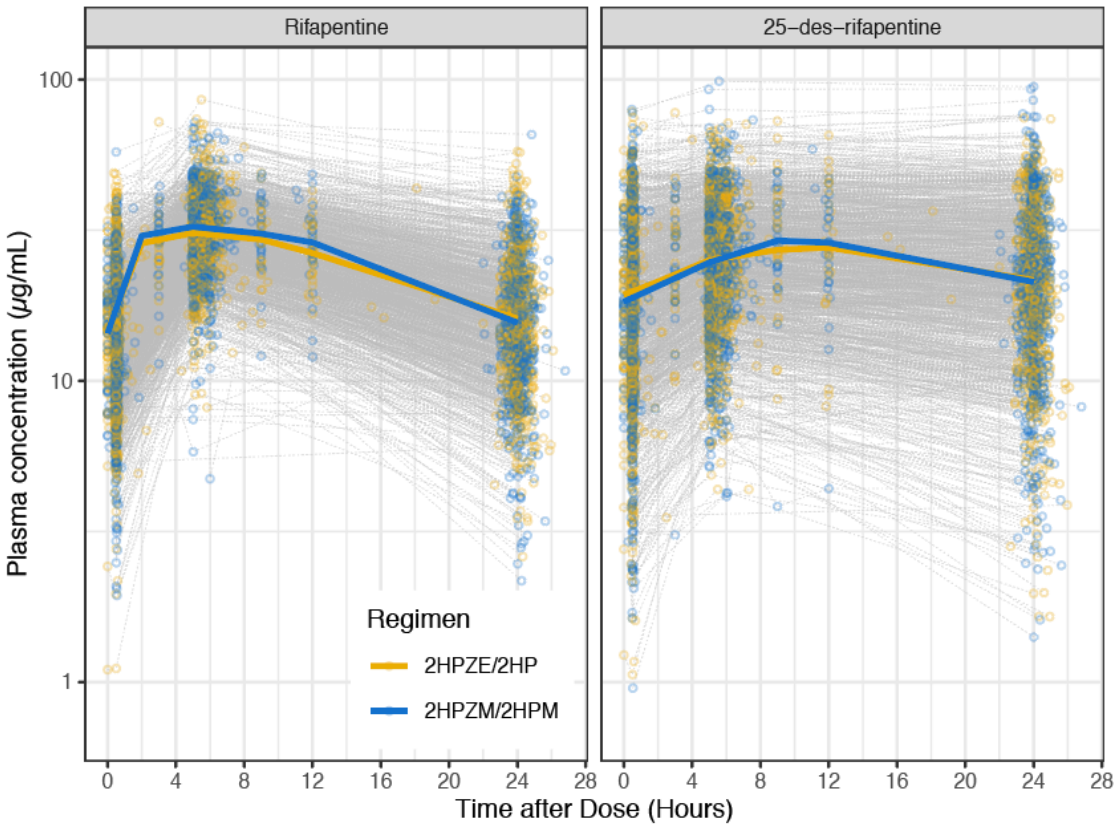

Figure 2-2 Observed rifapentine and 25-desacetyl rifapentine pharmacokinetic data were similar between 2HPZE/2HP and 2HPZM/2HPM regimens

Circles represent individual samples and solid lines represent medians. Data is stratified by regimen (yellow for HPZE and blue for HPZM), parent drug (left) and metabolite (right).

Pharmacokinetic Model

The one-compartment disposition model with linear metabolite clearance and transit compartment absorption best described the observed data. In the final model, the rifapentine steady state apparent CL/F was estimated to be 2.24 L/h (Relative Standard Error: 1.2%) and the V/F 47.4 L (2.7%) in the typical reference patient (male, Black, and HIV-). Two transit compartments best described the absorption phase with a mean transit time (MTT) of 3.68 hours (3.5%). Interindividual variability was supported on F=19.7% (20.4%), MTT=32.8% (21.3%), CL/F=32.3% (11.0%), and CL_m/F=47.5% (4.9%), with correlations between CL-F=41.2% (32.1%), F-CL_m=39.2% (36.9%), and CL-CL_m=58.1% (8.8%). The distribution of inter-individual variability on CLm was not normal and required a box cox transformation for metabolite clearance (CL_m) to improve model fit. (Table 2-2)

Table 2-2 Bootstrap of Final Model

(*) parameters are fixed.

	Final Full Model		
Parameters (units)	**Median**	**95% Confidence Interval**	**Relative Standard Error (%)**
CL/F (L/h)	2.24	2.19 – 2.29	1.17
V/F (L)	47.4	45.0 – 50.1	2.66
Mean transit time (h)	3.68	3.40 – 3.95	3.52
CL_m/F_m (L/h)	2.15	2.08 – 2.21	1.50
CL_m box cox transformation shape parameter	0.294	0.190 – 0.393	17.4
V_m/F_m (L)	11.3	10.4 – 12.1	4.04
F	1*	–	–
F_m	1*	–	–
N transit compartments	2*	–	–
Covariates (reference)			
Asian race effect on bioavailability (fraction relative to Black reference)	1.091	1.051 – 1.151	27.8
Female effect on bioavailability (fraction relative to male reference)	1.155	1.118 – 1.196	11.8
HIV infection effect on clearance (fraction relative to HIV-uninfected reference)	1.098	1.049 – 1.14	22.8
Between Subject Variability (units)			
Between-subject variability in CL (%CV)	32.3	28.4 – 35.4	11.0
Between-subject variability in MTT (%CV)	32.8	23.0 – 38.3	21.3
Between-subject variability in CL_m (%CV)	47.5	45.2 – 49.5	4.92
Between-subject variability in F (%CV)	20.9	16.3 – 25.3	20.4
Correlation CL-F	0.412	0.33 – 0.47	32.1
Correlation CL-CL_m	0.581	0.55 – 0.61	8.84
Correlation F-CL_m	0.392	0.30 – 0.46	36.9
Residual Error (units)			
Proportional error, parent (%)	15.5	14.0 – 17.1	4.84
Additive error, parent (μg/mL)	0.25*	–	–
Proportional error, metabolite (%)	14.6	13.7 – 16.1	3.91
Additive error, metabolite (μg/mL)	0.25*	–	–

Impact of Covariates on Pharmacokinetics

Rifapentine bioavailability was strongly influenced by race and sex ($P < 0.001$). In the final model, Asians had a 9.2% [relative standard error: 27.8%] increase in bioavailability relative to Black or Mixed race, and females had a 15.1% [11.8%] increase in bioavailability relative to males. Food, dose, and time dependent enzyme induction are well documented effects on rifapentine bioavailability[16], however since all participants in S31/A5349 were given the same 1200 mg dose with food with samples collected between 2-8 weeks (after induction has reached steady state) these effects could not be estimated. (Figure 2-3)

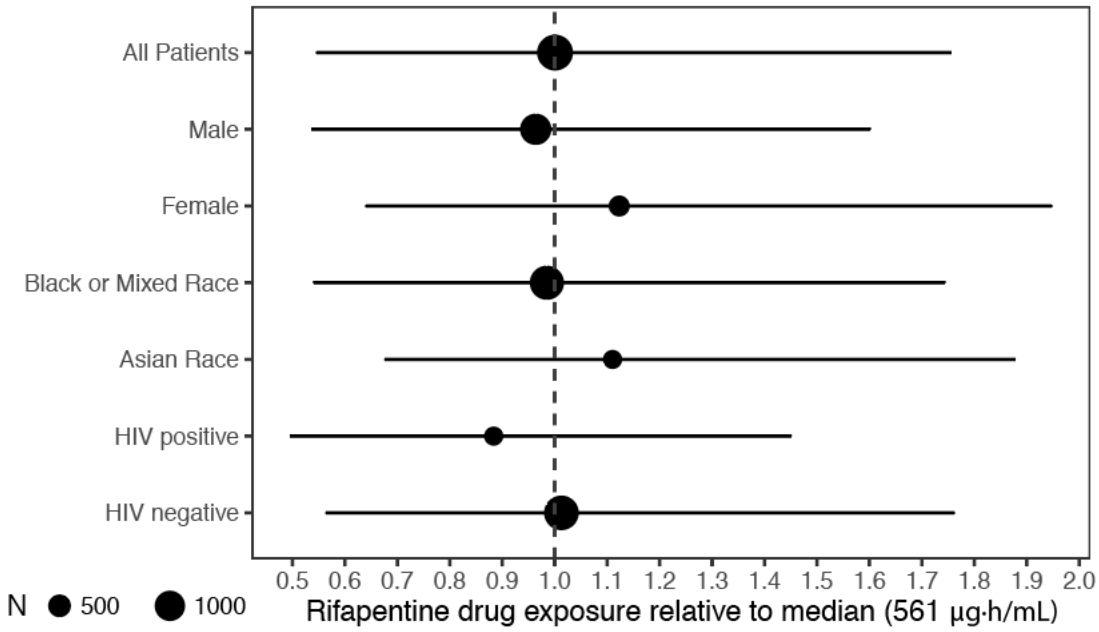

Figure 2-3 Forest plot of rifapentine exposures stratified by significant covariates, female sex, Asian race, and HIV seropositivity

Rifapentine exposure relative to median is shown. Range corresponds to 2.5th and 97.5th percentiles of relative rifapentine exposure. Point size is proportional to the number of participants in that subpopulation.

Body weight was statistically significant on apparent clearance (P<0.001), however apparent clearance only changed by 2.6% [34%] for every 10 kg change in body weight, a clinically insignificant effect size that explained little of the variability in clearance and did not appreciably change individual clearances (Supplemental Figure 2-3A). Additionally, individual clearance and weight had a weak relationship, R^2=0.0088 (Supplemental Figure 2-3B). Ultimately, the effect was removed from the final model for parsimony.

The raw pharmacokinetic profiles stratified by HIV status can be seen in Supplemental Figure 2-4A, along with box plots of model calculated AUCs stratified by HIV status in Supplemental Figure 2-4B where HIV seropositive patients had a median decrease of 14.6% in $AUC_{0\text{-}24h}$ relative to HIV-negative participants. HIV-coinfection significantly increased apparent clearance by 10% [22.8%] relative to HIV-negative participants (P<0.01).

In total, the three covariates, HIV status, sex, and race explain 25% of the variance in bioavailability and 15% in apparent clearance.

Model Evaluation and Validation

The goodness of fit plots and VPC of the basic structural model (built with training cohort data alone) shows that the model predicted the analysis cohort raw data well (Supplemental Figure 2-2A). Furthermore, we show that model-predicted concentrations matched the raw data of the validation cohort, which was not used in model development (Supplemental Figure 2-2B). After model validation, data from both cohorts were pooled, and parameters were re-estimated (Supplemental Table 2-1). VPCs of the final pharmacokinetic model for rifapentine and its metabolite are shown in Figure 2-4.

The final rifapentine pharmacokinetic structural model is shown in Supplemental Figure 2-1, and final bootstrap parameter estimates and confidence intervals in Table 2-2.

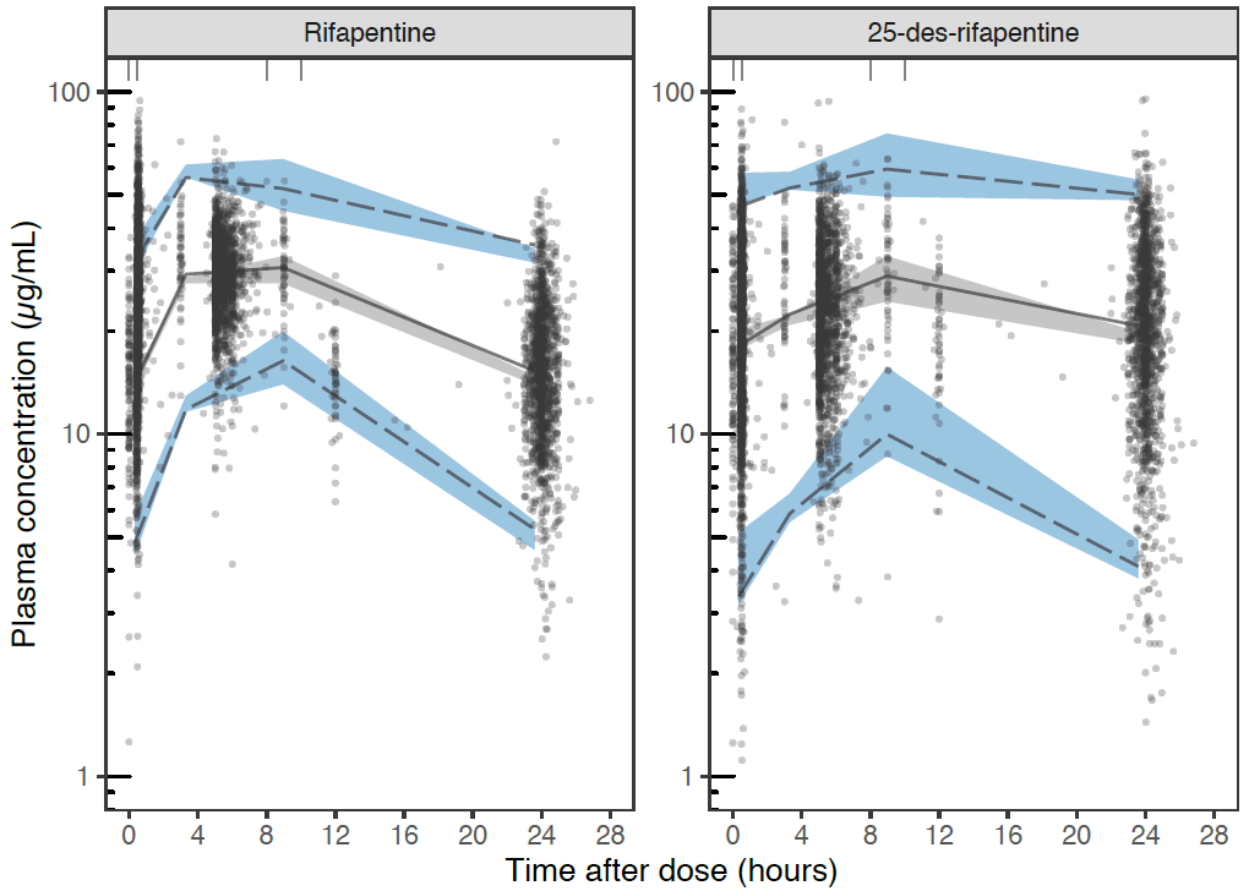

Figure 2-4 Prediction corrected visual predictive check of total cohort shows reasonable model fit

Points show observed concentration, solid black line show median of the observed data, dashed black lines show the 5th and 95th percentile of the observed data, shaded areas show 95% confidence interval of the 5th, median, and 95th percentile of model predicted simulations.

Pharmacokinetic-Safety Analysis

Higher rifapentine $AUC_{0\text{-}24h}$ or C_{max} were associated with a decreased risk for death (Odds Ratio, 0.50 for every 100 μg·h/mL increase in $AUC_{0\text{-}24h}$; 95% CI, 0.27 – 0.87 | OR, 0.31 for every 10 μg/mL increase in C_{max}; 95% CI, 0.09 – 0.91). Overall mortality, however, is low, 7/1681 in the safety population. Other safety outcomes were not significantly associated (threshold of $P < 0.05$) with rifapentine exposure (Figure 2-5 and Supplemental Table 2-2). Participants missing PK sampling in the safety population were more likely to have any grade 3 or higher adverse events, 27/93 (29.0%), compared to participants with PK sampling, 251/1580 (15.8%). Participants without pharmacokinetic sampling had a higher proportion of premature discontinuations of the assigned regimen in the microbiologically eligible population, 53/67 (79%), compared to participants with PK sampling, 38/1508 (2.5%).

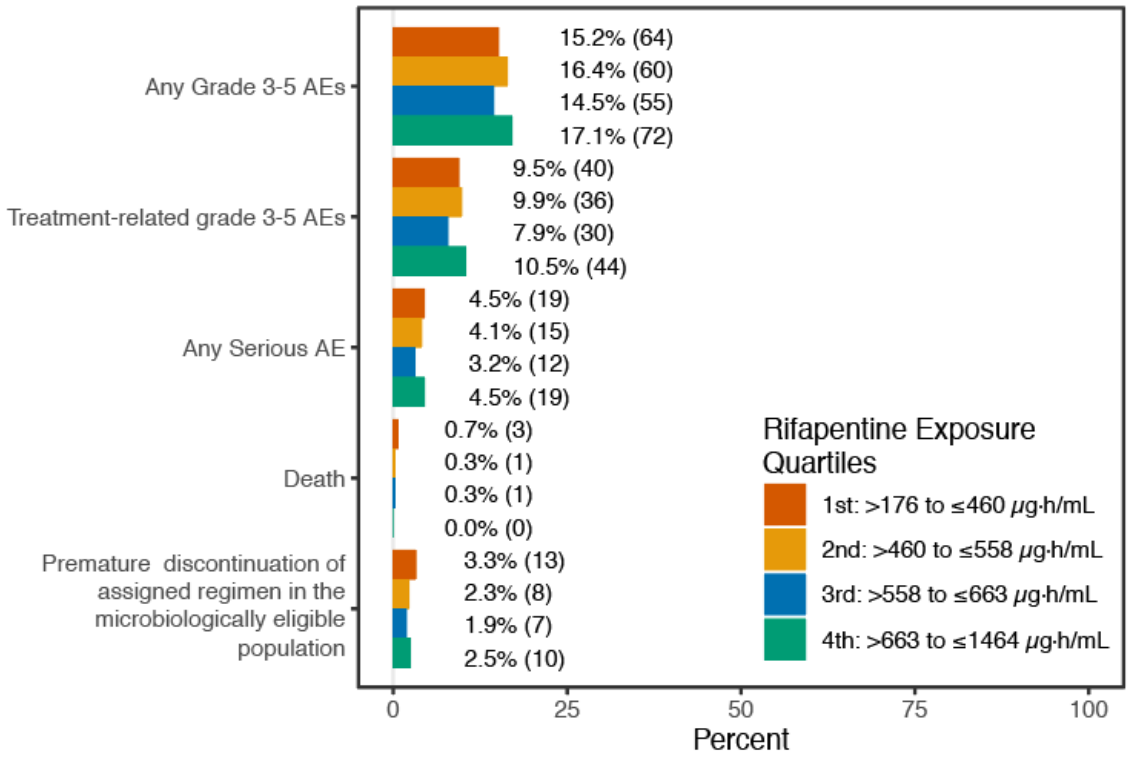

Figure 2-5 Rifapentine exposures were not associated with any predefined safety outcomes

Bars shows percentage of participants with safety outcomes by quartiles of rifapentine exposure. Tolerability was defined as premature discontinuation of the assigned regimen for any reason other than microbiological ineligibility. Participants without pharmacokinetic sampling were excluded from this figure. Percentages are calculated from the safety population for all safety outcomes except tolerability, which was calculated from the microbiologically eligible population.

Dosing Simulations

A 1200 mg flat dose only resulted in 47.3% (748/1580) of S31/A5239 participants achieving rifapentine exposures above the 570 µg·h/mL target. Importantly, some subpopulations had lower proportions: 45.7% of Black participants, 40.2% of male participants, and 30.2% of HIV seropositive participants achieved the 570 µg·h/mL exposure target. Combinations of these risk factors were at higher risk for low rifapentine exposure where only 16.2% of male and HIV seropositive participants achieved the target exposure. Simulations of two dosing strategies were compared to the observed flat 1200 mg dose, (1) flat 1500 mg dose, (2) flat 1800 mg dose (Figure 2-6). Further flat dosing simulations with the S31/A5349 participant population demonstrate that participants would benefit from higher doses where 70.7% and 80.8% of participants would achieve the target exposure with 1500 and 1800 mg rifapentine (Figure 2-6).

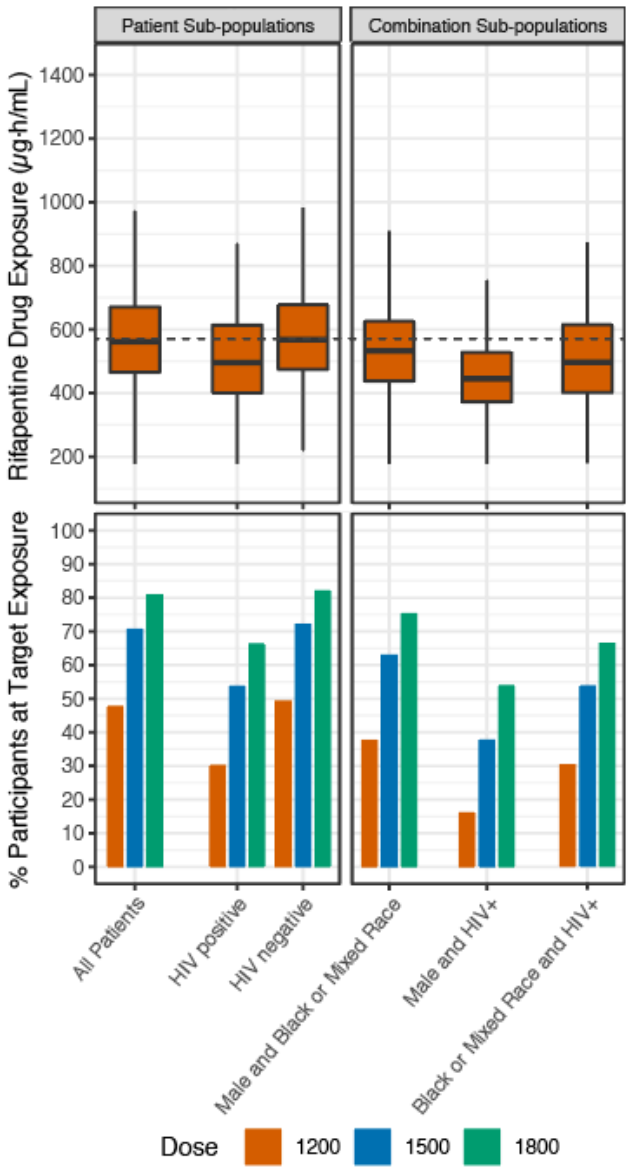

Figure 2-6 HIV seropositive, male and black or mixed race, male and HIV seropositive, and black or mixed race and HIV seropositive participants were at highest risk for low drug exposure with the flat 1200 mg dose

Top: Box plots represent the observed 1200 mg dose, model-derived, steady state $AUC_{0\text{-}24h}$ of participant subpopulations. Dashed line is the 570 µg·h/mL target exposure. **Bottom:** Bar graphs represent the percentage of the subpopulation achieving the 570 µg·h/mL target exposure at 1200, 1500, and 1800 mg doses. In the left panels, participants are stratified by single risk factors and in the right panels, stratified by combinations of risk factors.

Discussion

The study described here represents the largest single-trial analysis of rifapentine population pharmacokinetics to date. Considering the recent WHO rapid communication which recommended the new 4-month 2HPZM/2HPM regimen as a possible alternative to the 6-month 2HRZE/4HR regimen for the treatment of DS-TB[17] and our S31/A5349 PKPD analysis which identified rifapentine exposure as the single most important predictor for treatment success, further optimizing of the dosing of rifapentine could lead to even higher cure rates and potentially shorter regimens than the currently endorsed rifapentine

and moxifloxacin 4 month regimen. Rifapentine's highly variable PK in this study with $AUC_{0\text{-}24h}$ varying from 117 to 1444 µg·h/mL amongst 1580 participants all receiving a flat 1200 mg daily dose by directly observed therapy underscores the challenges in implementing this novel regimen in pragmatic settings. Although the heterogeneity in exposure is partly due to biochemical properties of rifapentine such as activation of pregnane X[18] receptor, induction of metabolizing enzymes[19,20], and high binding affinity to plasma proteins[14] which are outside the scope of our analysis, we have accounted for 25% of the variance in bioavailability and 15% in apparent clearance by thoroughly characterizing the between subject variability of F, CL, and Vc and their relationships with clinical characteristics and demographic covariates. Our results establish several findings that may help guide rifapentine dosing strategies: 1) the pharmacokinetic, efficacy, and safety data do not support weight-based dosing for rifapentine; 2) male, Black/Mixed race, and participants living with HIV are at higher risk for low exposure, especially intersections of these populations; 3) the data doesn't provide evidence of an exposure-toxicity relationship, and 4) our simulations suggest increasing the flat-dose to 1500 mg or 1800 mg, which will increase the proportion of patients who reach target exposures, especially in patients who are at high risk of low rifapentine exposures (male, Black/Mixed race, and/or participants living with HIV).

Currently, rifapentine is primarily used for the treatment of latent TB and current guidelines recommend weight-based dosing for rifapentine[14], which was not supported in our analysis. In four previously described rifapentine population pharmacokinetic models, weight did not influence rifapentine pharmacokinetics.[5,16,21,22] Furthermore, Savic et. al. supported flat dosing, which was implemented in this trial[5], because body weight did not significantly modulate clearance in the preceding phase II dose ranging trial. Hibma and Radtke et. al. identified a small weight effect of <10% change in CL for every 10kg change in body weight but concluded this effect to be clinically insignificant[16]. Contrarily, Langdon et. al. identified a large 24% increase in CL for every 10 kg increase in body weight although they dosed by weight and did not adjust for dose limiting bioavailability which would have likely decrease the estimated effect size[23]. In this study, with the largest cohort to date, a small weight effect compared to all other studies was observed (2% change in CL for every 10 kg change in body weight). Such a small

change in clearance along with little evidence of dose-limiting toxicity does not justify weight banded dosing.

The covariates selected in this Study 31/A5349 analysis, race, sex, and HIV status, were reported previously by Savic et. al[5]. However, for sex and HIV status Savic previously found sex to be a covariate on apparent clearance and HIV status on F. Our analysis here, found sex on bioavailability and HIV status on clearance to best describe the observed data. In 2008 when study 29/29x was initiated, prevailing WHO guidelines[24] for treating TB and HIV coinfected patients recommended that the priority was to treat TB first and defer ART until after the initial phase of TB treatment unless CD4 count <200/mm^3. In 2010, these guidelines[25,26] were updated to recommend initiating ART as soon as possible. Therefore, HIV seropositive participants in S29/29x were not on ART while 116/133 (87%) S31/A5349 HIV seropositive participants were on efavirenz-based ART prior to PK sampling and therefore had potential for drug-drug interactions. This could explain why HIV status was found to significantly modulate clearance instead of bioavailability in this study. We note that rifapentine exposure in participants taking antiretrovirals other than efavirenz may differ from what we observed.

Our findings with race on F were consistent with previous findings where Black or mixed race have lower F relative to White or Asian race. Savic and other authors have also previously reported that rifapentine administered with a high fat meal increases F by 20.5%. Given that race, geographic site, and type of meal are all confounded with each other, it is challenging to clearly disentangle the contributions of each. S31/A5349 pharmacogenomic data were collected but were not yet available for this study. Pharmacogenomic analysis may bring clarity to the exact contributions of race in modulating rifapentine pharmacokinetics. Previous pharmacogenomic analysis with rifampicin has identified rs4149032 polymorphism of *SLCO1B1* which explained an additional 21% of the between-subject variability in apparent clearance.[27,28] The model reported here may be updated pending pharmacogenomic analyses.

Increasing rifapentine exposure was associated with a decreased risk for death, however there were only 7 deaths in the rifapentine containing arms and no strong conclusions can be made. Other safety outcomes were not associated with rifapentine exposure. Interestingly, participants with missing PK sampling were more likely to have any grade 3 or higher adverse events and premature discontinuation of the assigned regimen. It's possible that participants missing PK sampling had higher exposures and therefore are masking an exposure-safety relationship. However, only 27/278 (9.7%) grade 3 or higher adverse events were missing PK samples and therefore are unlikely to change the overall finding that rifapentine exposures are not associated with any grade 3 or higher adverse events.

Rifapentine with its high between subject variability (31.6% in CL, 32.8% in MTT, and 47.3% in CL_m) and dose-limiting bioavailability means that all subpopulations have the potential for underexposure. Furthermore, we have shown that only 48% of 1580 S31/A5349 participants reached the 570 μg·h/mL target exposure with the 1200 mg dose, with lower proportions in subpopulations at risk for low exposure (Black/mixed race, male, and HIV+). Proportion of participants achieving target exposure drastically improves in all populations with a 1500 or 1800 mg dose, and these higher doses are particularly crucial for male and HIV seropositive participants who are at higher risk for poor outcomes because of low rifapentine exposure (rifapentine regimen: 10/45 [22.2%], rifapentine-moxifloxacin: 2/34 [5.9%]), compared to all other participants (rifapentine regimen: 65/739 [8.8%], rifapentine-moxifloxacin: 43/757 [5.7%]).

The strengths of this study included the exceptionally large study size, diverse racial makeup, breadth of covariates collected, and the remarkable consistency in study implementation across 13 countries and 34 sites. However, there was one major limitation in the analysis. High between subject variability is a well-known issue with rifamycin dosing, and although the study was conducted vigorously and robustly there remains substantial unexplained variability. The three covariates, HIV status, sex, and race only explain 25% of the between subjected variability in bioavailability and 15% in apparent clearance. Pending pharmacogenomic analyses may explain additional variability.

In conclusion, we have modeled the largest rifapentine pharmacokinetic dataset to date. We have previously shown that rifapentine exposure is the single most significant predictor for treatment failure and bacteriological relapse in participants receiving the novel 4-month rifapentine-moxifloxacin regimen. Whereas the 4 month regimen was successful, further optimized dosing may lead to additional advances in cure rates, especially in selected populations, or further treatment shortening broadly.. Our work suggests increasing the flat-dose to 1500 mg or 1800 mg, which will increase the proportion of patients who reach target exposures, especially in patients who are at high risk of low rifapentine exposures (male, Black/Mixed race, and/or participants living with HIV). At these higher doses, toxicity concerns are minimized because we did not identify evidence of increased safety outcomes with increased rifapentine exposure in the trial.

References

1. Aristoff, P. A., Garcia, G. A., Kirchhoff, P. D. & Hollis Showalter, H. D. Rifamycins – Obstacles and opportunities. *Tuberculosis* **90**, 94–118 (2010).
2. Roehr B. FDA approves rifapentine for the treatment of pulmonary tuberculosis.... Food and Drug Administration. J Int Assoc Physicians AIDS Care. 1998 Aug;4(8):19-25. PMID: 11365728.
3. Rosenthal, I. M., Zhang, M., Almeida, D., Grosset, J. H. & Nuermberger, E. L. Isoniazid or Moxifloxacin in Rifapentine-based Regimens for Experimental Tuberculosis? *Am. J. Respir. Crit. Care Med.* **178**, 989–993 (2008).
4. Dorman, S. E. *et al.* Daily Rifapentine for Treatment of Pulmonary Tuberculosis. A Randomized, Dose-Ranging Trial. *Am. J. Respir. Crit. Care Med.* **191**, 333–343 (2015).
5. Savic, R. *et al.* Defining the optimal dose of rifapentine for pulmonary tuberculosis: Exposure-response relations from two phase II clinical trials. *Clin. Pharmacol. Ther.* **102**, 321–331 (2017).
6. Dorman, S. E. *et al.* Substitution of Rifapentine for Rifampin During Intensive Phase Treatment of Pulmonary Tuberculosis: Study 29 of the Tuberculosis Trials Consortium. *J. Infect. Dis.* **206**, 1030–1040 (2012).
7. Burman, W. The Rifamycins: Renewed Interest in an Old Drug Class. 8.
8. Effects of Tuberculosis, Race, and Human Gene SLCO1B1 Polymorphisms on Rifampin Concentrations. https://journals.asm.org/doi/epub/10.1128/AAC.00353-10 doi:10.1128/AAC.00353-10.
9. Pharmacokinetics of Rifapentine at 600, 900, and 1,200 mg during Once-Weekly Tuberculosis Therapy. https://www.atsjournals.org/doi/epdf/10.1164/rccm.200311-1612OC doi:10.1164/rccm.200311-1612OC.
10. Dorman, S. E. *et al.* Four-Month Rifapentine Regimens with or without Moxifloxacin for Tuberculosis. *N. Engl. J. Med.* **384**, 1705–1718 (2021).
11. Dorman, S. E. *et al.* High-dose rifapentine with or without moxifloxacin for shortening treatment of pulmonary tuberculosis: Study protocol for TBTC study 31/ACTG A5349 phase 3 clinical trial. *Contemp. Clin. Trials* **90**, 105938 (2020).

12. Byon, W. *et al.* Establishing Best Practices and Guidance in Population Modeling: An Experience With an Internal Population Pharmacokinetic Analysis Guidance. *CPT Pharmacomet. Syst. Pharmacol.* **2**, 51 (2013).
13. Mould, D. & Upton, R. Basic Concepts in Population Modeling, Simulation, and Model-Based Drug Development-Part 2: Introduction to Pharmacokinetic Modeling Methods. *CPT Pharmacomet. Syst. Pharmacol.* **2**, 38 (2013).
14. Rifapentine (Priftin) [package insert]. Kansas City, KA: Hoechst Mar- ion Roussel, 1998.
15. Munsiff, S. S., Kambili, C. & Ahuja, S. D. Rifapentine for the Treatment of Pulmonary Tuberculosis. *Clin. Infect. Dis.* **43**, 1468–1475 (2006).
16. Hibma, J. E. *et al.* Rifapentine Population Pharmacokinetics and Dosing Recommendations for Latent Tuberculosis Infection. *Am. J. Respir. Crit. Care Med.* **202**, 866–877 (2020).
17. World Health Organization. *Treatment of drug-susceptible tuberculosis: rapid communication*. (World Health Organization, 2021).
18. Shehu, A. I., Li, G., Xie, W. & Ma, X. The pregnane X receptor in tuberculosis therapeutics. *Expert Opin. Drug Metab. Toxicol.* **12**, 21–30 (2016).
19. Williamson, B., Dooley, K. E., Zhang, Y., Back, D. J. & Owen, A. Induction of Influx and Efflux Transporters and Cytochrome P450 3A4 in Primary Human Hepatocytes by Rifampin, Rifabutin, and Rifapentine. *Antimicrob. Agents Chemother.* **57**, 6366–6369 (2013).
20. Induction and autoinduction properties of rifamycin derivatives: a review of animal and human studies. https://ehp.niehs.nih.gov/doi/epdf/10.1289/ehp.94102s9101 doi:10.1289/ehp.94102s9101.
21. Savic, R. M. *et al.* Population Pharmacokinetics of Rifapentine and Desacetyl Rifapentine in Healthy Volunteers: Nonlinearities in Clearance and Bioavailability. *Antimicrob. Agents Chemother.* **58**, 3035–3042 (2014).
22. Zvada, S. P. *et al.* Effects of Four Different Meal Types on the Population Pharmacokinetics of Single-Dose Rifapentine in Healthy Male Volunteers. *Antimicrob. Agents Chemother.* **54**, 3390–3394 (2010).
23. Langdon, G. *et al.* Population Pharmacokinetics of Rifapentine and Its Primary Desacetyl Metabolite in South African Tuberculosis Patients. *Antimicrob. Agents Chemother.* **49**, 4429–4436 (2005).
24. *TB/VIH manuel clinique*. (2005).

25. World Health Organization. *Antiretroviral Threapy for HIV Infection in Adults and Adolescents: Recommendations for a public health approach*. (WHO, 2010).
26. Schutz, C., Meintjes, G., Almajid, F., Wilkinson, R. J. & Pozniak, A. Clinical management of tuberculosis and HIV-1 co-infection. *Eur. Respir. J.* **36**, 1460–1481 (2010).
27. Swaminathan, S. & Ramachandran, G. Role of pharmacogenomics in the treatment of tuberculosis: a review. *Pharmacogenomics Pers. Med.* 89 (2012) doi:10.2147/PGPM.S15454.
28. Chigutsa, E. *et al.* The *SLCO1B1* rs4149032 Polymorphism Is Highly Prevalent in South Africans and Is Associated with Reduced Rifampin Concentrations: Dosing Implications. *Antimicrob. Agents Chemother.* **55**, 4122–4127 (2011).

Supplemental Information

Supplemental Table 2-1 Summary of Pharmacokinetic, Demographic, Clinical, and Safety data

(*) rifapentine and 25-desacetyl rifapentine were measured in each sample. N (%) given for categorical variables and median (95th percentiles) given for continuous variables. (▼) 12 participants were missing aggregate cavity size and disease extent, 3 participants were missing baseline smear grade.

	Training Dataset	Validation Dataset	Validation Dataset 2	Total
PHARMACOKINETIC SAMPLING*				
Total Patients	N=1053	N=462	N=65	N=1580
Intensive Sampling Patients	N=35 (624 samples)	N=18 (324 samples)	N=0 (0 samples)	N=53 (944 samples)
Sparse Sampling Patients	N=1018 (6094 samples)	N=444 (2670 samples)	N=65 (390 samples)	N=1527 (9112 samples)
Below Limit of Quantification	16 samples	8 samples	0 samples	24 samples
Arm 2: 2HPZE/2HP	N=532 (50)	N=220 (48)	N=34 (52)	N=786 (50)
Arm 3: 2HPZM/2HPM	N=521 (50)	N=242 (52)	N=31 (48)	N=794 (50)
DEMOGRAPHIC FACTORS				
Age [years]	30 (17 – 60)	31 (18 – 59)	35 (19 – 56)	31 (17-60)
Male Sex	758 (72.0)	321 (69)	46 (71)	1125 (71)
Height [cm]	167 (151 – 182)	167 (150 – 183)	167 (152 – 189)	167 (151 – 182)
Weight [kg]	53 (41 - 76)	54 (41 – 75.4)	54 (42 – 85.4)	53 (41 -76)
BMI [kg/m2]	18.92 (14.87 – 27.73)	19.08 (15.58 – 27.58)	19.05 (15.53 – 31.46)	19.00 (15.05 – 28.02)
Race				
Black	758 (72)	328 (71)	36 (55)	1122 (71)
Mixed/Multi-racial	160 (15)	73 (16)	27 (42)	260 (16)
Asian	122 (12)	56 (12)	0 (0)	178 (11)
White	13 (1)	5 (1)	2 (3)	20 (1)
CLINICAL FACTORS				
African Clinical Site	770 (73)	336 (73)	63 (97)	1169 (74)
Baseline Chest X-Ray Cavity	772 (73)	325 (70)	47 (73)	1145 (73)
Baseline Chest X-Ray Class ▼				
No cavities	269 (26)	135 (29)	17 (27)	421 (27)
Cavities < 4cm	351 (34)	143 (31)	26 (41)	520 (33)
Cavities ≥ 4cm	424 (41)	182 (40)	21 (33)	627 (40)
Baseline Chest X-Ray Extent ▼				
Lesions < 1/4 thoracic area	182 (17)	90 (20)	16 (25)	288 (18)
Lesions 1/4 to < 1/2 thoracic area	479 (46)	207 (45)	21 (33)	707 (45)
Lesions ≥ 1/2 thoracic area	383 (36)	165 (35)	27 (42)	573 (37)
Baseline Smear Grade ▼				
Negative	39 (4)	18 (4)	6 (9)	63 (4)
Scanty	185 18)	86 (19)	14 (22)	285 (18)
Grade 1	222 (21)	113 (25)	12 (18)	347 (22)
Grade 2	287 (27)	140 (30)	16 (25)	443 (28)
Grade 3	306 (29)	103 (22)	17 (26)	426 (27)
Positive WHO scale not used	13 (1)	1 (0)		14 (1)
Karnofsky Score	90 (70 - 100)	90 (70 - 100)	90 (70 - 100)	90 (70 – 100)
HIV	80 (8)	46 (10)	7 (11)	133 (8)
Diabetes	25 (2)	14 (3)	4 (6)	43 (3)

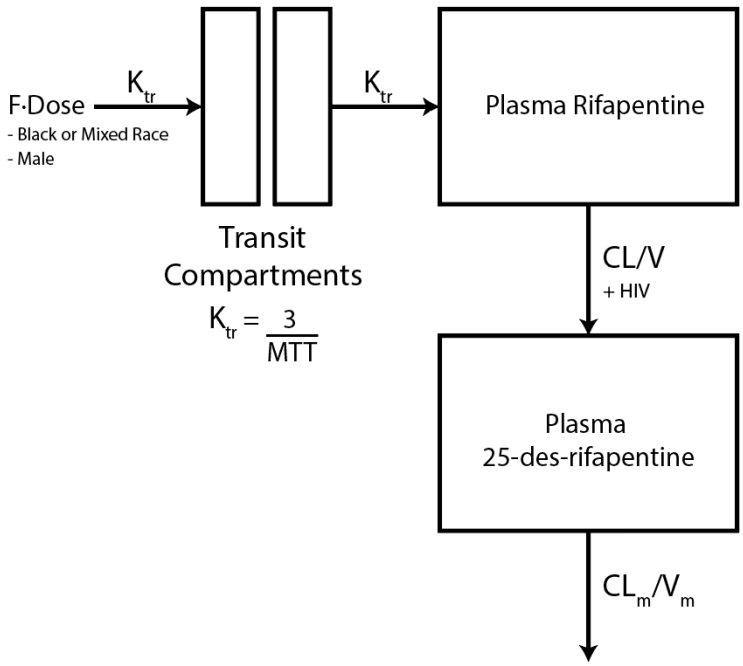

Supplemental Figure 2-1 Rifapentine Structural Pharmacokinetic Model

Pharmacokinetic data were well described with a one compartment model with linear metabolite clearance and two transit compartment delayed absorption. Male sex and Black/Mixed race participants had lower bioavailability, while HIV seropositive participants had higher apparent clearance.

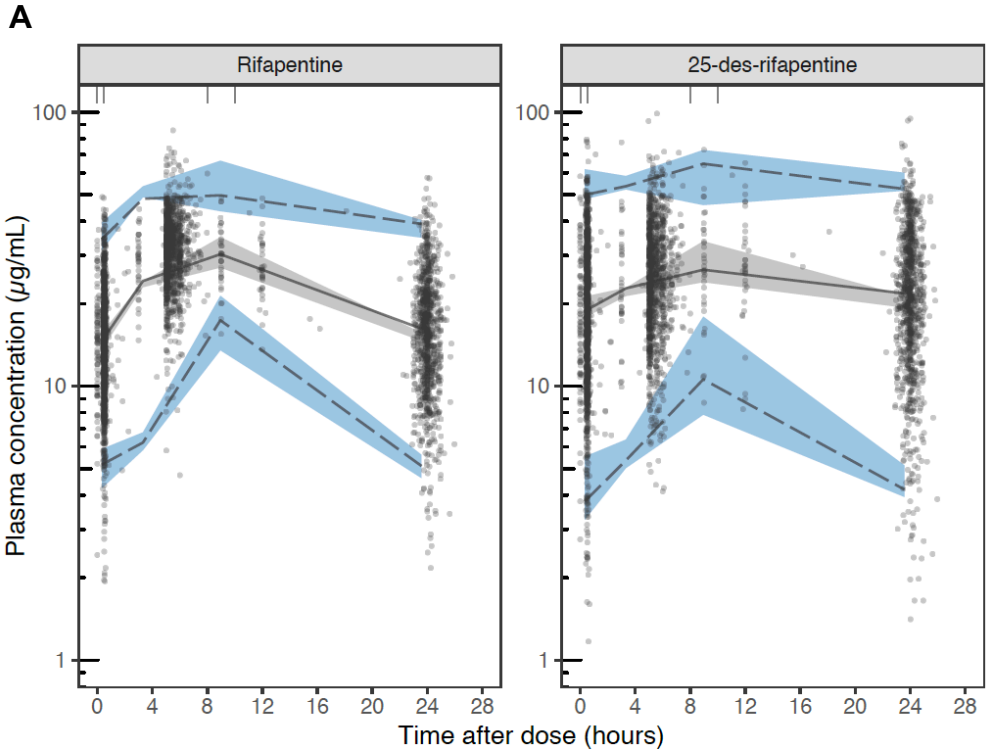

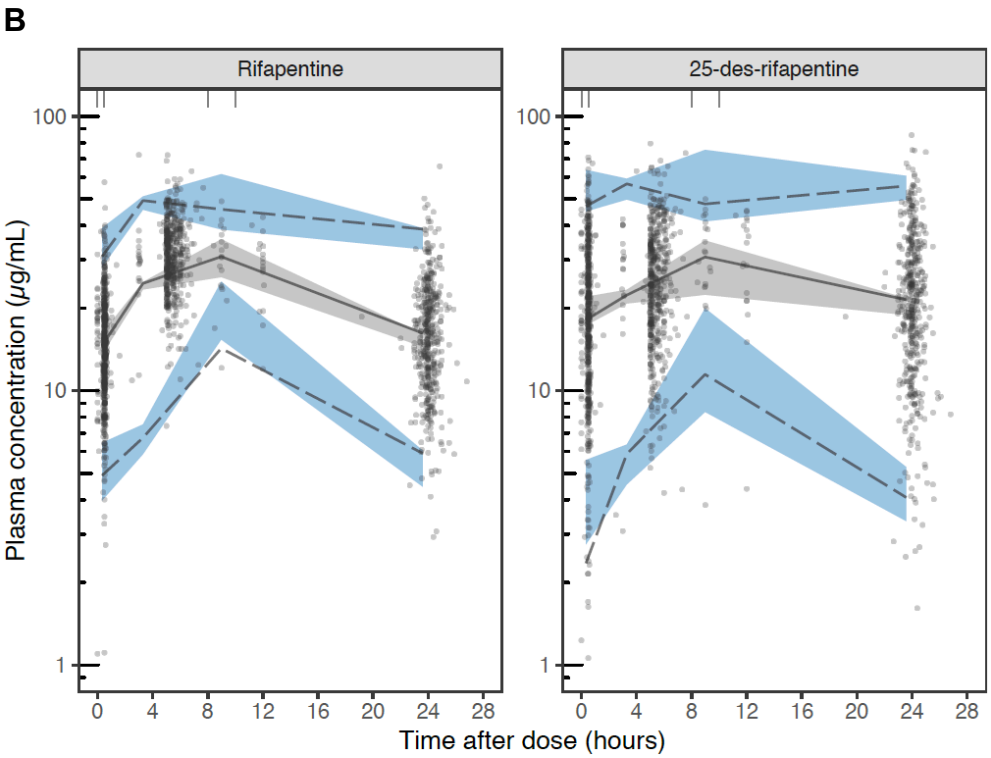

Supplemental Figure 2-2 Prediction Corrected Visual Predictive Checks of (A) Training and (B) Validation Cohorts

Points show observed concentration, solid black line show median of the observed data, dashed black lines show the 5th and 95th percentile of the observed data, shaded areas show 95% confidence interval of the 5th, median, and 95th percentile of model predicted simulations.

Supplemental Table 2-2 Training and Final Model Parameters

Parameters with (*) were fixed.

	Training Model		Final Full Model	
Parameters (units)	**Estimate (%RSE)**	**Between-subject Variability %CV (%RSE)**	**Estimate (%RSE)**	**Between-subject Variability %CV (%RSE)**
CL/F (L/h)	2.22 (1)	27.8 (7)	2.25 (1)	32.4 (4)
V/F (L)	42.9 (3)	--	47.3 (2)	--
MTT (h)	4.04 (4)	35.5 (7)	3.66 (3)	33.8 (9)
CL_m/F_m (L/h)	2.09 (1)	46.8 (4)	2.14 (2)	50.1 (3)
CL_m Box Cox transformation Shape parameter	0.392 (19)	--	0.354 (19)	--
V_m/F_m (L)	10 (3)	--	11.3 (3)	--
F	1*	2.9 (70)	1*	19.9 (8)
F_m	1*	--	1*	--
N Transit Compartments	2*	--	2*	--
Covariates (reference)				
Asian race effect on bioavailability (fraction relative to Black reference)	1.099 (49)	--	1.092 (28)	--
Female effect on bioavailability (fraction relative to male reference)	1.159 (18)	--	1.151 (15)	--
HIV infection effect on clearance (relative to HIV-uninfected reference)	1.091 (29)	--	1.10 (21)	--
Variability (units)				
Correlation CL-F	--	-0.99 (32)	--	0.382 (14)
Correlation CL-CLm	--	0.707 (7)	--	0.741 (5)
Correlation F-CLm	--	-0.707 (32)	--	0.20 (20)
Residual Error (units)				
Proportional Error, parent (%)	16.8 (4)	--	15.9 (4)	--
Additive Error, parent (ug/mL)	0.25*	--	0.25*	--
Proportional Error, metabolite (%)	15.5 (5)	--	14.9 (4)	--
Additive Error, metabolite (ug/mL)	0.25*	--	0.25*	--

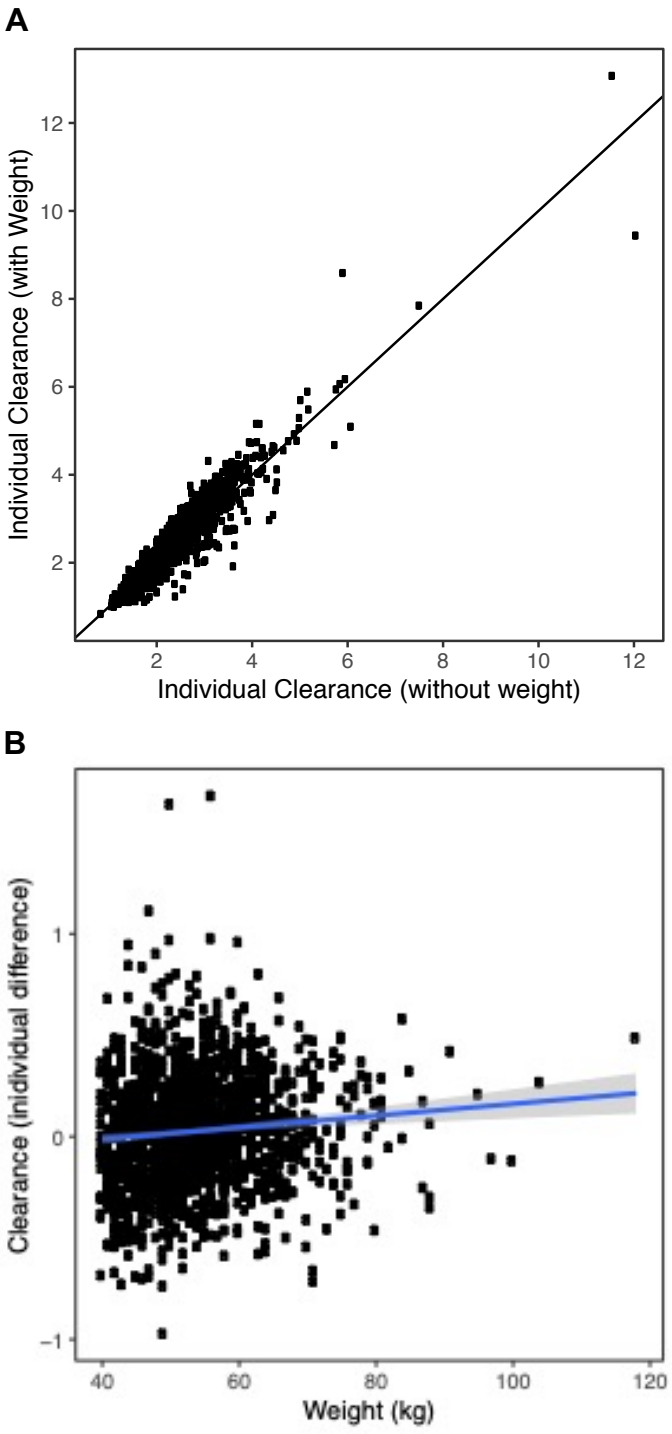

Supplemental Figure 2-3 Body weight does not significantly modulate rifapentine clearance

(A) Model derived individual clearance accounting for weight (y-axis) and not accounting for weight (x-axis). There is little change in clearance for individual participants. **(B)** Weak relationship between individual differences in clearance and weight, R^2=0.0088.

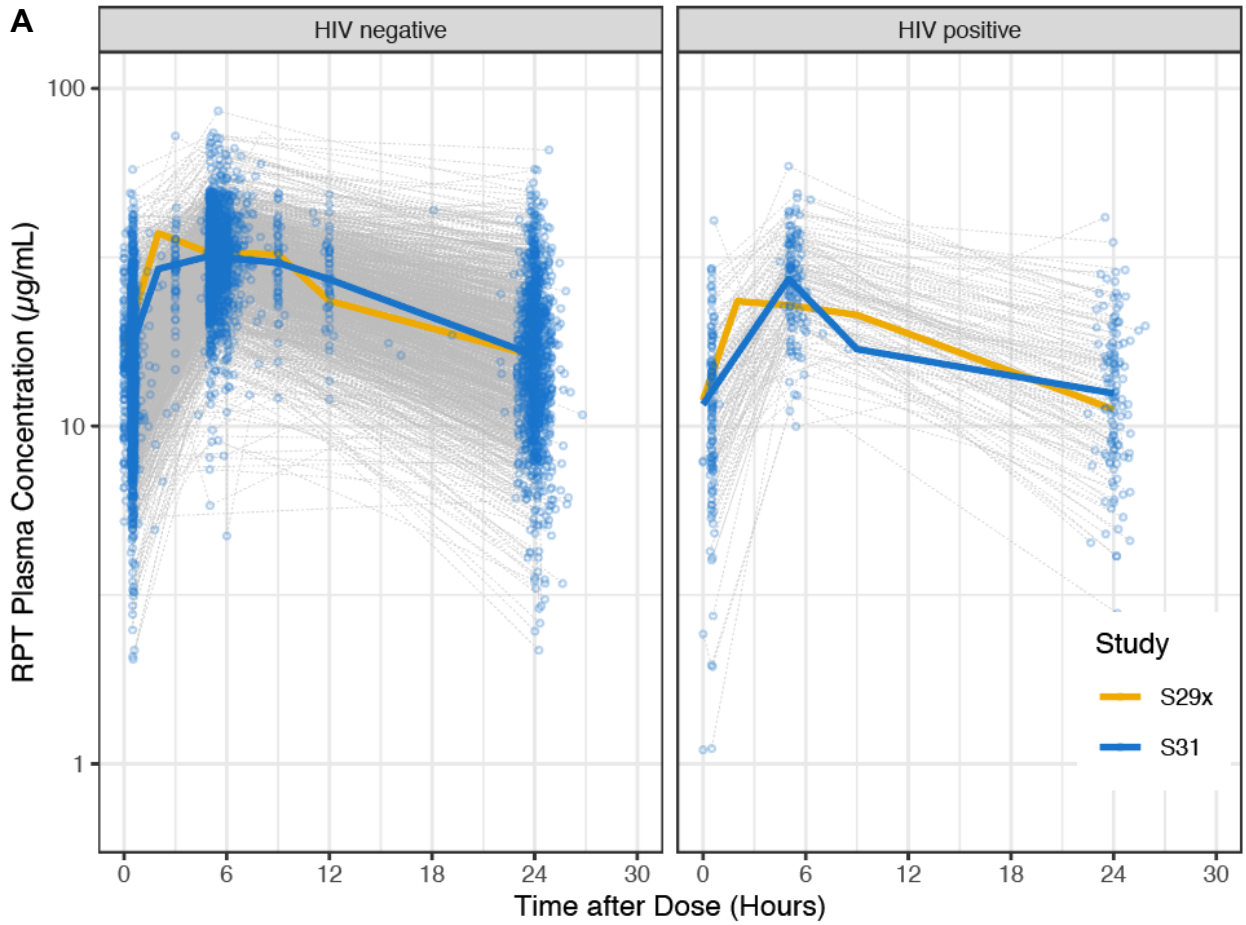

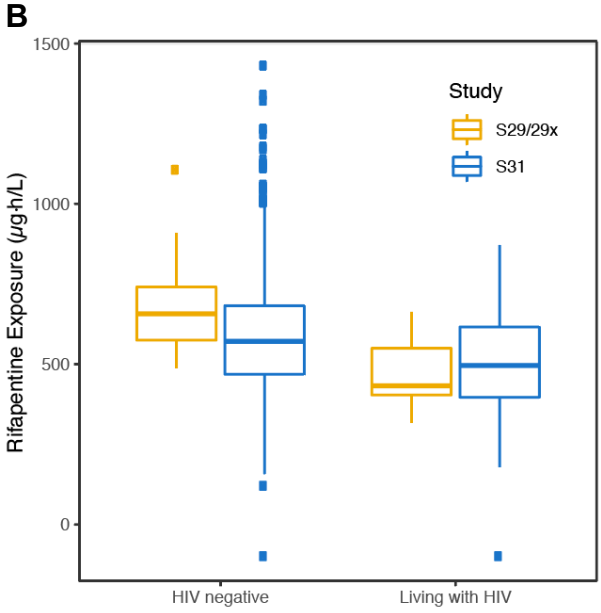

Supplemental Figure 2-4 HIV seropositive participants have lower exposure **(A)** Raw rifapentine pharmacokinetic profiles stratified by HIV status in S31/A5349 and S29/29x. S29/29x found the effect on bioavailability, in S31/A5349 we found the effect on apparent clearance, potentially due to S31/A5349 participants taking efavirenz based ART, which is also a potent CYP inducer. **(B)** Regardless of the effect on bioavailability or clearance, the exposures of HIV seropositive participants are comparable between the two studies.

Supplemental Table 2-3 Odds Ratios of Safety Outcomes for increase in Rifapentine Exposure

Odds ratios are adjusted for treatment group and are reported for every 100 µg·h/mL increase in rifapentine $AUC_{0\text{-}24h}$ and every 10 µg/mL increase in rifapentine C_{max}. The only safety outcome associated with an increase in rifapentine exposure is death (highlighted in green), but overall mortality is low 7/1681 and it is inversely correlated; higher rifapentine exposures have a lower probability of death.

Safety Outcome	Odds Ratio	95% CI	p-value
Rifapentine $AUC_{0\text{-}24h}$ (for every 100 µg·h/mL)			
Grade 3 or higher adverse event	1.03	0.95 – 1.10	0.51
Treatment-related grade 3 or higher adverse event	1.01	0.92 – 1.10	0.86
Any serious adverse event	0.94	0.81 – 1.07	0.34
Any grade 3 or higher adverse event within 28 weeks after randomization	1.03	0.96 – 1.10	0.45
Any adverse event resulting in discontinuation of assigned treatment	0.98	0.77 – 1.20	0.82
Premature discontinuation of assigned regimen for any reason in the microbiologically eligible population	0.97	0.85 – 1.09	0.59
ALT or AST level ≥5×ULN	1.07	0.86 – 1.29	0.53
ALT or AST level ≥10×ULN	0.95	0.62 – 1.36	0.79
Serum total bilirubin level ≥3×ULN	1.06	0.89 – 1.23	0.51
Hy's law criteria of ALT or AST level ≥3×ULN plus serum total bilirubin level ≥2×ULN	1.19	0.92 – 1.48	0.17
Neutropenia	1.01	0.99 – 1.03	0.19
Death	0.50	0.27 – 0.87	0.012
Rifapentine C_{max} (for every 10 µg/mL)			
Grade 3 or higher adverse event	1.03	0.88 – 1.20	0.72
Treatment-related grade 3 or higher adverse event	0.99	0.81 – 1.20	0.93
Any serious adverse event	0.84	0.62 – 1.12	0.24
Any grade 3 or higher adverse event within 28 weeks after randomization	1.02	0.87 – 1.12	0.82
Any adverse event resulting in discontinuation of assigned treatment	0.78	0.46 – 1.27	0.33
Premature discontinuation of assigned regimen for any reason in the microbiologically eligible population	0.78	0.59 – 1.03	0.08
ALT or AST level ≥5×ULN	1.13	0.71 – 1.73	0.59
ALT or AST level ≥10×ULN	0.87	0.35 – 1.89	0.74
Serum total bilirubin level ≥3×ULN	1.17	0.82 – 1.63	0.36
Hy's law criteria of ALT or AST level ≥3×ULN plus serum total bilirubin level ≥2×ULN	1.61	0.95 – 2.56	0.07
Neutropenia	1.03	0.98 – 1.07	0.21
Death	0.31	0.09 – 0.91	0.032

Chapter 3 - Moxifloxacin Population Pharmacokinetics in the Novel 4-Month Rifapentine-Moxifloxacin Regimen

Introduction

Moxifloxacin is a fluoroquinolone of great interest for tuberculosis treatment; it is first line for multi-drug resistant tuberculosis[1] (MDR-TB) and has been investigated for the potential to reduce treatment durations from 6 months to 4 months for drug susceptible tuberculosis (DS-TB). It has demonstrated potent activity against M. tuberculosis in preclinical[2] and clinical studies[3,4], where the single substitution of ethambutol for moxifloxacin increases early bactericidal activity and improves time to culture conversion. However, recent DS-TB phase III trials (OFLOTUB[5], ReMOX[6], and RIFAQUIN[7]) investigating single substitutions of isoniazid or ethambutol for a fluoroquinolone have all failed to achieve acceptable cure rates after reducing treatment duration to 4 months. Nevertheless, moxifloxacin remains of great interest due to good penetration into cellular lesions of tuberculosis granulomas in animal models[8], its well-documented and well-tolerated safety profile when used for extended periods of time in adults and children (7 years and above)[9–13], and is also widely available due to its approval in other indications[14].

Moxifloxacin is rapidly absorbed, with the majority of drug reaching systemic circulation within 2-3 hours. It has a long half-life of 12 ± 1.3 hours, which means drug is not completely eliminated before administration of the next dose (24h), important in preventing selection for antibiotic resistance. Moxifloxacin is a p-glycoprotein substrate with approximately 20% excreted unchanged renally, and 25% through feces. The remaining is metabolized by sulfotransferases and glucuronosyltransferases. Coadministration of moxifloxacin with rifapentine (or other rifamycins) decreases moxifloxacin exposure due to enzyme and transporter induction.[14]

Recently, the latest moxifloxacin investigation in DS-TB, Tuberculosis Trials Consortium study 31/ACTG A5349 (S31), an international, multicenter, randomized, open-label, phase III, noninferiority trial,

successfully demonstrated noninferiority of the short course 4-month regimen of high dose rifapentine, moxifloxacin, isoniazid, and pyrazinamide when compared to the 6-month standard of care regimen of rifampicin, isoniazid, pyrazinamide, and ethambutol[15,16]. Notably, S31/A5349 is the first phase III anti-tuberculosis agent trial that had near study-wide pharmacokinetic sampling for all drugs offering the first opportunity to build robust population pharmacokinetic models and characterize subpopulations at risk of low exposure with the largest single cohort and richest dataset in the history of TB trials.

Methods

Sample Collection and Assays

Samples were collected between the 2 week and 8 week visit windows, after enzyme induction reached steady state. Intensive sampling was performed on a small number of participants with samples taken at 0.5, 3, 5, 9, 12, and 24 hours. The study aimed to collect intensive pharmacokinetic samples from 53 participants for 85% power to detect up to an 8% difference in apparent clearance assuming 20% variance between individuals. The remaining participants were sampled sparsely with time points at 0.5, 5, and 24 hours. Plasma concentrations of moxifloxacin were determined using validated high-performance liquid chromatography mass spectroscopy assays.

Modeling Software and Methods

Pharmacokinetic data were randomly split into an analysis cohort for model development and validation cohort for model validation, where one-third of the data was conserved for the validation cohort and covariates (clinical site and HIV) were balanced between cohorts. Moxifloxacin plasma concentrations were analyzed using nonlinear mixed-effects modeling with NONMEM version 7.41 (ICON Development Solutions). Population pharmacokinetic model building followed standard procedures by first characterizing the base structural model and estimating typical pharmacokinetic parameters using a first-order conditional estimation method with ε–η interaction (FOCE INTER).[17] Interindividual variability, which describes the observed population variability in pharmacokinetic parameters, consists of individual η‘s that are assumed to follow a normal distribution and the variance of this distribution is estimated.

The structural models tested included one- and two-compartment models with first-order elimination. Different absorption models were explored, such as first-order absorption or a sequence of zero- and first-order absorption incorporating either lag times or transit compartment absorption.

Covariates, including age, sex, African/non-African site, race, weight, BMI, presence of cavitation, aggregate cavity size, extent of disease on chest radiograph, smear grade, HIV status, diabetes history and karnofsky score, were evaluated for potential inclusion as covariates on the PK parameters: bioavailability (F1), clearance (CL), volume of the central compartment (V_c), intercompartmental flow rate (Q), and volume of the peripheral compartment (V_P). Covariate effects were selected through a stepwise procedure with forward selection (P<0.05) and backward elimination (P<0.01). Final inclusion of covariates was based on statistical significance, scientific plausibility, and clinical relevance.[18]

Model development was guided by assessment of goodness of fit plots, condition number, and the likelihood ratio test. Simulation based diagnostics (e.g., visual predictive checks [VPCs] and bootstraps) were used for model development and evaluation.

R software (version 3.5.2; R Foundation for Statistical Computing) was used for all data management, analyses, and graphical visualization. The xpose (version 0.4.4) and vpc (version 1.0.1) packages were used for visual diagnostics. Nonparametric bootstrap and covariate modeling were performed with Perl-speaks-NONMEM (version 4.7.0).

Safety Outcomes and Analysis

The primary safety outcome in the trial was any grade 3 or higher adverse events during the on-treatment period (the time during which the participants were receiving the trial medications and up to 14 days after the last dose). Additional analyses were performed with treatment related grade 3 or higher adverse events, severe adverse events, tolerability, and death. Tolerability was defined as discontinuation of the assigned treatment for any reason other than microbiological ineligibility. Secondary safety outcomes, increased ALT and AST levels were investigated as well for a pharmacokinetic-toxicity relationship. See

Table 1 for counts of each of the safety outcomes. Moxifloxacin $AUC_{0\text{-}24h}$ and C_{max} were analyzed with independent logistic regressions with each of the safety outcomes described above.

Results

Study Design and Dataset

The S31/A5349 moxifloxacin pharmacokinetic data were received from the US Centers for Disease Control on July 20, 2020, and consisted of 744 participants, an additional cohort of data with 43 participants were received on June 30, 2021. All participants received 2HPZM/2HPM; 8 weeks of daily 400 mg moxifloxacin, 1200 mg rifapentine, 600 mg isoniazid, and weight-based pyrazinamide followed by 9 weeks of daily moxifloxacin, rifapentine, and isoniazid. 26 participants were intensively sampled and 741 participants were sparsely sampled. In total, 231 intensive samples and 2146 sparse samples were collected and measured for moxifloxacin plasma concentrations (see raw data in Figure 3-1). Participant demographics, clinical factors, and demographics were similar across the model development and validation datasets (Table 3-1 and Supplemental Table 3-1). There were only 9 samples reported as below the limit of quantification (lower limit of quantification=0.04 μg/mL), and were fixed to half the LLOQ concentration, 0.02 μg/mL.

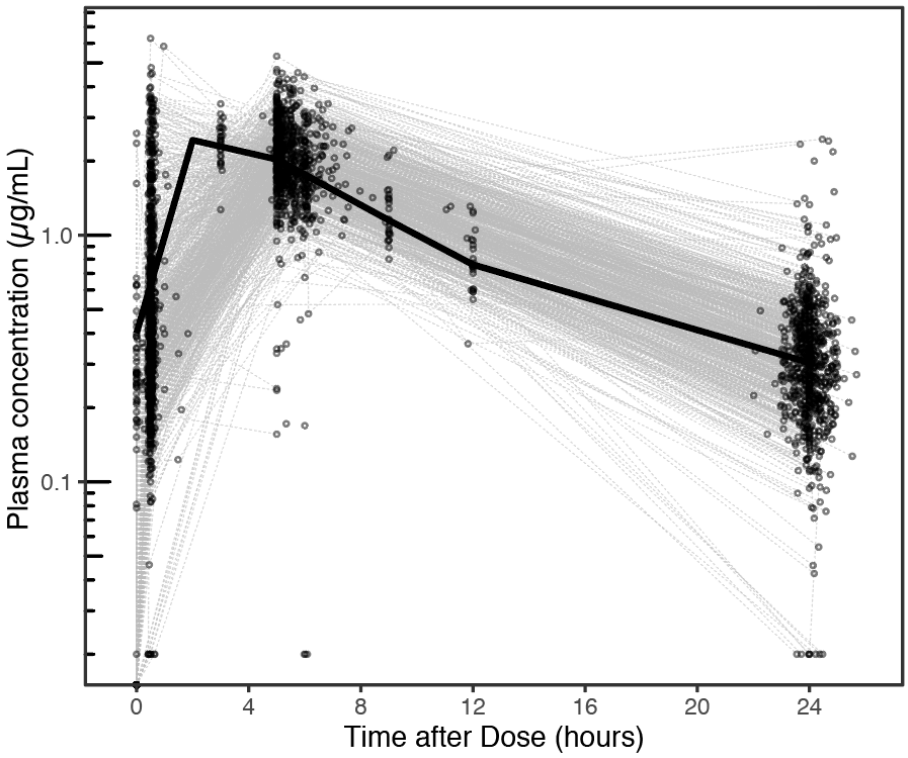

Figure 3-1 Moxifloxacin Raw Pharmacokinetic Data
Circles represent individual samples and solid lines represent medians.

Table 3-1 Summary of Moxifloxacin Pharmacokinetic, Demographic, Clinical, and Safety Data
n (%) given for categorical measures and median (95th percentiles) given for continuous measures

	Arm 3 2HPZM/2HPM	Missing
PHARMACOKINETIC SAMPLING		
Total Participants	N=787	--
Intensive Sampling Participants	N=26 (228 samples)	--
Sparse Sampling Participants	N=761 (2251 samples)	--
Below Limit of Quantification	9 samples	--
DEMOGRAPHIC FACTORS		
Age [years]	30 (17-60)	0 (0)
Male Sex	559 (71)	0 (0)
Height [cm]	167 (151 - 183)	0 (0)
Weight [kg]	53 (41 -76)	0 (0)
BMI [kg/m2]	18.99 (15.23 – 28.48)	0 (0)
Race		0 (0)
Black	551 (70)	
Asian	133 (17)	
Mixed/Multi-racial	91 (12)	
White	12 (2)	
CLINICAL FACTORS		
African Clinical Site	577 (73)	0 (0)
Baseline Chest X-Ray Cavity	572 (73)	0 (0)
Baseline Chest X-Ray Class		7 (0.9)
No cavities	206 (26)	
Cavities < 4cm	275 (35)	
Cavities ≥ 4cm	299 (38)	
Baseline Chest X-Ray Extent		7 (0.9)
Lesions < 1/4 thoracic area	151 (19)	
Lesions 1/4 to < 1/2 thoracic area	366 (47)	
Lesions ≥ 1/2 thoracic area	263 (34)	
Baseline Smear Grade		1 (0.1)
Negative	24 (3)	
Scanty	152 (19)	
Grade 1	168 (21)	
Grade 2	225 (29)	
Grade 3	211 (27)	
Karnofsky Score	90 (70 - 100)	0 (0)
HIV	65 (8)	0 (0)
History of Diabetes	29 (4)	0 (0)
SAFETY OUTCOMES		
Number of Patients (Safety Population)	846	--
Grade 3 or higher adverse event	159 (18.8)	--
Treatment-related grade 3 or higher adverse event	109 (12.9)	--
Any serious adverse event	37 (4.4)	--
Death	3 (0.4)	--
Any adverse event resulting in discontinuation of assigned treatment	16 (1.9)	--
Any grade 3 or higher adverse event within 28 weeks after randomization	194 (22.9)	--
ALT or AST level ≥5×ULN	16 (1.9)	--
ALT or AST level ≥10×ULN	4 (0.5)	--
Serum total bilirubin level ≥3×ULN	28 (3.3)	--
Hy's law criteria of ALT or AST level ≥3×ULN plus serum total bilirubin level ≥2×ULN	10 (1.2)	--
Premature discontinuation of assigned regimen for any reason in the microbiologically eligible population	55/791 (7.0)	--

Pharmacokinetic Model

The two-compartment model with linear clearance and transit compartment absorption best described the observed data. In the final model, the steady state apparent CL of moxifloxacin was estimated to be 16.7 L/h (relative standard error: 1.5%). In Figure 3-1, moxifloxacin PK profiles of S31/A5349 are compared to study NC-002 (NCT01498419), where moxifloxacin was administered without rifamycins and the steady state apparent CL was estimated to be 12.6 L/h. The V_c was estimated as 128 L (2.6%), intercompartmental flow rate (Q) was 4.59 L/h (6.3%), and V_p was 349 L (25.3%) in the typical reference patient (male, non-diabetic, and HIV-uninfected). Two transit compartments best described the absorption phase with a mean transit time (MTT) of 2.38 hours. Interindividual variability was supported on MTT=46.1% (11.6%) and CL=5.7% (9.8%). A box cox transformation for MTT improved model fit and was necessary as MTT η distribution was not normal. Proportional error 27.1% (4.7%) alone was sufficient to describe the data, additive error did not improve model fit. The final moxifloxacin pharmacokinetic structural model is shown in Supplemental Figure 3-1, and final bootstrap parameter estimates and confidence intervals in Table 3-2. All pharmacokinetic parameters were well estimated, with low relative standard errors (<30%).

Table 3-2 Bootstrap of Final Model
Standard errors are reasonable, demonstrating excellent model fit. Bioavailability (F) was fixed to 100% and number of transit compartments was fixed to 2.

	Final Full Model		
Parameters (units)	**Median**	**95% Confidence Interval**	**Relative Standard Error (%)**
CL/F (L/h)	16.7	16.24 – 17.26	1.45
V/F (L)	128.2	121.2 – 134.8	2.63
MTT (h)	2.38	2.19 – 2.49	3.06
MTT Box Cox transformation Shape parameter	-0.882	-0.353 – -0.995	15.3
Q (L/h)	4.59	3.93 – 5.19	6.34
V_p (L)	349	238 – 654	25.3
Covariates (reference)			
Diabetes effect on CL (relative to non-diabetic reference)	+27.5%	16.3% – 40.5%	20.7
HIV+ effect on CL (relative to HIV- reference)	+24.3%	16.6% – 33.2%	16.7
Female effect on V_c (relative to male reference)	-17.1%	-11.5% – -21.9%	14.8
Female effect on bioavailability (relative to male reference)	+19.1	12.3% – 24.6%	16.1
Between Subject Variability (units)			
Between-subject Variability in CL (% CV)	5.7	4.4 – 6.6	9.77
Between-subject Variability in MTT (% CV)	46.1	39.2 – 65.5	11.6
Residual Error (units)			
Proportional Error (%)	27.1	24.3 – 29.7	4.65

Impact of Covariates on Pharmacokinetics

Moxifloxacin bioavailability and volume of distribution of the central compartment was strongly influenced by sex (univariate P < 0.001). In the final model, females had a 19.1% (16.1%) increase in bioavailability and a 17.1% (14.8%) decrease in V_c relative to males. A female effect on bioavailability was needed to account for the differences in exposure (Figure 3-2), while the effect on V_c was needed to account for differences in C_{max} (Supplemental Figure 3-3).

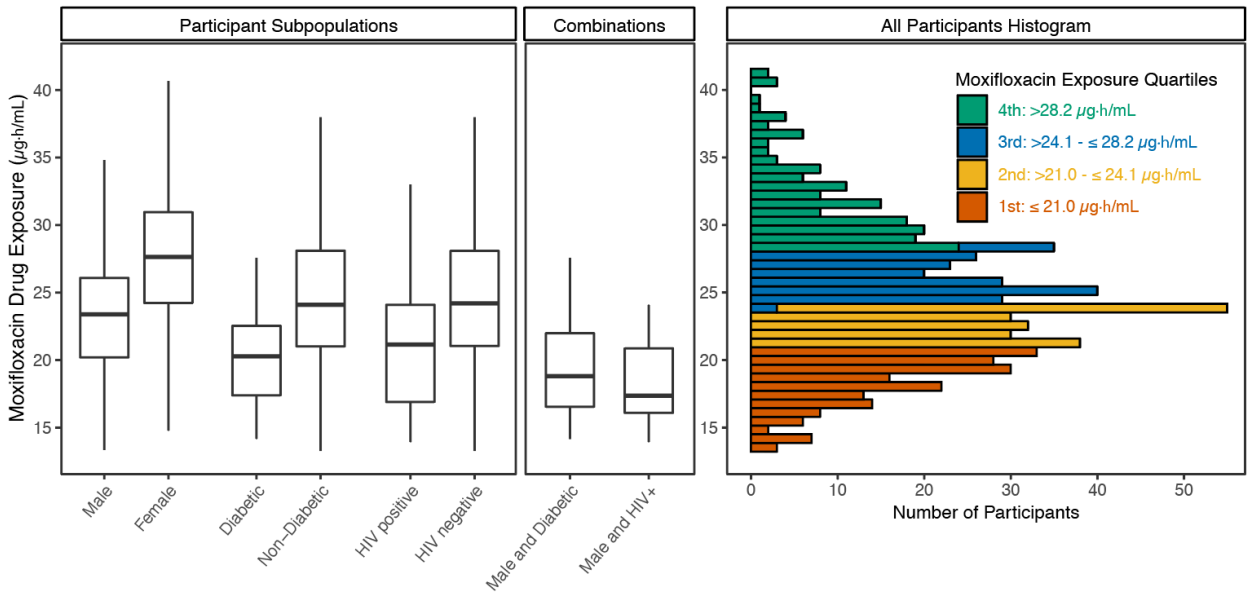

Figure 3-2 Male participants and participants living with HIV or diabetes were at risk for low moxifloxacin exposure
Combinations of these low exposure subpopulations were at higher risk for low exposure.

The raw pharmacokinetic profiles stratified by HIV status can be seen in Supplemental Figure 3-4, along with box plots of model derived AUCs stratified by HIV status in Figure 3-2 where the decrease in exposure in HIV seropositive participants can clearly be seen compared to HIV negative participants. HIV-positive status was significant on apparent clearance (univariate P<0.01), an increase of 24.3% (16.7%) in HIV-positive participants relative to HIV-negative participants.

Diabetes status was also significant on apparent clearance (univariate P<0.01), an increase of 27.5% (20.7%) in diabetic participants relative to non-diabetic participants. The raw pharmacokinetic profiles

stratified by diabetes status can be seen in Supplemental Figure 3-5A, and the large difference in exposure can be seen in Figure 3-2. This difference is independent of weight, as seen in Supplemental Figure 3-5B, diabetic participants had higher clearance irrespective of weight. Weight was statistically significant on bioavailability, but with little clinical or physiological justification for its impact on bioavailability, it was removed for parsimony.

Model Evaluation and Validation

The goodness of fit plots and VPC of the basic structural model (built with training cohort data alone) shows that the model predicted the analysis cohort raw data well: the median, 2.5th and 97.5th percentiles of raw data fell within or near the percentiles of model predicted concentrations for all time points (Supplemental Figure 3-2A). Furthermore, we show that model-predicted concentrations matched the raw data of the validation cohort, which was not used in model development (Supplemental Figure 3-2B). After model validation, all data were pooled, and parameters were re-estimated (Supplemental Table 3-2). VPCs of the final pharmacokinetic model for moxifloxacin are shown in Figure 3-3.

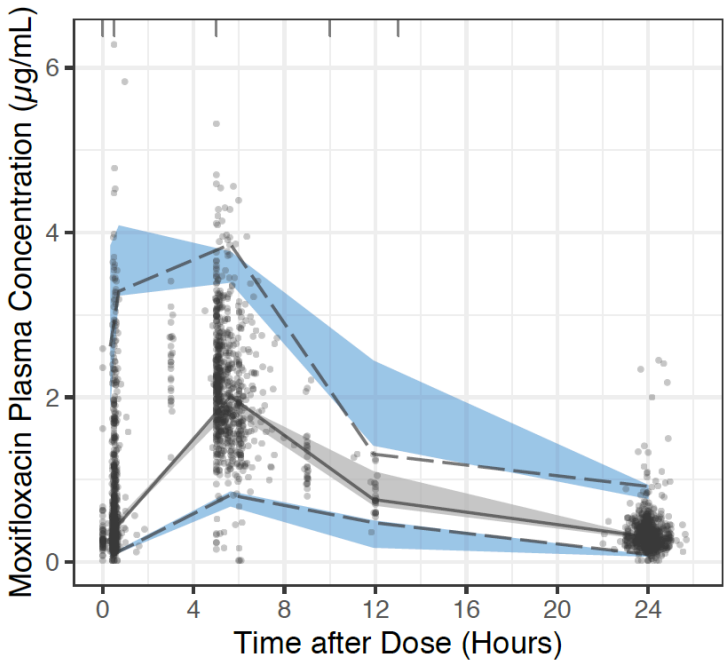

Figure 3-3 Visual predictive check shows reasonable model fit

Points show observed concentration, solid black line show median of the observed data, dashed black lines show the 5th and 95th percentile of the observed data, shaded areas show 95% confidence interval of the 5th, median, and 95th percentile of model predicted simulations.

Pharmacokinetic-Pharmacodynamic Analysis

We have previously described that moxifloxacin AUC as a continuous measure was not univariately significant by Cox regression. It was univariately significant as a categorical covariate of above or below the median AUC of 24 µg·h/mL (Figure 3-4: above median, 17/435 3.9%; below median, 28/356 7.9%; HR, 2.00; p = 0.02). Ultimately, moxifloxacin AUC was not included in the multivariable PKPD model, as rifapentine AUC alone was sufficient in explaining the previously cited differences.

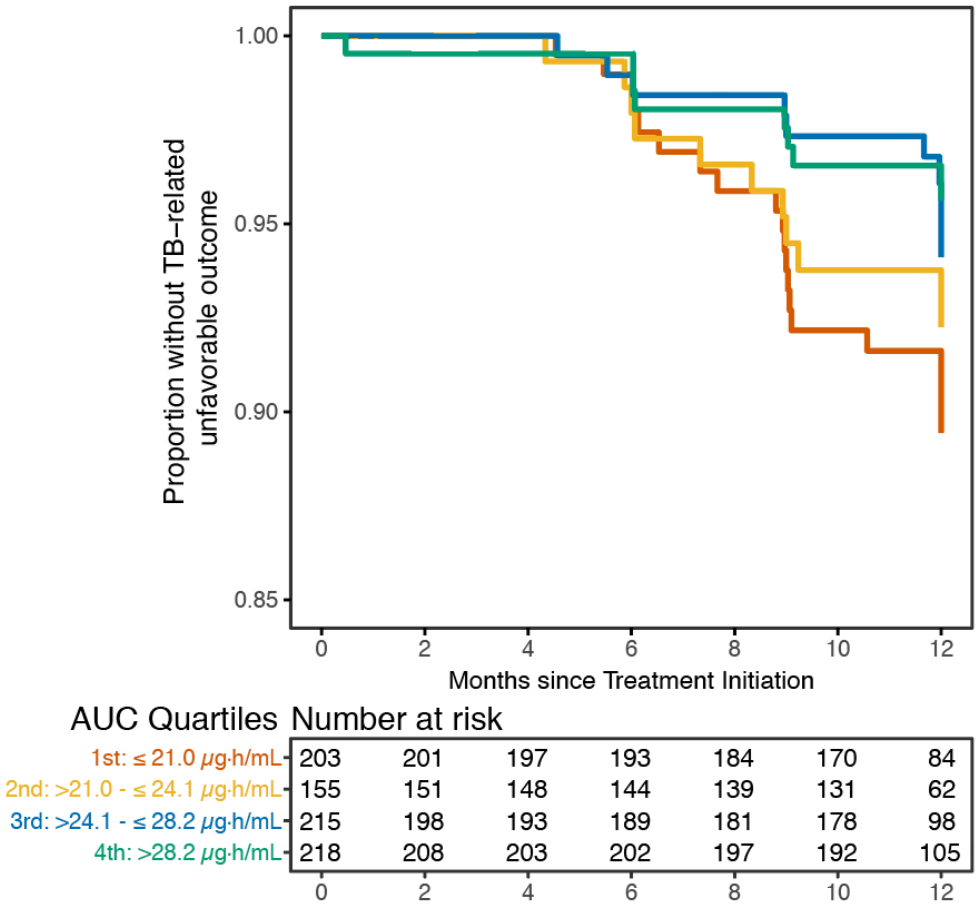

Figure 3-4 Kaplan Meier Estimates of TB-related Unfavorable Outcomes Demonstrate that Low Moxifloxacin Exposures are Associated with Higher Risk for TB-related Unfavorable Outcomes

Pharmacokinetic-Safety Analysis

None of the safety outcomes investigated were significantly associated (P < 0.05) with higher moxifloxacin $AUC_{0\text{-}24h}$ or C_{max} (Figure 3-5 and Supplemental Table 3-3).

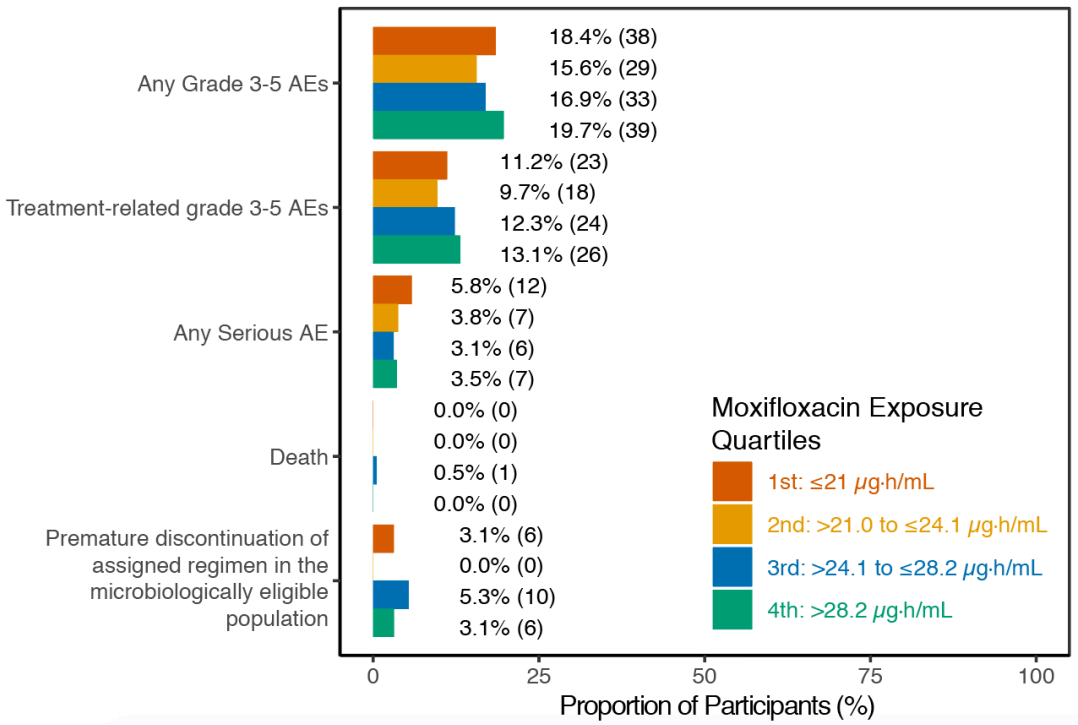

Figure 3-5 Moxifloxacin exposures were not associated with safety outcomes

Bars shows percentage of participants with safety outcomes by quartiles of moxifloxacin exposure. Tolerability was defined as premature discontinuation of the assigned regimen for any reason other than microbiological ineligibility. Participants without pharmacokinetic sampling were excluded from this figure. Percentages are calculated from the safety population for all safety outcomes except tolerability, which was calculated from the microbiologically eligible population.

Discussion

The study described here represents the largest single-trial analysis of moxifloxacin population pharmacokinetics to date (788 participants, 2479 samples). In our final model, clearance is estimated as 16.7 L/h, 31% higher than the clearance estimated in NC-002 (NCT01498419)[9] where moxifloxacin was administered without rifamycins[19]. We surmise that the increase in clearance is due to the induction of PGP, UGTs, and SULTs by rifapentine[20–23]. Approximately 50% of moxifloxacin is metabolized into glucuronide and sulfate conjugates, and while rifamycin induction of glucuronosyltransferases is better understood in literature, there is also some evidence of sulfotransferases also being induced by rifamycins[20,21].

HIV-positive patients were found have an increase in clearance by 24.3%. 55/62 HIV seropositive participants were on efavirenz based anti-retroviral treatment prior to PK sampling, which is well documented in literature to increase moxifloxacin clearance by PGP enzyme induction[24,25]. Again though, the clinical significance of this finding is also unclear, as HIV-infected individuals experienced 3/52 (4.8%) TB-related unfavorable outcomes and HIV-uninfected individuals 42/729 (5.7%) TB-related unfavorable outcomes (microbiologically eligible population).

Diabetic participants were also found to have an increase in clearance by 27.5%, confirming previously reported findings in the largest moxifloxacin pharmacokinetic study to date[26]. Moxifloxacin is excreted approximately 20% unchanged in the urine and the sulfate conjugate is also excreted renally[27]. However, the clinical significance of the increase in clearance is also unclear, as there were only 32 diabetic participants receiving moxifloxacin, and only 1 (3.1%) experienced a TB-related unfavorable outcome while for non-diabetic participants 44/759 (5.8%) (microbiologically eligible population). There were challenges in defining participants living with diabetes in S31/A5349 and the indicator for diabetes reported here was based on participant self-reporting. Although this data is not perfect, it was the most reliable based on all available clinical and laboratory data after consulting with CDC medical officers and protocol chairs.

Finally, female participants had a 19.1% increase in bioavailability and a 17.1% decrease in V_c relative to males. The difference in AUC and C_{max} has been observed in other studies, although this difference was reduced after accounting for body weight[28]. In this study however, body weight was not included in the final model, suggesting that the difference observed between genders is more than just differences in body weight. The clinical significance for the gender differences in exposure is also unclear, as 35/563 (6.2%) and 10/228 (4.4%) of male and female participants respectively experienced TB-related unfavorable outcomes. However, this difference was not significant univariately by Cox regression.

We have further confirmed the main safety findings of the primary analysis, which demonstrated no significant difference in any grade 3-5 adverse events between the rifapentine-moxifloxacin regimen and

the control regimen.[15] In this study, we have found that none of the primary or secondary safety outcomes are associated with increased moxifloxacin exposure; alleviating safety concerns of administering moxifloxacin for 4-months.

The strengths of this study included the exceptionally large study size, diverse racial makeup, breadth of covariates collected, and the remarkable consistency in study implementation across 34 sites. We identified four factors that significantly modulate moxifloxacin pharmacokinetics, however there are some limitations as the clinical implications of moxifloxacin pharmacokinetics are unclear. As we have described in Chapter 4, moxifloxacin AUC as a continuous measure was not univariately significant by Cox regression. It was univariately significant as a categorical covariate of above or below the median AUC of 24 μg·h/mL (above median, 17/435 3.9%; below median, 28/356 7.9%; HR, 2.00; p = 0.02). Ultimately, moxifloxacin AUC was not included in the multivariable PKPD model, as rifapentine AUC alone was sufficient in explaining the previously cited differences. However, despite the lack of clarity we believe that moxifloxacin exposure is still crucial in driving treatment response as the small number of TB-related unfavorable outcomes in the 2HPZM/2HPM arm 45/791 (5.9%) and the complex interplay between pharmacokinetics, baseline disease severity, and treatment outcomes gives us little power to detect but the largest risk factors. This lack of a target exposure for moxifloxacin is a major limitation that prevents us from making dose recommendations; however, although the clinical significance of low moxifloxacin exposure is still not well characterized, subpopulations at highest risk of low exposure, such as male patients living with HIV or diabetes (Figure 3), may be considered for a dose increase to ensure sufficient exposure. Finally, electrocardiograms were not collected which leaves us unable to evaluate the primary safety concern of fluoroquinolones, QT prolongation.

Considering the recent WHO rapid communication which recommended the new 4-month 2HPZM/2HPM regimen as a possible alternative to the 6-month 2HRZE/4HR regimen for the treatment of DS-TB, our findings suggest that selected populations may be at risk for lower exposures and programmatic awareness of these risks will be relevant as part of the global implementation of the regimen. The study described here, which is the largest moxifloxacin pharmacokinetic study in tuberculosis patients to date, provides a robust model with covariates that can be used to optimize dosing for all patients.

References

1. World Health Organization. *WHO consolidated guidelines on tuberculosis: module 4: treatment: drug-resistant tuberculosis treatment*. (World Health Organization, 2020).
2. Rodríguez, J. C., Ruiz, M., Climent, A. & Royo, G. In vitro activity of four fluoroquinolones against Mycobacterium tuberculosis. *International Journal of Antimicrobial Agents* **17**, 229–231 (2001).
3. Rustomjee, R. *et al.* A Phase II study of the sterilising activities of ofloxacin, gatifloxacin and moxifloxacin in pulmonary tuberculosis. *The International Journal of Tuberculosis and Lung Disease* **12**, 128–138 (2008).
4. Conde, M. B. *et al.* Moxifloxacin versus ethambutol in the initial treatment of tuberculosis: a double-blind, randomised, controlled phase II trial. *The Lancet* **373**, 1183–1189 (2009).
5. Merle, C. S. *et al.* A Four-Month Gatifloxacin-Containing Regimen for Treating Tuberculosis. *N Engl J Med* **371**, 1588–1598 (2014).
6. Gillespie, S. H. *et al.* Four-Month Moxifloxacin-Based Regimens for Drug-Sensitive Tuberculosis. *N Engl J Med* **371**, 1577–1587 (2014).
7. Jindani, A. *et al.* High-Dose Rifapentine with Moxifloxacin for Pulmonary Tuberculosis. *N Engl J Med* **371**, 1599–1608 (2014).
8. Sarathy, J. *et al.* Fluoroquinolone Efficacy against Tuberculosis Is Driven by Penetration into Lesions and Activity against Resident Bacterial Populations. *Antimicrob Agents Chemother* **63**, e02516-18 (2019).
9. Dawson, R. *et al.* Efficiency and safety of the combination of moxifloxacin, pretomanid (PA-824), and pyrazinamide during the first 8 weeks of antituberculosis treatment: a phase 2b, open-label, partly randomised trial in patients with drug-susceptible or drug-resistant pulmonary tuberculosis. *The Lancet* **385**, 1738–1747 (2015).
10. Thee, S. *et al.* Pharmacokinetics and Safety of Moxifloxacin in Children With Multidrug-Resistant Tuberculosis. *Clinical Infectious Diseases* **60**, 549–556 (2015).
11. Naidoo, A., Naidoo, K., McIlleron, H., Essack, S. & Padayatchi, N. A Review of Moxifloxacin for the Treatment of Drug-Susceptible Tuberculosis: Journal of Clinical Pharmacology. *The Journal of Clinical Pharmacology* **57**, 1369–1386 (2017).

12. Pranger, A. D. *et al.* Evaluation of moxifloxacin for the treatment of tuberculosis: 3 years of experience. *European Respiratory Journal* **38**, 888–894 (2011).
13. Xu, P. *et al.* Moxifloxacin is an effective and safe candidate agent for tuberculosis treatment: a meta-analysis. *International Journal of Infectious Diseases* **60**, 35–41 (2017).
14. Avelox (moxifloxacin hydrochloride). Package Insert. Bayer AG. 1999.
15. Dorman, S. E. *et al.* Four-Month Rifapentine Regimens with or without Moxifloxacin for Tuberculosis. *N Engl J Med* **384**, 1705–1718 (2021).
16. Dorman, S. E. *et al.* High-dose rifapentine with or without moxifloxacin for shortening treatment of pulmonary tuberculosis: Study protocol for TBTC study 31/ACTG A5349 phase 3 clinical trial. *Contemporary Clinical Trials* **90**, 105938 (2020).
17. Byon, W. *et al.* Establishing Best Practices and Guidance in Population Modeling: An Experience With an Internal Population Pharmacokinetic Analysis Guidance. *CPT: Pharmacometrics & Systems Pharmacology* **2**, 51 (2013).
18. Mould, D. & Upton, R. Basic Concepts in Population Modeling, Simulation, and Model-Based Drug Development-Part 2: Introduction to Pharmacokinetic Modeling Methods. *CPT: Pharmacometrics & Systems Pharmacology* **2**, 38 (2013).
19. Wang, Q. (2021) Determination of risk factors for time to culture conversion in tuberculosis patients receiving novel regimen [Poster Abstract 9847]. 2021 Populations Approach Group Europe, online. www.page-meeting.org/?abstract=9847.
20. Gufford, B. T. *et al.* Rifampin modulation of xeno- and endobiotic conjugating enzyme mRNA expression and associated microRNAs in human hepatocytes. *Pharmacol Res Perspect* **6**, e00386 (2018).
21. Niemi, M., Backman, J. T., Fromm, M. F., Neuvonen, P. J. & Kivistö, K. T. Pharmacokinetic Interactions with Rifampicin. *Clin Pharmacokinet* **42**, 819–850 (2003).
22. Dooley, K. *et al.* Repeated Administration of High-Dose Intermittent Rifapentine Reduces Rifapentine and Moxifloxacin Plasma Concentrations. *AAC* **52**, 4037–4042 (2008).
23. Nijland, H. M. J. *et al.* Rifampicin Reduces Plasma Concentrations of Moxifloxacin in Patients with Tuberculosis. *Clinical Infectious Diseases* **45**, 1001–1007 (2007).

24. Mouly, S. *et al.* Hepatic but not intestinal CYP3A4 displays dose-dependent induction by efavirenz in humans. *Clinical Pharmacology & Therapeutics* **72**, 1–9 (2002).
25. Naidoo, A. *et al.* Effect of rifampicin and efavirenz on moxifloxacin concentrations when co-administered in patients with drug-susceptible TB. *Journal of Antimicrobial Chemotherapy* **72**, 1441–1449 (2017).
26. Dekkers, B. G. J. *et al.* Reduced moxifloxacin exposure in patients with tuberculosis and diabetes. *Eur Respir J* **54**, 1900373 (2019).
27. Moise, P. A., Birmingham, M. C. & Schentag, J. J. Pharmacokinetics and metabolism of moxifloxacin. *Drugs Today* **36**, 229 (2000).
28. Sullivan, J. T., Lettieri, J. T., Liu, P. & Heller, A. H. The Influence of Age and Gender on the Pharmacokinetics of Moxifloxacin: *Clinical Pharmacokinetics* **40**, 11–18 (2001).
29. World Health Organization. *Treatment of drug-susceptible tuberculosis: rapid communication*. (World Health Organization, 2021).

Supplementary Information

Supplemental Table 3-1 Summary of Pharmacokinetic, Demographic, Clinical, and Safety data

Training and validation data split had similar characteristics. n (%) given for categorical measures and median (95th percentiles) given for continuous measures. (*) 7 participants were missing aggregate cavity size and disease extent, 1 participant was missing smear grade.

	Training Dataset	Validation Dataset	Validation Dataset 2	Total
PHARMACOKINETIC SAMPLING				
Total Patients	N=511	N=233	N=43	N=787
Intensive Sampling Patients	N=21 (185 samples)	N=5 (43 samples)	N=0 (0 samples)	N=26 (228 samples)
Sparse Sampling Patients	N=490 (1450 samples)	N=228 (676 samples)	N=43 (125 samples)	N=761 (2251 samples)
Below Limit of Quantification	6 samples	1 sample	2 samples	9 samples
DEMOGRAPHIC FACTORS				
Age [years]	30 (16 - 60)	31 (18 - 59)	33 (18 - 52)	30 (17-60)
Male Sex	353 (69)	175 (75)	31 (72)	559 (71)
Height [cm]	167 (150 - 183)	169 (151 - 183)	167 (156 - 186)	167 (151 - 183)
Weight [kg]	53 (41 - 78)	53 (41 – 74)	54 (44 – 75)	53 (41 -76)
BMI [kg/m2]	19.07 (15.34 – 28.46)	18.69 (15.03 – 27.23)	19.00 (15.59 – 28.71)	18.99 (15.23 – 28.48)
Race				
Black	362 (71)	167 (72)	22 (51)	551 (70)
Mixed/Multi-racial	83 (16)	30 (13)	20 (47)	133 (17)
Asian	59 (12)	32 (14)	0 (0)	91 (12)
White	7 (1)	4 (2)	1 (2)	12 (2)
CLINICAL FACTORS				
African Clinical Site	368 (72)	167 (72)	42 (98)	577 (73)
Baseline Chest X-Ray Cavity	370 (72)	169 (73)	33 (77)	572 (73)
Baseline Aggregate Cavity Size*				
No cavities	130 (26)	65 (28)	11 (26)	206 (26)
Cavities < 4cm	181 (36)	75 (32)	19 (44)	275 (35)
Cavities ≥ 4cm	194 (38)	92 (40)	13 (30)	299 (38)
Baseline Chest X-Ray Disease Extent*				
Lesions < 1/4 thoracic area	89 (18)	55 (24)	7 (16)	151 (19)
Lesions 1/4 to < 1/2 thoracic area	248 (49)	101 (44)	17 (40)	366 (47)
Lesions ≥ 1/2 thoracic area	168 (33)	76 (33)	19 (44)	263 (34)
Baseline Smear Grade*				
Negative	15 (3)	8 (3)	1 (2)	24 (3)
Scanty	90 (18)	50 (21)	12 (28)	152 (19)
Grade 1	111 (22)	50 (21)	7 (16)	168 (21)
Grade 2	150 (29)	62 (27)	13 (30)	225 (29)
Grade 3	139 (27)	62 (27)	10 (23)	211 (27)
WHO scale not used	5 (1)	1 (0)	0 (0)	6 (1)
Karnofsky Score	90 (70 - 100)	90 (70 - 100)	90 (70 - 100)	90 (70 - 100)
HIV	39 (8)	21 (9)	5 (12)	65 (8)
Diabetes	21 (4)	5 (2)	3 (7)	29 (4)

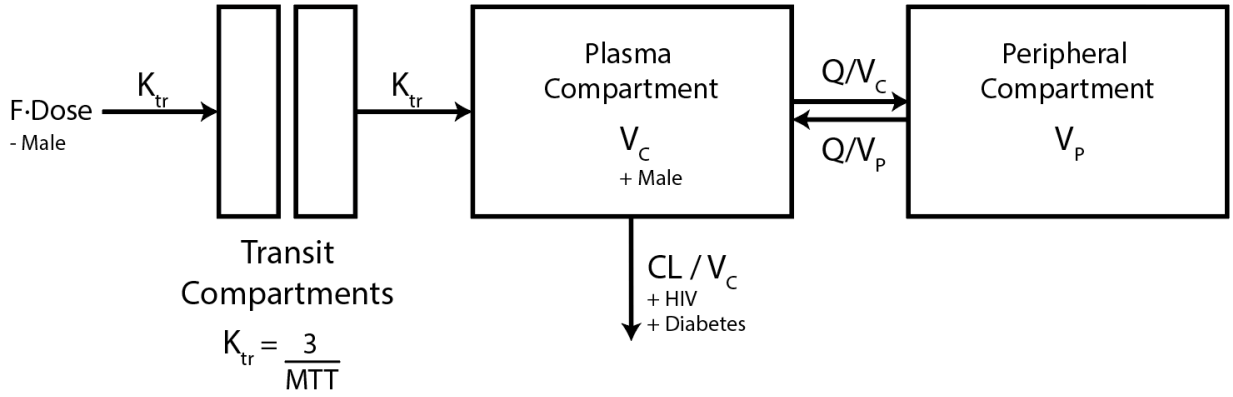

Supplemental Figure 3-1 Moxifloxacin Structural Pharmacokinetic Model

Pharmacokinetic data were well described with a two-compartment model with linear clearance and two transit compartment delayed absorption. Male participants had lower bioavailability and higher volume of distribution, while participants living with and participants living with diabetes had higher apparent clearance.

Supplemental Table 3-2 Training and Final Model Parameters

Bioavailability (F) was fixed to 100% and number of transit compartments were fixed to 2.

	Training Model		Final Full Model	
Parameters (units)	**Estimate (%RSE)**	**Between-subject Variability %CV (%RSE)**	**Estimate (%RSE)**	**Between-subject Variability %CV (%RSE)**
CL/F (L/h)	16.5 (1.6)	24 (5.3)	16.7 (1.3)	24 (4.7)
V/F (L)	130 (2.7)	--	129 (2.3)	--
MTT (h)	2.43 (3.2)	67 (5.0)	2.41 (3.5)	66 (2.8)
MTT Box Cox transformation Shape parameter	-0.892 (18)	--	-0.956 (11.7)	--
Q (L/h)	4.43 (9.3)	--	4.56 (7.0)	--
V_p (L)	323 (13)	--	336 (26)	--
Covariates (reference)				
Diabetes effect on CL (fraction relative to non-diabetic reference)	+23.5% (28)	--	+27.7% (18.5)	--
HIV+ effect on CL (fraction relative to HIV- reference)	+23.8% (23)	--	+24.1% (17.6)	--
Female effect on V (fraction relative to male reference)	-17.4% (18)	--	-17.6% (15.8)	--
Female effect on bioavailability (fraction relative to male reference)	+17% (23)	--	+19.6% (16.5)	--
Residual Error (units)				
Proportional Error (%)	27.2 (5.2)	--	27.2 (4.6)	--

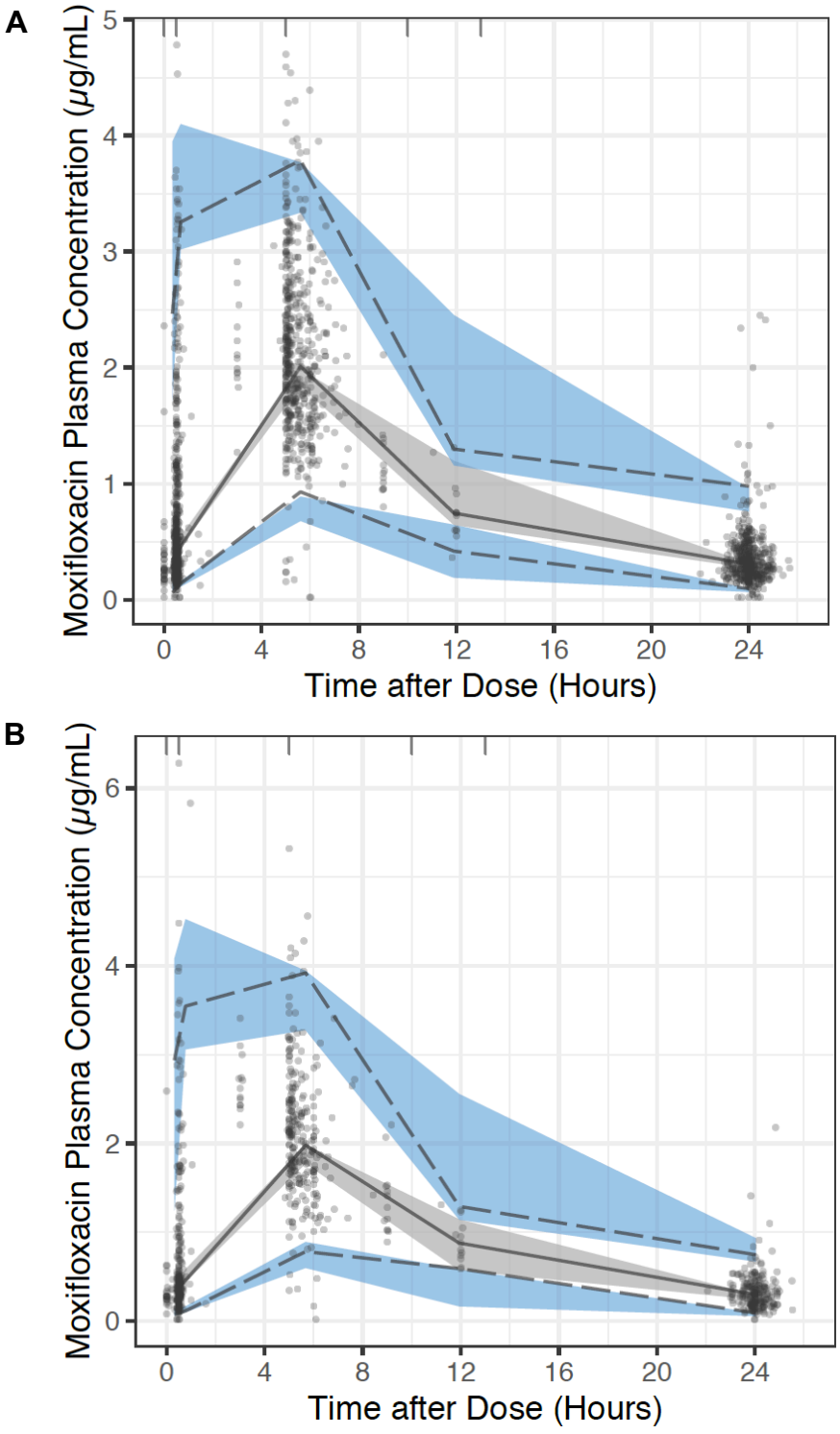

Supplemental Figure 3-2 Visual Predictive Checks of (A) Training and (B) Validation Cohorts

Points show observed concentration, solid black line show median of the observed data, dashed black lines show the 5th and 95th percentile of the observed data, shaded areas show 95% confidence interval of the 5th, median, and 95th percentile of model predicted simulations.

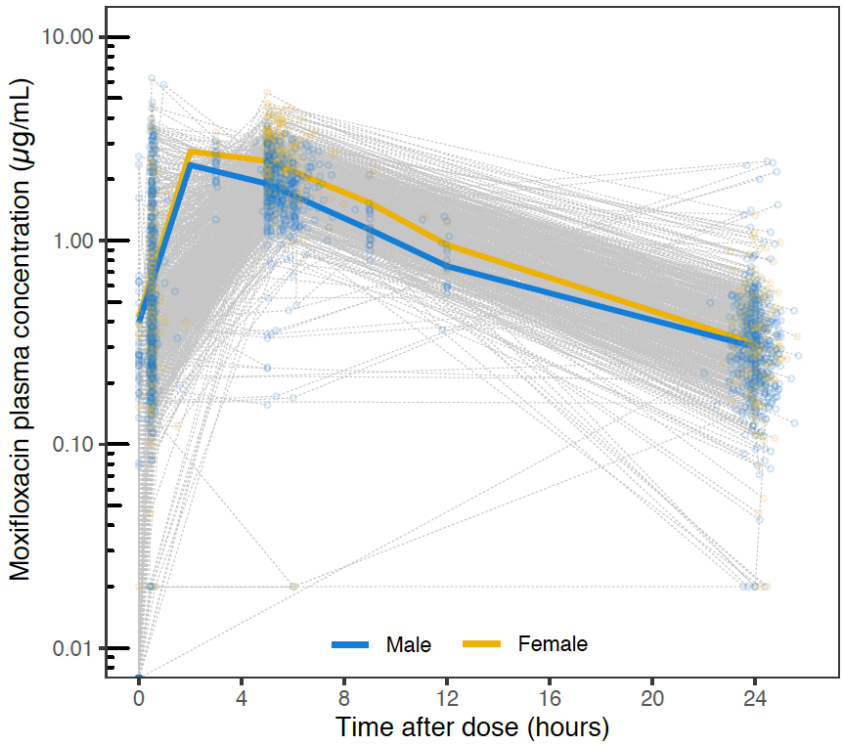

Supplemental Figure 3-3 Raw and median PK profiles stratified by sex demonstrate that females have higher plasma concentrations

Circles represent individual samples and solid lines represent medians. Data is colored by sex, yellow for female and blue for male.

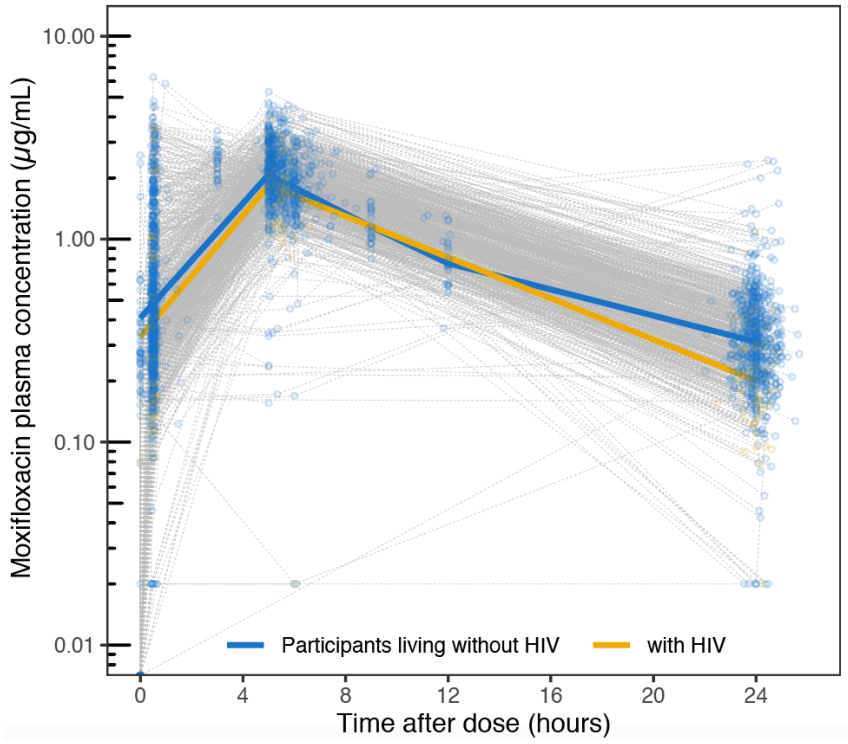

Supplemental Figure 3-4 Raw and median PK profiles stratified by participants living with and without HIV demonstrate that participants living without HIV have higher trough concentrations

Circles represent individual samples and solid lines represent medians. Data is colored by HIV status, yellow for participants living with HIV and blue for participants living without HIV.

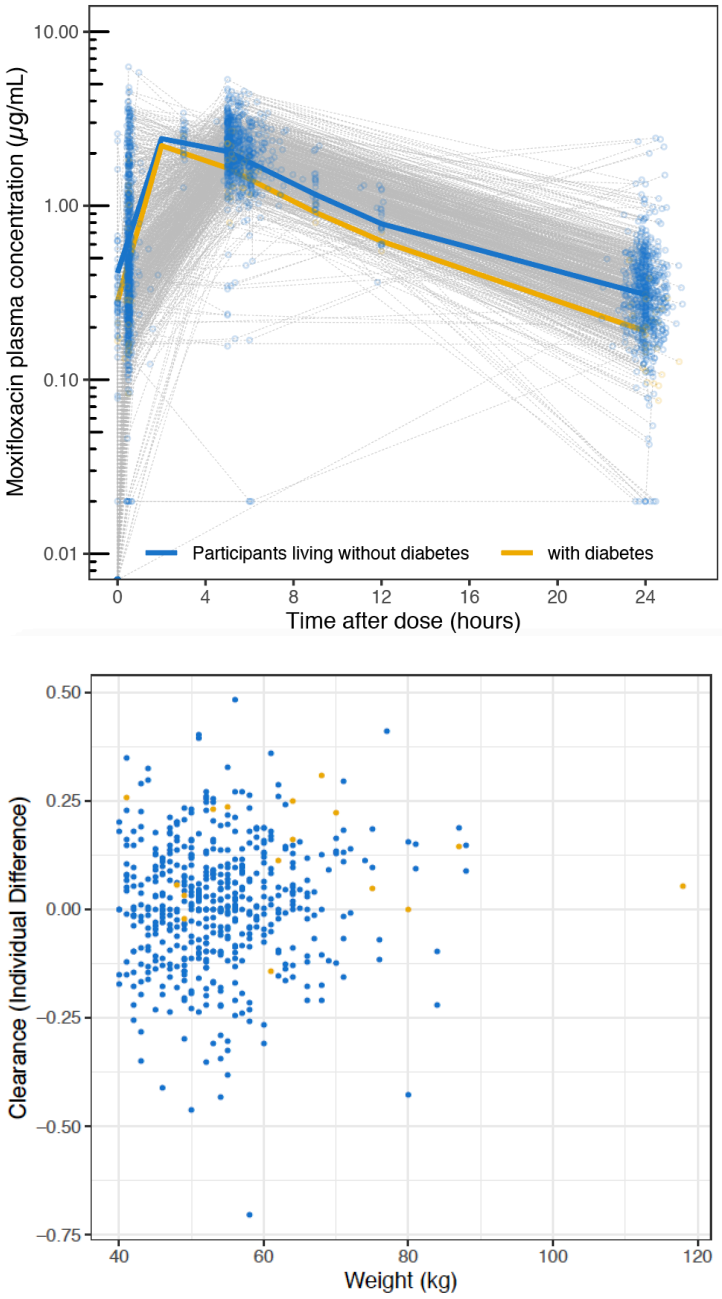

Supplemental Figure 3-5 Raw and median PK profiles stratified by diabetes status demonstrate that non-diabetic participants have higher plasma concentrations

(A) Circles represent individual samples and solid lines represent medians. Data is colored by diabetes status, yellow for participants living without diabetes and blue for with diabetes. **(B)** Points represent individual patients and their clearance (individual difference from median), diabetic patients had higher clearance irrespective of weight.

Supplemental Table 3-3 Odds Ratios of Safety Outcomes for increase in Moxifloxacin Exposure

Odds ratios are adjusted for treatment group and are reported for every 10 μg·h/mL increase in moxifloxacin $AUC_{0\text{-}24h}$ and every 10 μg/mL increase in moxifloxacin C_{max}. None of the safety outcomes are significantly associated with increased moxifloxacin exposure.

Safety Outcome	Odds Ratio	95% CI	p-value
Moxifloxacin AUC (for every 10 μg·h/mL)			
Grade 3 or higher adverse event	1.07	0.83 – 1.35	0.59
Treatment-related grade 3 or higher adverse event	1.09	0.82 – 1.43	0.51
Any serious adverse event	0.93	0.54 – 1.45	0.76
Any grade 3 or higher adverse event within 28 weeks after randomization	1.09	0.87 – 1.36	0.44
Any adverse event resulting in discontinuation of assigned treatment	1.17	0.79 – 1.64	0.49
Premature discontinuation of assigned regimen for any reason in the microbiologically eligible population	0.76	0.31 – 1.55	0.42
ALT or AST level ≥5×ULN	1.25	0.62 – 2.15	0.49
ALT or AST level ≥10×ULN	0.61	0.08 – 2.34	0.55
Serum total bilirubin level ≥3×ULN	0.79	0.41 – 1.37	0.43
Hy's law criteria of ALT or AST level ≥3×ULN plus serum total bilirubin level ≥2×ULN	0.73	0.23 – 1.76	0.54
Death	0.92	0.11 – 3.14	0.93
Moxifloxacin Cmax (for every 1 μg/mL)			
Grade 3 or higher adverse event	1.09	0.85 – 1.38	0.47
Treatment-related grade 3 or higher adverse event	1.04	0.78 – 1.37	0.77
Any serious adverse event	1.15	0.72 – 1.72	0.54
Any grade 3 or higher adverse event within 28 weeks after randomization	1.02	0.81 – 1.27	0.86
Any adverse event resulting in discontinuation of assigned treatment	0.49	0.18 – 1.16	0.11
Premature discontinuation of assigned regimen for any reason in the microbiologically eligible population	0.91	0.58 – 1.34	0.63
ALT or AST level ≥5×ULN	0.89	0.39 – 1.73	0.77
ALT or AST level ≥10×ULN	0.56	0.07 – 2.25	0.49
Serum total bilirubin level ≥3×ULN	1.04	0.59 – 1.69	0.87
Hy's law criteria of ALT or AST level ≥3×ULN plus serum total bilirubin level ≥2×ULN	1.08	0.39 – 2.20	0.87
Death	1.76	0.42 – 4.09	0.37

Chapter 4 - Risk Stratified Treatment for Drug-Susceptible Pulmonary Tuberculosis

Introduction

Study 31/A5349 (NCT02410772) was a phase III randomized controlled trial that compared 4-month regimens of daily isoniazid, rifapentine, and pyrazinamide plus either moxifloxacin (rifapentine-moxifloxacin regimen) or ethambutol (rifapentine regimen) to the 6-month standard treatment of isoniazid, rifampicin, pyrazinamide, and ethambutol (control regimen) for treatment of drug-susceptible pulmonary tuberculosis. The 4-month rifapentine-moxifloxacin regimen demonstrated noninferior efficacy and comparable safety to the control,[1,2] making it the first 4-month regimen endorsed by both the World Health Organization (WHO) and the U.S. Centers for Disease Control and Prevention (CDC) for the treatment of adolescents and adults with pulmonary tuberculosis.[3,4] While the rifapentine regimen was not shown to be noninferior to the control, 82% of participants receiving it were successfully cured.[2]

Globally, tuberculosis has long been treated with a one-size-fits-all approach, but the evidence in support of using stratified medicine approaches has been steadily growing.[5–8] The importance of considering severity of disease for stratifying patients into easy and hard-to-treat phenotypes has been previously reported.[5] Study 31/A5349 incorporated pharmacokinetic sampling for all drugs among all participants, thereby providing an unprecedented opportunity to establish the contribution of exposure-response relationships to clinical outcomes for all first-line antituberculosis drugs, and permitting insights into the complex interplay between disease severity, other patient factors, regimen potency, and regimen duration on long-term clinical outcomes. Here, we report the results of prespecified Study 31/A5349 secondary analyses that were designed to assess pharmacokinetic, clinical, and demographic markers for efficacy and safety outcomes among participants treated with the 4-month rifapentine or rifapentine-moxifloxacin regimens. Our objective was to inform and better define approaches for the optimal use of the novel 4-month rifapentine-moxifloxacin regimen in clinical practice.

Methods

Trial Design and Participants

Study 31/A5349 was a phase III randomized controlled trial conducted in 13 countries at 34 clinical sites by the CDC funded Tuberculosis Trials Consortium and the National Institutes of Health funded AIDS Clinical Trials Group (ACTG).[1,2] The participants were ≥12 years of age and had newly diagnosed pulmonary tuberculosis that was confirmed on culture to be susceptible to isoniazid, rifampicin, and fluoroquinolones. All participants provided written informed consent.

Pharmacokinetics

All participants who underwent randomization were included for steady state sparse and/or intensive pharmacokinetic sampling between weeks 2-8 of treatment. Plasma concentrations of all drugs were determined using validated high-performance liquid chromatography mass spectroscopy assays. Population pharmacokinetic models were developed for each of the drugs and steady state individual participant area under the concentration-time curve from 0-24 hours ($AUC_{0\text{-}24h}$) and maximal plasma concentration (C_{max}) were calculated and used as inputs for this study (unpublished data). Participants without pharmacokinetic samples had their $AUC_{0\text{-}24h}$ and C_{max} imputed by the population pharmacokinetic models.

Baseline Clinical Factors

We considered the following as baseline factors potentially associated with treatment efficacy: age, sex, race, trial site, weight, body-mass index, Karnofsky performance score, HIV status, diabetes, smoking history, AFB sputum smear grade, baseline time-to-positivity for *M. tuberculosis* growth in liquid mycobacterial sputum culture (Mycobacteria Growth Indicator Tube [MGIT], Becton Dickinson), GeneXpert cycle threshold for detection of *M. tuberculosis* in sputum (Xpert MTB/RIF, Cepheid), cavitary disease on chest radiography, aggregate cavity size, and extent of disease defined as percent involvement of the thoracic area on chest radiography. Participants were excluded from analyses if they had missing baseline covariates.

Efficacy Outcomes

The primary efficacy outcome of Study 31/A5349 was a composite unfavorable outcome that included tuberculosis-related unfavorable outcomes, tuberculosis-unrelated unfavorable outcomes, and not assessable outcomes.[1,2] The efficacy outcome in this analysis was time to tuberculosis-related unfavorable outcome. In brief, a tuberculosis-related unfavorable outcome was defined as: (1) two consecutive positive sputum cultures on or after week 17, (2) not seen at month 12 with last culture positive, or (3) clinical diagnosis of tuberculosis recurrence and treatment restarted. Tuberculosis-unrelated unfavorable outcomes and not assessable outcomes were right-censored at the time of event; favorable outcomes were right-censored at the time of last follow up visit.

Safety Outcomes

The primary safety outcome in the trial was any grade 3 or higher adverse event occurring while participants received trial medications and up to 14 days after the last dose. Additional safety outcomes considered were treatment-related grade 3 or higher adverse events, serious adverse events, tolerability, and death. Tolerability was defined as discontinuation of the assigned treatment for any reason other than microbiological ineligibility.

Statistical Analysis

We generated Kaplan-Meier estimates for all participants and stratified by $AUC_{0\text{-}24h}$ (dichotomized at median) for each of the six drugs. We performed univariable pharmacokinetic-pharmacodynamic Cox proportional hazards analysis comparing the two strata. Each arm and each drug were analyzed separately.

The analysis population consisted of the microbiologically eligible population from Study 31/A5349.[2] Separate Cox proportional hazards models were built to analyze each arm separately. Baseline clinical factors, pharmacokinetics, and demographics were tested in univariable and multivariable analyses to identify risk factors for tuberculosis-related unfavorable outcomes. We selected risk factors for the final multivariable model with a stepwise procedure testing of linear relationships in a forward inclusion (likelihood ratio test $P<0.05$) and a backwards exclusion ($P<0.01$) procedure. We evaluated and validated

models using Schoenfeld, Martingale, and deviance residuals to assess the proportional hazards assumption, examine influential outliers, and check for nonlinearity in covariates, respectively. The baseline clinical risk factors selected by the stepwise procedure were used to construct a risk stratification algorithm that stratified participants into low, moderate, and high-risk disease phenotypes. For each of the risk strata, we performed subgroup analyses calculating the risk difference and 95% Wald confidence interval; we compared the upper border of the confidence interval to a 6.6% margin, the threshold for noninferiority used in the primary analysis. We also tested prespecified risk group definitions from the TB-ReFLECT analysis by Imperial et. al.[5] We calculated interaction p-values for each of the identified single and composite risk factors.

We used logistic regression models to evaluate the association between $AUC_{0\text{-}24h}$ and C_{max} of all drugs and safety outcomes. We considered pharmacokinetic, demographic, and baseline clinical factors, described above, as potential predictors of any grade 3-5 adverse events in univariable and multivariable logistic regression. The selection of covariates for followed the same stepwise procedure described above.

Results

The 2343 participants in the microbiologically eligible population from Study 31/A5349 were included in the analysis, among which 2218 (95%) had pharmacokinetic data and the remaining 125 participants had their $AUC_{0\text{-}24h}$ and C_{max} imputed. The baseline demographic, clinical, and pharmacokinetic characteristics of these participants across the three treatment groups can be found in Table 4-1. Trial level Kaplan Meier estimates of tuberculosis-related unfavorable outcomes by regimen are shown in Supplemental Figure 4-1.

Table 4-1 Summary of Demographics, Clinical Factors, Pharmacokinetics, Treatment and Safety Outcomes in the Microbiologically Eligible Population from Study 31/A5349.

Abbreviations: AFB, acid-fast bacillus; $AUC_{0\text{-}24h}$, area under the concentration-time curve from 0-24 hours; BMI, body mass index; C_{max}, maximal plasma concentration; HIV, human immunodeficiency virus.
Data are shown as n (%) for categorical measures and median (2.5^{th} and 97.5^{th} percentiles) for continuous measures. Missing values are equally distributed across arms

	Rifapentine-Moxifloxacin 2HPZM/2HPM	Rifapentine 2HPZE/2HP	Control 2HRZE/4HR	Missing
Number of Participants	791	784	768	--
DEMOGRAPHIC FACTORS				
Age [years]	31 (17 - 60)	30 (18 - 59)	30 (18 - 60)	0 (0)
Male Sex	563 (71)	563 (72)	544 (71)	0 (0)
Height [cm]	167 (150 - 183)	167 (152 - 182)	167 (150 - 184)	0 (0)
Weight [kg]	53 (41 - 76)	53 (41 - 75)	53 (41 - 75)	1 (0)
BMI [kg/m2]	19.03 (15.23 – 27.90)	18.92 (14.87 – 27.54)	18.93 (15.03 – 27.37)	1 (0)
Race				5 (0.2)
Black	552 (70)	571 (73)	553 (72)	
Mixed/Multi-racial	136 (17)	111 (14)	111 (15)	
Asian	89 (11)	93 (12)	86 (11)	
White	13 (2)	8 (1)	15 (2)	
African Clinical Site	578 (73)	573 (73)	565 (74)	0 (0)
BASELINE CLINICAL FACTORS				
Xpert MTB/RIF cycle threshold	17.2 (11.4 – 25.6)	17.4 (11.3 – 26.3)	17.2 (11.5 – 25.5)	302 (13)
Time to Detection on Sputum Liquid Culture [days]	8.12 (3.64 – 19.00)	7.92 (3.54 – 18.00)	8.21 (3.73 – 19.3)	65 (3)
Cavitary Disease on Chest Radiography	572 (72)	572 (73)	557 (73)	0 (0)
Aggregate Cavity Size on Chest Radiography				15 (0.7)
No cavities	213 (27)	206 (26)	206 (27)	
Cavities < 4cm	277 (35)	246 (32)	251 (33)	
Cavities ≥ 4cm	295 (38)	327 (42)	307 (40)	
Extent of Disease on Chest Radiography				15 (0.7)
Lesions < 1/4 thoracic area	155 (20)	135 (17)	120 (16)	
Lesions 1/4 to < 1/2 thoracic area	360 (46)	343 (44)	343 (45)	
Lesions ≥ 1/2 thoracic area	270 (34)	301 (39)	301 (39)	
Sputum AFB Smear Grade				3 (0.1)
Negative	29 (4)	32 (4)	21 (3)	
Scanty	149 (19)	127 (16)	121 (16)	
Grade 1	168 (21)	173 (22)	188 (25)	
Grade 2	228 (29)	228 (29)	229 (30)	
Grade 3	209 (26)	214 (27)	198 (26)	
Positive (WHO scale not used)	7 (1)	9 (1)	10 (1)	
Karnofsky Score	90 (70 – 100)	90 (70 – 100)	90 (70 – 100)	0 (0)
HIV Infection	62 (8)	68 (9)	64 (8)	1 (0)
History of Diabetes	32 (4)	14 (2)	31 (4)	0 (0)
Smoking History				0 (0)
Never	431 (54)	409 (52)	391 (51)	
Current	185 (23)	175 (22)	181 (24)	
Former	175 (22)	200 (26)	196 (26)	
History of Liver Disease	6 (1)	6 (1)	5 (1)	0 (0)

	Rifapentine-Moxifloxacin 2HPZM/2HPM	Rifapentine 2HPZE/2HP	Control 2HRZE/4HR	Missing
Number of Participants	791	784	768	--
PHARMACOKINETICS				
Rifapentine $AUC_{0\text{-}24h}$ [µg·h/mL]	557.1 (276 – 983)	562.4 (302 – 1037)	--	67 (4)
Moxifloxacin $AUC_{0\text{-}24h}$ [µg·h/mL]	24.3 (15.3 – 44.1)	--	--	49 (6)
Isoniazid $AUC_{0\text{-}24h}$ [µg·h/mL]	10.2 (6.8 – 33.3)	10.2 (6.8 – 31.8)	13.8 (8.4 – 41.7)	153 (7)
Pyrazinamide $AUC_{0\text{-}24h}$ [µg·h/mL]	350 (229 – 590)	307 (214 – 553)	353 (258 – 577)	125 (5)
Ethambutol $AUC_{0\text{-}24h}$ [µg·h/mL]	--	15.7 (12.4 – 21.1)	15.0 (11.8 – 20.5)	138 (9)
Rifampicin $AUC_{0\text{-}24h}$ [µg·h/mL]	--	--	41.4 (22.1 – 147.1)	57 (6)
Rifapentine C_{max} [µg /mL]	32.8 (19.2 – 51.9)	32.4 (19.5 – 53.4)	--	67 (4)
Moxifloxacin C_{max} [µg /mL]	2.56 (1.72 – 4.35)	--	--	49 (6)
Isoniazid C_{max} [µg /mL]	2.6 (2.1 – 4.8)	2.6 (2.0 – 4.4)	3.7 (3.1 – 5.4)	153 (7)
Pyrazinamide C_{max} [µg /mL]	28.6 (19.0 – 44.8)	28.1 (22.3 – 42.8)	33.8 (26.9 – 46.6)	125 (5)
Ethambutol C_{max} [µg /mL]	--	1.68 (1.05 – 3.14)	1.83 (1.24 – 3.12)	138 (9)
TREATMENT OUTCOMES				
Tuberculosis-Related Unfavorable Outcomes	45 (5.7)	75 (9.5)	24 (3.1)	--
Not Tuberculosis-Related Unfavorable Outcomes	43 (5.4)	32 (4.1)	46 (5.9)	--
Total Unfavorable Outcomes	88 (11.1)	107 (13.6)	70 (9.1)	--
SAFETY OUTCOMES				
Number of Patients (Safety Population)	846	835	825	--
Grade 3 or higher adverse event	159 (18.8)	119 (14.3)	159 (19.3)	--
Treatment-related grade 3 or higher adverse event	109 (12.9)	64 (7.7)	81 (9.8)	--
Any serious adverse event	37 (4.4)	39 (4.7)	56 (6.8)	--
Death	3 (0.4)	4 (0.5)	7 (0.8)	--
Premature discontinuation of assigned regimen for any reason in the microbiologically eligible population	54/791 (6.8)	37/784 (4.7)	61/768 (7.9)	--

Risk Factors for TB-related Unfavorable Outcome

Stratified Kaplan-Meier estimates and univariate Cox regression analysis (Supplemental Figure 4-2) demonstrated that below median exposures were significantly associated with increased risk of TB-related unfavorable outcomes for rifapentine (rifapentine regimen: HR, 3.81; 95% CI, 2.22-6.55 | rifapentine-moxifloxacin: HR, 2.23; 95% CI, 1.18-4.20), moxifloxacin (HR, 2.00; 95% CI, 1.09-3.65), isoniazid (only significant in rifapentine regimen: HR, 1.79; 95% CI, 1.09 – 2.95), ethambutol (rifapentine regimen: HR, 1.73; 95% CI, 1.10-2.72 | control: HR, 2.43; 95% CI, 1.01-5.88), and pyrazinamide (control: HR, 2.46; 95% CI, 1.10-5.54) | rifapentine-moxifloxacin: HR, 1.85; 95% CI, 1.03 - 3.33 | not significant in rifapentine-regimen).

Multivariable analyses of pharmacokinetic and baseline clinical and demographic risk factors for tuberculosis-related unfavorable outcomes included 688 of 791 participants (87%) from the rifapentine-moxifloxacin regimen; 675 of 784 participants (86%) from the rifapentine regimen; and 667 of 768 participants (87%) from the control regimen. Among participants assigned to the experimental regimens,

lower baseline Xpert MTB/RIF cycle threshold was associated with an increased hazard of tuberculosis-related unfavorable outcomes (rifapentine regimen: HR 1.54 for every 3 cycle threshold increase; 95% CI, 1.24–1.93 | rifapentine-moxifloxacin regimen: HR 1.43 for every 3 cycle threshold increase; 95% CI, 1.07-1.91) while higher rifapentine $AUC_{0\text{-}24h}$ was associated with a decreased hazard of tuberculosis-related unfavorable outcomes (rifapentine regimen: HR 0.77 for every 100 μg·h/mL increase; 95% CI, 0.63–0.95 | rifapentine-moxifloxacin regimen: HR 0.65 for every 100 μg·h/mL increase; 95% CI, 0.54–0.77). All other pharmacokinetic-pharmacodynamic drug effects that were significant on univariable analysis were not significant after adjusting for rifapentine exposure. Among participants on the rifapentine-moxifloxacin regimen, extensive disease on chest radiography (defined as involvement of ≥50% lung area on chest radiograph) was associated with an increased hazard of tuberculosis-related unfavorable outcomes (HR 2.02; 95% CI, 1.07–3.82). Among participants on the rifapentine regimen, extensive disease was associated with an increased hazard of tuberculosis-related unfavorable outcomes in the baseline factors only multivariable model (Supplemental Figure 4-3) but not after adjusting for rifapentine exposure (HR 1.61 with involvement of ≥50% thoracic area; 95% CI, 0.98–2.65). Finally, in the rifapentine regimen only, we observed an increased hazard of tuberculosis-related unfavorable outcomes among older participants (HR 1.38 for every 10-year increase; 95% CI, 1.13–1.68) and increased hazard among participants with lower weight (HR 1.76 for every 10 kg decrease; 95% CI, 1.25–2.49). (Figure 4-1A and 4-1B)

Among participants assigned to the control regimen, lower baseline Xpert MTB/RIF cycle threshold was associated with an increased hazard and higher pyrazinamide $AUC_{0\text{-}24h}$ was associated with a decreased hazard of tuberculosis-related unfavorable outcomes (Xpert: HR 1.69 for every 3-cycle threshold decrease; 95% CI, 1.08-2.63 | Pyrazinamide: HR 0.35 for every 100 μg·h/mL increase; 95% CI 0.15–0.83) (Figure 4-1C).

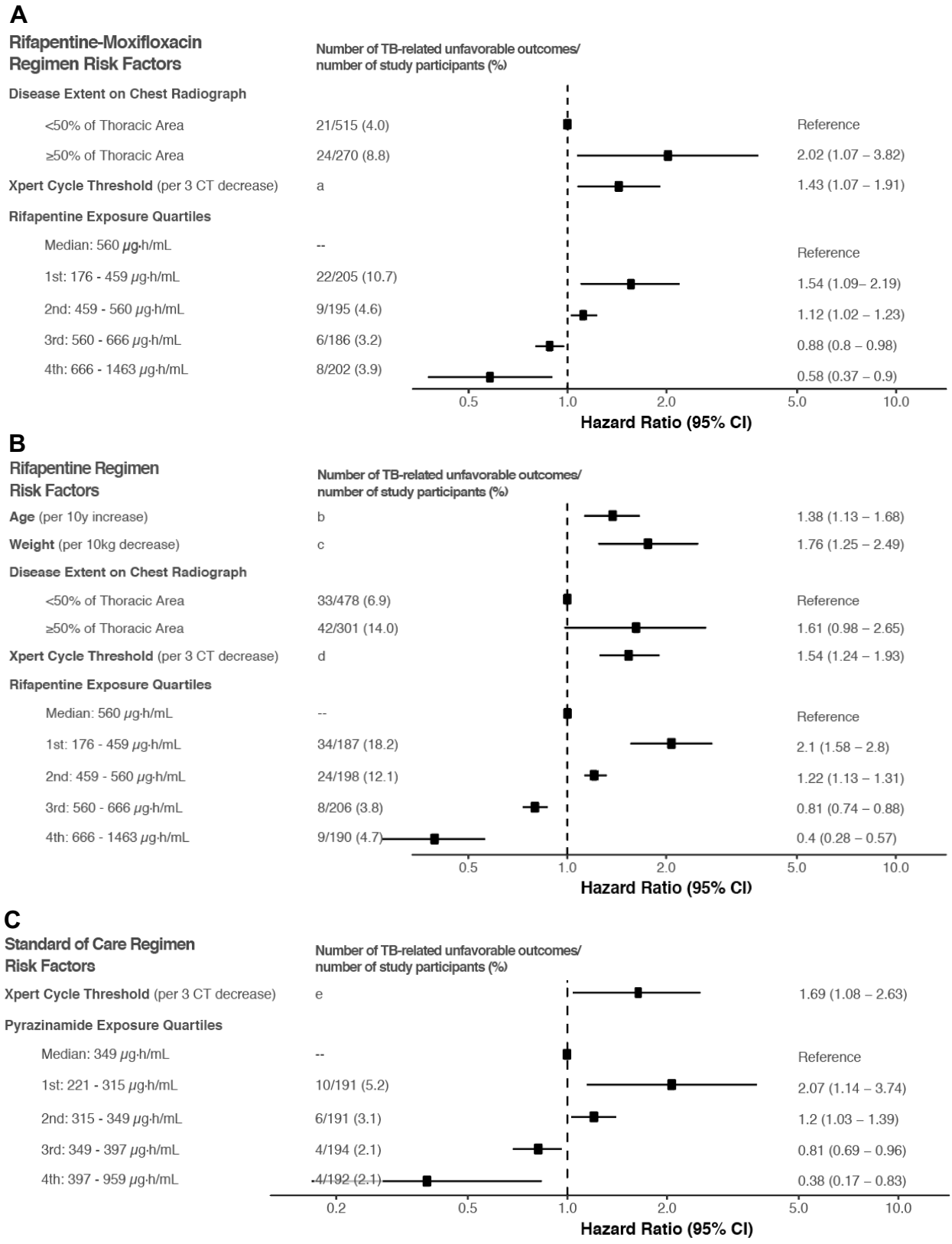

Figure 4-1 Multivariate hazard ratios for TB-related unfavorable outcomes.

Multivariate analysis of pharmacokinetic and baseline predictors for the rifapentine-moxifloxacin, rifapentine, and the control regimen. **(a)** Xpert cycle threshold < 18, 29/397 (7.3); Xpert cycle threshold ≥ 18, 10/296 (3.4), **(b)** Age < 30 years, 21/354 (5.9); Age ≥ 30 years, 54/430 (12.6), **(c)** Weight < 53 kg, 45/364 (12.4); Weight ≥ 53 kg, 30/419 (7.2), **(d)** Xpert cycle threshold < 18, 54/397 (13.6); Xpert cycle threshold ≥ 18, 13/284 (7.7), **(e)** Xpert cycle threshold < 18, 15/399 (3.7); Xpert cycle threshold ≥ 18, 5/268 (1.9). Hazard ratios and 95% confidence intervals of pharmacokinetic variables were reported for the median exposure within each quartile relative to the overall median exposure.

Univariable Cox proportional hazards analysis, sensitivity analyses of imputed pharmacokinetic values, and univariate subgroup analyses can be found in the supplement.

Risk Stratification Algorithm

We designed a simple risk algorithm for participants receiving the rifapentine-moxifloxacin regimen by stratifying participants by two routinely available major risk factors identified by our analysis: Xpert MTB/RIF cycle threshold stratified above and below the median (17.3 cycle threshold rounded to 18, the median cycle threshold value for participants with smear grade 1+, Supplemental Figure 4) and extent of disease on chest radiography (above and below 50% involvement of lung area). Rifapentine exposure was excluded from the risk algorithm as it is often not available to clinicians. The low-risk phenotype was defined as Xpert cycle threshold ≥18 and involvement of <50% lung area on chest radiography, the high-risk phenotype was defined as Xpert cycle threshold <18 and involvement of ≥50% lung area on chest radiography, while the remaining population was defined as the moderate-risk phenotype. Kaplan-Meier estimates stratified by regimen, risk phenotype, and rifapentine exposure demonstrate that among participants with above-median rifapentine exposure, no TB-related unfavorable outcomes occurred during the 4-month treatment period, and TB-related unfavorable outcome rates were comparable across arms and risk groups at 12 months post randomization. In contrast, in participants with below-median rifapentine exposure, the substitution of moxifloxacin for ethambutol improved 12-month outcomes across all risk groups low: 6.6% to 4.4%; moderate: 11.3% to 6.1%; high: 29.4% to 14.3%). (Figure 4-2)

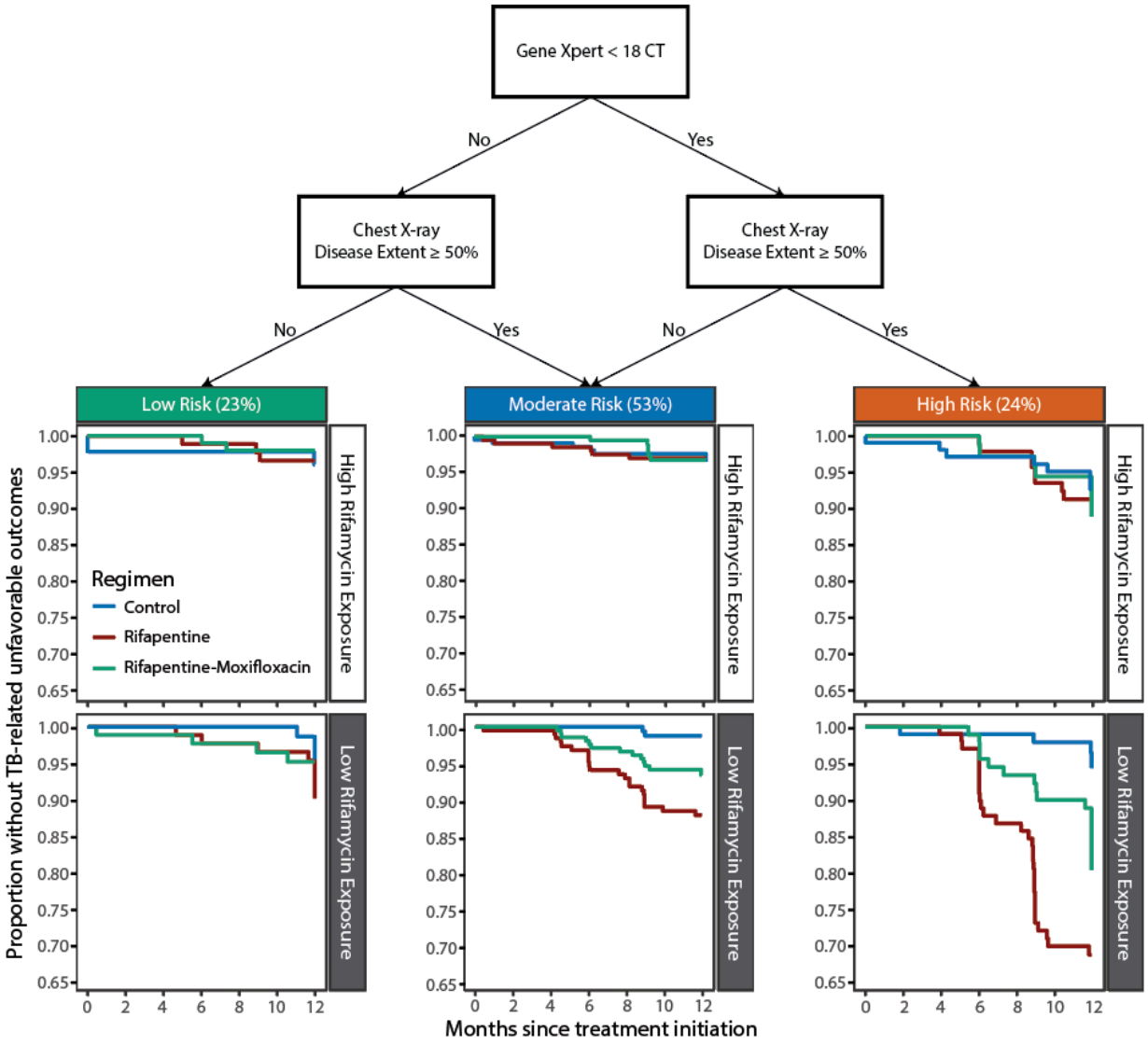

Figure 4-2 Xpert MTB/RIF cycle threshold and extent of disease on chest radiography stratify partcipants into low-risk, moderate-risk, and high-risk disease severity phenotypes.

Risk groups were defined by baseline Xpert MTB/RIF cycle threshold and extent of disease on chest radiography, defined as the percent involvement of the area of the thoracic area. Risk groups can be further stratified by rifamycin exposure, where Kaplan Meier estimates demonstrate that low risk participants do not need exposure optimization. Moderate risk participants receiving the rifapentine regimen require dose optimization to achieve optimal outcomes, while those receiving the rifapentine moxifloxacin regimen would benefit from dose optimization but is not required. The high-risk participants with high rifamycin exposure have promising percentage point differences, but none of the regimens achieve <5% tuberculosis-related unfavorable outcomes regardless of rifamycin exposure levels.

Phenotype Subgroup Analyses

The Study 31/A5349 risk phenotypes defined by our decision tree in Figure 3 demonstrated similar rates of tuberculosis-related unfavorable outcomes across the experimental and control regimens in the subpopulations at low risk (risk difference, 0.1%; 95% CI, -3.4% – 3.6%) and moderate-risk (risk difference, 2.5%; 95% CI, 0.1% – 4.9%). High risk participants who received the rifapentine-moxifloxacin regimen had higher tuberculosis-related unfavorable outcomes than the control (risk difference, 6.2%; 95% CI, 0.5% – 11.9%). Interaction p-values were not significant for all subpopulations (Figure 4-3A).

The Study 31/A5349 risk phenotypes defined by our decision tree in Figure 3 demonstrated similar rates of tuberculosis-related unfavorable outcomes across the rifapentine and control regimens in the subpopulations at low risk (risk difference, 2.1%; 95% CI, -2% – 6.1%). However, those classified as moderate risk and high risk experienced higher tuberculosis-related unfavorable outcomes than the control. (moderate risk: risk difference, 4.8%; 95% CI, 2% – 7.7% | high risk: risk difference, 13.9%; 95% CI, 7.6% – 20.2%). Interaction p-values were not significant for all subpopulations (Figure 4-3B).

We also validated the risk phenotypes previously described by Imperial et al. in the TB-ReFLECT analysis.[5] (Supplemental Figure 4-5)

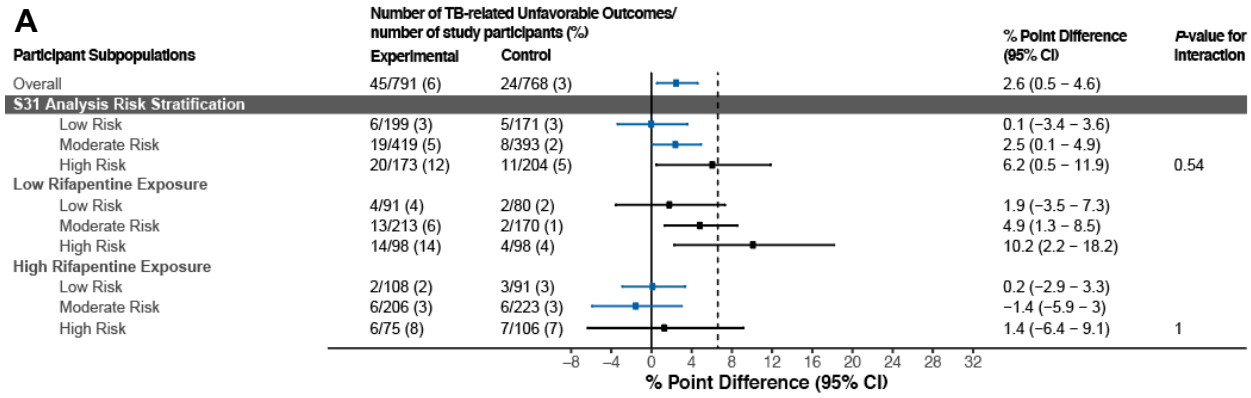

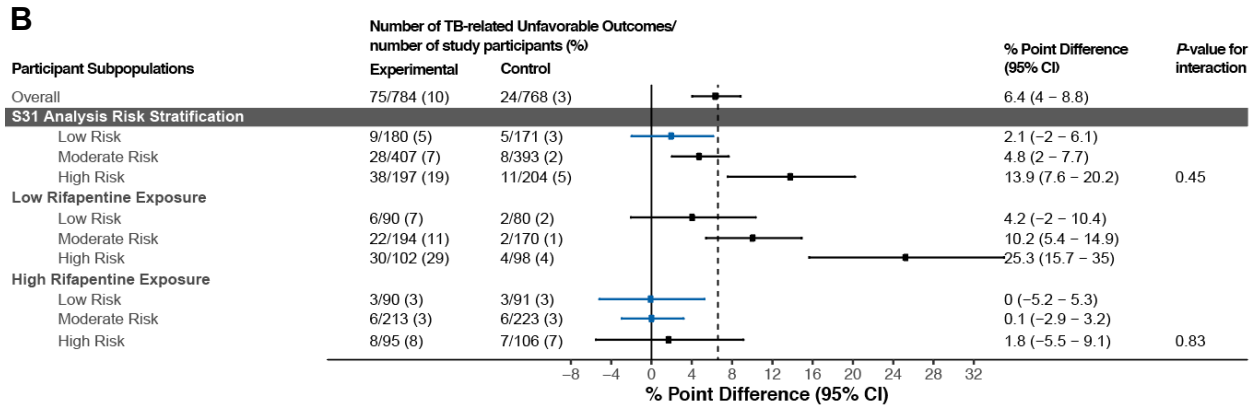

Figure 4-3 Risk Stratification Reveals a Low-risk Subgroup where Further Treatment Shortening and Simplification is Likely Possible and a High-risk Subgroup where Longer Treatment May Be Needed.

The figure shows the results of subgroup analyses of Study 31/A5349 risk groups. Low and high rifapentine subgroups in the experimental arms were compared to low and high rifampicin subgroups in the control arm. **(A)** Analysis of the rifapentine-moxifloxacin regimen demonstrates that the high-risk group, comprising 23% of the Study 31/A5349 population, requires a longer and/or more potent regimen than the rifapentine-moxifloxacin regimen. **(B)** Analysis of the rifapentine regimen demonstrates that the subpopulations at low risk, and moderate- or high-risk with high rifapentine exposure, comprising 60% of the Study 31/A5349 population, have small % point differences with the control. Additionally, in both rifapentine and rifapentine moxifloxacin regimens among participants with high rifapentine exposure, the differences between experimental and control regimens are not observed across all risk groups.

Safety

The primary safety outcome, any grade 3 or higher adverse events by regimen are reported in Supplemental Table 4-1 in MedDRA preferred terms.

In participants receiving rifapentine-moxifloxacin regimens, higher pyrazinamide exposures were associated with increased incidence of any grade 3 or higher adverse events (Odds Ratio, for every 100 μg·h/mL increase in $AUC_{0\text{-}24h}$ 1.22; 95% CI, 1.02 - 1.45) and treatment related grade 3 or higher adverse events (OR, for every 100 μg·h/mL increase in $AUC_{0\text{-}24h}$ 1.27; 95% CI, 1.04 - 1.55). Contrarily, there were no significant differences between quartiles of rifapentine exposure and any grade 3 or higher adverse events, treatment related grade 3 or higher adverse events, any serious adverse events, death, or tolerability. (Figure 4-4) In addition to pharmacokinetic factors, older age, shorter height, Karnofsky performance score, and history of liver disease were also univariately associated with grade 3 or higher adverse events (Supplemental Table 4-2). In multivariable analysis, older age (OR, 1.22 for every 10 year

increase, 95% CI, 1.06-1.41), shorter height (OR, 1.27 for every 10 cm decrease; 95% CI, 1.02-1.58), history of liver disease (OR, 7.90; 95% CI, 1.50-58.1), and higher pyrazinamide exposures (OR 1.22, 95% CI, 1.01-1.45) were associated with higher incidence of grade 3 or higher adverse events. Further sensitivity analyses to justify the inclusion of height are reported in the supplement.

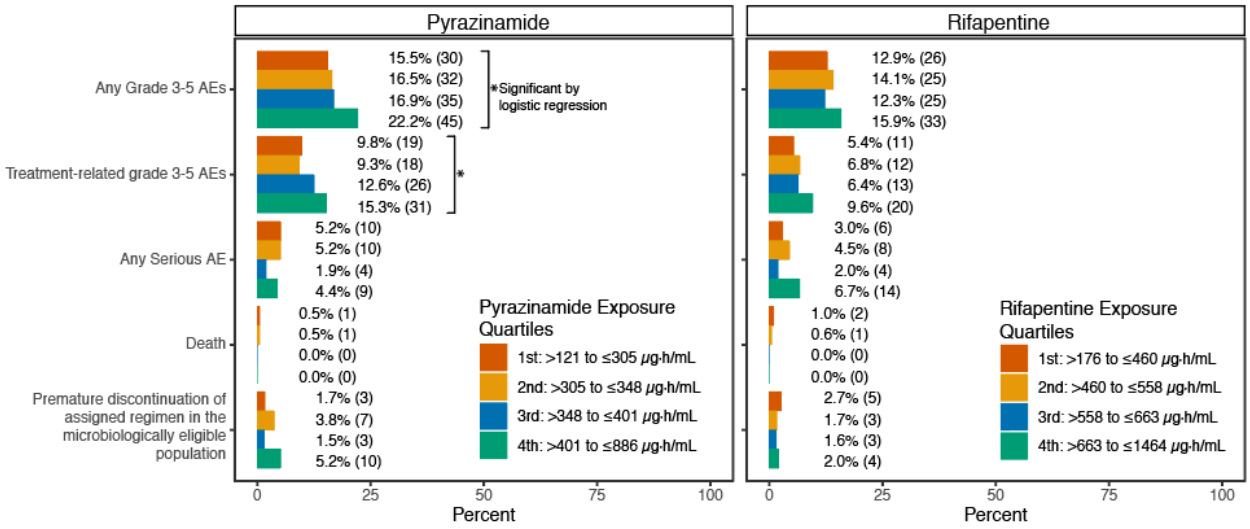

Figure 4-4 Among Participants Receiving Rifapentine-moxifloxacin Regimen, Higher Pyrazinamide Exposures are Associated with Primary Safety Outcome, Any Grade 3-5 Adverse Events, While Higher Rifapentine Exposures are Not Associated.

Higher pyrazinamide exposures were associated with increased incidence of any grade 3 or higher adverse events (Odds Ratio, for every 100 µg·h/mL increase in $AUC_{0\text{-}24h}$ 1.22; 95% CI, 1.02 - 1.45) and treatment related grade 3 or higher adverse events (OR, for every 100 µg·h/mL increase in $AUC_{0\text{-}24h}$ 1.27; 95% CI, 1.04 - 1.55). Contrarily, there is no significant difference between quartiles of rifapentine exposure and any grade 3 or higher adverse events, treatment related grade 3 or higher adverse events, any serious adverse events, death, or tolerability. Participants without pharmacokinetic sampling were excluded from this figure. Percentages are calculated from the safety population for all safety outcomes except tolerability, which was calculated from the microbiologically eligible population. For each quartile, percentage of participants with safety outcomes are reported with number of events in parentheses.

Among participants receiving the control regimen, univariable logistic regression found female sex, higher BMI, higher Gene Xpert, participants living with diabetes, current smokers (relative to nonsmokers), ethambutol $AUC_{0\text{-}24h}$, and pyrazinamide C_{max} to be associated with any grade 3 or higher adverse events (threshold $P<0.05$, Supplemental Table 4-3). Multivariable analysis the following factors to be associated with any grade 3 or higher adverse events: male sex (OR, 0.55 relative to female sex; 95% CI, 0.37 -

0.82), Gene Xpert (OR, 0.83 for every 3 cycle threshold decrease; 95% CI, 0.71 - 0.97), and ethambutol $AUC_{0\text{-}24h}$ (OR, 1.44 for every 5 μg·h/mL increase; 95% CI, 1.01 - 2.06). Furthermore, among participants receiving the rifapentine regimen, higher ethambutol $AUC_{0\text{-}24h}$ was also a factor that drove any grade 3 or above adverse events (OR, 1.39 for every 5 μg·h/mL increase; 95% CI, 1.02 - 1.98).

Univariable and multivariable safety analyses of rifapentine regimen and sensitivity analyses of imputed pharmacokinetic values can be found in the supplement.

Discussion

We have shown that baseline disease severity (defined by lower Xpert MTB/RIF cycle threshold and greater extent of disease on chest radiography), older age, and lower weight were baseline risk factors for TB-related unfavorable outcomes in the 4-month arms. Low rifapentine exposure was also a strong predictor of TB-related unfavorable outcome, even after adjusting for baseline risk factors. In contrast, low rifampicin exposure was not a risk factor for TB-related unfavorable outcomes in the control arm, suggesting that longer treatment durations can reduce treatment outcome differences due to differences in drug exposure. The 4-month rifapentine-moxifloxacin regimen had comparable efficacy to the control arm across a wide range of subgroups, demonstrating the robustness of the trial-level finding of non-inferiority. Furthermore, we identified low and moderate risk subgroups comprising 76% of trial participants where the risk of TB-related unfavorable outcome was comparably low in all three treatment regimens, indicating an opportunity for exploring further treatment shortening or further simplification of treatment.

Nunn, Savic, Imperial and others have previously reported aggregate cavity size as the most informative and predictive chest radiography measure of baseline disease burden. While aggregate cavity size was statistically and clinically significant, we found that extent of disease measured by percent involvement of the total thoracic area to be more informative for 12-month outcomes. Extent of disease, while well correlated with aggregate cavity size, may be measuring something slightly different, where aggregate cavity size measures the progression of pulmonary tuberculosis pathology, disease extent is a two-dimensional representation of various pathologies, such as infiltration, fibrosis, and cavitation of lung tissue.

Additionally, disease extent is easier to interpret in the field, as a clinician only need to count the number of quadrants affected by lesions on chest radiography as opposed to estimating and summing cavity diameter. This finding that disease extent is a more robust and statistically significant risk factor for TB-related unfavorable outcomes suggests that 12-month durable cures may depend more on the extent of lung tissue affected.

In the largest ever randomized controlled trial of the treatment of active pulmonary tuberculosis where all participants were sampled for pharmacokinetic analysis, there was no evidence that high rifapentine exposure was associated with an increase in adverse events or intolerability. In contrast, in participants receiving the rifapentine-moxifloxacin regimen, older age, shorter height, history of liver disease, and higher pyrazinamide exposures were associated with an increased incidence of adverse events (grade 3 or more). Shorter height as a risk factor for adverse events represents a continuation of an ongoing debate, whether height can be used as a measure of lifetime nutrition and therefore a prognostic marker for efficacy or safety. The debate has primarily been centered around how malnutrition affects cell based immunity and thus treatment outcomes and mortality[9,10], but conflicting evidence has been published thus far.[11,12] The finding here provides retrospective evidence in a large phase III trial that shorter height is strongly associated with adverse events and is a measure of lifetime [mal]nutrition. Finally, in control and rifapentine regimens, we found that higher ethambutol exposure was a consistent driver of adverse events in univariable and multivariable analyses. A follow-up ethambutol pharmacokinetic and pharmacodynamic study carefully defining the therapeutic window is being performed to assess the risk-benefit for its inclusion in tuberculosis treatment regimens.

Our findings have implications for design of future tuberculosis treatment trials. Previous analyses have identified a low-risk subpopulation for which shorter treatments may be possible and a high-risk subpopulation where large differences in treatment response between regimens are observed[5,13]. Our analysis confirmed these findings and found that, mitigating these differences in the high-risk subpopulation were key to the rifapentine-moxifloxacin regimen successfully demonstrating noninferiority whereas the rifapentine regimen failed. Specifically, these large differences in treatment response were mitigated by

sufficient rifapentine exposure and the substitution of moxifloxacin for ethambutol. In low resource settings, therapeutic dose monitoring remains impractical compared to increasing the rifapentine dose to ensure adequate exposure; on the other hand, therapeutic dose monitoring can be beneficial in high resource settings since individual rifapentine exposure is highly variable (Supplemental Figure 6).[14] Finally, despite careful dose-ranging trials[15,16] prior to the phase III trial, many participants nevertheless had suboptimal rifapentine exposures. Collection of pharmacokinetic samples and prespecified comprehensive pharmacokinetic-pharmacodynamic analyses in phase III trials is immensely valuable and can further provide critical information that guides clinical use of the new regimen.

Our study has limitations. Since the drugs were all tested as combination regimens, we could not distinguish relative contributions of each individual drug aside from comparing moxifloxacin versus ethambutol. Second, we acknowledge the risks involved with subgroup analyses in trials with a noninferiority design,[17] and whereas exploration of risk factors was prespecified in the parent protocol, the definitions of the low, moderate, and high-risk phenotypes presented here were not. We did, however, validate the prespecified easy, moderate, hard-to-treat phenotypes defined by Imperial et al.[5] and the definitions have been updated with a contemporary measure (i.e., Xpert MTB/RIF cycle threshold) of baseline disease burden. A third limitation is that no definite conclusions could be made regarding noninferiority given limited power. A clinical trial under development by the ACTG (A5414/SPECTRA-TB) incorporates stratified medicine principles in the evaluation of dose-optimized rifapentine and moxifloxacin containing ultra-short regimens. The design of that trial will provide adequate power for trial-level and stratum-level testing. Finally, a S31/A5349 eligibility criterion of sputum smear microscopy positive (or the equivalent as assessed by Xpert MTB/RIF) skewed the study population towards the more severe end of the pulmonary tuberculosis spectrum of severity. While this is unlikely to have impacted the risk factor analysis or stratification algorithm, our findings do not directly address patients with sputum smear-negative pulmonary tuberculosis, estimated to account for about 40-50% of pulmonary tuberculosis cases.[18,19]

In conclusion, achieving a high exposure to rifapentine in the 4-month rifapentine-moxifloxacin regimen reduces the risk of TB-related unfavorable outcomes, especially in individuals with more severe pulmonary

TB. Furthermore, patients can be stratified by baseline disease burden into a low-risk subgroup in which further treatment shortening and simplification are likely to be possible and a high-risk subgroup in which longer treatment may be needed.

References

1. Dorman, S. E. *et al.* High-dose rifapentine with or without moxifloxacin for shortening treatment of pulmonary tuberculosis: Study protocol for TBTC study 31/ACTG A5349 phase 3 clinical trial. *Contemporary Clinical Trials* **90**, 105938 (2020).
2. Dorman, S. E. *et al.* Four-Month Rifapentine Regimens with or without Moxifloxacin for Tuberculosis. *N Engl J Med* **384**, 1705–1718 (2021).
3. World Health Organization. *Treatment of drug-susceptible tuberculosis: rapid communication*. (World Health Organization, 2021).
4. Carr, W. *et al.* Interim Guidance: 4-Month Rifapentine-Moxifloxacin Regimen for the Treatment of Drug-Susceptible Pulmonary Tuberculosis — United States, 2022. *MMWR Morb. Mortal. Wkly. Rep.* **71**, 285–289 (2022).
5. Imperial, M. Z. *et al.* A patient-level pooled analysis of treatment-shortening regimens for drug-susceptible pulmonary tuberculosis. *Nat Med* **24**, 1708–1715 (2018).
6. Lange, C. *et al.* Perspective for Precision Medicine for Tuberculosis. *Frontiers in Immunology* **11**, (2020).
7. Imperial, M. Z., Phillips, P. P. J., Nahid, P. & Savic, R. M. Precision-Enhancing Risk Stratification Tools for Selecting Optimal Treatment Durations in Tuberculosis Clinical Trials. *Am J Respir Crit Care Med* **204**, 1086–1096 (2021).
8. Turkova, A. *et al.* Shorter Treatment for Nonsevere Tuberculosis in African and Indian Children. *N Engl J Med* **386**, 911–922 (2022).
9. Cegielski, J. P. & McMurray, D. N. The relationship between malnutrition and tuberculosis: evidence from studies in humans and experimental animals. 13.
10. Chandrasekaran, P., Saravanan, N., Bethunaickan, R. & Tripathy, S. Malnutrition: Modulator of Immune Responses in Tuberculosis. *Front. Immunol.* **8**, 1316 (2017).
11. Bach, F., Wejse, C., Storgaard, M. & Patsche, C. B. Is body height a prognostic marker for outcome of tuberculosis treatment? *Infectious Diseases* **54**, 538–541 (2022).
12. Faurholt-Jepsen, D. *et al.* Height as a prognostic marker for survival during antituberculous therapy. *Infectious Diseases* **47**, 515–516 (2015).

13. Aber, V. R. & Nunn, A. J. [Short term chemotherapy of tuberculosis. Factors affecting relapse following short term chemotherapy]. *Bull Int Union Tuberc* **53**, 276–280 (1978).
14. Pharmacokinetics of Rifapentine at 600, 900, and 1,200 mg during Once-Weekly Tuberculosis Therapy. https://www.atsjournals.org/doi/epdf/10.1164/rccm.200311-1612OC doi:10.1164/rccm.200311-1612OC.
15. Dorman, S. E. *et al.* Daily Rifapentine for Treatment of Pulmonary Tuberculosis. A Randomized, Dose-Ranging Trial. *Am J Respir Crit Care Med* **191**, 333–343 (2015).
16. Savic, R. *et al.* Defining the optimal dose of rifapentine for pulmonary tuberculosis: Exposure-response relations from two phase II clinical trials. *Clin. Pharmacol. Ther.* **102**, 321–331 (2017).
17. Wang, R., Lagakos, S. W., Ware, J. H., Hunter, D. J. & Drazen, J. M. Statistics in Medicine — Reporting of Subgroup Analyses in Clinical Trials. *N Engl J Med* **357**, 2189–2194 (2007).
18. Asadi, L. *et al.* How much do smear-negative patients really contribute to tuberculosis transmissions? Re-examining an old question with new tools. *eClinicalMedicine* **43**, 101250 (2022).
19. Linguissi, L. S. G. *et al.* Diagnosis of smear-negative pulmonary tuberculosis based on clinical signs in the Republic of Congo. *BMC Res Notes* **8**, 804 (2015).
20. Najjingo, I. *et al.* Comparison of GeneXpert cycle threshold values with smear microscopy and culture as a measure of mycobacterial burden in five regional referral hospitals of Uganda- A cross-sectional study. *PLoS ONE* **14**, e0216901 (2019).
21. Merle, C. S. *et al.* A Four-Month Gatifloxacin-Containing Regimen for Treating Tuberculosis. *N Engl J Med* **371**, 1588–1598 (2014).
22. Gillespie, S. H. *et al.* Four-Month Moxifloxacin-Based Regimens for Drug-Sensitive Tuberculosis. *N Engl J Med* **371**, 1577–1587 (2014).
23. Jindani, A. *et al.* High-Dose Rifapentine with Moxifloxacin for Pulmonary Tuberculosis. *N Engl J Med* **371**, 1599–1608 (2014).

Supplementary Information

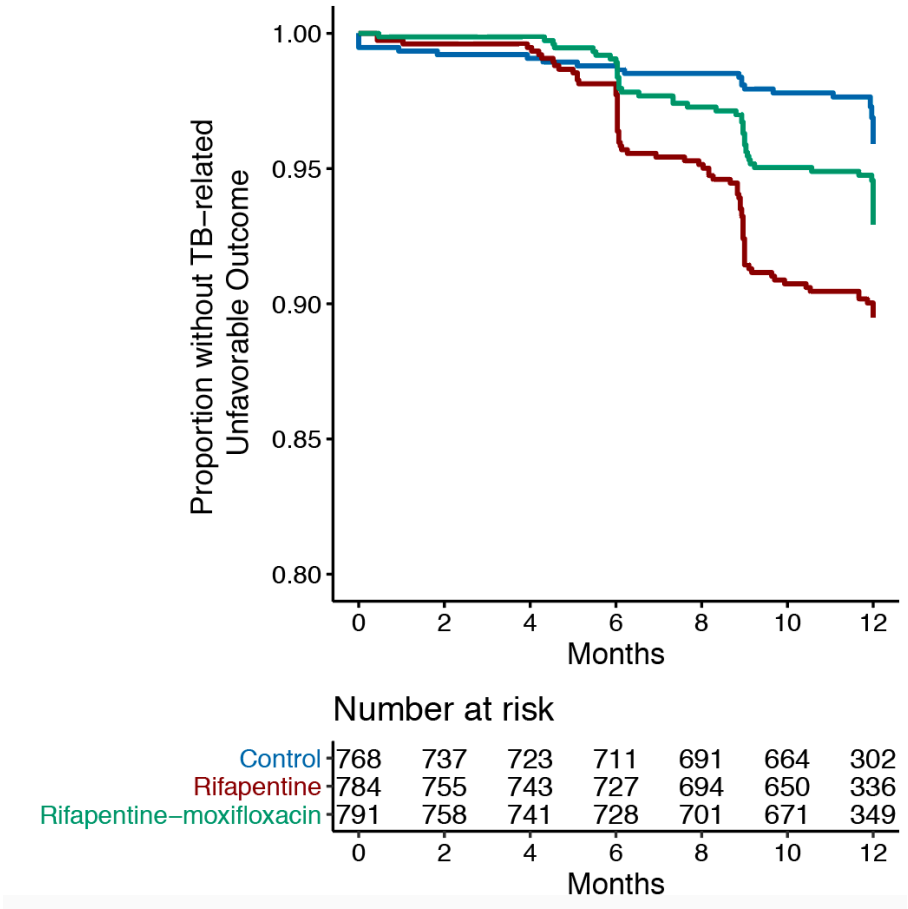

Supplemental Figure 4-1 Kaplan-Meier Estimates of Time to Tuberculosis-Related Unfavorable Outcomes by Regimen

Favorable outcomes and not tuberculosis-related unfavorable outcomes were right censored at the time of last visit and time to event

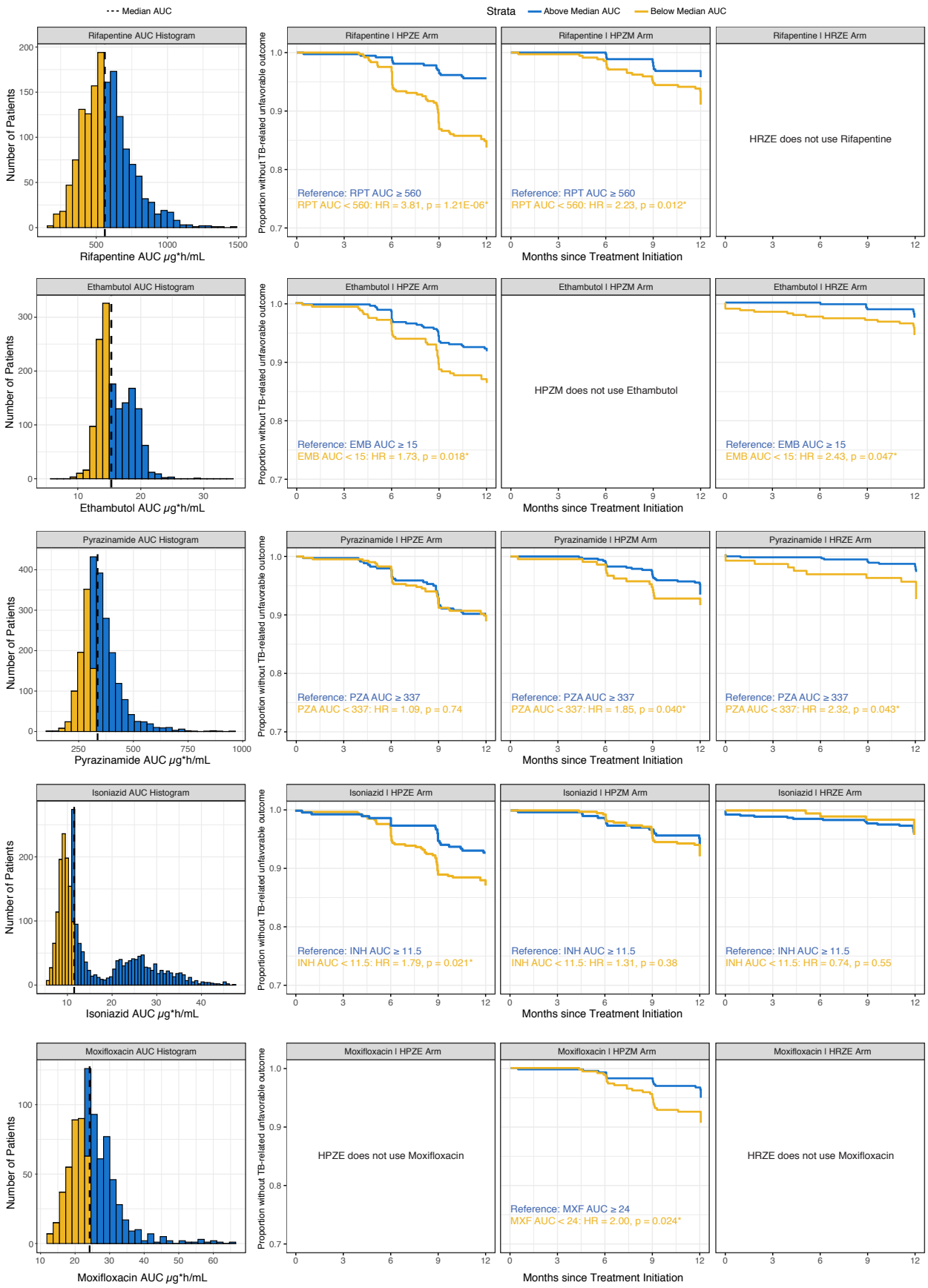
Median AUC
Strata
Above Median AUC
Below Median AUC
Rifapentine AUC Histogram
Rifapentine I HPZE Arm
Rifapentine I HPZM Arm
Rifapentine I HRZE Arm
Number of Patients
Proportion without TB-related unfavorable outcome
Rifapentine AUC μg*h/mL
Reference: RPT AUC ≥ 560
RPT AUC < 560: HR = 3.81, p = 1.21E-06*
Reference: RPT AUC ≥ 560
RPT AUC < 560: HR = 2.23, p = 0.012*
HRZE does not use Rifapentine
Months since Treatment Initiation
Ethambutol AUC Histogram
Ethambutol I HPZE Arm
Ethambutol I HPZM Arm
Ethambutol I HRZE Arm
Ethambutol AUC μg*h/mL
Reference: EMB AUC ≥ 15
EMB AUC < 15: HR = 1.73, p = 0.018*
HPZM does not use Ethambutol
Reference: EMB AUC ≥ 15
EMB AUC < 15: HR = 2.43, p = 0.047*
Pyrazinamide AUC Histogram
Pyrazinamide I HPZE Arm
Pyrazinamide I HPZM Arm
Pyrazinamide I HRZE Arm
Pyrazinamide AUC μg*h/mL
Reference: PZA AUC ≥ 337
PZA AUC < 337: HR = 1.09, p = 0.74
Reference: PZA AUC ≥ 337
PZA AUC < 337: HR = 1.85, p = 0.040*
Reference: PZA AUC ≥ 337
PZA AUC < 337: HR = 2.32, p = 0.043*
Isoniazid AUC Histogram
Isoniazid I HPZE Arm
Isoniazid I HPZM Arm
Isoniazid I HRZE Arm
Isoniazid AUC μg*h/mL
Reference: INH AUC ≥ 11.5
INH AUC < 11.5: HR = 1.79, p = 0.021*
Reference: INH AUC ≥ 11.5
INH AUC < 11.5: HR = 1.31, p = 0.38
Reference: INH AUC ≥ 11.5
INH AUC < 11.5: HR = 0.74, p = 0.55
Moxifloxacin AUC Histogram
Moxifloxacin I HPZE Arm
Moxifloxacin I HPZM Arm
Moxifloxacin I HRZE Arm
Moxifloxacin AUC μg*h/mL
HPZE does not use Moxifloxacin
Reference: MXF AUC ≥ 24
MXF AUC < 24: HR = 2.00, p = 0.024*
HRZE does not use Moxifloxacin

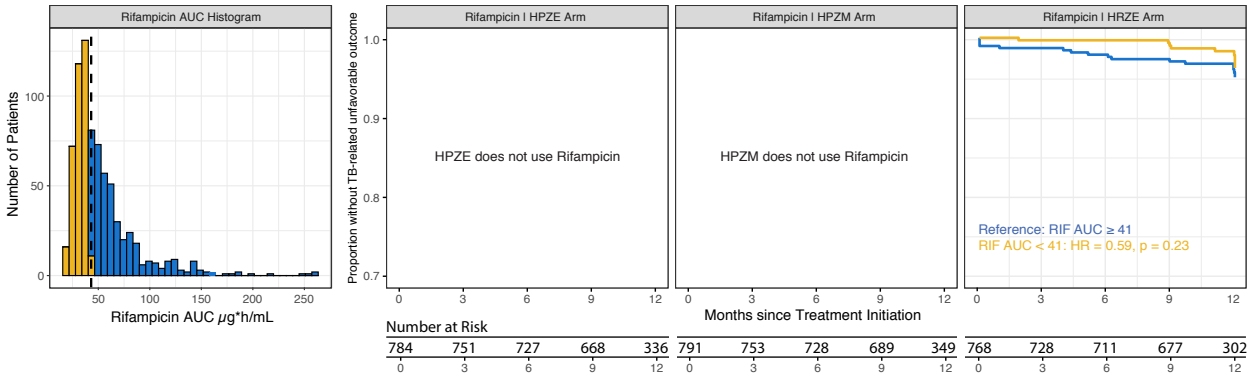

Supplemental Figure 4-2 Study 31 Steady State $AUC_{0\text{-}24h}$ Histograms of Each Drug and Kaplan Meier Estimate of Time to Tuberculosis-related Unfavorable Outcome for experimental arms stratified by arm and drug exposure. Hazard ratios and p values for logrank test are reported in each plot respectively.

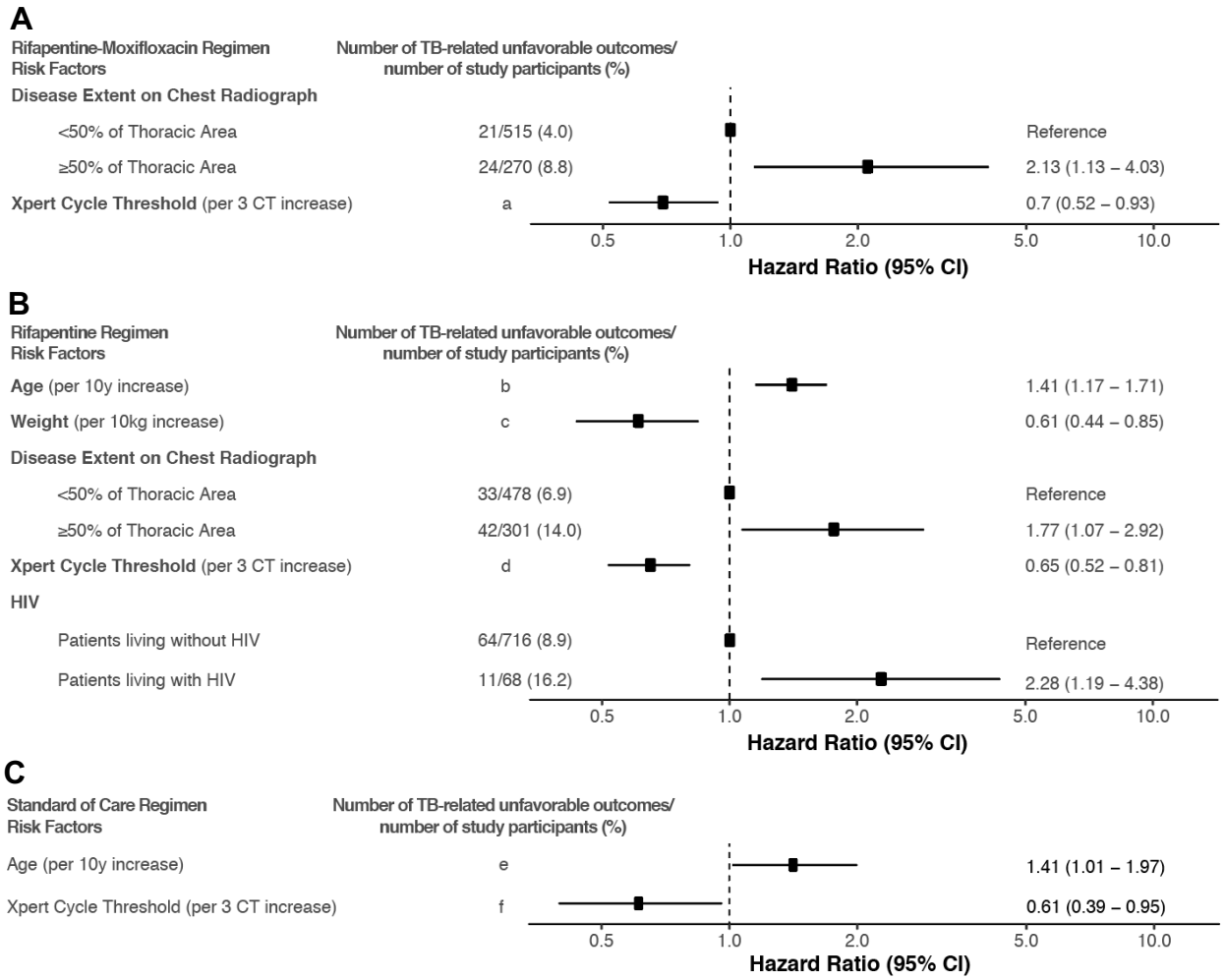

Supplemental Figure 4-3 Multivariate Hazard Ratios for Tuberculosis-Related Unfavorable Outcomes with only Baseline Predictors

Multivariate analysis of baseline predictors (without pharmacokinetic predictors) for the rifapentine-moxifloxacin, rifapentine, and the control regimen. **(a)** Xpert cycle threshold < 18, 29/397 (7.3); Xpert cycle threshold ≥ 18, 10/296 (3.4), **(b)** Age < 30 years, 21/354 (5.9); Age ≥ 30 years, 54/430 (12.6), **(c)** Weight < 53 kg, 45/364 (12.4); Weight ≥ 53 kg, 30/419 (7.2), **(d)** Xpert cycle threshold < 18, 54/397 (13.6); Xpert cycle threshold ≥ 18, 13/284 (7.7), **(e)** Age < 30 years, 4/353 (1.1); Age ≥ 30 years, 20/415 (4.8), **(f)** Xpert cycle threshold < 18, 15/399 (3.7); Xpert cycle threshold ≥ 18, 5/268 (1.9)

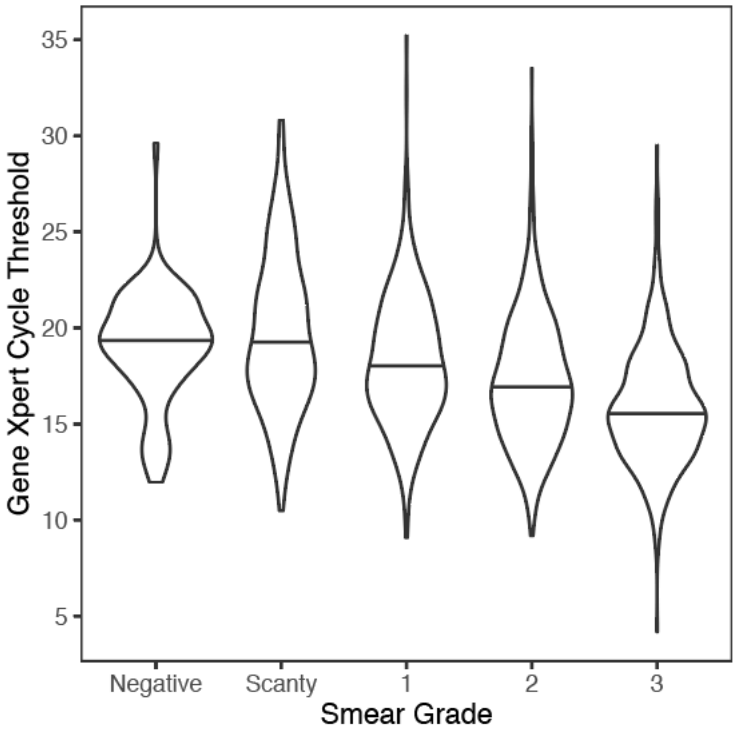

Supplemental Figure 4-4 Violin Plot of Gene Xpert Cycle Threshold Values by Smear Grade

The central line in each violin represents the median value. Gene Xpert and smear grade do not have a perfect translation, but cycle threshold decreases with increasing smear grade. Negative smear grade = 19.4 median cycle threshold, scanty smear grade = 19.1 median cycle threshold, smear grade 1+ = 18 median cycle threshold, smear grade 2+ = 16.9 median cycle threshold, smear grade 3+ = 15.5 median cycle threshold.

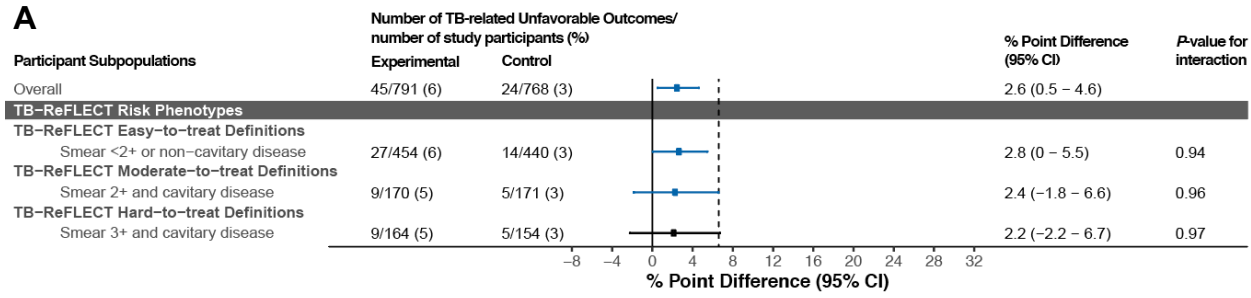

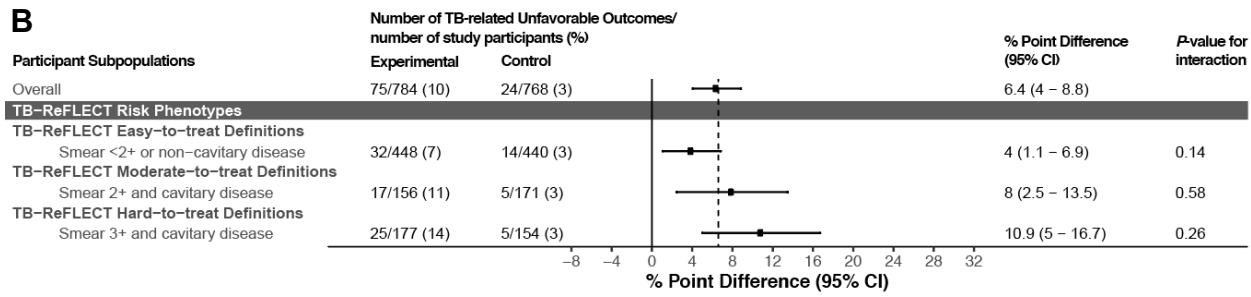

Supplemental Figure 4-5 Prespecified Risk Phenotype Definitions from TB-ReFLECT Analysis are Validated in the Rifapentine Regimen

The figure shows the results of subgroup analyses of TB-ReFLECT risk groups as defined by Imperial et al.[5] **(A)** Percentage point differences remain small across all TB-ReFLECT risk phenotypes in the rifapentine-moxifloxacin regimen. **(B)** The expected graded response is observed in the rifapentine regimen, where the easy-to-treat phenotype has small % point differences relative to control and the hard-to-treat phenotype has large % point differences.

Supplemental Table 4-1 MedDRA coded grade 3 or higher Adverse Events by Regimen

Number of patients (% of patients) are reported in the first column of each regimen, then the number of events in the second column.

SYSTEM ORGAN CLASS	PREFERRED TERM	CONTROL REGIMEN N=825		RIFAPENTINE N=835		RIFAPENTINE-MOXIFLOXACIN N=846	
		N (%)	N events	N (%)	N events	N (%)	N events
BLOOD AND LYMPHATIC SYSTEM DISORDERS	ANAEMIA	5 (0.61)	5	1 (0.12)	1	5 (0.59)	5
	HAEMOLYTIC ANAEMIA	1 (0.12)	1	0 (0)	0	0 (0)	0
	HYPOCHROMIC ANAEMIA	1 (0.12)	1	0 (0)	0	0 (0)	0
	IRON DEFICIENCY ANAEMIA	1 (0.12)	1	0 (0)	0	0 (0)	0
	LEUKOCYTOSIS	0 (0)	0	0 (0)	0	1 (0.12)	1
	LEUKOPENIA	0 (0)	0	3 (0.36)	3	1 (0.12)	1
	LYMPHOPENIA	0 (0)	0	0 (0)	0	3 (0.35)	3
	MICROCYTIC ANAEMIA	1 (0.12)	1	0 (0)	0	0 (0)	0
	NEUTROPENIA	47 (5.7)	53	33 (3.95)	36	56 (6.62)	67
	THROMBOCYTOPENIA	0 (0)	0	1 (0.12)	1	1 (0.12)	1
	THROMBOTIC THROMBOCYTOPENIC PURPURA	0 (0)	0	0 (0)	0	1 (0.12)	1
HEPATOBILIARY DISORDERS	CHOLELITHIASIS	0 (0)	0	1 (0.12)	1	0 (0)	0
	GAMMA GT RAISED	0 (0)	0	0 (0)	0	1 (0.12)	1
	HEPATITIS	26 (3.15)	27	25 (2.99)	28	38 (4.49)	40
	HYPERBILIRUBINAEMIA	0 (0)	0	1 (0.12)	1	2 (0.24)	2
VASCULAR DISORDERS	AORTIC ANEURYSM	0 (0)	0	0 (0)	0	1 (0.12)	1
	AORTIC THROMBOSIS	1 (0.12)	1	0 (0)	0	0 (0)	0
	DEEP VEIN THROMBOSIS	3 (0.36)	3	1 (0.12)	1	1 (0.12)	1
	HYPERTENSION	16 (1.94)	18	16 (1.92)	18	13 (1.54)	18
INFECTIONS AND INFESTATIONS	BODY TINEA	0 (0)	0	0 (0)	0	1 (0.12)	1
	BONE TUBERCULOSIS	1 (0.12)	1	0 (0)	0	0 (0)	0
	CONJUNCTIVITIS	0 (0)	0	0 (0)	0	1 (0.12)	1
	CONJUNCTIVITIS VIRAL	1 (0.12)	1	0 (0)	0	0 (0)	0
	DENGUE FEVER	0 (0)	0	1 (0.12)	1	0 (0)	0
	DISSEMINATED TUBERCULOSIS	0 (0)	0	1 (0.12)	1	0 (0)	0
	EXTRAPULMONARY TUBERCULOSIS	0 (0)	0	1 (0.12)	1	0 (0)	0
	GASTROENTERITIS	1 (0.12)	1	0 (0)	0	0 (0)	0
	HEPATITIS A	0 (0)	0	1 (0.12)	1	0 (0)	0
	HEPATITIS C	0 (0)	0	0 (0)	0	1 (0.12)	1
	HIV INFECTION CDC GROUP IV SUBGROUP C1	0 (0)	0	1 (0.12)	1	0 (0)	0
	LOWER RESPIRATORY TRACT INFECTION	0 (0)	0	1 (0.12)	1	0 (0)	0
	LUNG ABSCESS	0 (0)	0	1 (0.12)	1	0 (0)	0
	MALARIA	3 (0.36)	5	0 (0)	0	2 (0.24)	2
	OOPHORITIS	0 (0)	0	1 (0.12)	1	0 (0)	0
	ORCHITIS	0 (0)	0	1 (0.12)	1	0 (0)	0
	PARACOCCIDIOIDES INFECTION	1 (0.12)	1	0 (0)	0	0 (0)	0
	PELVIC INFLAMMATORY DISEASE	2 (0.24)	2	0 (0)	0	0 (0)	0
	PERICARDITIS TUBERCULOUS	0 (0)	0	0 (0)	0	1 (0.12)	1
	PNEUMOCYSTIS JIROVECII PNEUMONIA	1 (0.12)	1	0 (0)	0	0 (0)	0
	PNEUMONIA	2 (0.24)	2	1 (0.12)	1	4 (0.47)	5
	PNEUMONIA BACTERIAL	2 (0.24)	2	2 (0.24)	2	1 (0.12)	1
	PULMONARY TUBERCULOSIS	0 (0)	0	2 (0.24)	2	2 (0.24)	2
	RESPIRATORY TRACT INFECTION	1 (0.12)	1	0 (0)	0	0 (0)	0
	SEPSIS	1 (0.12)	1	0 (0)	0	0 (0)	0
	TUBERCULOSIS	1 (0.12)	1	0 (0)	0	0 (0)	0
	URINARY TRACT INFECTION	1 (0.12)	1	1 (0.12)	1	0 (0)	0
	VULVOVAGINAL CANDIDIASIS	0 (0)	0	0 (0)	0	1 (0.12)	1
PREGNANCY, PUERPERIUM AND PERINATAL CONDITIONS	ABORTION SPONTANEOUS	0 (0)	0	0 (0)	0	1 (0.12)	1
	COMPLICATION OF PREGNANCY	0 (0)	0	0 (0)	0	1 (0.12)	1
	PRE-ECLAMPSIA	1 (0.12)	2	0 (0)	0	0 (0)	0
	PREGNANCY	20 (2.42)	22	9 (1.08)	10	10 (1.18)	11
	PRETERM PREMATURE RUPTURE OF MEMBRANES	0 (0)	0	0 (0)	0	1 (0.12)	1
METABOLISM AND NUTRITION DISORDERS	ABNORMAL LOSS OF WEIGHT	0 (0)	0	0 (0)	0	1 (0.12)	1
	ABNORMAL WEIGHT GAIN	0 (0)	0	1 (0.12)	1	0 (0)	0
	DIABETES MELLITUS	1 (0.12)	1	0 (0)	0	0 (0)	0
	DIABETES MELLITUS INADEQUATE CONTROL	3 (0.36)	5	2 (0.24)	2	3 (0.35)	6
	DIABETIC KETOACIDOSIS	0 (0)	0	0 (0)	0	1 (0.12)	2
	GOUT	1 (0.12)	1	0 (0)	0	0 (0)	0
	HYPERGLYCAEMIA	1 (0.12)	1	1 (0.12)	1	1 (0.12)	1
	HYPERKALAEMIA	4 (0.48)	4	0 (0)	0	2 (0.24)	2
	HYPOALBUMINAEMIA	0 (0)	0	2 (0.24)	2	0 (0)	0
	HYPOGLYCAEMIA	1 (0.12)	1	0 (0)	0	0 (0)	0
	HYPONATRAEMIA	0 (0)	0	1 (0.12)	2	1 (0.12)	1
	PSEUDOHYPERKALAEMIA	1 (0.12)	1	0 (0)	0	1 (0.12)	1
	TYPE 2 DIABETES MELLITUS	0 (0)	0	0 (0)	0	1 (0.12)	1
RESPIRATORY, THORACIC AND MEDIASTINAL DISORDERS	BRONCHIECTASIS	0 (0)	0	0 (0)	0	1 (0.12)	1
	BRONCHOSPASM	0 (0)	0	0 (0)	0	1 (0.12)	1
	CHRONIC OBSTRUCTIVE PULMONARY DISEASE	1 (0.12)	2	0 (0)	0	0 (0)	0
	DYSPNOEA	0 (0)	0	2 (0.24)	2	0 (0)	0
	HAEMOPTYSIS	5 (0.61)	6	3 (0.36)	3	3 (0.35)	3
	PLEURAL EFFUSION	0 (0)	0	0 (0)	0	1 (0.12)	1
	PNEUMOTHORAX	0 (0)	0	0 (0)	0	1 (0.12)	1
	PULMONARY EMBOLISM	3 (0.36)	3	1 (0.12)	1	0 (0)	0

SYSTEM ORGAN CLASS	PREFERRED TERM	CONTROL REGIMEN N=825		RIFAPENTINE N=835		RIFAPENTINE-MOXIFLOXACIN N=846	
		N (%)	N events	N (%)	N events	N (%)	N events
INJURY, POISONING AND PROCEDURAL COMPLICATIONS	ALCOHOL POISONING	0 (0)	0	1 (0.12)	1	0 (0)	0
	CRANIOCEREBRAL INJURY	0 (0)	0	1 (0.12)	1	0 (0)	0
	DOCUMENTED HYPERSENSITIVITY TO ADMINISTERED PRODUCT	1 (0.12)	1	0 (0)	0	0 (0)	0
	EYE INJURY	1 (0.12)	1	0 (0)	0	0 (0)	0
	HAND FRACTURE	1 (0.12)	1	0 (0)	0	0 (0)	0
	HUMERUS FRACTURE	1 (0.12)	1	0 (0)	0	0 (0)	0
	INJURY	0 (0)	0	0 (0)	0	1 (0.12)	1
	LIMB INJURY	1 (0.12)	1	0 (0)	0	0 (0)	0
	OVERDOSE	1 (0.12)	1	1 (0.12)	1	0 (0)	0
	ROAD TRAFFIC ACCIDENT	0 (0)	0	1 (0.12)	1	0 (0)	0
	STAB WOUND	0 (0)	0	2 (0.24)	2	0 (0)	0
	THERMAL BURN	1 (0.12)	1	0 (0)	0	0 (0)	0
	TIBIA FRACTURE	1 (0.12)	1	0 (0)	0	0 (0)	0
	ULNA FRACTURE	1 (0.12)	1	0 (0)	0	0 (0)	0
SKIN AND SUBCUTANEOUS TISSUE DISORDERS	ANGIOEDEMA	0 (0)	0	1 (0.12)	1	0 (0)	0
	DRUG REACTION WITH EOSINOPHILIA AND SYSTEMIC SYMPTOMS	1 (0.12)	1	0 (0)	0	0 (0)	0
	PRURITUS	0 (0)	0	1 (0.12)	1	1 (0.12)	1
	RASH GENERALISED	0 (0)	0	1 (0.12)	1	1 (0.12)	1
	RASH MACULO-PAPULAR	0 (0)	0	0 (0)	0	1 (0.12)	1
	RASH PRURITIC	0 (0)	0	2 (0.24)	2	0 (0)	0
	URTICARIA	0 (0)	0	1 (0.12)	1	4 (0.47)	4
NERVOUS SYSTEM DISORDERS	CENTRAL NERVOUS SYSTEM LESION	1 (0.12)	2	0 (0)	0	0 (0)	0
	CEREBRAL INFARCTION	0 (0)	0	0 (0)	0	1 (0.12)	1
	CEREBROVASCULAR ACCIDENT	0 (0)	0	0 (0)	0	1 (0.12)	1
	EPILEPSY	1 (0.12)	1	0 (0)	0	0 (0)	0
	GUILLAIN-BARRE SYNDROME	0 (0)	0	0 (0)	0	1 (0.12)	1
	NEUROPATHY PERIPHERAL	0 (0)	0	1 (0.12)	1	0 (0)	0
	SEIZURE	1 (0.12)	1	0 (0)	0	0 (0)	0
	SYNCOPE	0 (0)	0	0 (0)	0	2 (0.24)	2
	TEMPORAL LOBE EPILEPSY	1 (0.12)	1	0 (0)	0	0 (0)	0
EYE DISORDERS	ASTIGMATISM	0 (0)	0	0 (0)	0	1 (0.12)	1
	BLEPHARITIS	0 (0)	0	1 (0.12)	1	0 (0)	0
	CATARACT	0 (0)	0	0 (0)	0	1 (0.12)	1
	CONJUNCTIVITIS ALLERGIC	0 (0)	0	0 (0)	0	1 (0.12)	1
	DIABETIC RETINOPATHY	1 (0.12)	1	0 (0)	0	0 (0)	0
	OPTIC NEUROPATHY	1 (0.12)	1	0 (0)	0	0 (0)	0
	REFRACTION DISORDER	0 (0)	0	0 (0)	0	1 (0.12)	1
	VISUAL ACUITY REDUCED	2 (0.24)	2	0 (0)	0	0 (0)	0
	VITRITIS	0 (0)	0	0 (0)	0	1 (0.12)	1
INVESTIGATIONS	BLOOD BILIRUBIN INCREASED	0 (0)	0	0 (0)	0	1 (0.12)	1
	BLOOD PRESSURE INCREASED	1 (0.12)	1	2 (0.24)	2	2 (0.24)	2
	PREGNANCY TEST FALSE POSITIVE	1 (0.12)	1	1 (0.12)	1	1 (0.12)	1
	WEIGHT DECREASED	1 (0.12)	1	0 (0)	0	0 (0)	0
NEOPLASMS BENIGN, MALIGNANT AND UNSPECIFIED (INCL CYSTS AND POLYPS)	ANOGENITAL WARTS	1 (0.12)	1	0 (0)	0	0 (0)	0
	BLADDER TRANSITIONAL CELL CARCINOMA	0 (0)	0	1 (0.12)	1	0 (0)	0
	BREAST CANCER	1 (0.12)	1	0 (0)	0	0 (0)	0
	LYMPHOMA	0 (0)	0	1 (0.12)	1	0 (0)	0
	NEOPLASM MALIGNANT	1 (0.12)	1	0 (0)	0	0 (0)	0
	OESOPHAGEAL CARCINOMA	0 (0)	0	0 (0)	0	1 (0.12)	1
	PAPILLARY THYROID CANCER	1 (0.12)	1	0 (0)	0	0 (0)	0
	PERIPHERAL NERVE SHEATH TUMOUR MALIGNANT	1 (0.12)	1	0 (0)	0	0 (0)	0
	SQUAMOUS CELL CARCINOMA	1 (0.12)	1	0 (0)	0	0 (0)	0
	SQUAMOUS CELL CARCINOMA OF THE TONGUE	1 (0.12)	1	0 (0)	0	0 (0)	0
GASTROINTESTINAL DISORDERS	GASTRITIS	0 (0)	0	0 (0)	0	1 (0.12)	1
	PANCREATITIS ACUTE	1 (0.12)	1	0 (0)	0	0 (0)	0
	PEPTIC ULCER	0 (0)	0	0 (0)	0	1 (0.12)	1
	PNEUMATOSIS INTESTINALIS	1 (0.12)	2	0 (0)	0	0 (0)	0
	SMALL INTESTINAL OBSTRUCTION	1 (0.12)	1	0 (0)	0	0 (0)	0
	VOMITING	0 (0)	0	1 (0.12)	1	0 (0)	0
GENERAL DISORDERS AND ADMINISTRATION SITE CONDITIONS	ADVERSE DRUG REACTION	0 (0)	0	0 (0)	0	2 (0.24)	3
	DEATH	1 (0.12)	1	1 (0.12)	1	0 (0)	0
	DRUG INTOLERANCE	1 (0.12)	1	0 (0)	0	0 (0)	0
	PYREXIA	1 (0.12)	1	0 (0)	0	0 (0)	0
MUSCULOSKELETAL AND CONNECTIVE TISSUE DISORDERS	ARTHRALGIA	2 (0.24)	2	0 (0)	0	1 (0.12)	1
	COSTOCHONDRITIS	1 (0.12)	1	0 (0)	0	0 (0)	0
	INTERVERTEBRAL DISC DISORDER	0 (0)	0	1 (0.12)	1	0 (0)	0
	SACROILIITIS	1 (0.12)	1	0 (0)	0	0 (0)	0
	SPINAL OSTEOARTHRITIS	1 (0.12)	1	0 (0)	0	0 (0)	0
CARDIAC DISORDERS	CARDIAC FAILURE CONGESTIVE	0 (0)	0	0 (0)	0	1 (0.12)	2
	COR PULMONALE	1 (0.12)	1	0 (0)	0	0 (0)	0
	LONG QT SYNDROME	0 (0)	0	0 (0)	0	1 (0.12)	1
	RIGHT VENTRICULAR FAILURE	0 (0)	0	0 (0)	0	1 (0.12)	1
PSYCHIATRIC DISORDERS	BRIEF PSYCHOTIC DISORDER, WITH POSTPARTUM ONSET	1 (0.12)	1	0 (0)	0	0 (0)	0
	DISORIENTATION	0 (0)	0	0 (0)	0	1 (0.12)	1
	SUICIDE ATTEMPT	0 (0)	0	1 (0.12)	1	1 (0.12)	1
IMMUNE SYSTEM DISORDERS	DRUG HYPERSENSITIVITY	0 (0)	0	0 (0)	0	2 (0.24)	2
RENAL AND URINARY DISORDERS	RENAL IMPAIRMENT	0 (0)	0	0 (0)	0	1 (0.12)	1
	RENAL TUBULAR NECROSIS	0 (0)	0	0 (0)	0	1 (0.12)	1
CONGENITAL, FAMILIAL AND GENETIC DISORDERS	CONGENITAL ANOMALY	0 (0)	0	1 (0.12)	1	0 (0)	0

Supplemental Table 4-2 Univariable and Multivariable Safety Analysis of Any Grade 3 or Higher Adverse Events in Participants Receiving Rifapentine-Moxifloxacin Regimen in the Safety Population.

Baseline clinical factors and individual drug pharmacokinetic estimates were evaluated in univariable and multivariable logistic regression models as potential risk factors for the occurrence of any grade 3 or higher adverse events.

Predictor	Unadjusted Odds Ratio	Unadjusted 95% CI	Unadjusted p-value	Adjusted Odds Ratio	Adjusted 95% CI	Adjusted p-value
DEMOGRAPHIC FACTORS						
Age (for every 10 years)	**1.23**	**1.07 - 1.42**	**0.00415**	**1.22**	**1.06 - 1.41**	**0.0057**
Male sex (relative to female)	0.88	0.61 - 1.28	0.49			
Height (for every 10 cm decrease)	**1.27**	**1.03 - 1.57**	**0.028**	**1.27**	**1.02 - 1.58**	**0.030**
WT (for every 10 kg)	0.94	0.77 - 1.12	0.49			
BMI (for every 5 units)	1.08	0.83 - 1.37	0.57			
Asian Race (relative to Black)	1.27	0.75 - 2.07	0.36			
Mixed Race (relative to Black)	0.76	0.44 - 1.27	0.31			
African clinical site (relative to non-African)	1.02	0.70 - 1.52	0.91			
BASELINE CLINICAL FACTORS						
Gene Xpert (for every 3 CT decrease)	1.05	0.90 - 1.23	0.51			
Time to Detection on Sputum Liquid Culture (for every 5 day increase)	0.96	0.77 - 1.17	0.68			
Presence of Cavitation	0.90	0.62 - 1.33	0.60			
Aggregate cavity size <4cm (relative to no cavities)	0.82	0.53 - 1.28	0.39			
Aggregate cavity size ≥4cm (relative to no cavities)	0.80	0.52 - 1.24	0.32			
Extent of disease (<25% relative to 25-50%)	1.06	0.67 - 1.73	0.81			
Extent of disease (>50% relative to 25-50%)	1.22	0.75 - 2.03	0.42			
Smear grade 0.5 relative to 0	0.78	0.32 - 2.11	0.60			
Smear grade 1 relative to 0	0.76	0.32 - 2.05	0.57			
Smear grade 2 relative to 0	0.89	0.38 - 2.33	0.79			
Smear grade 3 relative to 0	0.70	0.30 - 1.87	0.45			
Karnofsky score (for every 10)	**1.32**	**1.01 - 1.75**	**0.05**			
HIV-infected (relative to HIV-uninfected)	0.68	0.32 - 1.29	0.27			
Diabetes (relative to non-diabetic)	1.78	0.80 - 3.67	0.14			
Smoking history (former relative to nonsmoker)	1.01	0.65 - 1.54	0.96			
Smoking history (current relative to nonsmoker)	0.75	0.47 - 1.16	0.21			
History of Liver Disease	**8.84**	**1.71 - 64.2**	**0.012**	**7.90**	**1.50 - 58.1**	**0.019**
PHARMACOKINETIC FACTORS						
Rifapentine $AUC_{0\text{-}24h}$ (for every 100 µg·h/mL)	1.02	0.92 - 1.13	0.70			
Rifapentine C_{max} (for every 10 µg/mL)	1.00	0.81 - 1.24	0.98			
Moxifloxacin $AUC_{0\text{-}24h}$ (for every 5 µg·h/mL)	1.03	0.91 - 1.16	0.59			
Moxifloxacin C_{max} (for every 1 µg/mL)	1.09	0.85 - 1.38	0.47			
Pyrazinamide $AUC_{0\text{-}24h}$ (for every 100 µg·h/mL)	**1.22**	**1.02 - 1.45**	**0.03**	**1.22**	**1.01 - 1.45**	**0.034**
Pyrazinamide C_{max} (for every 10 µg/mL)	1.17	0.93 - 1.46	0.17			
Isoniazid $AUC_{0\text{-}24h}$ (for every 5 µg·h/mL)	1.08	0.97 - 1.19	0.17			
Isoniazid C_{max} (for every 1 µg/mL)	1.10	0.87 - 1.36	0.42			

Supplemental Table 4-3 Univariable and Multivariable Safety Analysis of Any Grade 3 or Higher Adverse Events in Participants Receiving Control Regimen in the Safety Population.

Baseline clinical factors and individual drug pharmacokinetic estimates were evaluated in univariable and multivariable logistic regression models as potential risk factors for the occurrence of any grade 3 or higher adverse events.

Predictor	Unadjusted Odds Ratio	Unadjusted 95% CI	Unadjusted p-value	Adjusted Odds Ratio	Adjusted 95% CI	Adjusted p-value
DEMOGRAPHIC FACTORS						
Age (for every 10 years)	1.05	0.90 - 1.21	0.54			
Male sex (relative to female)	**0.64**	**0.45 - 0.92**	**0.016**	**0.55**	**0.37 - 0.82**	**0.00308**
Height (for every 10 cm decrease)	1.15	0.94 - 1.41	0.18			
WT (for every 10 kg)	1.13	0.93 - 1.36	0.21			
BMI (for every 5 units)	**1.30**	**1.01 - 1.68**	**0.04**			
Asian Race (relative to Black)	0.97	0.55 - 1.64	0.92			
Mixed Race (relative to Black)	0.60	0.32 - 1.06	0.093			
African clinical site (relative to non-African)	0.85	0.58 - 1.25	0.40			
BASELINE CLINICAL FACTORS						
Gene Xpert (for every 3 CT decrease)	**0.81**	**0.70 - 0.94**	**0.0049**	**0.83**	**0.71 - 0.97**	**0.016**
Time to Detection on Sputum Liquid Culture (for every 5 day increase)	1.09	0.88 - 1.33	0.39			
Presence of Cavitation	0.82	0.56 - 1.20	0.30			
Aggregate cavity size <4cm (relative to no cavities)	0.87	0.56 - 1.34	0.52			
Aggregate cavity size ≥4cm (relative to no cavities)	0.72	0.47 - 1.10	0.13			
Extent of disease (<25% relative to 25-50%)	1.10	0.66 - 1.88	0.73			
Extent of disease (>50% relative to 25-50%)	1.31	0.79 - 2.25	0.31			
Smear grade 0.5 relative to 0	1.26	0.47 - 4.03	0.66			
Smear grade 1 relative to 0	0.94	0.35 - 2.95	0.90			
Smear grade 2 relative to 0	1.08	0.42 - 3.36	0.88			
Smear grade 3 relative to 0	0.83	0.31 - 2.61	0.72			
Karnofsky score (for every 10)	0.81	0.63 - 1.05	0.11			
HIV-infected (relative to HIV-uninfected)	1.16	0.61 - 2.05	0.64			
Diabetes (relative to non-diabetic)	**2.53**	**1.14 - 5.35**	**0.017**			
Smoking history (former relative to nonsmoker)	0.88	0.58 - 1.33	0.55			
Smoking history (current relative to nonsmoker)	**0.57**	**0.35 - 0.90**	**0.02**			
History of Liver Disease	0.84	0.04 - 5.24	0.87			
PHARMACOKINETIC FACTORS						
Rifampicin $AUC_{0\text{-}24h}$ (for every 10 µg·h/mL)	1.03	0.98 - 1.07	0.26			
Rifampicin C_{max} (for every 1 µg/mL)	1.03	0.99 - 1.06	0.12			
Ethambutol $AUC_{0\text{-}24h}$ (for every 5 µg·h/mL)	**1.40**	**1.01 - 1.94**	**0.045**	**1.44**	**1.01 - 2.06**	**0.043**
Ethambutol C_{max} (for every 1 µg/mL)	1.40	0.99 - 1.94	0.051			
Pyrazinamide $AUC_{0\text{-}24h}$ (for every 100 µg·h/mL)	1.16	0.94 - 1.42	0.15			
Pyrazinamide C_{max} (for every 10 µg/mL)	**1.52**	**1.11 - 2.06**	**0.00792**			
Isoniazid $AUC_{0\text{-}24h}$ (for every 5 µg·h/mL)	1.02	0.94 - 1.11	0.62			
Isoniazid C_{max} (for every 1 µg/mL)	1.17	0.90 - 1.52	0.24			

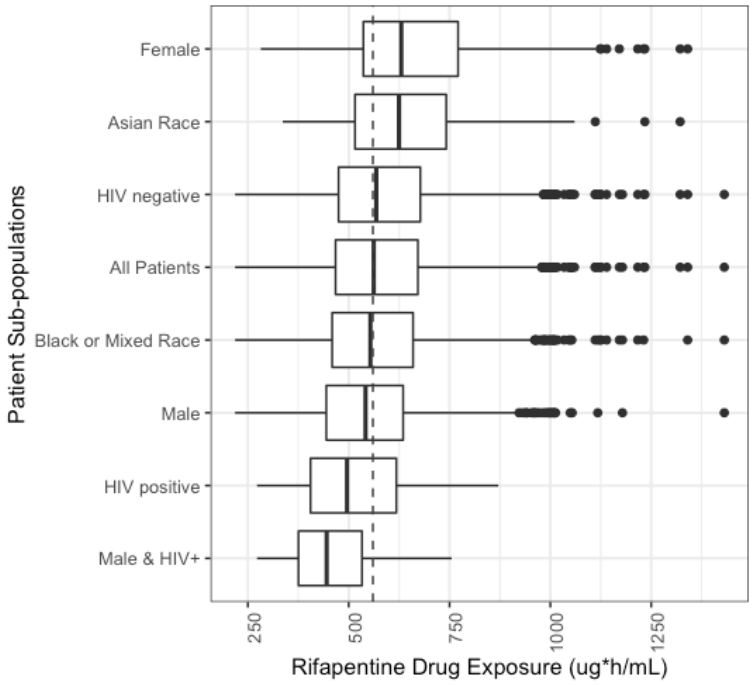

Supplemental Figure 4-6 All Patients Have the Potential for Low Rifapentine Exposure, but Male Patients and Patients Living with HIV are at Higher Risk of Low Drug Exposure

Low rifapentine exposure also greatly increases the risk for tuberculosis-related unfavorable outcomes, therefore identifying subpopulations at risk of low rifapentine exposure is important. Although any patient has the potential for low rifapentine exposure, male or patients living with HIV have the highest risk of low rifapentine exposure.

Supplemental Methods

As an additional pharmacokinetic-pharmacodynamic analysis, rifapentine and rifapentine-moxifloxacin regimens dichotomized by median rifapentine exposure were compared by Cox proportional hazards analysis (the main text made these comparisons by regimen).

Univariable Cox proportional hazards analysis were performed on all demographic, baseline clinical, and pharmacokinetic factors. Multivariable analyses were reported in the main text. Sensitivity analysis including and excluding imputed pharmacokinetic values were performed on univariable and multivariable analyses. Subgroup analyses of risk factors identified in multivariable analysis were performed comparing risk differences dichotomized by the median value of each risk factor. TB-ReFLECT risk phenotype definitions were validated with Study 31/A5349 data by calculating risk differences and calculating the 95% Wald confidence interval.

Univariable and multivariable logistic regression of any grade 3 or higher adverse events were performed for participants receiving rifapentine and control regimens (rifapentine-moxifloxacin regimen in the main text). Sensitivity analysis including and excluding imputed pharmacokinetic values were also performed on univariable and multivariable safety analyses.

Follow up sensitivity analyses were performed to justify the inclusion of height in multivariate logistic regression model for any grade 3 or higher adverse events. Models were adjusted for age, weight, sex, and race.

Supplemental Results

Among participants with above-median rifapentine exposure, only two TB-related unfavorable outcomes occurred during the 4-month treatment period, both were not seen at the 12-month follow-up visit and their last culture was positive and taken during the treatment period. TB-related unfavorable rates were comparable across arms at 12 months post randomization (rifapentine-moxifloxacin regimen HR, 0.86 relative to rifapentine regimen; 95% CI, 0.42-1.75) at 12 months post randomization. (Supplemental Figure

7). In contrast, in participants with below-median rifapentine exposure, the substitution of moxifloxacin for ethambutol improved 12-month outcomes from 14.5% in those who received the rifapentine regimen to 9.8% in those who received the rifapentine-moxifloxacin regimen (rifapentine-moxifloxacin HR, 0.49 relative to rifapentine regimen; 95% CI, 0.32-0.77). The main text of the manuscript demonstrated this finding stratified by regimen, risk group, and rifamycin exposure; it is reiterated here stratified by regimen and rifamycin exposure for robustness.

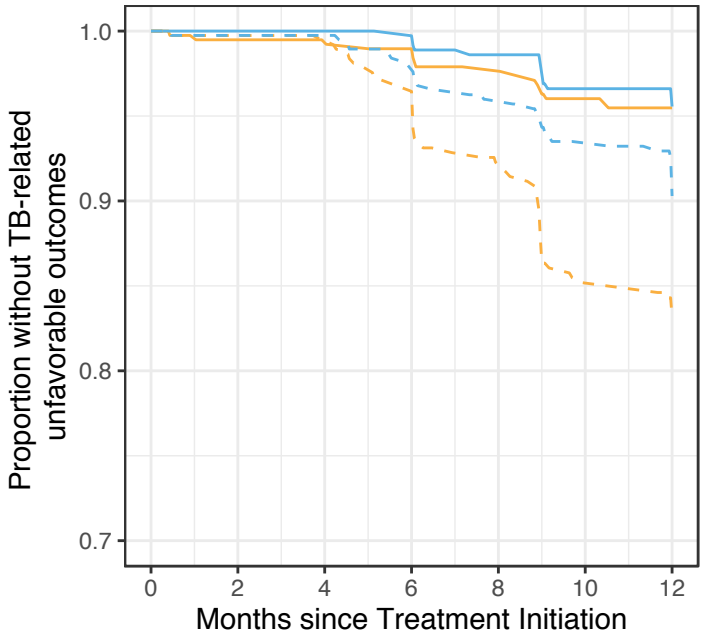

RPT AUC	Regimen	Number at Risk						
Above Median	HPZE	395	380	378	375	366	355	190
Below Median	HPZE	386	375	365	352	328	295	146
Above Median	HPZM	386	373	365	361	349	335	184
Below Median	HPZM	402	384	375	366	351	335	164

Supplemental Figure 4-7 Rifapentine Exposure is Crucial in Driving Treatment Response

Above median rifapentine exposure participants (solid lines) have comparable cure rates regardless of receiving the rifapentine regimen (yellow solid) or the rifapentine-moxifloxacin (blue solid) regimen. Below median rifapentine exposure patients (dotted lines) markedly improve cure rates with the substitution of moxifloxacin for ethambutol.

Among participants receiving the rifapentine-moxifloxacin regimen, univariable cox proportional hazards analysis identified Black race (relative to Asian), lower gene Xpert cycle threshold, lower rifapentine AUC_{0-24h}, lower rifapentine C_{max}, lower pyrazinamide AUC_{0-24h}, and lower isoniazid AUC_{0-24h} as associated with TB-related unfavorable outcomes (threshold $P<0.05$, Supplemental Table 4). Among participants receiving the rifapentine regimen, factors univariably associated with TB-related unfavorable outcomes included: older age, male sex, lower weight, lower BMI, lower Gene Xpert, shorter time to detection on sputum liquid culture, aggregate cavity size >4cm, extent of disease involvement of >50% lung area on chest radiography, living with HIV, living with diabetes, history of liver disease, lower rifapentine AUC_{0-24h}, lower rifapentine C_{max}, lower ethambutol AUC_{0-24h}, lower ethambutol C_{max}, lower isoniazid AUC_{0-24h}, and lower isoniazid C_{max} (threshold $P<0.05$, Supplemental Table 5). Among participants receiving the control regimen, factors univariably associated with TB-related unfavorable outcomes included: older age, lower Gene Xpert cycle threshold, current smoker (relative to nonsmoker), lower pyrazinamide AUC_{0-24h}, lower pyrazinamide C_{max}, and lower isoniazid C_{max} (threshold $P<0.05$, Supplemental Table 6). Multivariable results were presented in the main text.

Univariate and multivariable analyses were repeated excluding all imputed pharmacokinetic values. Findings were consistent with those reported in the main text for participants receiving rifapentine-mofloxacin and rifapentine regimens. For participants receiving control regimen, pyrazinamide C_{max} was no longer significant univariably after excluding imputed pharmacokinetic values, and in the multivariable model pyrazinamide AUC_{0-24h} was also no longer significant. (Supplemental Table 7 and 8)

Supplemental Table 4-4 Unadjusted and Adjusted Hazard Ratios for Rifapentine-Moxifloxacin Regimen Participants in Microbiologically Eligible Population

Predictor	Unadjusted Hazard Ratio	Unadjusted 95% CI	Unadjusted p-value	Adjusted Hazard Ratio	Adjusted 95% CI	Adjusted p-value
DEMOGRAPHIC FACTORS						
Age (for every 10 year increase)	1.08	0.85 - 1.37	0.55	--	--	--
Male sex (relative to female)	0.69	0.34 - 1.40	0.31	--	--	--
WT (for every 10 kg increase)	0.89	0.64 - 1.25	0.51	--	--	--
BMI (for every 1 unit increase)	0.95	0.86 - 1.06	0.36	--	--	--
Asian Race (relative to Black)	**0.47**	**0.24 - 0.94**	**0.034**	--	--	--
Mixed Race (relative to Black)	0.54	0.19 - 1.55	0.25	--	--	--
African clinical site (relative to non-African)	0.89	0.45 - 1.75	0.73	--	--	--
BASELINE CLINICAL FACTORS						
Gene Xpert (for every 3 CT decrease)	**1.47**	**1.10 - 1.97**	**0.00988**	**1.43**	**1.07 - 1.91**	**0.015**
Time to Detection on Sputum Liquid Culture (for every 1 day increase)	0.99	0.92 - 1.07	0.88	--	--	--
Presence of Cavitation	0.93	0.49 - 1.78	0.83	--	--	--
Cavity Class >4 cm (relative to <4cm/no cavities)	1.61	0.90 - 2.88	0.11	--	--	--
Extent of disease (>50% relative to <25%/25-50%)	**2.23**	**1.24 - 4.01**	**0.0073**	**2.03**	**1.08 - 3.83**	**0.029**
Smear grade 0.5 relative to 0	0	0 - Inf	0.99	--	--	--
Smear grade 1 relative to 0	1.04	0.45 - 2.40	0.93	--	--	--
Smear grade 2 relative to 0	1.04	0.46 - 2.35	0.92	--	--	--
Smear grade 3 relative to 0	0.98	0.45 - 2.12	0.96	--	--	--
Karnofsky score (for every 10)	0.74	0.49 - 1.12	0.16	--	--	--
HIV-infected (relative to HIV-uninfected)	0.83	0.26 - 2.67	0.75	--	--	--
Diabetes (relative to non-diabetic)	0.55	0.08 - 3.98	0.55	--	--	--
Smoking history (former relative to nonsmoker)	0.59	0.29 - 1.20	0.15	--	--	--
Smoking history (current relative to nonsmoker)	1.08	0.50 - 2.34	0.84	--	--	--
History of Liver Disease	0	0 - Inf	0.99	--	--	--
PHARMACOKINETIC FACTORS						
Rifapentine $AUC_{0\text{-}24h}$ (for every 100 µg·h/mL)	**0.77**	**0.64 - 0.93**	**0.00648**	**0.77**	**0.63 - 0.95**	**0.015**
Rifapentine C_{max} (for every 10 µg/mL)	**0.77**	**0.63 - 0.93**	**0.00828**	--	--	--
Moxifloxacin $AUC_{0\text{-}24h}$ (for every 5 µg·h/mL)	0.82	0.64 - 1.05	0.12	--	--	--
Moxifloxacin C_{max} (for every 1 µg/mL)	0.78	0.49 - 1.24	0.29	--	--	--
Pyrazinamide $AUC_{0\text{-}24h}$ (for every 100 µg·h/mL)	**0.60**	**0.40 - 0.91**	**0.016**	--	--	--
Pyrazinamide C_{max} (for every 10 µg/mL)	0.63	0.38 - 1.06	0.080	--	--	--
Isoniazid $AUC_{0\text{-}24h}$ (for every 5 µg·h/mL)	**0.78**	**0.62 - 0.98**	**0.033**	--	--	--
Isoniazid C_{max} (for every 1 µg/mL)	0.82	0.54 - 1.24	0.34	--	--	--

Supplemental Table 4-5 Unadjusted and Adjusted Hazard Ratios for Rifapentine Regimen Participants in Microbiologically Eligible Population

Predictor	Unadjusted Hazard Ratio	Unadjusted 95% CI	Unadjusted p-value	Adjusted Hazard Ratio	Adjusted 95% CI	Adjusted p-value
DEMOGRAPHIC FACTORS						
Age (for every 10 year increase)	**1.45**	**1.22 - 1.71**	**<0.0001**	**1.37**	**1.13 - 1.67**	**0.00166**
Male sex (relative to female)	**0.38**	**0.2 - 0.74**	**0.0044**			
WT (for every 10 kg increase)	**0.61**	**0.44 - 0.83**	**0.00152**	**0.57**	**0.40 - 0.80**	**0.00124**
BMI (for every 1 unit increase)	**0.86**	**0.79 - 0.95**	**0.00208**			
Asian Race (relative to Black)	1.49	0.68 - 3.26	0.32			
Mixed Race (relative to Black)	1.54	0.57 - 4.14	0.39			
African clinical site (relative to non-African)	0.58	0.32 - 1.05	0.072			
BASELINE CLINICAL FACTORS						
Gene Xpert (for every 3 CT decrease)	**1.63**	**1.32 - 2.02**	**<0.0001**	**1.54**	**1.93 - 1.24**	**0.00012**
Time to Detection on Sputum Liquid Culture (for every 1 day increase)	**0.90**	**0.83 - 0.97**	**0.00515**			
Presence of Cavitation	1.23	0.72 - 2.08	0.45			
Cavity Class >4 cm (relative to <4cm/no cavities)	**1.67**	**1.06 - 2.64**	**0.026**			
Extent of disease (>50% relative to <25%/25-50%)	**2.09**	**1.32 - 3.29**	**0.00156**	**1.61**	**0.98 - 2.65**	**0.060**
Smear grade 0.5 relative to 0	0.28	0.04 - 2.04	0.21			
Smear grade 1 relative to 0	0.37	0.14 - 0.96	0.042			
Smear grade 2 relative to 0	0.65	0.33 - 1.29	0.22			
Smear grade 3 relative to 0	1.42	0.84 - 2.40	0.20			
Karnofsky score (for every 10)	0.93	0.66 - 1.31	0.66			
HIV-infected (relative to HIV-uninfected)	**1.95**	**1.03 - 3.71**	**0.040**			
Diabetes (relative to non-diabetic)	**6.53**	**2.83 - 15.1**	**<0.0001**			
Smoking history (former relative to nonsmoker)	**0.52**	**0.30 - 0.91**	**0.023**			
Smoking history (current relative to nonsmoker)	1.00	0.56 - 1.77	0.99			
History of Liver Disease	**5.27**	**1.29 - 21.5**	**0.020**			
PHARMACOKINETIC FACTORS						
Rifapentine $AUC_{0\text{-}24h}$ (for every 100 µg·h/mL)	**0.65**	**0.55 - 0.76**	**<0.0001**	**0.65**	**0.54 - 0.77**	**<0.0001**
Rifapentine C_{max} (for every 10 µg/mL)	**0.62**	**0.52 - 0.74**	**<0.0001**			
Ethambutol $AUC_{0\text{-}24h}$ (for every 5 µg·h/mL)	**0.54**	**0.33 - 0.86**	**0.00983**			
Ethambutol C_{max} (for every 1 µg/mL)	**0.56**	**0.34 - 0.92**	**0.022**			
Pyrazinamide $AUC_{0\text{-}24h}$ (for every 100 µg·h/mL)	0.87	0.64 - 1.19	0.38			
Pyrazinamide C_{max} (for every 10 µg/mL)	0.60	0.35 - 1.02	0.060			
Isoniazid $AUC_{0\text{-}24h}$ (for every 5 µg·h/mL)	**0.80**	**0.67 - 0.95**	**0.011**			
Isoniazid C_{max} (for every 1 µg/mL)	**0.53**	**0.35 - 0.81**	**0.00295**			

Supplemental Table 4-6 Unadjusted and Adjusted Hazard Ratios for Control Regimen Participants in Microbiologically Eligible Population

Predictor	Unadjusted Hazard Ratio	Unadjusted 95% CI	Unadjusted p-value	Adjusted Hazard Ratio	Adjusted 95% CI	Adjusted p-value
DEMOGRAPHIC FACTORS						
Age (for every 10 year increase)	**1.41**	**1.05 - 1.90**	**0.023**			
Male sex (relative to female)	1.45	0.63 - 3.30	0.38			
WT (for every 10 kg increase)	0.64	0.37 - 1.11	0.11			
BMI (for every 1 unit increase)	0.88	0.75 - 1.04	0.13			
Asian Race (relative to Black)	0.71	0.24 - 2.09	0.53			
Mixed Race (relative to Black)	0.49	0.09 - 2.70	0.42			
African clinical site (relative to non-African)	0.97	0.39 - 2.45	0.95			
BASELINE CLINICAL FACTORS						
Gene Xpert (for every 3 CT decrease)	**1.66**	**1.07 - 2.57**	**0.024**	**1.69**	**1.08 - 2.63**	**0.021**
Time to Detection on Sputum Liquid Culture (for every 1 day increase)	0.98	0.88 - 1.09	0.72			
Presence of Cavitation	1.34	0.50 - 3.58	0.56			
Cavity Class >4 cm (relative to <4cm/no cavities)	1.46	0.66 - 3.26	0.35			
Extent of disease (>50% relative to <25%/25-50%)	1.29	0.58 - 2.88	0.53			
Smear grade 0.5 relative to 0	0	0 - Inf	1			
Smear grade 1 relative to 0	0.78	0.21 - 2.94	0.71			
Smear grade 2 relative to 0	1.13	0.41 - 3.13	0.81			
Smear grade 3 relative to 0	0.88	0.31 - 2.54	0.82			
Karnofsky score (for every 10)	0.73	0.42 - 1.27	0.27			
HIV-infected (relative to HIV-uninfected)	0.53	0.07 - 3.94	0.54			
Diabetes (relative to non-diabetic)	2.38	0.56 - 10.1	0.24			
Smoking history (former relative to nonsmoker)	2.51	0.56 - 11.3	0.23			
Smoking history (current relative to nonsmoker)	**5.26**	**1.16 - 23.7**	**0.031**			
History of Liver Disease	0	0 - Inf	1			
PHARMACOKINETIC FACTORS						
Rifampicin $AUC_{0\text{-}24h}$ (for every 10 µg·h/mL)	1.02	0.93 - 1.11	0.67			
Rifampicin C_{max} (for every 1 µg/mL)	1.02	0.95 - 1.10	0.63			
Ethambutol $AUC_{0\text{-}24h}$ (for every 5 µg·h/mL)	1.09	0.91 - 1.30	0.37			
Ethambutol C_{max} (for every 1 µg/mL)	1.10	0.60 - 2.03	0.75			
Pyrazinamide $AUC_{0\text{-}24h}$ (for every 100 µg·h/mL)	**0.38**	**0.17 - 0.82**	**0.013**	**0.36**	**0.15 - 0.83**	**0.016**
Pyrazinamide C_{max} (for every 10 µg/mL)	**0.35**	**0.14 - 0.90**	**0.029**			
Isoniazid $AUC_{0\text{-}24h}$ (for every 5 µg·h/mL)	0.49	0.20 - 1.16	0.10			
Isoniazid C_{max} (for every 1 µg/mL)	**0.34**	**0.12 - 0.96**	**0.041**			

Supplemental Table 4-7 Univariate Cox Proportional Hazards of TB-related Unfavorable Outcomes Sensitivity Analysis of Pharmacokinetic Factors Including and Excluding Imputed Values.

(A) Rifapentine-Moxifloxacin Regimen, (B) Rifapentine Regimen, (C) Control Regimen.

Rifapentine-Moxifloxacin Regimen	**Main Analysis Including Imputed PK**			**Sensitivity Analysis Excluding Imputed PK**		
Predictor	Unadjusted Hazard Ratio	Unadjusted 95% CI	Unadjusted p-value	Unadjusted Hazard Ratio	Unadjusted 95% CI	Unadjusted p-value
PHARMACOKINETIC FACTORS						
Rifapentine $AUC_{0\text{-}24h}$ (for every 100 µg·h/mL)	**0.77**	**0.64 - 0.93**	**0.00648**	**0.76**	**0.63 - 0.93**	**0.00697**
Rifapentine C_{max} (for every 10 µg/mL)	**0.77**	**0.63 - 0.93**	**0.00828**	**0.77**	**0.63 - 0.94**	**0.011**
Moxifloxacin $AUC_{0\text{-}24h}$ (for every 5 µg·h/mL)	0.82	0.64 - 1.05	0.12	0.82	0.63 - 1.06	0.13
Moxifloxacin C_{max} (for every 1 µg/mL)	0.78	0.49 - 1.24	0.29	0.80	0.49 - 1.30	0.37
Pyrazinamide $AUC_{0\text{-}24h}$ (for every 100 µg·h/mL)	**0.60**	**0.40 - 0.91**	**0.016**	**0.59**	**0.39 - 0.91**	**0.017**
Pyrazinamide C_{max} (for every 10 µg/mL)	0.63	0.38 - 1.06	0.080	0.61	0.36 - 1.04	0.069
Isoniazid $AUC_{0\text{-}24h}$ (for every 5 µg·h/mL)	**0.78**	**0.62 - 0.98**	**0.033**	**0.78**	**0.62 - 0.98**	**0.033**
Isoniazid C_{max} (for every 1 µg/mL)	0.82	0.54 - 1.24	0.34	0.82	0.54 - 1.24	0.34

Rifapentine Regimen	**Main Analysis Including Imputed PK**			**Sensitivity Analysis Excluding Imputed PK**		
Predictor	Unadjusted Hazard Ratio	Unadjusted 95% CI	Unadjusted p-value	Unadjusted Hazard Ratio	Unadjusted 95% CI	Unadjusted p-value
PHARMACOKINETIC FACTORS						
Rifapentine $AUC_{0\text{-}24h}$ (for every 100 µg·h/mL)	**0.65**	**0.55 - 0.76**	**<0.0001**	**0.64**	**0.54 - 0.76**	**<0.0001**
Rifapentine C_{max} (for every 10 µg/mL)	**0.62**	**0.52 - 0.74**	**<0.0001**	**0.61**	**0.51 - 0.73**	**<0.0001**
Ethambutol $AUC_{0\text{-}24h}$ (for every 5 µg·h/mL)	**0.54**	**0.33 - 0.86**	**0.00983**	**0.54**	**0.33 - 0.88**	**0.015**
Ethambutol C_{max} (for every 1 µg/mL)	**0.56**	**0.34 - 0.92**	**0.022**	**0.56**	**0.34 - 0.94**	**0.029**
Pyrazinamide $AUC_{0\text{-}24h}$ (for every 100 µg·h/mL)	0.87	0.64 - 1.19	0.38	0.87	0.63 - 1.19	0.37
Pyrazinamide C_{max} (for every 10 µg/mL)	0.60	0.35 - 1.02	0.060	0.58	0.34 - 1.00	0.051
Isoniazid $AUC_{0\text{-}24h}$ (for every 5 µg·h/mL)	**0.80**	**0.67 - 0.95**	**0.011**	**0.80**	**0.67 - 0.95**	**0.011**
Isoniazid C_{max} (for every 1 µg/mL)	**0.53**	**0.35 - 0.81**	**0.00295**	**0.53**	**0.35 - 0.81**	**0.00295**

Control Regimen	**Main Analysis Including Imputed PK**			**Sensitivity Analysis Excluding Imputed PK**		
Predictor	Unadjusted Hazard Ratio	Unadjusted 95% CI	Unadjusted p-value	Unadjusted Hazard Ratio	Unadjusted 95% CI	Unadjusted p-value
PHARMACOKINETIC FACTORS						
Rifampicin $AUC_{0\text{-}24h}$ (for every 10 µg·h/mL)	1.02	0.93 - 1.11	0.67	1.00	0.90 - 1.12	0.95
Rifampicin C_{max} (for every 1 µg/mL)	1.02	0.95 - 1.10	0.63	1.01	0.93 - 1.10	0.78
Ethambutol $AUC_{0\text{-}24h}$ (for every 5 µg·h/mL)	1.09	0.91 - 1.30	0.37	1.09	0.91 - 1.30	0.38
Ethambutol C_{max} (for every 1 µg/mL)	1.10	0.60 - 2.03	0.75	1.10	0.60 - 2.03	0.76
Pyrazinamide $AUC_{0\text{-}24h}$ (for every 100 µg·h/mL)	**0.38**	**0.17 - 0.82**	**0.013**	**0.44**	**0.20 - 0.99**	**0.048**
Pyrazinamide C_{max} (for every 10 µg/mL)	**0.35**	**0.14 - 0.90**	**0.029**	0.46	0.17 - 1.23	0.12
Isoniazid $AUC_{0\text{-}24h}$ (for every 5 µg·h/mL)	0.49	0.20 - 1.16	0.10	0.66	0.26 - 1.69	0.39
Isoniazid C_{max} (for every 1 µg/mL)	0.34	0.12 - 0.96	0.041	0.53	0.19 - 1.48	0.22

Supplemental Table 4-8 Multivariable Cox Proportional Hazards of TB-related Unfavorable Outcomes Sensitivity Analysis of Pharmacokinetic Factors Including and Excluding Imputed Values.

(A) Rifapentine-Moxifloxacin Regimen, (B) Rifapentine Regimen, (C) Control Regimen.

Rifapentine-Moxifloxacin Regimen	**Main Analysis Including Imputed PK**			**Sensitivity Analysis Excluding Imputed PK**		
Predictor	Adjusted Hazard Ratio	Adjusted 95% CI	Adjusted p-value	Adjusted Hazard Ratio	Adjusted 95% CI	Adjusted p-value
Rifapentine $AUC_{0\text{-}24h}$ (for every 100 µg·h/mL)	0.77	0.63 - 0.95	0.015	0.76	0.61 - 0.95	0.015
Gene Xpert (for every 3 CT decrease)	1.43	1.07 - 1.91	0.015	1.55	1.14 - 2.10	0.00521
Extent of disease (>50% relative to <25%/25-50%)	2.03	1.08 - 3.83	0.029	2.17	1.12 - 4.23	0.022

Rifapentine Regimen	**Main Analysis Including Imputed PK**			**Sensitivity Analysis Excluding Imputed PK**		
Predictor	Adjusted Hazard Ratio	Adjusted 95% CI	Adjusted p-value	Adjusted Hazard Ratio	Adjusted 95% CI	Adjusted p-value
Rifapentine $AUC_{0\text{-}24h}$ (for every 100 µg·h/mL)	0.65	0.54 - 0.77	<0.0001	0.65	0.54 - 0.77	<0.0001
Gene Xpert (for every 3 CT decrease)	1.54	1.93 - 1.24	0.00012	1.60	1.28 - 2.01	<0.0001
Extent of disease (>50% relative to <25%/25-50%)	1.61	0.98 - 2.65	0.060	1.68	1.01 - 2.78	0.047
Age (for every 10 year increase)	1.37	1.13 - 1.67	0.00166	1.38	1.14 - 1.69	0.00130
WT (for every 10 kg increase)	0.57	0.40 - 0.80	0.00124	0.55	0.38 - 0.78	<0.0001

Control Regimen	**Main Analysis Including Imputed PK**			**Sensitivity Analysis Excluding Imputed PK**		
Predictor	Adjusted Hazard Ratio	Adjusted 95% CI	Adjusted p-value	Adjusted Hazard Ratio	Adjusted 95% CI	Adjusted p-value
Pyrazinamide $AUC_{0\text{-}24h}$ (for every 100 µg·h/mL)	0.36	0.15 - 0.83	0.016	0.43	0.18 - 1.03	0.06
Gene Xpert (for every 3 CT decrease)	1.69	1.08 - 2.63	0.021	1.95	1.16 - 3.28	0.011

Univariate Subgroup Analyses

The rifapentine-moxifloxacin regimen was noninferior to the control at the trial level. We therefore sought to identify high-risk subpopulations of participants that had large risk differences relative to control and for whom the rifapentine-moxifloxacin regimen might not be appropriate. Among participants who received the rifapentine-moxifloxacin regimen, those with ≥50% disease extent on chest radiography and those with low rifapentine exposure experienced higher tuberculosis-related unfavorable outcomes compared to the control (≥50% disease extent: risk difference, 5.2%; 95% CI, 1.9% – 8.6% | low rifapentine exposure: risk difference, 5.4%; 95% CI, 2.4% – 8.5%). Participants with an Xpert MTB/RIF cycle threshold of <18 had 3.5% increased risk of tuberculosis-related unfavorable outcomes when compared to the control, but the upper border of the 95% CI exceeded the 6.6% margin (95% CI, 0.4 – 6.7). All other subpopulations stratified by single risk factors (age and weight) had small risk differences. Rifapentine exposure had a significant interaction with regimen ($P < 0.03$), while no other interactions were significant. (Supplemental Figure 8A)

The rifapentine regimen did not achieve noninferiority compared to the control at the trial level. We therefore sought to identify subpopulations of participants that had small risk differences relative to control and help define the low-risk subpopulations. Among participants receiving the rifapentine regimen, those with high rifapentine exposure had similar rates of tuberculosis-related unfavorable outcomes compared to the control group (risk difference, 0.5%; 95% CI, -2.2% – 3.2%). Participants with Xpert MTB/RIF cycle threshold of ≥18 and those with <50% disease extent on chest radiography also had similar rates of tuberculosis-related unfavorable outcomes at 12 months across the experimental and control regimens (Xpert cycle threshold ≥18: risk difference, 2.7%; 95% CI, -0.2% – 5.6% | <50% disease extent: risk difference, 4.1%; 95% CI, 1.4% – 6.8%). All other subpopulations stratified by single risk factors (age and weight) had large risk differences or wide confidence intervals. Rifapentine exposure had a significant interaction with regimen ($P < 0.001$), while no other interactions were significant. (Supplemental Figure 8B)

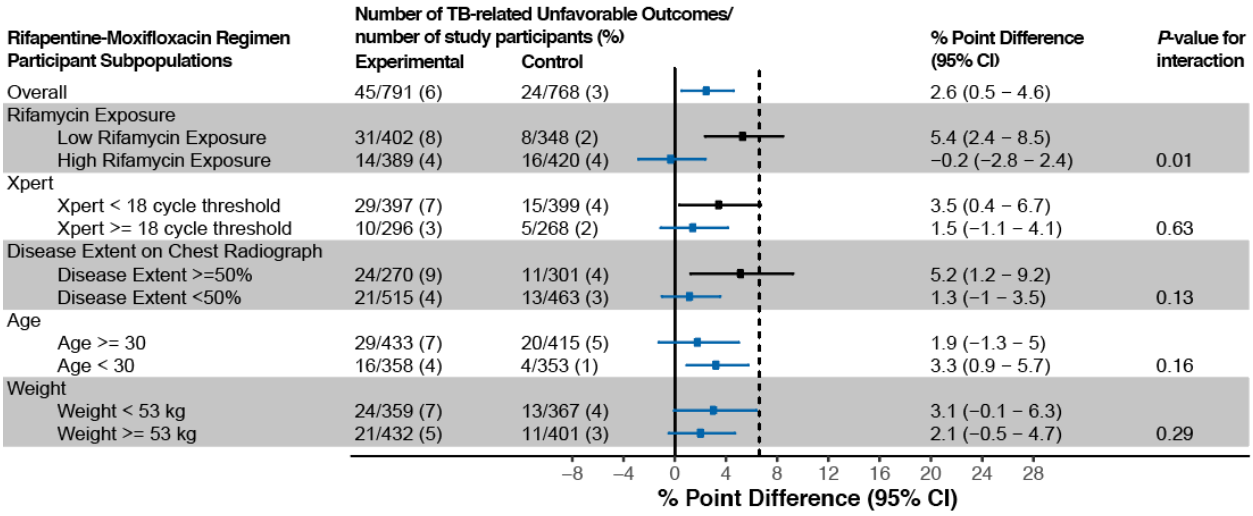

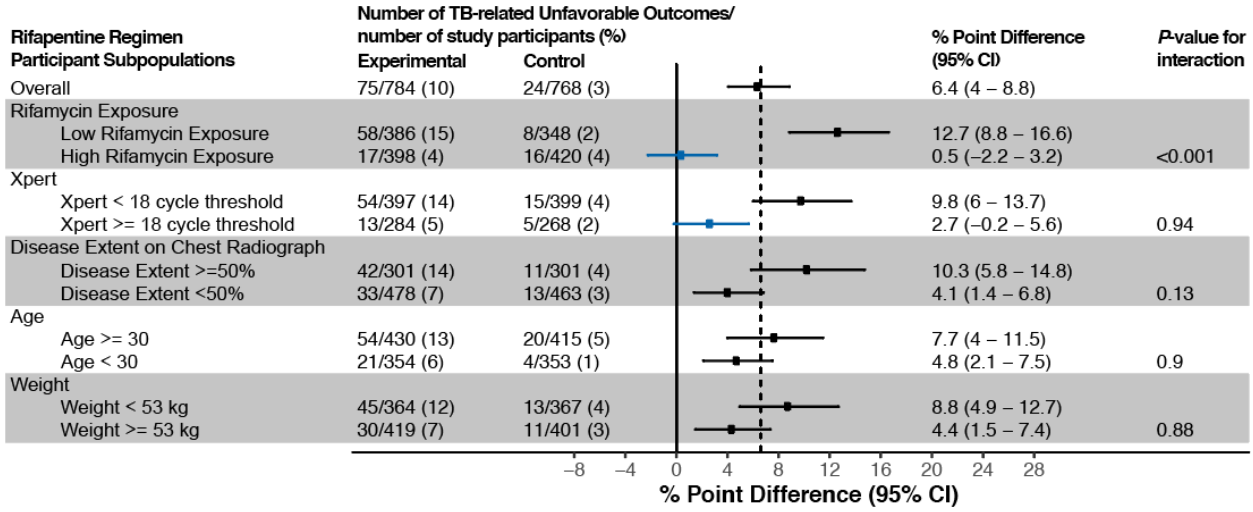

Supplemental Figure 4-8 Subgroup analyses of identified risk factors

(A) Rifapentine-moxifloxacin and (B) Rifapentine regimens are stratified by median value further supports risk stratification based on rifamycin exposure, Xpert cycle threshold, and disease extent on chest radiograph, the top three risk factors that demonstrate the greatest separation in outcomes between above and below median subgroups. For the experimental regimens low and high rifamycin exposure referred to rifapentine and for the control, rifampicin.

Prespecified Risk Phenotype Validation

We validated prespecified risk group definitions in the TB-ReFLECT analysis by Imperial et al[5]; whereby easy-to-treat participants defined as sputum AFB smear grade <2 or non-cavitary disease had similar rates of tuberculosis-related unfavorable outcome across the experimental and control regimens, and in the hard-to-treat phenotypes, defined as sputum AFB smear grade ≥3 and cavitary disease, the experimental group experienced higher tuberculosis-related treatment outcomes than the control. For those receiving rifapentine-moxifloxacin regimen, TB-ReFLECT defined easy-to-treat participants had similar rates of tuberculosis-related unfavorable outcome across the experimental and control regimens (easy-to-treat: risk difference, 2.8%; 95% CI, 0% – 5.5%). Hard-to-treat participants defined by the TB-ReFLECT analysis also experienced similar rates of tuberculosis-related unfavorable outcome, however the u pper bound of the confidence interval was beyond the 6.6% margin (risk difference, 2.2%; 95% CI, -2.2% – 6.7%). (Supplemental Figure 4-5A)

For those receiving rifapentine regimen, participants classified as easy-to-treat by the TB-ReFLECT definition had a small risk difference compared to the control, however the upper bound of the confidence interval was just beyond the 6.6% margin (risk difference, 4.0%; 95% CI, 1.1% – 6.9%); participants classified as hard-to-treat by the TB-ReFLECT definition had a large risk difference compared to the control (hard-to-treat: risk difference, 10.9%; 95% CI, 5% – 16.7%). %). (Supplemental Figure 4-5B)

Despite the lack of a clear graded response across TB-ReFLECT risk phenotypes in the rifapentine-moxifloxacin regimen, we believe that TB-ReFLECT risk groups still exist in the rifapentine-moxifloxacin regimen. However, there were only 5.7% TB-related unfavorable outcomes in the rifapentine-moxifloxacin regimen which gave little resolution to observe the differences between risk groups. Additionally, sputum AFB smear grade and presence of cavitation are lower resolution measurements than Xpert MTB/RIF cycle threshold[20] and disease extent on chest radiograph, and the more potent noninferior rifapentine-moxifloxacin regimen needs finer measurements to tease out the high-risk strata. Finally, the TB-ReFLECT risk strata were defined from regimens that all failed to achieve noninferiority (OFLOTUB[21], ReMOX[22], RIFAQUIN[23]), we therefore see a clear validation of the TB-ReFLECT risk phenotypes in the

rifapentine regimen which is a more similar comparison but not as clear in participants receiving the rifapentine-moxifloxacin regimen.

Safety

Among participants receiving the rifapentine regimen, univariable logistic regression found older age, shorter height, Asian race (relative to Black), non-African clinical site (relative to African), history of liver disease, and higher ethambutol exposure to be associated with any grade 3 or higher adverse events (threshold $P<0.05$, Supplemental Table 9). Multivariable analysis the following factors to be associated with any grade 3 or higher adverse events: height (OR, 1.50 for every 10 cm shorter; 95% CI, 1.16 - 1.94), Asian race (OR, 2.18 relative to Black race; 95% CI, 1.29 - 3.61), history of liver disease (OR, 6.16; 95% CI, 1.29 - 32.48), and ethambutol $AUC_{0\text{-}24h}$ (OR, 1.39 for every 5 μg·h/mL increase; 95% CI, 1.02 - 1.98).

Supplemental Table 4-9 Univariable and Multivariable Safety Analysis of Any Grade 3 or Higher Adverse Events in Participants Receiving Rifapentine Regimen in the Safety Population

Baseline clinical factors and individual drug pharmacokinetic estimates were evaluated in univariable and multivariable logistic regression models as potential risk factors for the occurrence of any grade 3 or higher adverse events.

Predictor	Unadjusted Odds Ratio	Unadjusted 95% CI	Unadjusted p-value	Adjusted Odds Ratio	Adjusted 95% CI	Adjusted p-value
DEMOGRAPHIC FACTORS						
Age (for every 10 years)	**1.20**	**1.03 - 1.39**	**0.020**			
Male sex (relative to female)	0.72	0.48 - 1.09	0.12			
Height (for every 10 cm decrease)	**1.50**	**1.17 - 1.92**	**0.00139**	**1.5**	**1.16 - 1.94**	**0.00192**
WT (for every 10 kg)	0.91	0.72 - 1.14	0.44			
BMI (for every 5 units)	1.18	0.88 - 1.55	0.25			
Asian Race (relative to Black)	**2.59**	**1.55 - 4.24**	**0.00021**	**2.18**	**1.29 - 3.61**	**0.00281**
Mixed Race (relative to Black)	0.91	0.48 - 1.62	0.76			
African clinical site (relative to non-African)	**0.64**	**0.43 - 0.97**	**0.033**			
BASELINE CLINICAL FACTORS						
Gene Xpert (for every 3 CT decrease)	0.90	0.76 - 1.07	0.22			
Time to Detection on Sputum Liquid Culture (for every 5 day increase)	1.09	0.87 - 1.33	0.43			
Presence of Cavitation	0.86	0.57 - 1.33	0.50			
Aggregate cavity size <4cm (relative to no cavities)	1.06	0.66 - 1.73	0.80			
Aggregate cavity size ≥4cm (relative to no cavities)	0.66	0.41 - 1.08	0.099			
Extent of disease (25-50% relative to <25%)	1.84	1.07 - 3.34	0.035			
Extent of disease (>50% relative to <25%	0.87	0.47 - 1.66	0.67			
Smear grade 0.5 relative to 0	1.60	0.56 - 5.76	0.41			
Smear grade 1 relative to 0	1.69	0.62 - 5.94	0.35			
Smear grade 2 relative to 0	1.74	0.65 - 6.05	0.32			
Smear grade 3 relative to 0	1.11	0.40 - 3.96	0.85			
Karnofsky score (for every 10)	1.25	0.92 - 1.72	0.17			
HIV-infected (relative to HIV-uninfected)	1.25	0.62 - 2.32	0.51			
Diabetes (relative to non-diabetic)	2.81	0.87 - 7.88	0.06			
Smoking history (former relative to nonsmoker)	1.17	0.73 - 1.84	0.51			
Smoking history (current relative to nonsmoker)	0.96	0.58 - 1.57	0.88			
History of Liver Disease	**8.27**	**1.80 - 42.4**	**0.00611**	**6.16**	**1.29 - 32.48**	**0.021**
PHARMACOKINETIC FACTORS						
Rifapentine $AUC_{0\text{-}24h}$ (for every 100 µg·h/mL)	1.03	0.92 - 1.15	0.59			
Rifapentine C_{max} (for every 10 µg/mL)	1.06	0.83 - 1.34	0.62			
Ethambutol $AUC_{0\text{-}24h}$ (for every 5 µg·h/mL)	1.33	0.99 - 1.81	0.057	**1.39**	**1.02 - 1.98**	**0.053**
Ethambutol C_{max} (for every 1 µg/mL)	1.26	0.95 - 1.67	0.099			
Pyrazinamide $AUC_{0\text{-}24h}$ (for every 100 µg·h/mL)	0.96	0.74 - 1.22	0.75			
Pyrazinamide C_{max} (for every 10 µg/mL)	1.19	0.82 - 1.70	0.34			
Isoniazid $AUC_{0\text{-}24h}$ (for every 5 µg·h/mL)	0.99	0.87 - 1.11	0.81			
Isoniazid C_{max} (for every 1 µg/mL)	1.12	0.83 - 1.50	0.43			

Univariate and multivariable analyses were repeated excluding all imputed pharmacokinetic values. Findings were mostly consistent with those reported in the main text. For participants receiving the rifapentine-moxifloxacin regimen, univariable sensitivity analysis excluding imputed pharmacokinetic values were consistent with the main analysis. In multivariable sensitivity analysis excluding imputed pharmacokinetic values, height and history of liver disease were no longer significant. For participants receiving the rifapentine regimen, in the main analysis ethambutol $AUC_{0\text{-}24h}$ was not univariably significant but was univariably significant in the sensitivity analysis excluding imputed pharmacokinetic values. In multivariable sensitivity analysis excluding imputed pharmacokinetic values, history of liver disease was no longer significant. For participants receiving the control regimen, in the main analysis ethambutol C_{max} was not univariably significant but was univariably significant in the sensitivity analysis excluding imputed pharmacokinetic values. In multivariable sensitivity analysis excluding imputed pharmacokinetic values findings were consistent with those reported in the main analysis and text. (Supplemental Table 10 and 11)

Supplemental Table 4-10 Univariate Logistic Regression Safety Sensitivity Analysis of Pharmacokinetic Factors Including and Excluding Imputed Values

Rifapentine-Moxifloxacin Regimen	**Main Analysis Including Imputed PK**			**Sensitivity Analysis Excluding Imputed PK**		
Predictor	Unadjusted Odds Ratio	Unadjusted 95% CI	Unadjusted p-value	Unadjusted Odds Ratio	Unadjusted 95% CI	Unadjusted p-value
PHARMACOKINETIC FACTORS						
Rifapentine $AUC_{0\text{-}24h}$ (for every 100 µg·h/mL)	1.02	0.92 - 1.13	0.70	1.02	0.92 - 1.12	0.77
Rifapentine C_{max} (for every 10 µg/mL)	1.00	0.81 - 1.24	0.98	1.02	0.81 - 1.26	0.88
Moxifloxacin $AUC_{0\text{-}24h}$ (for every 5 µg·h/mL)	1.03	0.91 - 1.16	0.59	1.04	0.91 - 1.17	0.55
Moxifloxacin C_{max} (for every 1 µg/mL)	1.09	0.85 - 1.38	0.47	1.06	0.82 - 1.36	0.63
Pyrazinamide $AUC_{0\text{-}24h}$ (for every 100 µg·h/mL)	**1.22**	**1.02 - 1.45**	**0.03**	**1.01**	**1.00 - 1.02**	**0.026**
Pyrazinamide C_{max} (for every 10 µg/mL)	1.17	0.93 - 1.46	0.17	1.01	0.99 - 1.04	0.29
Isoniazid $AUC_{0\text{-}24h}$ (for every 5 µg·h/mL)	1.08	0.97 - 1.19	0.17	4.32	0.51 - 34.2	0.17
Isoniazid C_{max} (for every 1 µg/mL)	1.10	0.87 - 1.36	0.42	2.50	0.26 - 22.4	0.42

Rifapentine Regimen	Main Analysis Including Imputed PK			Sensitivity Analysis Excluding Imputed PK		
Predictor	Unadjusted Odds Ratio	Unadjusted 95% CI	Unadjusted p-value	Unadjusted Odds Ratio	Unadjusted 95% CI	Unadjusted p-value
PHARMACOKINETIC FACTORS						
Rifapentine $AUC_{0\text{-}24h}$ (for every 100 µg·h/mL)	1.03	0.92 - 1.15	0.59	1.03	0.92 - 1.15	0.62
Rifapentine C_{max} (for every 10 µg/mL)	1.06	0.83 - 1.34	0.62	1.07	0.84 - 1.36	0.57
Ethambutol $AUC_{0\text{-}24h}$ (for every 5 µg·h/mL)	1.33	0.99 - 1.81	0.057	**1.40**	**1.02 - 1.96**	**0.037**
Ethambutol C_{max} (for every 1 µg/mL)	1.26	0.95 - 1.67	0.099	1.31	0.98 - 1.75	0.061
Pyrazinamide $AUC_{0\text{-}24h}$ (for every 100 µg·h/mL)	0.96	0.74 - 1.22	0.75	1.00	0.99 - 1.01	0.93
Pyrazinamide C_{max} (for every 10 µg/mL)	1.19	0.82 - 1.70	0.34	1.02	0.99 - 1.06	0.21
Isoniazid $AUC_{0\text{-}24h}$ (for every 5 µg·h/mL)	0.99	0.87 - 1.11	0.81	0.74	0.06 - 8.70	0.81
Isoniazid C_{max} (for every 1 µg/mL)	1.12	0.83 - 1.50	0.43	3.21	0.16 - 56.1	0.43

Control Regimen	Main Analysis Including Imputed PK			Sensitivity Analysis Excluding Imputed PK		
Predictor	Unadjusted Odds Ratio	Unadjusted 95% CI	Unadjusted p-value	Unadjusted Odds Ratio	Unadjusted 95% CI	Unadjusted p-value
PHARMACOKINETIC FACTORS						
Rifampicin $AUC_{0\text{-}24h}$ (for every 10 µg·h/mL)	1.03	0.98 - 1.07	0.26	1.01	0.96 - 1.06	0.70
Rifampicin C_{max} (for every 1 µg/mL)	1.03	0.99 - 1.06	0.12	1.02	0.98 - 1.06	0.27
Ethambutol $AUC_{0\text{-}24h}$ (for every 5 µg·h/mL)	**1.4**	**1.01 - 1.94**	**0.045**	**1.47**	**1.03 - 2.10**	**0.032**
Ethambutol C_{max} (for every 1 µg/mL)	1.4	0.99 - 1.94	0.051	**1.56**	**1.10 - 2.22**	**0.013**
Pyrazinamide $AUC_{0\text{-}24h}$ (for every 100 µg·h/mL)	1.16	0.94 - 1.42	0.15	1.01	1.00 - 1.02	0.061
Pyrazinamide C_{max} (for every 10 µg/mL)	**1.52**	**1.11 - 2.06**	**0.00792**	**1.05**	**1.02 - 1.09**	**0.00192**
Isoniazid $AUC_{0\text{-}24h}$ (for every 5 µg·h/mL)	1.02	0.94 - 1.11	0.62	1.53	0.28 - 7.96	0.62
Isoniazid C_{max} (for every 1 µg/mL)	1.17	0.90 - 1.52	0.24	4.83	0.33 - 65.8	0.24

Supplemental Table 4-11 Multivariable Logistic Regression Safety Sensitivity Analysis of Pharmacokinetic Factors Including and Excluding Imputed Values

Rifapentine-Moxifloxacin Regimen	Main Analysis Including Imputed PK			Sensitivity Analysis Excluding Imputed PK		
Predictor	Adjusted Odds Ratio	Adjusted 95% CI	Adjusted p-value	Adjusted Odds Ratio	Adjusted 95% CI	Adjusted p-value
Pyrazinamide $AUC_{0\text{-}24h}$ (for every 100 µg·h/mL)	1.22	1.01 - 1.45	0.034	1.22	1.01 - 1.46	0.035
Age (for every 10 years)	1.22	1.06 - 1.41	0.0057	1.2	1.03 - 1.39	0.018
Height (for every 10 cm decrease)	1.27	1.02 - 1.58	0.030	1.23	0.99 - 1.55	0.067
History of Liver Disease	7.90	1.50 - 58.1	0.019	4.06	0.48 - 34.5	0.17

Rifapentine Regimen	Main Analysis Including Imputed PK			Sensitivity Analysis Excluding Imputed PK		
Predictor	Adjusted Odds Ratio	Adjusted 95% CI	Adjusted p-value	Adjusted Odds Ratio	Adjusted 95% CI	Adjusted p-value
Ethambutol $AUC_{0\text{-}24h}$ (for every 5 µg·h/mL)	1.42	1.05 - 1.99	0.032	1.46	1.05 - 2.10	0.033
Height (for every 10 cm decrease)	1.55	1.21 - 1.99	0.000655	1.45	1.90 - 1.11	0.00735
History of Liver Disease	8.55	1.84 - 44.4	0.00578	3.01	0.38 - 19.1	0.24
Asian Race (relative to Black)	2.18	1.29 - 3.61	0.00281	1.87	1.05 - 3.21	0.028

Control Regimen	Main Analysis Including Imputed PK			Sensitivity Analysis Excluding Imputed PK		
Predictor	Adjusted Odds Ratio	Adjusted 95% CI	Adjusted p-value	Adjusted Odds Ratio	Adjusted 95% CI	Adjusted p-value
Ethambutol $AUC_{0\text{-}24h}$ (for every 5 μg·h/mL)	1.44	1.01 - 2.06	0.043	1.33	1.00 - 1.77	0.049
Gene Xpert (for every 3 CT decrease)	0.83	0.71 - 0.97	0.016	0.84	0.74 - 0.94	0.0035
Male sex (relative to female)	0.55	0.37 - 0.82	0.00308	0.62	0.45 - 0.85	0.00306

Among participants receiving the rifapentine-moxifloxacin regimen, height remained significant by likelihood ratio test (P=0.040) after adjusting for age, sex, and race (OR, 1.32 for every 10cm decrease; 95% CI, 1.01 - 1.73). However, after adjusting for only weight, height was not significant by likelihood ratio test (P=0.058). Weight was not significant in univariable or multivariable analyses.

Among participants receiving the rifapentine regimen, height remained significant by likelihood ratio test (P=0.015) after adjusting for age, race, and weight (OR, 1.42 for every 10 cm decrease; 95% CI, 1.07 - 1.87). However, after adjusting for sex in addition to age, race, and weight, height was not significant by likelihood ratio test (P=0.14). Age and race were significant risk factors for any grade 3 or higher adverse events in univariable analyses, while Asian race was significant in multivariable analyses, but weight and sex were not significant in univariable or multivariable analyses.

Chapter 5 - A comparison of clinical development pathways for tuberculosis regimen development.

Introduction

Tuberculosis kills more people than any other single pathogen. 1.2 million people died from TB in 2020 and, while this number was slowly decreasing in recent years from 1.7 million in 2000, progress was halted in 2020 with the first increase in TB mortality in decades as a result of the COVID-19 pandemic[1] . The unprecedented number of new drugs in development for the treatment of TB (more than fifteen in phase I or II clinical trials [https://www.newtbdrugs.org/pipeline/clinical, January 2022]) and the recent success of the 4-month regimen with rifapentine and moxifloxacin[2] provide hope that the 50-year-old 6-month first-line regimen for the world's oldest disease could be replaced with shorter, safer, more effective regimens. Unlike previous approvals of single drugs for the treatment of TB, with limited information about use in combination[3], the development and approval of TB drugs is now focused on the combination regimen as a whole. A recent example would be the approval of a novel pretomanid-based regimen for the treatment of multidrug-resistant TB and extensively drug-resistant TB by the US FDA in 2019 and the EMA in 2020. Nonetheless, there are challenges in interpreting the data from the small uncontrolled trial that led to approval of the pretomanid-based regimen BPaL[4,5], and consequent need for better trial designs.

With a rich pipeline of new drugs and urgent need for tools to end the TB epidemic, the conventional clinical development strategy of testing single substitutions in series is recognized as too inflexible, slow and resource intensive. With this strategy, it is impossible to evaluate all the new therapeutics and their combinations, increasing the likelihood of missing promising ones[6,7]. Conversely, the efficiencies in adaptive clinical trial designs are well known in other disease areas[8], and the potential has been recognized in TB[9,10]. A small number of TB clinical trials with adaptive designs have been initiated, including Simon's two-stage design[11], a Multi-Arm Multi-Stage (MAMS) design[12] (NCT03474198), a Bayesian response-adaptive (BAR) design[13] (NCT02754756), and an adaptive dose-finding design

(NCT04044001). Adaptive trial designs are frequently used in dose-finding trials but are also particularly effective in platform trials, where multiple interventions are simultaneously compared to a single control group. Each of these designs have advantages, limitations, and contexts of use that have not been comprehensively described and evaluated in the setting of TB drug development. Additionally, with funding levels for TB research and development at half of what is required[14], it is imperative that these trials employ designs that can quickly and accurately identify the most promising regimens to fund and continue development. These trials must also generate strong evidence to support regulatory approval, inclusion in international practice guidelines, and programmatic implementation.

Our objective was to conduct a clinical trial simulation study to evaluate and compare innovative late-stage clinical trial development pathways in TB drug development. We compared Phase II/Phase III sequential and seamless approaches, including Bayesian adaptive response and multi-arm multi-stage designs in terms of their efficiency and ability to identify successful regimens. We then provide recommendations for when, where, and how these innovative development strategies could be applied.

Methods

General considerations

We focused on the late-stage clinical development pathway from phase II to phase III. For any regimen entering this pathway, we assumed that all drugs had been shown to have promising anti-TB activity in early-phase clinical trial(s) and that adequate early clinical and non-clinical safety studies had been undertaken to permit evaluation of the combination regimens being given for up to 4 months. We assumed that all pathways had these five main characteristics.

1. The main objective of all pathways is to identify short treatment durations of 12 weeks or less that are noninferior to the control.
2. All pathways included the same control arm, the standard 6-month rifampicin-based regimen to benchmark the trial to historical data (necessary as culture conversion and other treatment response biomarkers vary even between studies of the same regimen[15]).

3. We did not consider more complex platform trial designs where treatment arms are added during the trial.
4. Recruitment to treatment arms can be stopped early for lack of benefit based on interim analysis results (design-dependent), but not for intermediate indicators of overwhelming efficacy. Potentially promising TB regimens based on interim analyses still require full enrollment of all patients to allow for precise estimates of efficacy.
5. All recruited patients in phase II are followed up to 78 weeks post-randomization to collect data on phase III clinical endpoints, e.g. TB-related unfavorable outcomes. Application of this standard feature of phase III designs allows for the data-enrichment of phase II designs and enables better learning opportunities.[16]

Clinical Trial Designs

We evaluated two main adaptive trial designs, the Multi-Arm Multi-Stage (MAMS) and Bayesian Response Adaptive Randomization (BAR) designs (described below). These designs are currently in use for TB regimen development (NCT03474198 and NCT03259269[13]) which gives evidence that they are considered by TB clinical trialists as suitable innovative approaches. The setting of phase III is non-inferiority as compared to control. We have evaluated five distinct drug development pathways:

A. **Conventional Sequential TB regimen development**. The standard clinical development pathway takes a single combination regimen candidate through a learning phase II using an intermediate endpoint, then a confirmatory phase III using the final clinical endpoint. The pretomanid-moxifloxacin-pyrazinamide (PaMZ) regimen was the first combination regimen to follow this pathway and will therefore be our non-adaptive comparator case study.
B. **Multi-Arm Multi-Stage (MAMS) Phase IIC with a separate Phase III**. This design evaluates several potential regimens with the objective to quickly identify poorly performing arms and stop enrollment to them. A fixed number of interim analyses are conducted with each intervention arm compared to control using an intermediate endpoint (time to culture conversion) with recruitment terminated to arms with insufficient evidence of benefit according to prespecified criteria (Figure 5-1A). The MAMS trial design adapted for the context of TB has been previously described[10,12].

C. **Bayesian Response Adaptive Randomization (BAR) Phase IIC with a separate Phase III**. The objective is to continuously evaluate the efficacy of regimens and enroll more patients and gather more data about the most promising regimens. The BAR trial design adapted for the context of TB has been previously described[13,17], where accumulating intermediate endpoint data throughout the trial is evaluated each week of the trial with randomization probability weighted in favor of better performing arms (Figure 5-1B).

D. **Seamless MAMS Phase IIC/III.** Where the phase IIC designs will only enroll a maximum of 100 patients per arm, the seamless trial combines the learning phase II and the confirmatory phase III, relying on adaptive elements to stop poor experimental regimens while enrollment continues for promising experimental regimens until phase III sample size (400+ per arm) is reached. Compared to the phase IIC MAMS design, the larger sample size of the seamless MAMS trial permits more interim analyses and adequately powered evaluation of final clinical endpoint of each regimen. The longer trial duration also permits the accumulation of final clinical endpoint data to perform interim analyses of final clinical endpoint.

E. **Seamless BAR Phase IIC/Phase III**. The seamless BAR design utilizes the same framework as the phase IIc design, but with a larger maximum sample size and adaptive randomization modified to also depend on a later endpoint to simultaneously evaluate regimens by intermediate endpoint and final clinical endpoint.

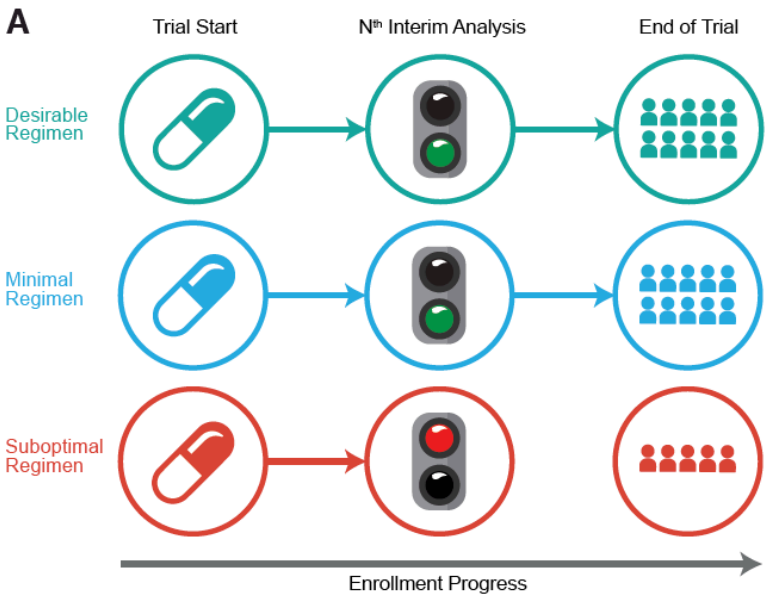
A
Trial Start
Nth Interim Analysis
End of Trial
Desirable Regimen
Minimal Regimen
Suboptimal Regimen
Enrollment Progress

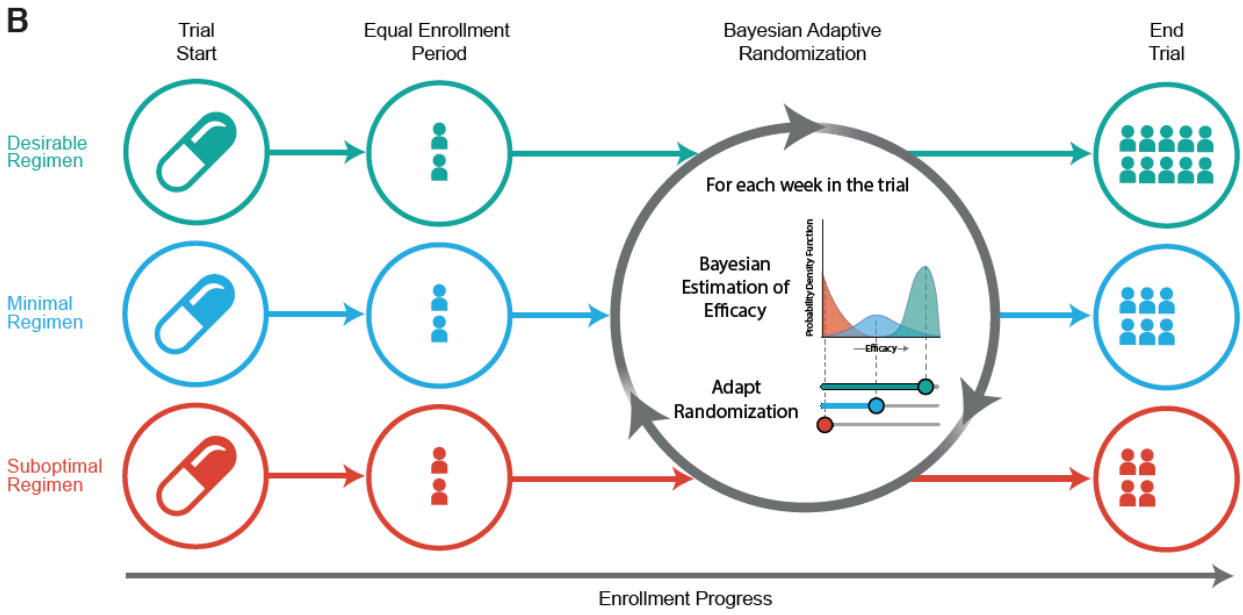
B
Trial Start
Equal Enrollment Period
Bayesian Adaptive Randomization
End Trial
Desirable Regimen
Minimal Regimen
Suboptimal Regimen
For each week in the trial
Bayesian Estimation of Efficacy
Probability Density Function
Efficacy
Adapt Randomization
Enrollment Progress

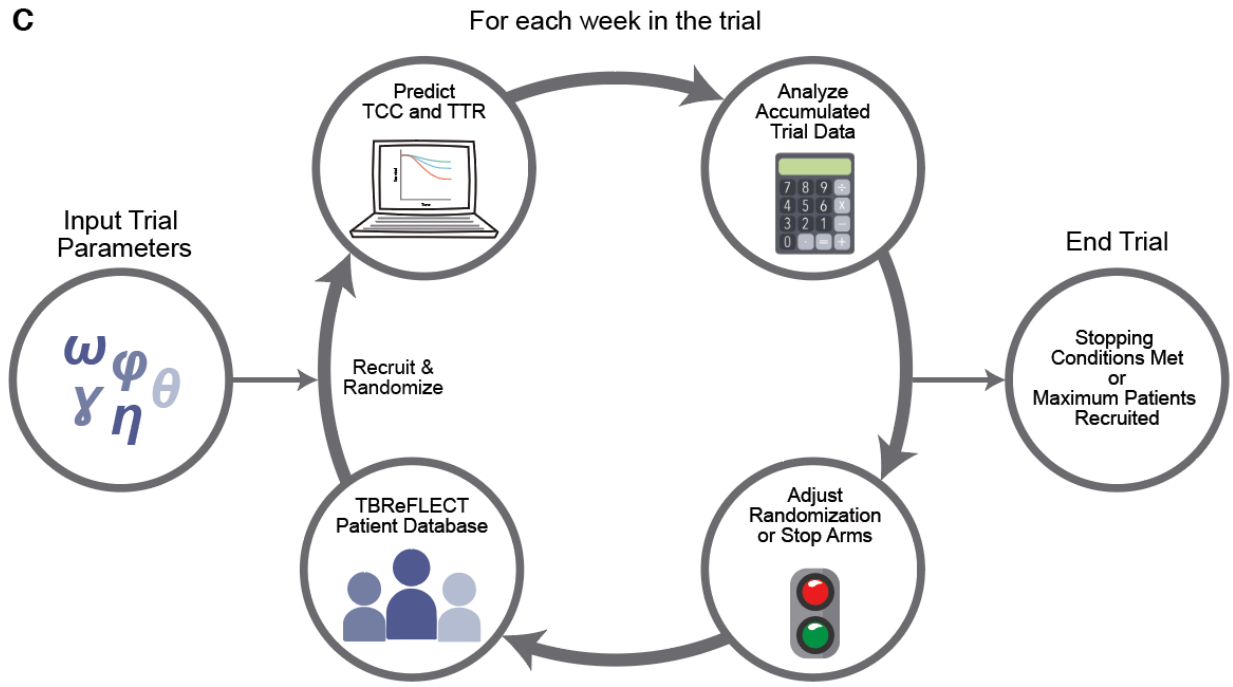

Figure 5-1 MAMS, BAR, & Simulation workflow schematics.

(A) Basic schematic of Multi-Arm Multi-Stage adaptive trial design, where each experimental regimen must pass a predefined criteria at interim analysis to continue recruitment. **(B)** Basic schematic of Bayesian Adaptive Randomization adaptive trial design, where each week the efficacy of each experimental arm is estimated and randomization probabilities are weighted in favor of well performing arms. **(C)** Trial simulation workflow schematic, where simulation trial and design parameters were inputted and for each week in the trial patients are recruited and randomized, their individual TCC and TTR are calculated, and accumulated trial data is analyzed, and then randomization is adjusted or arms are stopped as needed. This is repeated until trial stopping conditions are met or the maximum number of patients are recruited.

Our goal was to describe the operating characteristics of the pathways that graduated desirable regimens (defined in the next paragraph) from phase II to phase III in at least 95% of simulations and suboptimal regimens in no more than 10% of simulations. Given the scarcity of regimens with excellent safety profiles with a high chance of substantial treatment shortening, we decided to limit the risk of falsely stopping a desirable regimen at the expense of graduating a suboptimal regimen to phase III in 10% of occasions. This is analogous to limiting the false positive error (Type I error) rate to 10% while maintaining a high power in phase II.

For seamless phase III trials, to control type I error to <5%, designs were optimized so that <5% of simulations graduate suboptimal regimens and demonstrate noninferiority. We used the 16-week suboptimal regimen (Arm 9) to evaluate type I error and a 5.5% noninferiority margin (the true difference between the median cure rate of Arm 9 and control, see Table 1) was selected for a two-tailed 95% confidence interval noninferiority test.

Regimen Characteristics

We assumed that the trial is evaluating 3 experimental regimens in comparison to the standard of care control arm, with the goal of treatment shortening from 24 weeks to 16 weeks. The simulated regimens were designed to have various characteristics (desirable, minimal, suboptimal) with respect to WHO treatment target regimen profile shortening goals[18] (Table 5-1). The *desirable and minimal regimens* have efficacy comparable to the 24-week standard of care when given for 12 weeks and 16 weeks respectively. A *suboptimal regimen* has efficacy that is only slightly better than the 24week standard of care when given for 24 weeks. Each experimental regimen is evaluated at 3 durations (8, 12, 16 weeks), which brings the total number of arms to 10. See supplemental figure S1 for a graphical representation of the relationship between regimen potency, treatment duration, time to culture conversion, and time to TB-related unfavorable outcome. The relationship between time to culture conversion and time to TB-related unfavorable outcome is based on the relationship observed in TB-ReFLECT (Pooled database of OFLUTUB, ReMOX, and RIFAQUIN fluoroquinolone trials) and is described further in the *Data Generating Mechanism* sections later in the methods and supplemental methods.

Table 5-1 Simulated regimens designed according to 2016 treatment shortening target regimen profile[18].

Median cure rate is drawn from 1000 simulations of 2000 patients per arm with equal representation of easy, moderate, and hard-to-treat subpopulations within and between each arm drawn from the TB-ReFLECT database. The top regimens in order from best to worst: Arm 3, 2, 6, 1.

Arm	Regimen	Duration (Weeks)	Assumed TCC Hazard Ratio	Assumed TTR Hazard Ratio	Median Cure Rate
0	Control (HRZE)	24	Reference	Reference	92.0%
1	Desirable (Meets targets)	8	3.4	0.6	90.0%
2		12			92.5%
3		16			93.5%
4	Minimal (Minimum targets)	8	1.9	0.7	86.5%
5		12			87.5%
6		16			90.5%
7	Suboptimal (Below minimum targets)	8	1.2	0.85	81.0%
8		12			84.0%
9		16			86.5%

Clinical Endpoints

Time to culture conversion (TCC) of sputum liquid culture was used as the intermediate clinical endpoint and time to TB-related unfavorable outcome as the final clinical endpoint. TB-related unfavorable outcomes include treatment failure, relapse, and death for up to 78 weeks post-randomization; henceforth abbreviated as relapse or time to relapse (TTR)[19,20] since relapses make up most of TB-related unfavorable outcomes. The BAR design utilizes Bayesian estimates of binary endpoints as a measure of efficacy, so individual patient TCC and TTR were converted into binary outcomes at week 8, 24, 52, and 78 labeled as treatment success at 8 weeks or TS-8, TS-24, TS-52, and TS-78.

Data Generating Mechanism

The clinical trial data was simulated in R utilizing integrated parametric survival models[19] for intermediate endpoint TCC (up to 26 weeks) and final clinical endpoint TTR (up to 78 weeks). Sputum samples were taken from patients at 1, 2, 4, 6, 8, 12, 17, 22, 26, 39, 52, 65, and 78 weeks. The models quantify relationships between clinical, demographic and regimen features with phase II and phase III outcomes. To reliably represent the population of TB patients, we sampled patients with replacement from the TB-ReFLECT trial participant database with 3411 participants from the modified intent-to-treat analyses of

three large TB phase III trials[19]. We used definitions of easy/moderate/hard-to-treat patient populations from Imperial et. al.[20] to weight the sampling so that all three risk strata groups are equally represented in each simulated trial.

The joint parametric survival models for intermediate (TCC) and final (TTR) endpoint were used to generate individual patient outcomes for each of the regimens. In the models, in addition to treatment effects, time to culture conversion was delayed by older age, higher smear grade, or African clinical site (vs. non-African). Patients with delayed time to culture conversion, male sex, HIV-positive status, or cavitation on baseline chest x-ray had higher risk for TB-related unfavorable outcomes (final endpoint). Patients with the same characteristics will have identical probability functions for TCC and TTR, however the actual observed times for each patient are not deterministic, but randomly and independently drawn from these probability distributions. Models are described in more detail in the supplement and in Imperial et. al.[20]

MAMS Design Parameters

There are three MAMS design parameters to optimize: number of interim analyses, interim timing, and interim criteria. The timing of the interim analysis is crucial; too early and too little data is available to make adequately confident decisions, too late and too many patients have been enrolled into poorly performing regimens. Interim criteria were framed as a minimum TCC hazard ratio and maximum absolute relapse rate (at 52 weeks) that each arm must not pass to continue enrolling until the end of trial. The control arm matches enrollment to the investigational arms and the trial continues until the maximum sample size is reached in arms that are not stopped. These parameters were explored in a grid-like fashion with the goal of maximizing the probability of stopping suboptimal regimens and minimizing the probability of stopping desirable regimens, with the earliest interim timing and the least number of interim analyses.

Bayesian Response Adaptive Randomization

The BAR design estimates efficacy in each arm after a week of participants are randomized and randomization probabilities are adjusted proportionally to the efficacy of each arm. Randomization into the control arm matches the experimental arm with the highest randomization probability, so that the two will have approximately equal sample sizes. Two stopping rules were used: (1) recruitment to an arm is stopped after reaching a maximum sample size (recruitment continues to the other arms and control), and (2) the trial ends when *n* arms reach maximum sample size, where we allowed n to range from 1 to 5. These rules were designed to recruit rapidly to the best performing arms and stop the trial as soon as the top *n* arms have recruited enough patients for sufficient statistical power to demonstrate efficacy.

We modified a Bayesian adaptive randomization framework that has been described elsewhere[13,17], our modifications are briefly described here but also in more detail in the supplement. Two BAR tuning parameters, γ and η, determine how aggressively (γ) the BAR algorithm and when (η) adaptations to randomization probability are weighed in favor of well performing arms. We measured the aggressiveness of adaptive randomization by measuring the ratio of patients allocated to the 16-week desirable regimen over the 8-week suboptimal regimen, while the variability in patient allocation across arms between simulations was quantified by the % coefficient of variation (%CV) of that ratio. These two parameters were explored in a grid-like fashion across a range of reasonable values. Further, parameters were optimized to maximize aggressiveness of randomization and to minimize variability in allocation ratio between simulations with the goal of graduating clinically noninferior arms and stopping suboptimal arms. For phase IIc and seamless designs respectively, *graduation* of an arm was defined as greater than 80 and 350 patients recruited into the arm and *stopping* of an arm defined as less than 50 and 200 patients recruited (analogous to stopping at MAMS first and second interims respectively). The equal recruitment period (before the allocation ratio is changed by the algorithm) was adjusted in the range 10-50 patients per arm in the seamless design and fixed to 10 patient per arm in the phase IIc design due to its short recruitment period. The complete design parameter space explored for trial design optimization is summarized in Table 5-2.

Table 5-2 Simulation conditions, assumptions, and trial design parameter space.
* indicates trial design parameters that were explores and optimized

Parameters	MAMS		BAR	
	Phase IIc	**Seamless II/III**	**Phase IIc**	**Seamless II/III**
Maximum Patients	100 per arm	400 per arm	100 per arm	400 per arm
Recruitment Rate	10 patients/week		10 patients/week	
Culture & Data Lag Time	6 weeks		6 weeks	
Proportion of easy/moderate/hard to treat sub-populations	0.33 | 0.33 | 0.33		0.33 | 0.33 | 0.33	
Intermediate and Surrogate Endpoints Evaluated	TCC HR	TCC HR TS-52	TS-8 TS-24	TS-8 TS-24 TS-52
Number of Interim Analyses	1-2*	2-3*	--	--
Timing of Interim Analysis	10 - 100 patients*	100 - 400 patients*	--	--
Interim Criteria	TCC HR threshold: 1.1 – 2.3* Relapse % threshold: 4 – 20%*		--	--
Equal Recruitment Period (before adaptive algorithm is initiated)	--	--	10 patients per arm	10-50 patients per arm*
Bayesian adaptive randomization tuning parameters	--	--	Nonaggressive - Aggressive γ = 1 – 25* η = 0.1 – 2.0*	
Trial Stopping Rules	--	--	4 Arms reach max N	3 Arms reach max N
Priors	--	--	--	Optimistic* Skeptical*

Simulation Tool

Recruitment to the simulated trials was fixed at a total of 10 patients per week, selected as a reasonable estimate for a global multi-center TB trial[18-20]. It was assumed that TCC and TTR were available for statistical analysis 6 weeks after the actual event to account for the biological assay time and for the results to be entered into the database. For each week of the trial simulations:

1. 10 patients are 'recruited' from TB-ReFLECT patient database
2. Patients are randomized into arms/regimens; their individual intermediate (TCC) and final (TTR) endpoints simulated by the aforementioned integrated parametric survival models. Prior to any adaptive modifications, patients in each simulated trial were randomly allocated with equal probability to either a control arm or one of nine intervention arms.
3. For the BAR design, available data are analyzed, and randomization probabilities are updated. For the MAMS design, available data are only analyzed when interim analyses are triggered, then randomization is updated accordingly.

4. Proceed to the next week.
5. Steps 1-4 are repeated for each week of the trial until maximum number of patients have been recruited or trial stopping rules have been met.

MAMS and BAR design parameter space were explored with 1000 simulations performed for each set of parameter values to identify optimal sets with desired characteristics. Further details of design parameters have been explained above and the parameter space explored defined in Table 5-2; the simulation workflow is shown in Figure 5-1C.

Performance Measures

Each of the five optimized clinical development pathways were compared based on the following performance measures: total study and pathway duration, total recruitment, enrollment per arm, bias in estimation of treatment effects, number of observed relapse events per arm, and the probability of correctly selecting treatment shortening arms and stopping undesirable arms.

Sensitivity Analyses

Sensitivity analyses were performed to assess how recruitment rate, the assumed relationships in the parametric survival models, longer data lag times, and different compositions of desirable, minimal, and suboptimal regimens in the trials affect our conclusions. Further details can be found in supplemental methods.

Results

Results are summarized for each distinct design first, followed with a comparison between designs. Since differences in treatment duration impact the final endpoint and not the intermediate endpoint, treatment duration does not impact phase IIc stopping criteria (based on the intermediate endpoint of TCC) and therefore different durations of the same regimen are combined in the presentation of the phase IIc results.

Multi-Arm Multi-Stage (MAMS) Phase IIc

We found that one interim analysis that occurs after 50 patients (Fig. 5-2A) have been recruited in each arm and an interim criteria hazard ratio threshold of 1.7 (Fig. 5-2B) meets our criteria for an optimal design. In this setting, the desirable and suboptimal regimens graduated in 99.8% and 8.2% of simulations respectively. Minimal regimens graduated in 65.2% of simulations (Fig. 5-2C). Setting a lower hazard threshold or an earlier interim analysis will decrease the graduation rate of desirable regimens without appreciably increasing the stopping rate of suboptimal regimens. A second interim was explored but did not add value. With the suboptimal regimen already being stopped in 91.8% of simulations after the first interim analysis, the logistical cost of a second interim analysis did not justify the small potential benefit of stopping additional suboptimal regimens.

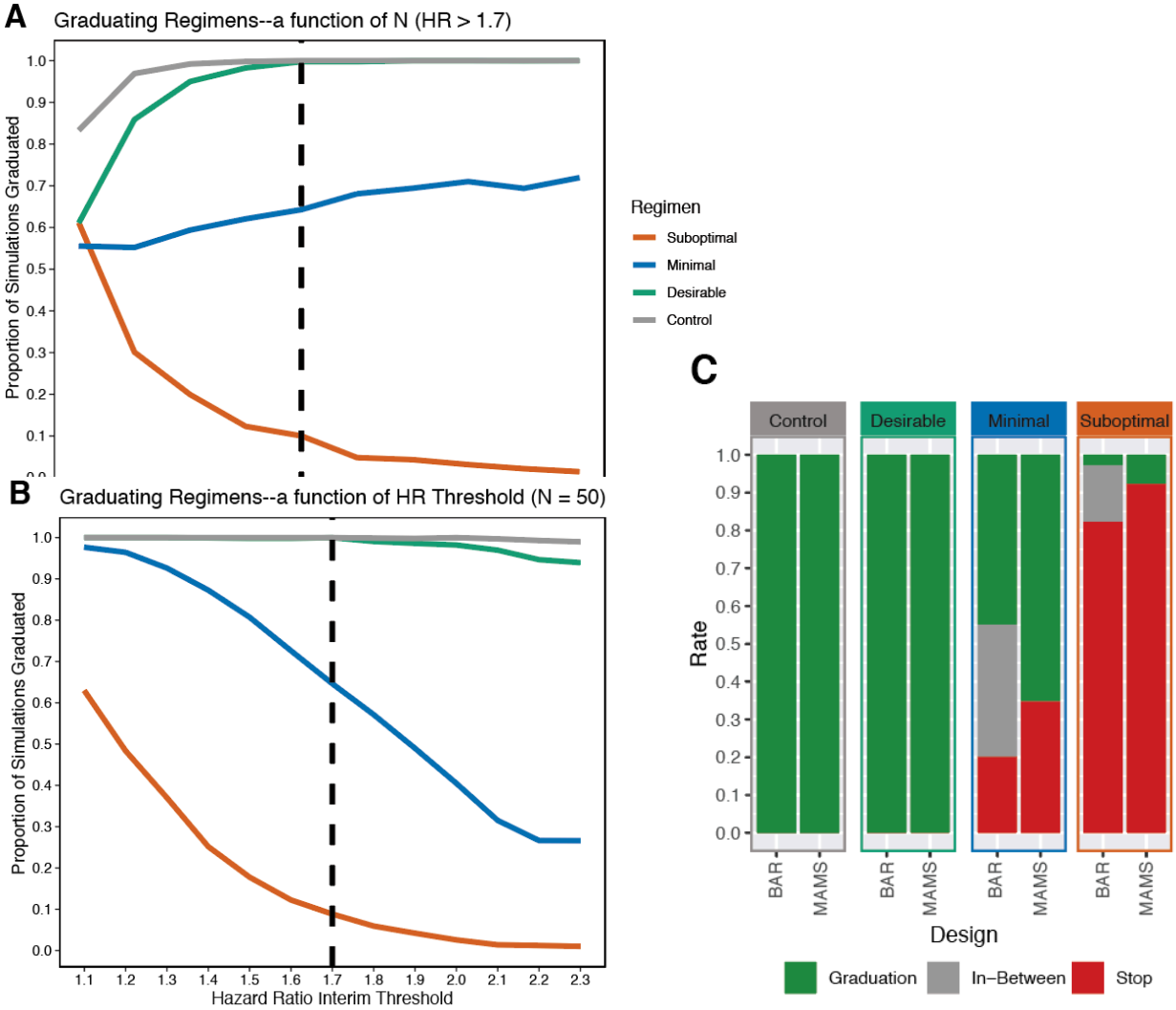

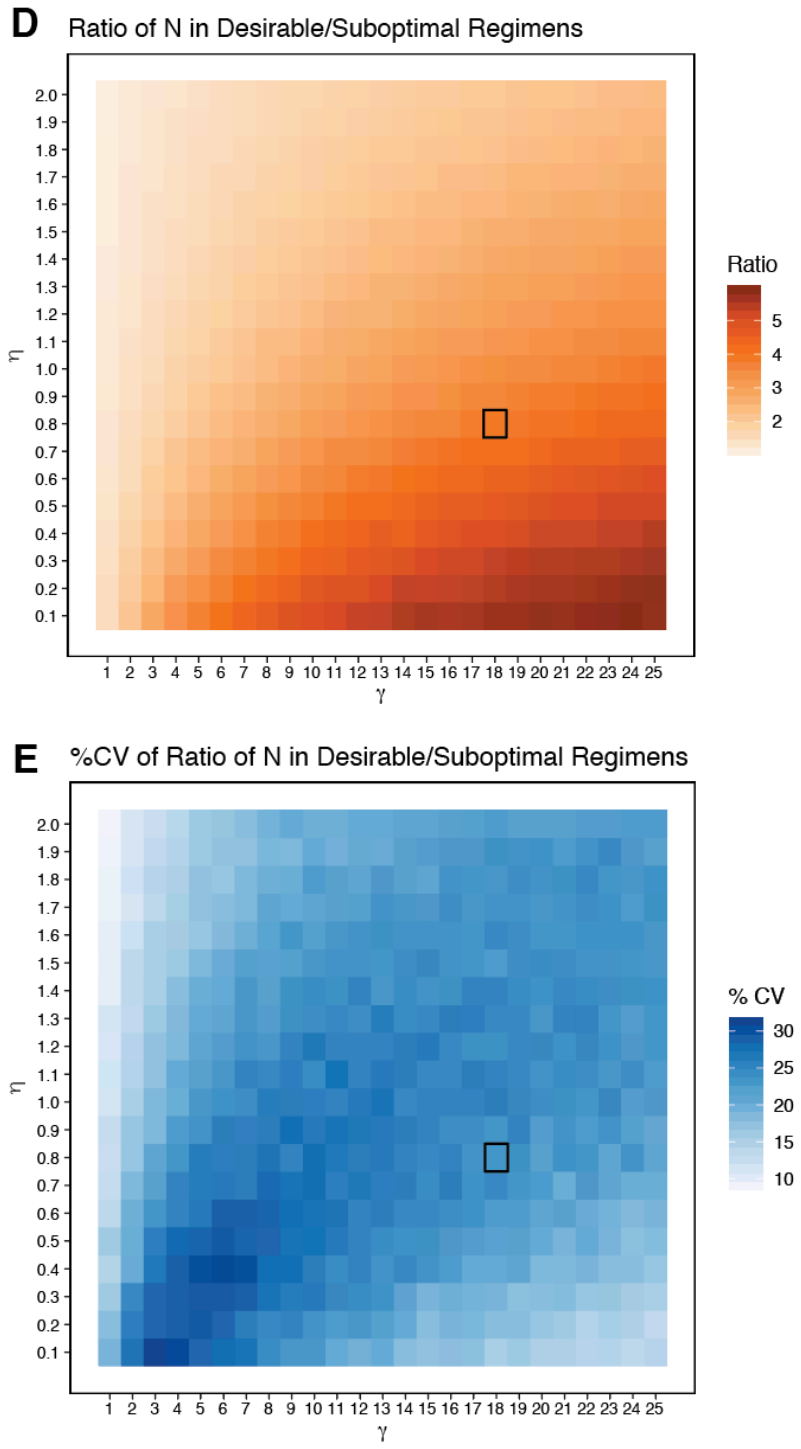

Figure 5-2 Phase IIc MAMS and BAR optimization and comparison.

(A) Fraction of simulations graduated for Phase IIC MAMS trials with interim criteria fixed at TCC HR > 1.7 while changing interim timing from 10 – 100 patients recruited into the control arm, at 10 patients/week interim timing is approximately study week 10 – 100. **(B)** Fraction of simulations graduated for Phase IIC MAMS trials with interim timing fixed to 50 patients and changes TCC HR criteria from 1.1 to 2.3. Dotted lines show the chosen optimized conditions, where an interim timing of 50 patients per arm

is the earliest timing in which the risk of stopping the desirable regimen is negligible and an interim criteria of TCC HR > 1.7 is the strictest criteria in which the risk of stopping the desirable regimen is negligible. The control in grey, represents the proportion of simulations in which the trial was not stopped prematurely due to all investigational arms being stopped. **(C)** Comparison of graduation and stopping rates of optimized Phase IIc MAMS and BAR designs. The continuous nature of the BAR recruitment was translated into a semi-discrete outcome for comparison to the MAMS design, *graduation* of an arm was defined as greater than 80 patients recruited into the arm, *stopping* of an arm defined as less than 50 patients recruited (analogous to stopping at MAMS interim) and *in-between* defined as 50-80 patients recruited into the arm. Both designs meet our target criteria graduating > 95% of desirable regimens and < 10% of suboptimal regimens. **(D)** Heatmap quantifying the aggressiveness of Bayesian adaptive randomization as the ratio of patients allocated to the desirable regimen/suboptimal regimen across a range of reasonable ɣ and η values. **(E)** Heatmap of the variability expressed as %CV in the ratio shown in D across 1000 simulations. The optimal condition outlined in black was chosen for its aggressiveness and limited variability while meeting our target critiera.

Bayesian Response Adaptive Randomization (BAR) Phase IIc

We identified a set of BAR tuning parameter values (γ =18, η =0.8) that meets our criteria for an optimal design. This optimized BAR design aggressively randomizes 2.5 times (Fig. 5-2D) more patients into the desirable regimen (median N = 100, see Supplemental Fig. 5-2B) over the suboptimal regimen (median N = 40) while limiting % CV of this ratio to less than 20% (Fig. 5-2E). The desirable regimen graduated in 99.5% of simulations (where graduation is defined as the sample size reaching 80 or more), and was stopped in 0.1% of simulations (where stopping was defined as the sample size not exceeding 50, Figure 5-2C). For minimal regimens 49.5% graduated and 18.3% were stopped. For suboptimal regimens 2.7% graduated and 81.0% stopped. The heatmap in Fig 5-2D shows the γ and η parameter space explored to optimize the aggressiveness of adaptive randomization, other sets of γ and η values might be suitable for trials with different objectives.

Seamless MAMS Phase II/III

Building off the optimized phase IIc MAMS design, we found that a second interim occurring after 200 patients (Fig. 5-3A) have been enrolled in each continuing arm with an interim criteria of a 12% relapse threshold (Fig. 5-3B) met our criteria for an optimal seamless design. Because the differences in treatment duration largely manifest as differences in relapse rate, a relapse rate threshold is able to distinguish between different durations of the same regimen. Therefore, the second interim served primarily to stop regimens that have a favorable intermediate endpoint (TCC) profile, but underwhelming

efficacy measured by final endpoint, e.g. relapse rate (Fig. 5-3C). Under these conditions, desirable regimens at 8, 12, and 16 week durations have a 2.2%, 1.3%, and 0% chance of being stopped respectively, minimal regimens 65.8%, 38.6%, and 37.5%, and suboptimal regimens 99.7%, 97.5%, and 95.3%. Only 9/1000 (0.9%) simulations graduated and demonstrated noninferiority for the 16-week suboptimal regimen (analogous to type I error). A third interim was explored, but since a two interim design well exceeded our aforementioned trial objective of graduating >95% of desirable regimens and <10% of suboptimal regimens, a third interim would provide limited benefit and was considered unnecessary.

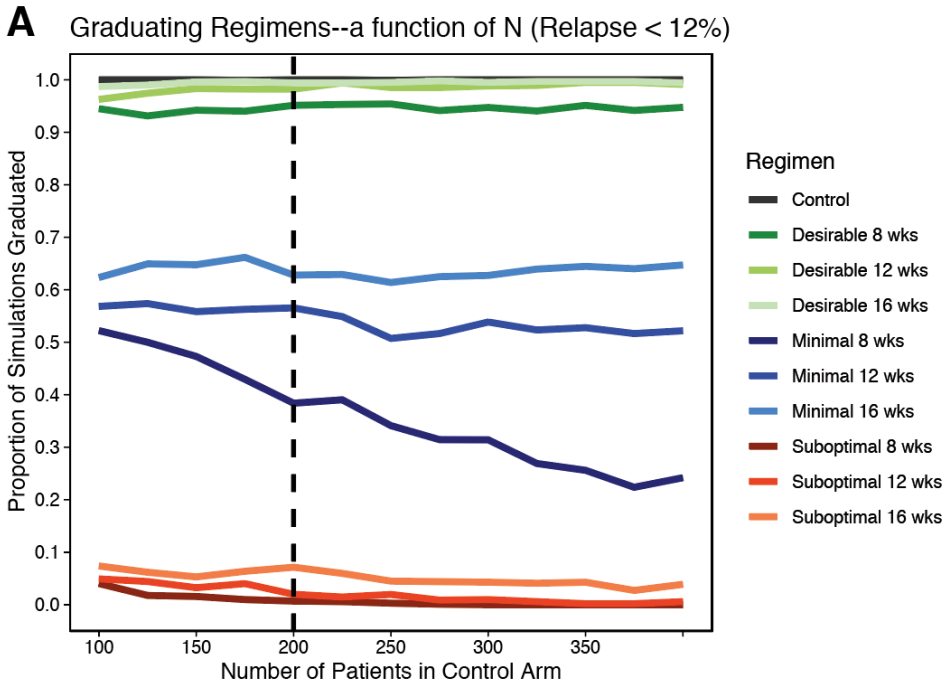

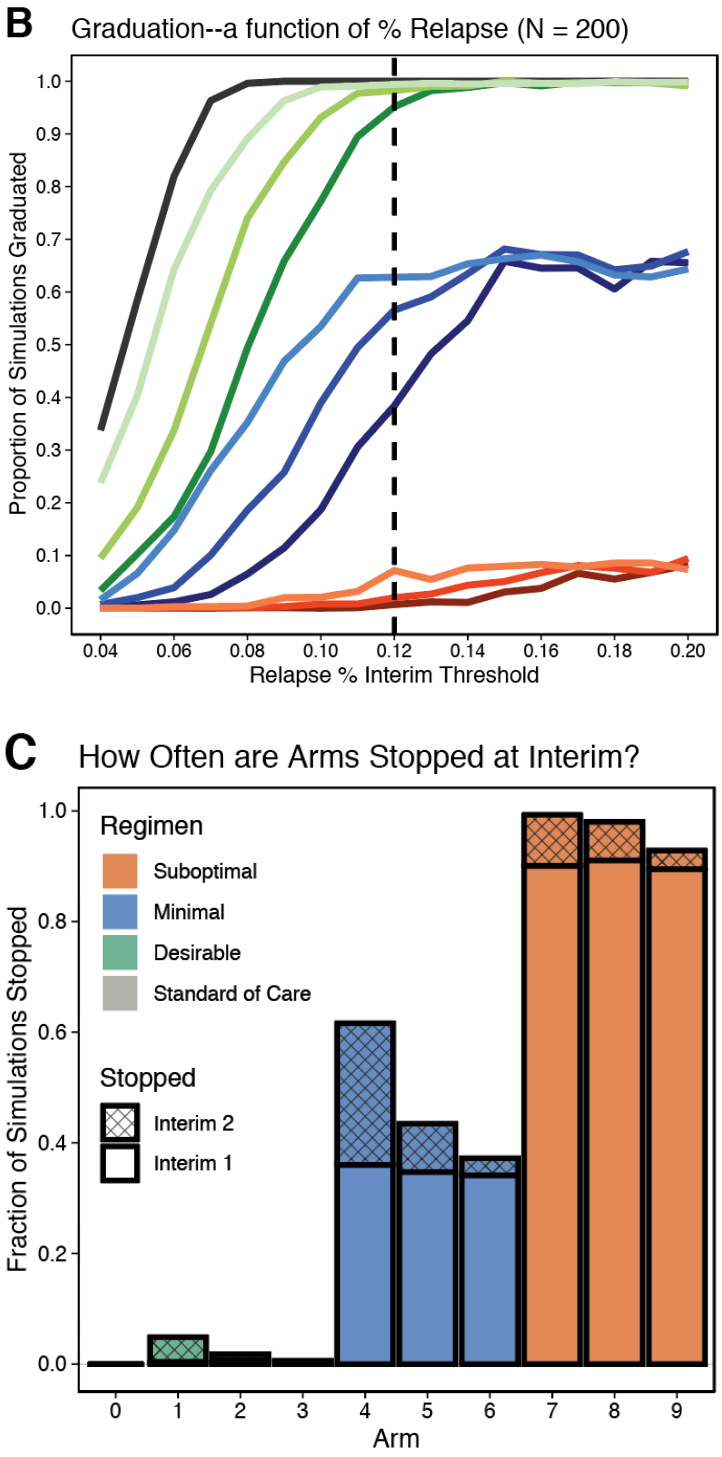

Figure 5-3 Seamless MAMS interim timing and criteria optimization.

(A) Fraction of simulations graduated for Seamless MAMS trials with second interim criteria fixed at relapse rate < 12% while exploring second interim timing. The control in grey, represents the proportion of simulations in which the trial was not stopped prematurely due to all investigational arms being stopped. **(B)** Fraction of simulations graduated for Seamless MAMS trials with second interim timing fixed at 200 patients per arm while exploring second interim criteria. Dotted line represents selected optimized second

interim conditions, where an interim timing of 200 patients per arm is the earliest timing in which the risk of stopping the desirable regimen is negligible and an interim criteria of relapse rate < 12% is the strictest criteria in which the risk of stopping the desirable regimen is negligible. **(C)** Fraction of arms stopped in interim 1 and 2. Note that interim 2 can distinguish between different durations of the same regimen, whereas interim 1 cannot.

Seamless BAR Phase II/III

We found that less aggressive BAR tuning parameters (γ =8, η =0.3) compared to the more aggressive phase IIc BAR tuning parameters, were better suited for our criteria for an optimal seamless trial. This optimized BAR design randomizes 5.9 times (Fig 5-4A) more patients into the 16-week desirable regimen (median N = 400) over the 8-week suboptimal regimen (median N = 67) while limiting the variability across simulations to < 50% (Fig 5-4B). Although the heatmap (Fig 5-4A) reveals more aggressive options for γ and η, the goals of phase IIc and seamless phase II/III differ where a seamless trial must not only distinguish between different durations of the same regimen but also evaluate regimens by the 52-week relapse endpoint. We found that a moderately aggressive randomization was more suitable for this purpose; in Fig. 5-4C, representations of aggressive and less-aggressive BAR simulations demonstrates that less-aggressive adaptation allows more time for 52-week relapse data to accumulate and therefore affect randomization. At 1100-1200 patients randomized, the 8-week desirable regimen recruitment begins to slow down while the 16-week minimal regimen speeds up in the less aggressive design eventually overtaking 8-week desirable regimen recruitment as compared to the more aggressive design. This is the consequence of the accumulation of incoming long term relapse data and demonstrating the benefit of slower adaptation in this context. Supplemental Figure 2 further demonstrates the desired behavior where the enrollment distribution in each arm produced a graded allocation of patients across the different treatment durations where the phase IIc design did not.

The desirable regimens at 8, 12, and 16 week durations graduated in 57.2%, 82.6%, and 93.8% of simulations respectively and stopped in 24.5%, 9.4%, and 3.5% of simulations respectively (Figure 5-4D). Although this set of design parameters falls just short of our 95% graduation target, the graded response of the BAR design makes a difficult translation to a binary graduation-stop result and we believe that this set of parameters is suitable for our trial objectives. Minimal regimens at 8, 12, and 16 week durations

graduated in 8.6%, 23.5%, and 58.9% of simulations respectively and stopped in 75.5%, 54.1%, and 23.9% of simulations respectively. Suboptimal regimens graduated in 0%, 0% and 1.3% of simulations and stopped in 99.6%, 98.9%, and 94.2% of simulations. Additionally, only 3.5% of simulations falsely rejected the null hypothesis for the 16-week suboptimal regimen (analogous to type I error).

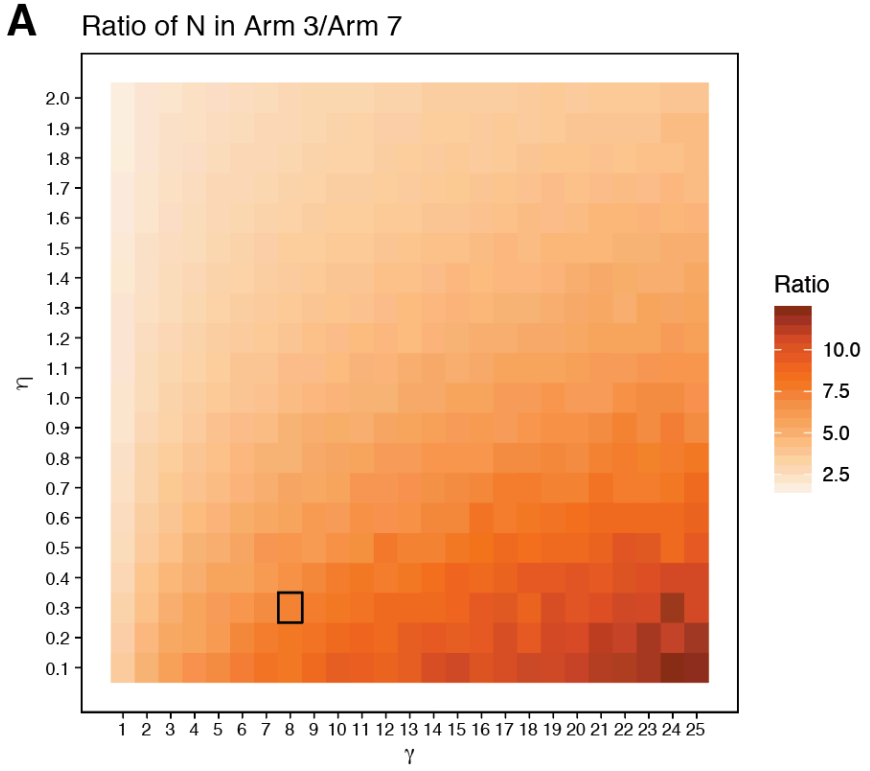

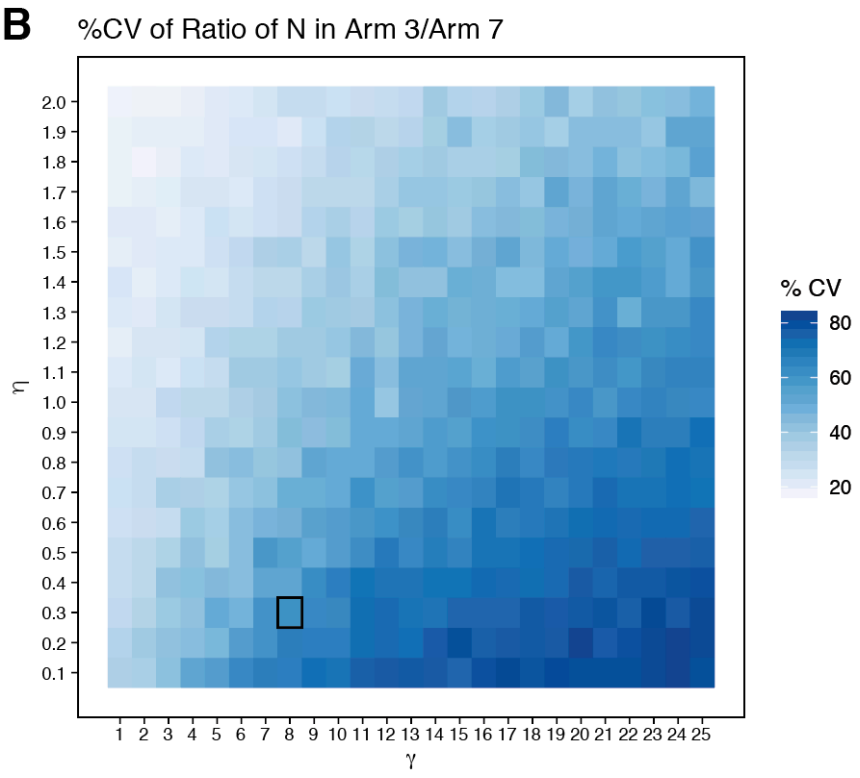
B
%CV of Ratio of N in Arm 3/Arm 7
η
γ
% CV
80
60
40
20

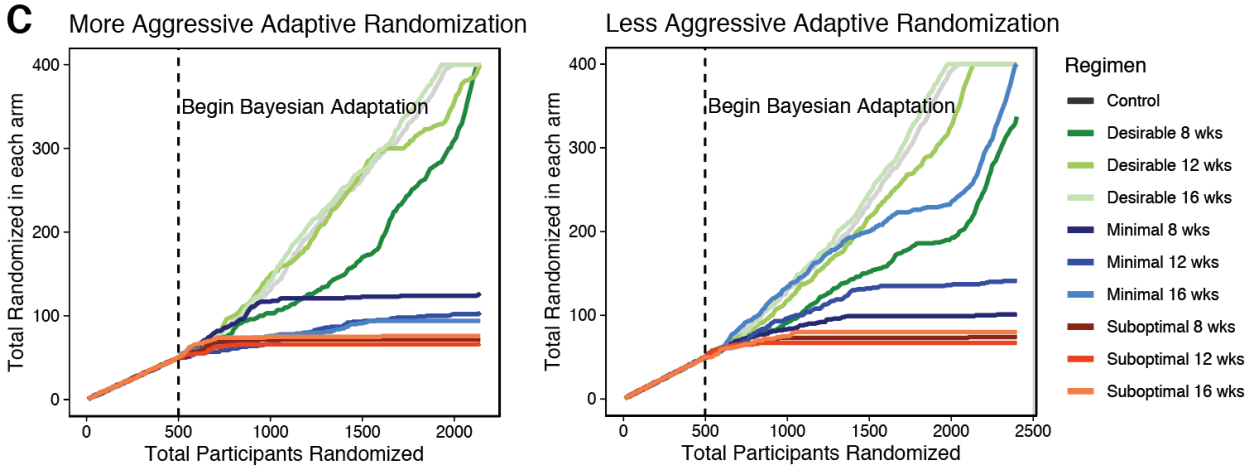
C
More Aggressive Adaptive Randomization
Less Aggressive Adaptive Randomization
Begin Bayesian Adaptation
Total Randomized in each arm
Total Participants Randomized
Regimen
Control
Desirable 8 wks
Desirable 12 wks
Desirable 16 wks
Minimal 8 wks
Minimal 12 wks
Minimal 16 wks
Suboptimal 8 wks
Suboptimal 12 wks
Suboptimal 16 wks

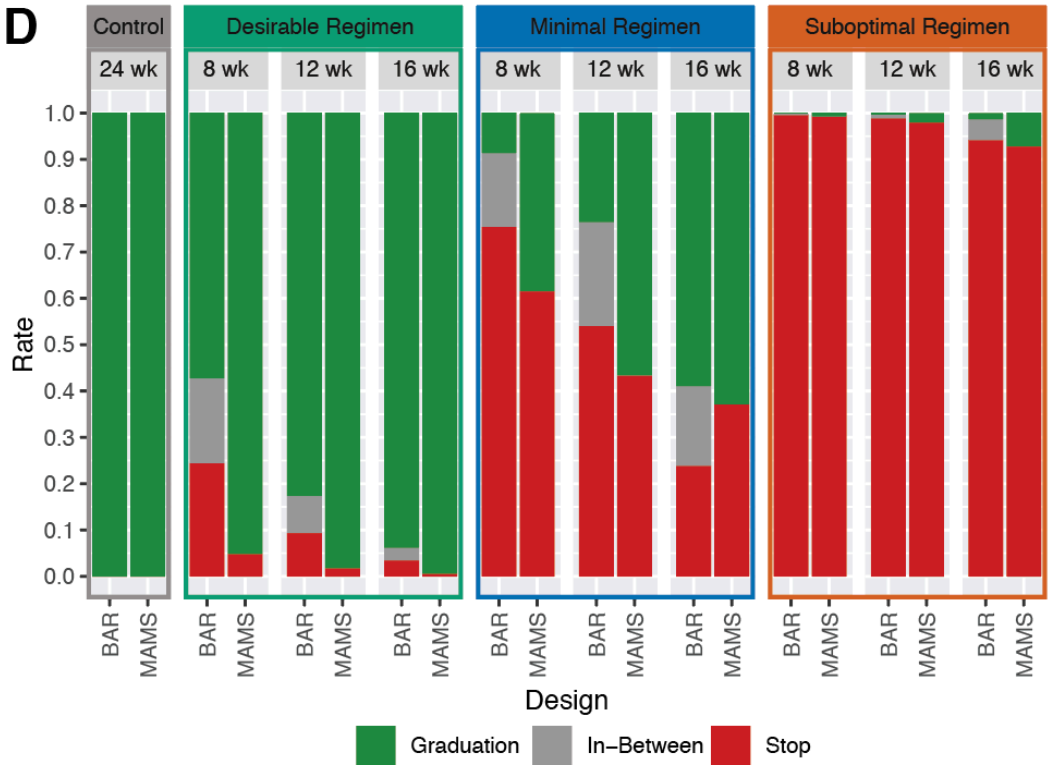

Figure 5-4 Seamless BAR optimization.

(A) Heatmap quantifying the aggressiveness of Bayesian adaptive randomization across a range of ɣ and η values. **(B)** Variability of patient distribution across simulations represented as % CV. (**C)** Representations of aggressive and less-aggressive BAR designs shows the suitability of less-aggressive adaptation for the seamless design. Less-aggressive adaptation allows relapse data to be taken into account and adjust randomization. At 1100-1200 patients randomized Arm 1 recruitment slows down while Arm 6 speeds up, reflecting incoming relapse data that reduces confidence in Arm 1 and increases confidence in Arm 6. **(D)** Graduation and stop plot comparing Seamless MAMS and BAR. The continuous nature of the BAR recruitment was translated into a semi-discrete outcome for comparison to the MAMS design, *graduation* of an arm was defined as greater than 350 patients recruited into the arm, *stopping* of an arm defined as less than 200 patients recruited (analogous to stopping at MAMS interim) and *in-between* defined as 200-350 patients recruited into the arm. Both designs are comparable and are suitable for our purposes, but BAR excels at penalizing and thus stopping poorly performing arms.

Overall Comparison of Trial Designs

BAR designs offer a clear advantage in identifying the most promising regimens more quickly with fewer patients than MAMS designs; BAR designs recruited 80 and 420 patients less in phase IIc and seamless trials respectively. Both MAMS and BAR designs were much more efficient compared to the conventional sequential approach which would recruit 1000 patients for phase IIc and 4000 for the seamless design (Figure 5-5). A major contributing factor to the observed recruitment advantage of the BAR design, is that

for MAMS, patient recruitment by arm is clustered around the interim analyses (50 and 200 patients) and trial end (400 patients), while BAR's patient distributions are continuous with each arm's median scaling with efficacy (Supplemental Figures 5-2B and 5-3). Both MAMS and BAR designs produce accurate efficacy estimates consistent with values produced by unbiased simulations (Supplemental Fig 4A and 4C), however the precision in estimating efficacy is directly proportional to the number of observed relapse events (Supplemental Fig 4B) and thus number of patients (Supplemental Fig 3) randomized into that arm. None of the designs introduced significant bias (<±7% median bias, Supplemental Fig 4C) except for 12% median underestimation of relapse rate in Phase IIc BAR suboptimal regimens due to the small sample size (N = 40).

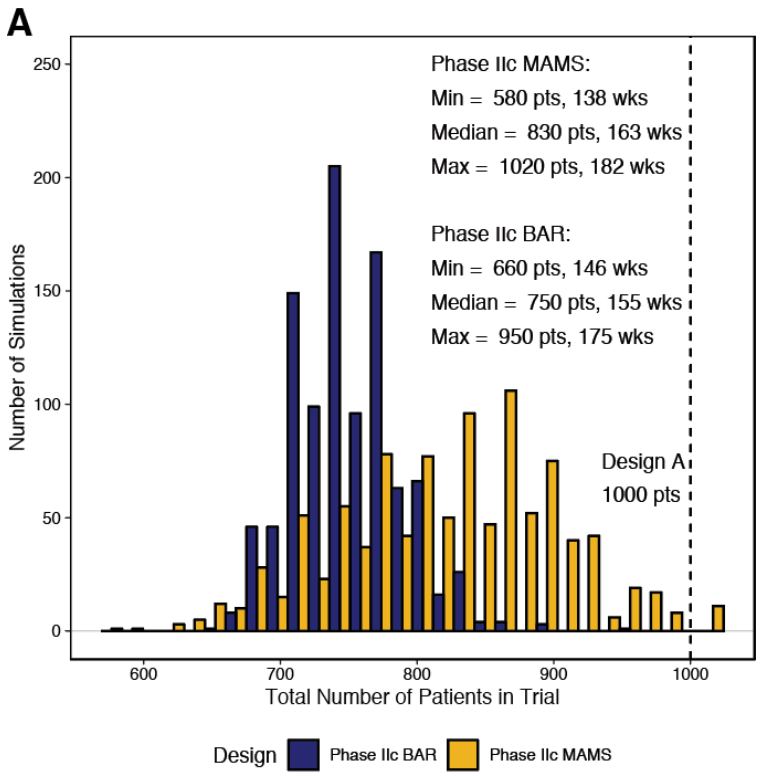

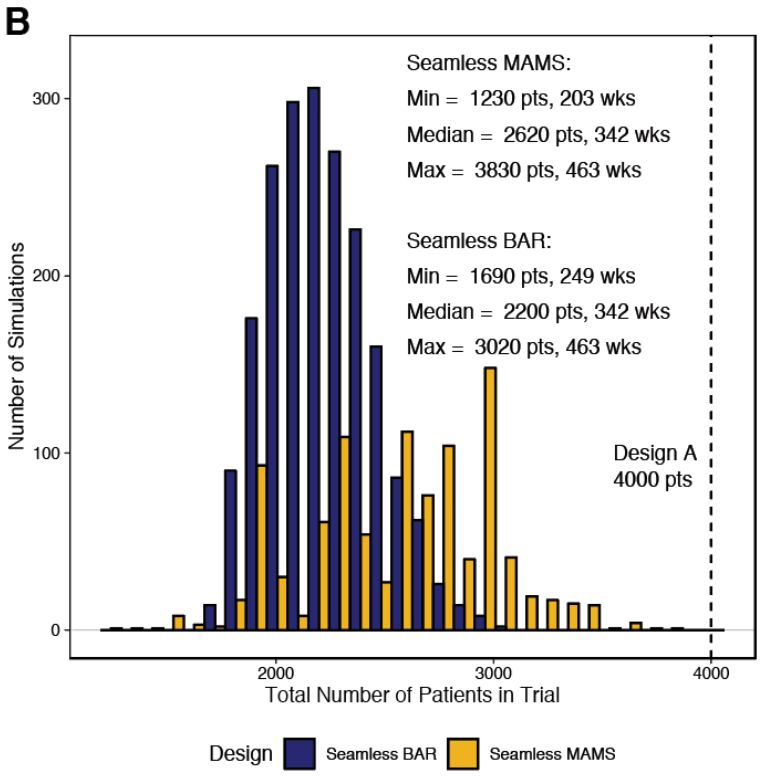

Figure 5-5 Study Duration and Total Recruitment Comparison of BAR and MAMS.

(A) Phase IIc and **(B)** Seamless Phase II/III comparisons. BAR and MAMS designs have comparable performance in graduating the best regimens and stopping the suboptimal regimens (demonstrated previously) while BAR consistently outperforms MAMS in study duration and total recruitment. Although both MAMS and BAR provide enormous time and patient savings compared to conventional clinical trials, the median Phase IIc BAR enrolls 80 fewer patients and saves 8 weeks of time compared to the Phase IIc MAMS and the median Seamless BAR enrolls 420 fewer patients and saves 42 weeks of time compared to the Seamless MAMS.

Sensitivity Analyses

Recruitment rates of 5-15 patients per week did not significantly change the results of the optimized adaptive trial designs, MAMS and BAR graduation rates changed less than an absolute 5%. However, a faster enrollment of 30 patients per week was too fast to allow for TCC or relapse data to accumulate in time for MAMS interim analyses or significantly affect BAR randomization probabilities. BAR designs were more sensitive to changes in recruitment rate because graduation is dependent on patient randomization which is directly dependent on the accumulation of data. All graduation decisions benefitted from a slower recruitment rate, but the benefit was minimal in the range 5-15 patients per week. Sensitivity analyses are presented in more detail in the supplement.

Discussion

In this study, we have demonstrated the suitability of adaptive trial designs for TB regimen development and have described optimal MAMS and BAR designs in the phase IIC and seamless phase II/III settings. In the seamless phase II/III designs, suboptimal regimens graduated in less than 10% of simulations with desirable regimens graduating in more than 95% of simulations. Both designs were able to discriminate between different durations of the same regimens where the 16-week minimal regimen graduated in 62% and 58.6% of simulations and the 8-week minimal regimen graduated in 33% and 8.6% of simulations for MAMS and BAR designs respectively. Additionally, both designs were able to reliably select the noninferior regimens (12 and 16 week desirable regimen) in at least 80% of simulations; bias was minimal in arms that graduated. In the phase IIC designs, desirable regimens graduated in >99% of simulations, while suboptimal regimens graduated in 8% and 2.7% of simulations for the MAMS and BAR designs respectively. Importantly, since adaptation in the smaller phase IIC trials is based only on the intermediate endpoint, TCC, which is independent of treatment duration, these phase IIc designs were not able to discriminate between different durations of the same regimen.

Recommendations regarding BAR and MAMS

Our objective was to compare the operating characteristics of different designs that have utility for TB regimen development, and specifically to describe particular designs that met our objectives of a typical regimen development program. From a broad view, adaptive trial designs offer a clear advantage in simultaneously evaluating more intervention arms with similar numbers of patients in a shorter time frame. Indeed, we found that the BAR designs require the least number of patients and also allow for more flexibility in trial objectives. For example, the ɣ and η parameters of the BAR design can be modified to have a less aggressive adaptive algorithm so that less weight is put on early data and the algorithm waits for more data before substantially changing randomization probabilities. Importantly, the adaptation algorithm in BAR weighs randomization in favor of the best performing arms relative to control. Therefore, while there is not necessarily an *direct* comparison with the other arms, the final sample sizes and trial durations are influenced by the *indirect* comparative efficacy of the arms. In other words, a trial with all equivalent suboptimal regimens will randomize patients equally between arms, as will a trial with all

equivalent desirable regimens. Therefore, the BAR design is most efficient for multi-arm trials with a combination of regimens of unknown efficacy potentially spanning suboptimal to desirable. In contrast, the MAMS design depends only on comparisons against the control arm and therefore whether a particular arm stops or continues does not depend on other arms in the trial, although that doesn't rule out comparisons between two active arms in an indirect fashion. Additionally, MAMS designs are more efficient and result in smaller sample sizes compared to BAR when all evaluated treatments are underperforming and fail to achieve minimum efficacy targets[21,22].

Critically, the choice of design and specification of design parameters, including timing of the interim analysis and target efficacy thresholds for the MAMS design, and randomization tuning parameters and stopping rules for the BAR design, will very much depend on the sponsor's objectives. If the objective is to consider each regimen on its own merit as compared to control, then the MAMS design is better suited, but if the objective is to rapidly select amongst a number of regimens that are likely to include a range of regimens from suboptimal to desirable then the BAR design is perhaps better suited. In the current landscape of TB drug development, with over ten new drug candidates, a MAMS design would select all regimens that meet the minimum target criteria, while the BAR design would efficiently rank the regimens and recruit greater numbers of patients to the top regimens to generate further evidence of efficacy. If the BAR design is modified to permit stopping for futility (see section on additional design modifications below) then the benefits (and limitations) of both MAMS and BAR would likely be combined – exploration of this was beyond the scope of this paper.

There are other considerations of MAMS and BAR designs that cannot be described with clinical trial simulations and make each design more or less suited to trial objectives. Adaptations can only occur at a limited number of interim analyses in the MAMS design which means a data and safety monitoring board can still have oversight over stopping decisions and incorporate safety considerations in their deliberations. Ongoing adaptation in the BAR design adds additional burdens on clinical trial conduct, workflow, and data management to ensure that data is available on the database with as few errors as possible at each point throughout the trial[23], whereas this is only needed at specific times when interim

analyses are being conducted in the MAMS design. On the other hand, MAMS can be less efficient than a BAR design when there are large differences between regimens as no adaptations can occur until the first interim analysis.

The typical delay in culture assay results (up to 6 weeks to perform assays) introduces some complexities in implementing adaptive trial designs in TB clinical development. Ideally, adaptive trial designs base interim analyses on early, accurate, and fast prognostic biomarkers. TCC is anything but early and fast, with most patients' culture converting between 4 – 8 weeks and therefore assay results not available until 10-14 weeks post-treatment initiation. Nevertheless, the follow up period is long, up to 78 weeks, which in combination with the slow recruitment rate (approximately 10 per week for a large global multicenter trial) allows for plenty of time for the adaptive elements of a trial design to be effective even with a slow intermediate endpoint like TCC.

Notably, seamless designs are especially time efficient; in addition to the time saved from reduced patient enrollment and thus reduced enrollment period, moving seamlessly between phases eliminates the need for two treatment follow up periods (each 18 months after enrollment of the last patient) and a 12-18 month analysis and planning period between trial phases[24]. However, seamless designs require careful planning, rapid and efficient data management, large upfront investment of logistics and resources, and steadfast sponsors and stakeholders to complete a prescribed seamless trial, not all of which are usually present which means seamless designs are rare in practice. In total, the seamless approach can accelerate TB regimen clinical development timelines by 2-4 years.

The effect of recruitment rate

We have shown that modest changes in recruitment rate have limited impact in the scenarios we explored. It is true that a substantial increase in recruitment rate can reduce efficiencies in adaptive designs with late outcome measurements, but this effect is limited unless recruitment is very fast relative to the overall study size. This means that it would normally be worth adding a new site to increase the

rate of recruitment while reducing the overall duration of the trial with only a modest impact on design efficiencies.

Additional Design Modifications

Besides the parameters and designs described thus far, there are many additional levers and interesting tools that can be adapted to suit various objectives: (1) Adding new regimens and arms in an ongoing phase IIc screening trial is of particular interest and there are case studies in oncology and COVID where this has been done with a BAR[25] or MAMS[26,27] design. (2) Stopping for overwhelming efficacy/futility is another often considered rule. Although stopping for overwhelming efficacy was not considered within the context of our work due to potential power issues, this feature can easily be added to MAMS interim analyses (which stop for futility). Stopping for overwhelming efficacy/futility can also be added to a BAR design, instead of only relying on the adaptive randomization algorithm, thereby attaining some of the benefits of the MAMS design. However, these features must be implemented with planned interim analyses and appropriate sample size adjustments to control type I error[28-30]. (3) REMoxTB, RIFAQUIN, OFLUTUB, and ACTG5349/Study 31 phase III trials have all demonstrated the complex interplay between regimen potency, disease severity, and treatment duration[19]. Patient subpopulation enrichment which enrolls and enriches for hard or easy-to-treat patients—is a strategy employed to control the disease severity representation in the trial. It can be used to increase trial efficiency and likelihood of success. Hard-to-treat subpopulations have a higher probability for treatment failure and bacteriological relapse thus, in this population, one might observe the same number of unfavorable events with a smaller sample size. Opting to enrich for hard-to-treat subpopulations instead of including all patients must be carefully approached. While higher outcome rates are likely to be observed, and therefore the design will have greater power to distinguish regimens, these types of trials might have other limitations when extrapolating efficacy and safety findings to the unstudied patient subpopulations. (4) Finally, treatment duration represents another manipulable variable which heavily impacts regimen efficacy and trial success, and TB trialists have turned to duration randomization trials[31,32] to optimize treatment duration prior to large confirmatory trials. The trial designs described here can be altered to estimate duration response curves or to select the shortest treatment duration that exceeds a minimum likelihood threshold

for noninferiority. Each of these design modifications could change operating characteristics of MAMS and BAR trials; additional simulations would be needed to explore this.

Limitations

There are a few limitations in the work described here. First, we explored a limited set of possible arm and regimen configurations, along with a limited set of parameters and trial rules. Given the vast parameter space and the flexibility of trial designs, we wanted to limit the scope of this study within the context of a large platform adaptive trial while highlighting the possible mechanisms that can be adjusted for a different set of trial objectives. Second, the models used to predict individual patient intermediate and final endpoints are based on data generated from rifamycin containing regimens, and the risk factors for culture conversion and relapse may not hold true for novel regimens with a different mechanism of action. However, with the recent success of high dose rifapentine with moxifloxacin in Study 31/A5349, it is clear that rifamycin-containing regimens will remain first line for drug sensitive TB for the foreseeable future. Finally, although we have confirmed that desirable regimens graduate in >95% of simulations (analogous to power) and suboptimal regimens graduate and demonstrate noninferiority in <5% of simulations (analogous to type I error), an in-depth power and type I error analysis was not explored in this study. To that end, we have assumed that a sample size of 400 is sufficient for a noninferiority confirmatory trial with a 6.6% margin to achieve 80% power and limit type I error to 5%. Instead, we focused on optimizing and reviewing the graduating and stopping decisions of the five pathways, which remain previously undiscussed in the context of TB.

Conclusions

We have developed a flexible clinical trial simulation tool integrated with parametric survival models to accurately simulate the potential range of real-world trial outcomes[20]. We have also demonstrated the efficiencies of MAMS and BAR designs over conventional approaches for a platform adaptive trial and provided sets of optimized design parameters. Through our ongoing collaborations, this work described here will be used by international consortia for TB regimen development and sets the stage for future adaptive trial design studies within the context of TB.

References

1. World Health Organization. Global Tuberculosis Report 2021. Geneva: World Health Organization; 2021.
2. Dorman SE, Nahid P, Kurbatova EV, et al. Four-Month Rifapentine Regimens with or without Moxifloxacin for Tuberculosis. *N Engl J Med* 2021; **384**(18): 1705-18.
3. Cox E, Laessig K. FDA approval of bedaquiline--the benefit-risk balance for drug-resistant tuberculosis. *N Engl J Med* 2014; **371**(8): 689-91.
4. Conradie F, Diacon AH, Ngubane N, et al. Treatment of Highly Drug-Resistant Pulmonary Tuberculosis. *N Engl J Med* 2020; **382**(10): 893-902.
5. Thwaites G, Nahid P. Triumph and Tragedy of 21st Century Tuberculosis Drug Development. *N Engl J Med* 2020; **382**(10): 959-60.
6. Phillips PPJ, Mitnick CD, Neaton JD, Nahid P, Lienhardt C, Nunn AJ. Keeping phase III tuberculosis trials relevant: Adapting to a rapidly changing landscape. *PLoS Med* 2019; **16**(3): e1002767.
7. Lienhardt C, Nahid P. Advances in clinical trial design for development of new TB treatments: A call for innovation. *PLoS Med* 2019; **16**(3): e1002769.
8. Kia TM, Marshall JC, Murthy S. Stakeholder perspectives on adaptive clinical trials: a scoping review. *Trials* 2020; **21**(1).
9. Davies GR, Phillips PP, Jaki T. Adaptive clinical trials in tuberculosis: applications, challenges and solutions. *Int J Tuberc Lung Dis* 2015; **19**(6): 626-34.
10. Phillips PPJ, Gillespie SH, Boeree M, et al. Innovative trial designs are practical solutions for improving the treatment of tuberculosis. *J Infect Dis* 2012; **205 Suppl 2**: S250-7.
11. Dawson R, Narunsky K, Carman D, et al. Two-stage activity-safety study of daily rifapentine during intensive phase treatment of pulmonary tuberculosis. *Int J Tuberc Lung Dis* 2015; **19**(7): 780-6.
12. Boeree MJ, Heinrich N, Aarnoutse R, et al. High-dose rifampicin, moxifloxacin, and SQ109 for treating tuberculosis: a multi-arm, multi-stage randomised controlled trial. *Lancet Infect Dis* 2017; **17**(1): 39-49.
13. Cellamare M, Ventz S, Baudin E, Mitnick CD, Trippa L. A Bayesian response-adaptive trial in tuberculosis: The endTB trial. *Clin Trials* 2017; **14**(1): 17-28.

14. Barr L, Treatment Action Group. Tuberculosis Research Funding Trends 2005-2018. 2019.
15. Bonnett LJ, Ken-Dror G, Koh G, Davies GR. Comparing the Efficacy of Drug Regimens for Pulmonary Tuberculosis: Meta-analysis of Endpoints in Early-Phase Clinical Trials. *Clin Infect Dis* 2017; **65**(1): 46-54.
16. Phillips PP, Dooley KE, Gillespie SH, et al. A new trial design to accelerate tuberculosis drug development: the Phase IIC Selection Trial with Extended Post-treatment follow-up (STEP). *BMC Med* 2016; **14**(1): 51.
17. Cellamare M, Milstein M, Ventz S, Baudin E, Trippa L, Mitnick CD. Bayesian adaptive randomization in a clinical trial to identify new regimens for MDR-TB: the endTB trial. *Int J Tuberc Lung Dis* 2016; **20**(12): 8-12.
18. World Health Organization. Target regimen profiles for TB treatment. Geneva: World Health Organization; 2016.
19. Imperial MZ, Nahid P, Phillips PPJ, et al. A patient-level pooled analysis of treatment-shortening regimens for drug-susceptible pulmonary tuberculosis. *Nature Medicine* 2018; **24**(11): 1708-15.
20. Imperial MZ, Phillips PPJ, Nahid P, Savic RM. Precision-Enhancing Risk Stratification Tools for Selecting Optimal Treatment Durations in Tuberculosis Clinical Trials. *Am J Respir Crit Care Med* 2021; **204**(9): 1086-96.
21. Wason JM, Trippa L. A comparison of Bayesian adaptive randomization and multi-stage designs for multi-arm clinical trials. *Stat Med* 2014; **33**(13): 2206-21.
22. Lin J, Bunn V. Comparison of multi-arm multi-stage design and adaptive randomization in platform clinical trials. *Contemp Clin Trials* 2017; **54**: 48-59.
23. Gallo P, Maurer W. Challenges in Implementing Adaptive Designs: Comments on the Viewpoints Expressed by Regulatory Statisticians. *Biometrical Journal* 2006; **48**(4): 591-7.
24. Tweed CD, Dawson R, Burger DA, et al. Bedaquiline, moxifloxacin, pretomanid, and pyrazinamide during the first 8 weeks of treatment of patients with drug-susceptible or drug-resistant pulmonary tuberculosis: a multicentre, open-label, partially randomised, phase 2b trial. *Lancet Respir Med* 2019; **7**(12): 1048-58.

25. Barker AD, Sigman CC, Kelloff GJ, Hylton NM, Berry DA, Esserman LJ. I-SPY 2: an adaptive breast cancer trial design in the setting of neoadjuvant chemotherapy. *Clin Pharmacol Ther* 2009; **86**(1): 97-100.
26. Choodari-Oskooei B, Bratton DJ, Gannon MR, Meade AM, Sydes MR, Parmar MK. Adding new experimental arms to randomised clinical trials: Impact on error rates. *Clin Trials* 2020; **17**(3): 273-84.
27. DeMichele A, Berry DA, Zujewski J, et al. Developing safety criteria for introducing new agents into neoadjuvant trials. *Clin Cancer Res* 2013; **19**(11): 2817-23.
28. Bassler D, Briel M, Montori VM, et al. Stopping randomized trials early for benefit and estimation of treatment effects: systematic review and meta-regression analysis. *JAMA* 2010; **303**(12): 1180-7.
29. Cairns JA, Wittes J, Wyse DG, et al. Monitoring the ACTIVE-W trial: some issues in monitoring a noninferiority trial. *Am Heart J* 2008; **155**(1): 33-41.
30. Goldman B, LeBlanc M, Crowley J. Interim futility analysis with intermediate endpoints. *Clin Trials* 2008; **5**(1): 14-22.
31. Quartagno M, Walker AS, Carpenter JR, Phillips PP, Parmar MK. Rethinking non-inferiority: a practical trial design for optimising treatment duration. *Clin Trials* 2018: 1740774518778027.
32. Pouwels KB, Yin M, Butler CC, et al. Optimising trial designs to identify appropriate antibiotic treatment durations. *Bmc Medicine* 2019; **17**.
33. Nunn AJ, Phillips PPJ, Mitchison DA. Timing of relapse in short-course chemotherapy trials for tuberculosis [Short communication]. *Int J Tuberc Lung D* 2010; **14**: 241-2(2).

Supplementary Information

Data Generating Mechanism

The model described in Imperial et. al. utilized individual-level data (n = 3405) from three international, randomized phase III trials (Ofloxacine-Containing, Short-Course Regimen for the Treatment of Pulmonary Tuberculosis [OFLOTUB] trial, NCT00216385; Rapid Evaluation of Moxifloxacin in TB [REMoxTB] trial, NCT00864383; and High-Dose Rifapentine with Moxifloxacin for Pulmonary Tuberculosis [RIFAQUIN] trial, ISRCTN44153044) that compared 4-month fluoroquinolone-containing regimens to the standard 6-month regimen for treatment of drug-susceptible TB.

The hazard risk for TB-related outcomes was best described with a surge function [EQ1]. Fewer treatment days increased the baseline hazard risk (λ) of TB-related outcomes (29% [percent relative standard error (%RSE) = 9] increase per 28-day decrease in number of treatment days. Baseline factors that increased hazard risk included HIV coinfection (86% [%RSE = 29] increase), higher smear grade (68% [36] increase for smear 3+ relative to smear 1+ or negative), male sex (64% [32] increase), presence of cavitary disease (26% [57] increase), and lower body mass index (BMI) (18% [41] increase per 5 kg/m2 decrease). Inclusion of time to culture conversion improved discrimination with an increase in ROC AUC from 0.69 (95% CI, 0.66–0.72) to 0.72 (0.69–0.75).

EQ1 $h(t,xi) = \lambda(x_i)t^{\beta}\exp(-\alpha t)$

The hazard risk for culture conversion was also best described with a surge function. There were several baseline factors that increased the baseline hazard risk (λ) for culture conversion including: younger age (8.8% [21] increase for every 10 years younger), lower smear grade (162% [24] increase for smear 1+ and 101% [28] increase for smear 2+ relative to smear 3+), clinical site (79% [6] decrease for Asia site and 156% [52] increase for India site relative to sub-Saharan Africa site). Additionally there were several baseline factors that increased the shape hazard risk (β) for culture conversion including: lower smear grade (44% [22] increase for smear 1+ and 36% [26] increase for smear 2+ relative to smear 3+) and

clinical site (49% [13] decrease for Asia site and 22% [78] increase for India site relative to sub-Saharan Africa site).

Individual survival probability density functions are calculated for each individual participant for culture conversion using the factors described above plus the regimen hazard ratios as described in Table 1. Then a random number between 0 and 1 is assigned to that participant and where it intersects the probability density function determines the TCC. The regimen hazard ratios, TCC, and aforementioned factors are used to calculate another survival probability density function for TB-related unfavorable outcomes. Another random number is assigned to that participant and the individual participant TTR calculated.

Bayesian Response Adaptive Randomization

Intermediate and Final Endpoints

The primary endpoint measured is treatment success at 78 weeks (TS-78) after randomization, and is defined as relapse free survival up to 78 weeks post randomization (TTR ≥ 78 weeks). Three intermediate endpoints will be measured at 8 weeks (TS-8: TCC ≤ 8 weeks), 24 weeks (TS-24: TCC ≤ 24 weeks AND TTR ≥ 24 weeks), and 52 weeks (TS-52: TTR ≥ 52 weeks). We expect a strong correlation to be observed between the intermediate endpoints TS-24 and TS-52 with the final endpoint TS-78; therefore, Phase IIc will adaptively randomize based on TS-24 and seamless Phase II/III based on TS-52. Incorporating relapse data into adaptive randomization is feasible for a seamless Phase III trial as the longer recruitment period permits the accumulation of relapse data in time to affect the course of the trial. As the majority of relapses (75-85%)[33] occur within 6 months post-treatment, TS-52 was chosen as reasonable predictor for treatment outcomes at 78 weeks. Individual patient endpoints were model generated as TCC and TTR then converted into binary TS-8, -24, -52, and -78 and used to update priors as data accumulates.

Adaptive Randomization

Phase IIc BAR is dependent on the Bayesian probability that TS-24 in arm *k* is better than the control arm. Essentially, as evidence accumulates of arm *k* performing better than the control arm, the randomization probability to arm *k* will be adjusted higher. For the control, the randomization probability is defined so that the control sample size approximately matches the investigational arm with the highest number of enrolled patients. The mathematical framework was drawn from Cellamare et. al. 2016 which implemented a BAR design for the endTB trial. Two randomization tuning parameters γ and η, where γ tunes how heavily randomization probabilities are weighed in favor of well performing arms and η tunes how quickly adaptive randomization responds to incoming data—$\eta > 1$ weighs early data higher and responds quickly, $\eta < 1$ penalizes early data and waits for more data before responding to accumulated data. These parameters were explored in a grid-like fashion across a range of reasonable values and optimized for graduating clinically noninferior arms and stopping suboptimal arms.

$$EQ2\colon\ P\big(\mathrm{TS}-52\ (k)\big) = \psi_{1.1}(k)\phi(k)\omega(k) + \psi_{0.1}(k)\big(1-\phi(k)\big)\omega(k) + \psi_{1.0}(k)\phi(k)\big(1-\omega(k)\big) + \psi_{0.0}(k)\big(1-\phi(k)\big)\big(1-\omega(k)\big)$$

The Phase II/III seamless Bayesian design was constructed using the same framework, but modified so that adaptive randomization is dependent on TS-52 instead, which is estimated by [EQ2] where $\phi(k)$ represents the probability of TS-8, $\omega(k)$ represents the probability of TS-24, and $\psi_{i,j}(k)$ represents the conditional probability of TS-52 given the four combinations of positive or negative TS-8 and TS-24. The priors for TS-8 and TS-24 are uniform distributions, the priors for the TS-52 conditional probabilities are: $\psi_{1.1}$ = (10,1) where $\psi_{1.1}$ represents a positive TS-8 and TS-24, $\psi_{1.0}$ = (1,10) where $\psi_{1.0}$ represents a positive TS-8 and negative TS-24, $\psi_{0.1}$ = (10,1), $\psi_{0.0}$ = (0.1,10). Optimistic (10,1) and skeptical (3,8) priors for $\psi_{0.1}$ were tested to determine the effects of confidence in the relationship between month 2 culture status and relapse.

A maximum N per arm rule was designed to stop enrollment to arms in which a sufficient number of patients have already been enrolled, 100 patients for phase IIC and 400 for seamless (same maximums as MAMS). Stopping rules for the Bayesian trial designs were designed to graduate a maximum number

of arms, 4 for Phase IIc and 3 for seamless Phase II/III, to reflect the desired number of candidates to advance to Phase III or submission to regulatory approval.

Sensitivity Analyses

Decoupling the model assumed relationship between individual TCC and TTR did not significantly affect the conclusions of each of the designs. Since MAMS evaluates arms as a whole, graduation and stop decisions were not affected. For BAR however, because the definition of TS-24 (TCC ≤ 24 weeks AND TTR ≥ 24 weeks) relies on an individual's TCC-TTR relationship, each arm's TS-24 rate changed slightly. Since the Phase IIc BAR design randomizes based on each arm's TS-24 rate relative to other arms, adaptive randomization responded appropriately to the decoupled TS-24 profile and shifted patients from desirable to minimal regimens. We believe our conclusions are not affected because the BAR design does not inherently assume an individual's TCC-TTR relationship, and the observed differences are an artifact of model implementation and the TS-24 definition, not a weakness of the BAR design. In practice, even if the relationship between TCC and TTR is different from what has been observed in prior trials each arm's TS-24 rate would remain the same. In support of this conclusion, seamless BAR, which randomizes based on TS-52, remained unaffected.

Changing the composition of regimens changed BAR patient allocation across arms in expected ways. Since adaptive randomization is dependent on each arm's performance relative to other arms, the BAR design will allocate patients very similarly between a scenario with 4 desirable and 4 minimal regimens and a scenario with 4 minimal and 4 suboptimal regimens. In other words, without additional trial rules a BAR design would allocate resources to the best regimens from a pool of suboptimal candidates and it is therefore not possible to design such a trial that achieves our goals of stopping suboptimal regimens x% of the time when there are few desirable regimens.

We are simulating data for time to relapse from a parametric survival model (based on previous work) and therefore the 'true relapse rate' for a particular simulation depends upon the exact individual patients recruited into each arm, in addition to the stochastic survival model, there is no underlying 'true relapse

rate' for an arm. Therefore, percent bias was assessed using the median relapse rate from unbiased non-adaptive trial simulations (Table 5-1) as reference, where 2000 patients were recruited into each arm using fixed randomization. Percent bias was calculated for each arm *k* as 100*(pathway relapse $rate_k$ – median unbiased relapse $rate_k$)/ median unbiased relapse $rate_k$.

A long delay in biomarker data results in inefficiency of an adaptive design. We ran simulations comparing the 6-week lag time (used in all simulations in the main text) to an 8 week lag time as a sensitivity analysis. Minimal differences were observed, with graduation and stopping rates changing less than 2% for *desirable* or *suboptimal* regimens and less than 5% for *minimal* regimens.

Sources of Variation

Important to consider while interpreting simulation results is the sources of variation. There are two sources of variation in this study: (1) The stochastic nature of parametric survival models. Each individual patient has an individual distribution of potential TCC and TTR based on their individual clinical and disease characteristics. Each patient's distribution is calculated and sampled upon their recruitment and due to not fixing the random seed, recruiting the same patient multiple times will result in slightly different TCC and TTR. (2) The randomization of patients into arms. Although randomization is balanced so that easy, moderate, and hard-to-treat patients are equally represented in all arms, with enough simulations an arm could be comprised of higher risk patients from each group, thus underestimating the efficacy of said arm.

Implications of Variation

Although this variation makes interpreting the simulation results more challenging and nuanced, simulating this variation (instead of assuming a fixed culture conversion rate and relapse rate in each arm as previous studies have done) is reflective of the full range of what may be observed in reality. Interestingly, the variation affects the course of MAMS and BAR trials differently. As the MAMS design compares each regimen to the control independently, the variation in other experimental arms is irrelevant to the comparison at hand. For example, if a suboptimal regimen has a higher survival rate than

its true rate due to variation in patient response and randomization, the suboptimal regimen may be graduated but it is irrelevant to the evaluation of the other experimental arms in the trial. However, for a BAR design, since randomization is dependent on the performance of other arms, the variation in a particular arm affects the course of the trial as a whole. Using the same example, if a suboptimal regimen has a higher survival rate than its 'true' rate (median cure rate from Table 1), then patient allocation shifts from other arms to the suboptimal regimen. In this scenario for patient enrollment across arms to be the same as the true scenario, all arms would also have to have a proportionally higher survival rate than its true rate.

Supplementary Figures

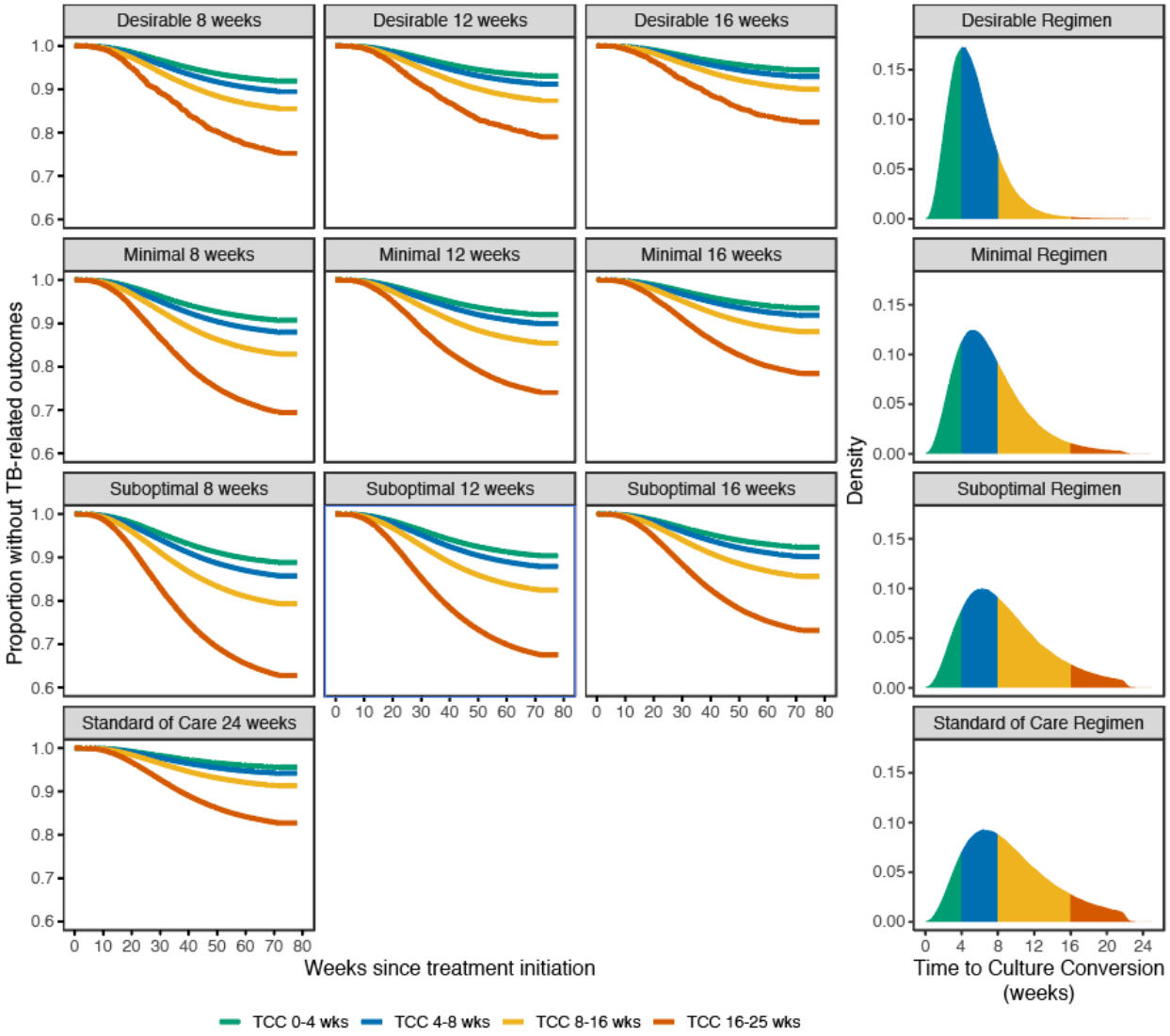

Supplemental Figure 5-1 Simulated regimens time to relapse Kaplan Meier estimates stratified by time to culture conversion.

In green are patients whose time to culture conversion is ≤4 weeks, in blue is >4 and ≤8 weeks, in yellow is >8 and ≤16 weeks, and in red is >16 and ≤25 weeks. On the right are density plots of time to culture conversion for each of the regimens, more potent the regimens cause patients to culture convert earlier and thus the distribution becomes more right skewed. Together, the plots demonstrate the relationship between regimen potency, treatment duration, time to culture conversion, and time to relapse.

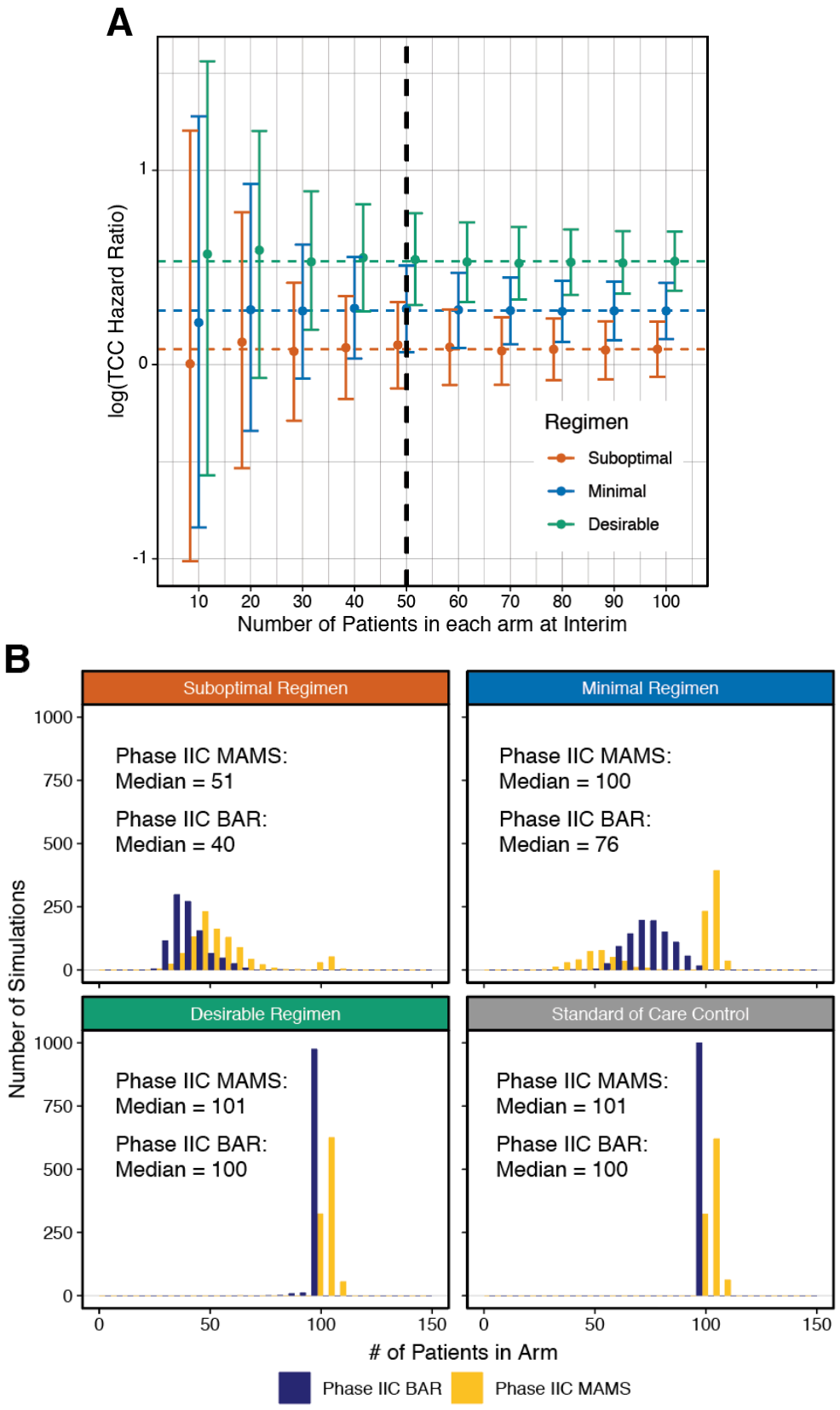

Supplemental Figure 5-2 Phase IIc Supporting optimization figures.

(A) points and the error bars represent the mean simulation HR estimation and 95% CI respectively. The accuracy of the HR estimate improves with increasing number of patients; interim timing at N = 50 is where the median estimate stabilizes and provides sufficient accuracy to make interim decisions. (B) Histogram of patient enrollment per simulation in each regimen across 1000 simulations of optimized BAR and MAMS trials. BAR's graded response is clearly demonstrated in the median enrollment in each of the regimens. Within each regimen, BAR simulations also produce a distribution of patient enrollment, contrasting with MAMS simulations with patient enrollment clustered around 50 and 100 (interim and trial end).

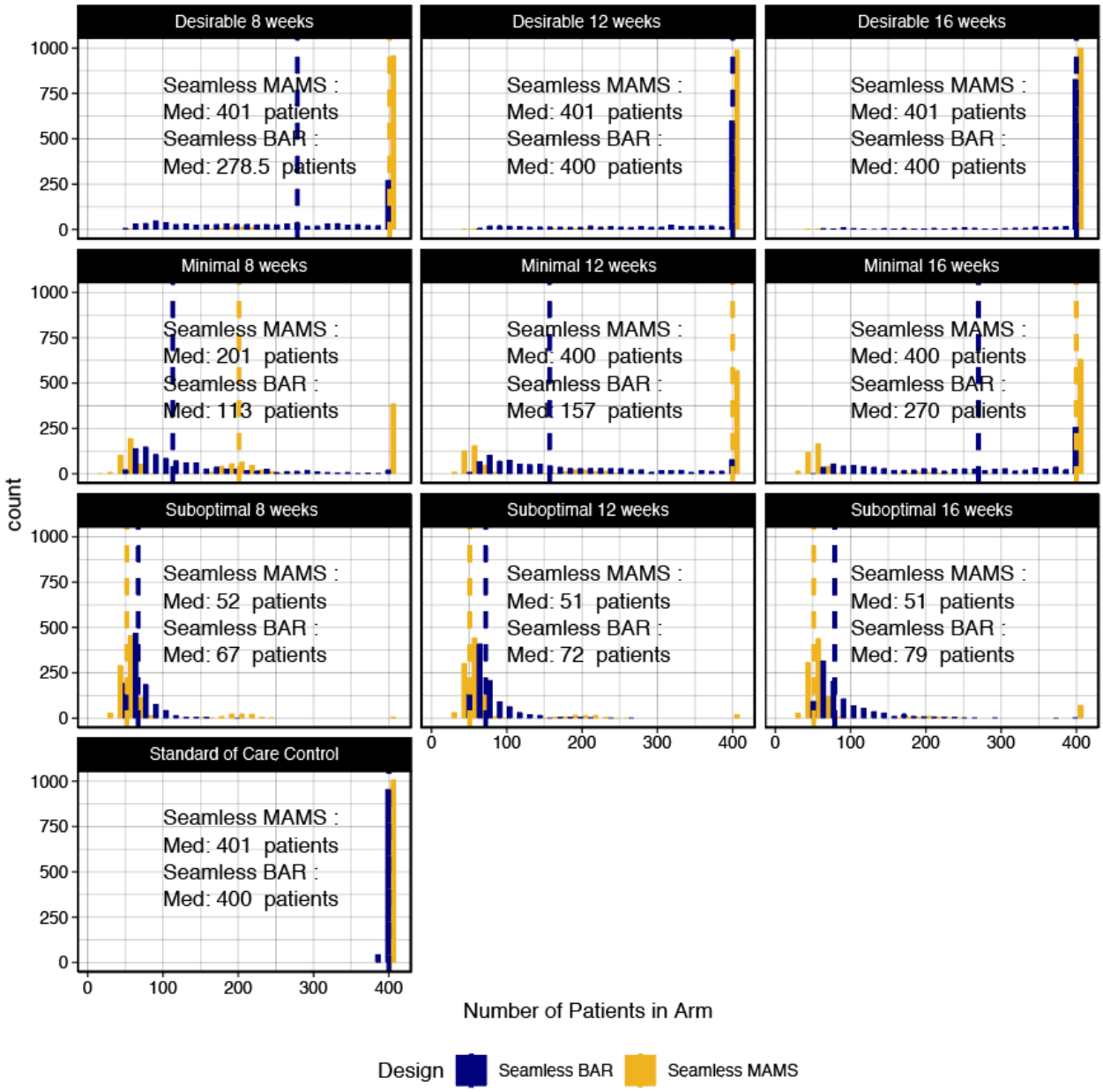

Supplemental Figure 5-3 Seamless Phase II/III enrollment per arm.

Histogram of patient enrollment per simulation in each arm across 1000 simulations of optimized BAR and MAMS trials. BAR's graded response is clearly demonstrated in seamless designs as well.

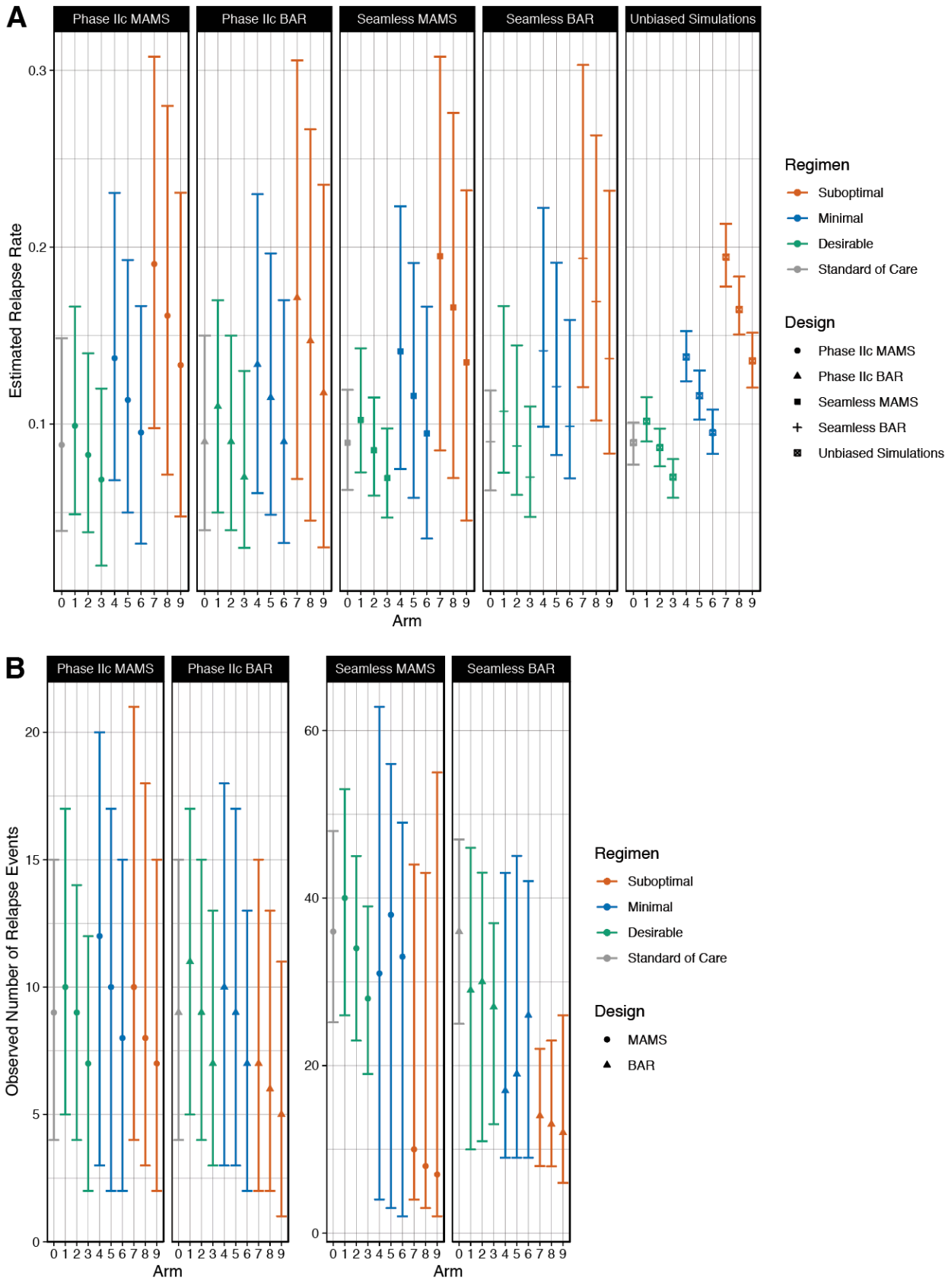
A
Phase IIc MAMS
Phase IIc BAR
Seamless MAMS
Seamless BAR
Unbiased Simulations
Estimated Relapse Rate
0.3
0.2
0.1
0 1 2 3 4 5 6 7 8 9
Arm
Regimen
Suboptimal
Minimal
Desirable
Standard of Care
Design
Phase IIc MAMS
Phase IIc BAR
Seamless MAMS
Seamless BAR
Unbiased Simulations
B
Phase IIc MAMS
Phase IIc BAR
Seamless MAMS
Seamless BAR
Observed Number of Relapse Events
20
15
10
5
0
60
40
20
0
0 1 2 3 4 5 6 7 8 9
Arm
Regimen
Suboptimal
Minimal
Desirable
Standard of Care
Design
MAMS
BAR

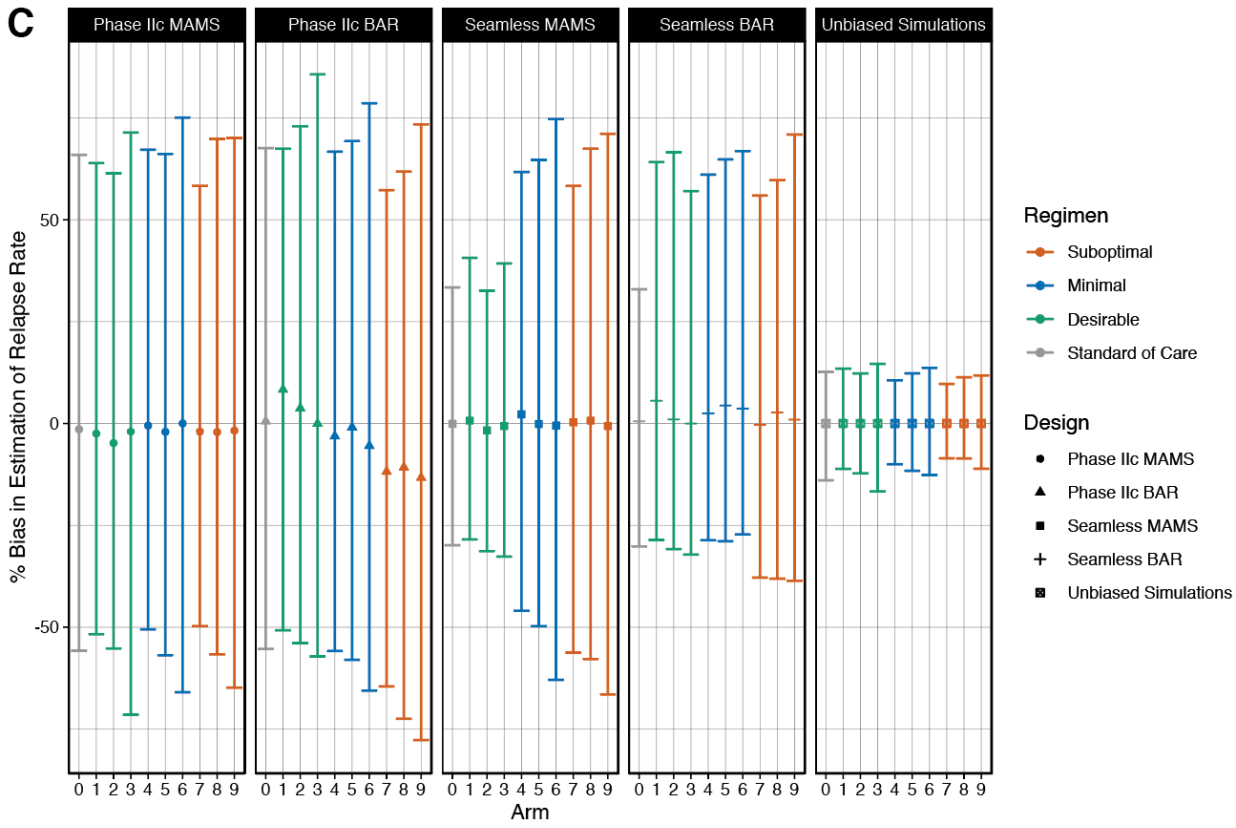

Supplemental Figure 5-4 Comparison of performance measures.

(A) Estimated relapse rate across arms and trial designs is accurate when compared to unbiased simulations. Lower accuracy and higher 95% prediction intervals are observed in arms with very low sample size, i.e. phase IIC BAR arms 7, 8, 9. (B) The higher number of relapse events observed in BAR designs' desirable regimens provide greater evidence of efficacy for the best regimens. Given the low relapse rate in better regimens, higher sample size is particularly needed in the best regimens to observe an appreciable number of relapse events to produce an accurate relapse rate estimate. (C) Minimal bias is observed in estimation of relapse rate across designs, except for phase IIC BAR arms 7, 8, 9 where the low sample size produces a consistent underestimation of relapse rate. Overall, both MAMS and BAR designs provides excellent accuracy and precision in relapse rate estimation. The bias in suboptimal regimens is inconsequential as these arms would quickly be abandoned for lack of efficacy.

Chapter 6 - Conclusion

The work presented in this dissertation improves the understanding of pharmacokinetics and pharmacodynamics of TB treatment. Quantitative, model-based tools were developed to provide evidence-based recommendations on optimal treatment regimens and strategies that i.) maximize durable cure in all patients, ii.) identify patients at higher risk for adverse events, iii.) maximize success of late-stage clinical development, and iv.) encourage the adoption of adaptive trial designs in anti-TB therapeutic development.

Chapters 2 and 3 describe the largest to date population pharmacokinetic analysis in the tuberculosis infected population of rifapentine and moxifloxacin, two of the six drugs administered in Study 31/A5349. Robust population pharmacokinetic models identified male sex, Black race, and HIV seropositivity as risk factors for low rifapentine exposure. While, male sex, HIV seropositivity, and patients living with diabetes as risk factors for low moxifloxacin exposure. Pharmacokinetic-safety analyses found no evidence of an exposure-toxicity relationship with any of the predefined safety outcomes or other known rifamycin or fluoroquinolone toxicities. While we were unable to determine a target exposure for moxifloxacin, we have demonstrated that male patients living with HIV or diabetes are at risk for low moxifloxacin exposures and dosing simulations demonstrated that they may benefit from a higher dose. Rifapentine dosing simulations found that although subpopulations at risk for low exposure would benefit most from a higher rifapentine dose, all patients would benefit from an increase to 1500 or 1800 mg.

The first ever phase III study-wide pharmacokinetic-pharmacodynamic analysis with long term clinical outcomes is reported in Chapter 4. Data from Study 31/A5349 was analyzed with parametric time to event modeling to identify risk factors for TB-related unfavorable outcome from demographic, clinical, and pharmacokinetic factors. Of the pharmacokinetic factors, higher rifapentine exposures were found to drive treatment response in rifapentine and rifapentine-moxifloxacin regimens, while higher pyrazinamide exposures were found to drive treatment response in the control regimen. We also found that higher baseline disease burden measured by Gene Xpert MTB/RIF (polymerase chain reaction based measurement) and extent of lung area affected by TB disease on chest radiograph were consistent risk factors across all three regimens used in Study 31/A5349. Furthermore, patients can be stratified by

these measures of baseline disease burden into a low-risk subgroup in which further treatment shortening and simplification are likely to be possible and a high-risk subgroup in which longer treatment may be needed.

The integrated models built from this work were used in a variety of additional simulation work. First, a clinical trial simulation tool was developed which simulated treatment outcomes from individual patient characteristics drawn from a patient database consisting of four recent phase III trials (Study 31/A5349, ReMOX, RIFAQUIN, and OFLOTUB). The random sampling from a real patient database in combination with the simulation of individual patient treatment outcomes allows for more realistic simulations that capture the potential variability that might be observed due to random sampling. By adding adaptive design frameworks to the simulation tool, multi-arm multi-stage and Bayesian adaptive randomization designs were explored for suitability and optimized for phase II and III anti-tuberculosis regimen trials. Chapter 5 presents the results of this work which have been reviewed by the UNITE4TB initiative, an international collaboration of non-governmental organizations, academia, and industry to accelerate the development of new anti-TB therapeutics. Finally, although this work is not presented in this dissertation, this simulation tool has also been used in the design of a novel phase II risk-stratification, duration-randomization trial by the AIDS clinical trial group (A5414).

In summary, quantitative, model-based approaches better characterize treatment response in TB patients and provide evidence-based tools that can be used to improve treatment outcomes and accelerate the development of anti-TB therapeutics. The presented work has contributed to the optimization and implementation of shorter, efficacious, and better tolerated regimens and development of new ultra-short therapeutics. Overall, this dissertation brings humanity one step closer to ending the TB epidemic.

Publishing Agreement

It is the policy of the University to encourage open access and broad distribution of all theses, dissertations, and manuscripts. The Graduate Division will facilitate the distribution of UCSF theses, dissertations, and manuscripts to the UCSF Library for open access and distribution. UCSF will make such theses, dissertations, and manuscripts accessible to the public and will take reasonable steps to preserve these works in perpetuity.

I hereby grant the non-exclusive, perpetual right to The Regents of the University of California to reproduce, publicly display, distribute, preserve, and publish copies of my thesis, dissertation, or manuscript in any form or media, now existing or later derived, including access online for teaching, research, and public service purposes.

DocuSigned by:
0931068BDC6749F...
Author Signature

12/13/2022
Date